LEVEL II

AD A056912

DDC FILE COPY
AD No.

AFFDL-TR-78-43

THE STATISTICAL NATURE OF FATIGUE CRACK PROPAGATION

D. A. VIRKLER
B. M. HILLBERRY
P. K. GOEL
SCHOOL OF MECHANICAL ENGINEERING
PURDUE UNIVERSITY
WEST LAFAYETTE, INDIANA

DDC
RECEIVED
AUG 2 1978
F

APRIL 1978

TECHNICAL REPORT AFFDL-TR-78-43
Final Report – June 1976 to May 1978

Approved for public release; distribution unlimited.

78 07 31 001

AIR FORCE FLIGHT DYNAMICS LABORATORY
AIR FORCE WRIGHT AERONAUTICAL LABORATORIES
AIR FORCE SYSTEMS COMMAND
WRIGHT-PATTERSON AIR FORCE BASE, OHIO 45433

NOTICE

When Government drawings, specifications, or other data are used for any purpose other than in connection with a definitely related Government procurement operation, the United States Government thereby incurs no responsibility nor any obligation whatsoever; and the fact that the government may have formulated, furnished, or in any way supplied the said drawings, specifications, or other data, is not to be regarded by implication or otherwise as in any manner licensing the holder or any other person or corporation, or conveying any rights or permission to manufacture, use, or sell any patented invention that may in any way be related thereto.

This report has been reviewed by the Information Office (OI) and is releasable to the National Technical Information Service (NTIS). At NTIS, it will be available to the general public, including foreign nations.

This technical report has been reviewed and is approved for publication.

Margery E. Artley

MARGERY E. ARTLEY,
Project Engineer

R.M. Bader

ROBERT M. BADER, Chf
Structural Integrity Br

FOR THE COMMANDER

Ralph L. Kuster Jr.

RALPH L. KUSTER, JR., Col, USAF
Chief, Structural Mechanics Division

"If your address has changed, if you wish to be removed from our mailing list, or if the addressee is no longer employed by your organization please notify, AFFDL/FBE, W-PAFB, OH 45433 to help us maintain a current mailing list".

Copies of this report should not be returned unless return is required by security considerations, contractual obligations, or notice on a specific document.

AIR FORCE/86780/10 July 1978 — 475

UNCLASSIFIED

SECURITY CLASSIFICATION OF THIS PAGE (When Data Entered)

REPORT DOCUMENTATION PAGE

READ INSTRUCTIONS BEFORE COMPLETING FORM

1. REPORT NUMBER: AFFDL-TR-43-78	2. GOVT ACCESSION NO.
3. RECIPIENT'S CATALOG NUMBER: Rept.	
4. TITLE (and Subtitle): THE STATISTICAL NATURE OF FATIGUE CRACK PROPAGATION.	5. TYPE OF REPORT & PERIOD COVERED: FINAL JUN 76 – MAY 78
	6. PERFORMING ORG. REPORT NUMBER
7. AUTHOR(s): D. A. VIRKLER, B. M. HILLBERRY, P. K. GOEL	8. CONTRACT OR GRANT NUMBER(s): AFOSR-76-3018
9. PERFORMING ORGANIZATION NAME AND ADDRESS: SCHOOL OF MECHANICAL ENGINEERING, PURDUE UNIVERSITY, WEST LAFAYETTE, INDIANA 47907	10. PROGRAM ELEMENT, PROJECT, TASK AREA & WORK UNIT NUMBERS: 2307-01-10
11. CONTROLLING OFFICE NAME AND ADDRESS: AIR FORCE OFFICE OF SCIENTIFIC RESEARCH/NA, BLDG. 410, BOLLING AIR FORCE BASE, DC 20332	12. REPORT DATE: MAR 77
	13. NUMBER OF PAGES: 42
14. MONITORING AGENCY NAME & ADDRESS (if different from Controlling Office): FATIGUE, FRACTURE AND RELIABILITY, STRUCTURAL INTEGRITY BRANCH, STRUCTURAL MECHANICS DIVISION, AIR FORCE FLIGHT DYNAMICS LABORATORY, WPAFB, OHIO	15. SECURITY CLASS. (of this report): UNCLASSIFIED
	15a. DECLASSIFICATION/DOWNGRADING SCHEDULE

16. DISTRIBUTION STATEMENT (of this Report)

Approved for public release; distribution unlimited.

DDC RECEIVED AUG 2 1978 F

17. DISTRIBUTION STATEMENT (of the abstract entered in Block 20, if different from Report)

18. SUPPLEMENTARY NOTES

19. KEY WORDS (Continue on reverse side if necessary and identify by block number)

FATIGUE
CRACK PROPAGATION
STATISTICAL DISTRIBUTION
NORMAL
LOG-NORMAL
WEIBULL
GAMMA
DIFFERENTIATION METHOD

20. ABSTRACT (Continue on reverse side if necessary and identify by block number)

A statistical investigation of the fatigue crack propagation process was conducted. Sixty-eight replicate constant amplitude crack propagation tests were conducted on 2024-T3 aluminum alloy. Distribution determination programs were written for the variables $\Delta N/\Delta a$, N, da/dN, and dN/da. The following distributions were considered: two-parameter normal distribution, three-parameter log-normal distribution, three-parameter Weibull distribution, two-parameter gamma distribution, three-parameter gamma distribution, the

over

DD FORM 1 JAN 73 1473 EDITION OF 1 NOV 65 IS OBSOLETE

UNCLASSIFIED

SECURITY CLASSIFICATION OF THIS PAGE (When Data Entered)

292 074 78 07 31 001

the generalized three-parameter gamma distribution, and the generalized four-parameter gamma distribution. From the experimental data, the distribution of N as a function of crack length was best represented by the three-parameter log-normal distribution.

Six growth rate calculation methods were investigated and the method which introduced the least amount of error into the growth rate data was found to be a modified secant method. Based on the distribution of da/dN, which varied moderately as a function of crack length, replicate a vs. N data were predicted. This predicted data reproduced the mean behavior but not the variant behavior of the actual a vs. N data.

FOREWORD

This report describes an investigation of the variability in fatigue crack propagation under constant ampltiude loading sponsored by AFOSR-78-3018, and performed under Air Force Project 2307, Solid Mechanics, Task 2307Ø110, Variability in Fatigue Crack Growth. Technical monitor for the project was Dr. J.P. Gallagher, formerly of AFFDL/FBE. Ms. M.E. Artley (AFFDL/FBE) assumed responsibility for the project February 1978. The project period was June 1976 to May 1978.

This program was conducted by the School of Mechanical Engineering Purdue University, W. Lafayette, Indiana. Principal Investigator was Professor B.M. Hillberry; the graduate research assistant was Mr. D.A. Virkler. Professor P.K. Goel was the statistician. Materials for the test specimens were provided by the Aluminum Company of America.

This report was submitted by the authors April 1978.

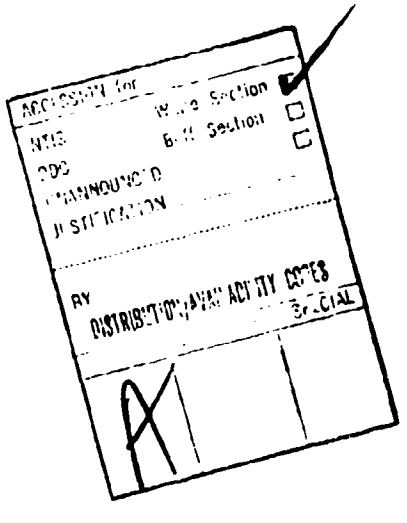

TABLE OF CONTENTS

PRECEDING PAGE BLANK-NOT FILMED

TABLE OF CONTENTS (Cont'd)

LIST OF TABLES

LIST OF TABLES

LIST OF TABLES (Cont'd)

LIST OF ILLUSTRATIONS

LIST OF ILLUSTRATIONS (Cont'd)

LIST OF ILLUSTRATIONS (Cont'd)

LIST OF ILLUSTRATIONS (Cont'd)

LIST OF SYMBOLS

A	chi-square tail area
a	half crack length (in. or mm.).
a_f	final half crack length (in. or mm.).
a_i	any discrete half crack length (in. or mm.).
$\overline{a_i}$	average half crack length used by the secant method (in. or mm.).
a_o	initial half crack length (in. or mm.).
B	Weibull slope.
B_2	curvature used in the Golden Section search method.
b	scale parameter for the MLE 3-parameter Weibull distribution.
b_o	least squares Y intercept.
b_1	least squares slope.
b_2	least squares curvature.
C^2	closeness.
C_1	scaling constant used by the incremental polynomial methods for the mean of the strip data.
C_2	scaling constant used by the incremental polynomial methods for the range of the strip data.
C_+	constant approaching positive infinity.
C_V	constant in the covariance matrix.
c	shape parameter for the MLE 3-parameter Weibull distribution.
D	maximum deviation in the Kolmogorov-Smirnov test.
d	convergence constant for the interior point penalty function algorithm.

da/dN	fatigue crack growth rate (in./cycle).
da/dN_i	any discrete value of fatigue crack growth rate (in./cycle).
da/dN_{max}	maximum fatigue crack growth rate (in./cycle).
da/dN_{min}	minimum fatigue crack growth rate (in./cycle).
dN/da	inverse fatigue crack growth rate (cycles/in.).
e	Napierian base (2.718281828).
$\exp(\chi)$	e raised to the χ power.
e_i	expected frequencies in the chi-square test.
$F(\chi_c)$	cumulative density function of corrected data.
F_g^{-1}	inverse cumulative density function for the generalized 4-parameter gamma distribution.
$f(\chi)$	density function of a random variable.
$G(z)$	standard normal probability function.
g	shape/power parameter for the gamma distributions.
H	Golden Section search constant (0.618033989).
$H(z)$	gamma probability function.
I	vairable used in deriving C^2.
J	variable used in deriving C^2.
j	iteration counter for the interior point penalty function algorithm.
K	variable used in deriving C^2.
k	number of equiprobable intervals for the chi-square test.
L	maximum likelihood estimator function.
$\ln$	natural logarithm (base e).
$\log_{10}$	logarithm (base 10).
m	slope.
N	cumulative load cycle count.

N_f	final cumulative load cycle count.
N_i	any discrete cumulative load cycle count.
$\overline{N_i}$	average cumulative load cycle count used by the secant method.
N_{LS}	log (base 10) scaled cycle count data used by the log-log incremental polynomial methods.
N_S	scaled cycle count data used by the incremental polynomial methods.
n	number of data points in a data set.
n_{HS}	number of data points lost at each end of the data by the incremental polynomial methods.
n_p	number of distribution parameters.
n_{STRIP}	number of data points in the incremented strip in the incremental polynomial methods.
o_i	observed frequencies in the chi-square test.
P	objective function used by the interior point penalty function algorithm.
P_{max}	maximum applied load during the load cycle (lbs.).
P_{min}	minimum applied load during the load cycle (lbs.).
q_i	chi-square test class end points.
R	R ratio.
R^2	coefficient of multiple determination.
r	iteration variable in the interior point penalty function algorithm.
S_E	standard deviation of the errors.
S_S	standard deviation of the standard deviations.
S.E.	standard error.
SSRES	residual sum of squares.
T	location parameter in the Golden Section search method.
TCSS	total corrected sum of squares.

t	variable in the gamma probability function.
U	variable used in deriving da/dN for the quadratic log-log 7-point incremental polynomial method.
u	variable of integration in the chi-square tail area equation.
V	covariance matrix.
v	inverse covariance matrix.
X	variable to be plotted on the abscissa.
$\overline{X_E}$	mean of the errors.
$\overline{X_S}$	mean of the standard deviations.
Y	variable to be plotted on the ordinate.
Z	Kolmogorov-Smirnov test statistic.
z	standarized distribution variate.
α	power parameter in the gamma distributions.
α_a	hypothesis acceptance level.
β	shape parameter in the log normal distributions.
Γ	gamma function.
γ	Euler's constant (0.5772157).
Δa	distance between two consecutive half crack length data points (in. or mm.).
ΔK	charge in stress intensity during the load cycle (ksi-square root in.).
ΔK_i	any discrete value of ΔK (ksi-square root in.).
ΔN	number of cumulative load cycles between two consecutive cumulative load cycle count data points.
$\Delta N/\Delta a$	change in cumulative load cycle count normalized by the change in half crack length (cycles/in.).
ΔP	change in applied load during the load cycle (lbs.).
ϵ	convergence criterion constant.
ϵ_+	positive constant approaching zero.

θ	characteristic value of the 3-parameter Weibull distribution.
μ	scale parameter (sometimes the mean) of a distribution.
ν	degrees of freedom.
π	Pi (3.141592654).
σ	shape parameter (sometimes the standard deviation) of a distribution.
τ	location parameter (sometimes the terminus) of a distribution.
χ	random variable.
χ^2	chi-square test statistic.
χ_c	corrected random variable data.
χ_i	any discrete value of a random variable.
χ_{min}	minimum value of a random variable.
χ_o	expected minimum value of the 3-parameter Weibull distribution.
ψ	digamma function.
ψ'	trigamma function.
$\hat{}$	hat (symbolizes an estimated variable).

SECTION I

INTRODUCTION

Throughout the course of history, it has always been desirable to be able to predict the life of a given design under expected service conditions. Life prediction in metal structures has necessitated a need for knowledge about the metal fatigue phenomenon. The metal fatigue process, as it is known today, is complex and is still not fully understood. There are many variables which influence the life of a metal structure, such as the material, loading, and geometric characteristics of the particular structure. This investigation involves only the determination of the effect of material properties on life prediction.

One of the primary mechanisms by which metal fatigue occurs is the propagation of microscopic cracks [1]. The study of fatigue crack propagation behavior has been widely conducted for some time in an effort to understand metal fatigue more fully. The information obtained from crack propagation studies is then used in estimating the fatigue life of structures and components. Ideally, it is desirable that this estimated life will exactly predict the actual life. Unfortunately, there are many variables which influence this prediction and some are not well understood. One of the most important of these variables is how well the empirical crack growth relationships obtained from experimental data actually represent the observed crack propagation behavior.

The raw data from a fatigue crack propagation test are the half crack length, a, and the number of cumulative load cycles, N, needed to

grow the crack to that length from some reference initial crack length for slightly increasing stress intensity level load conditions, called constant amplitude loading. A plot of typical raw fatigue crack propagation data is shown in Figure 1. The current interpretation of this raw data focuses upon the fatigue crack growth rate as a function of an applied stress intensity parameter, usually ΔK, the change of the stress intensity during the load cycle. The fatigue crack growth rate is defined as the rate of extension of the crack with respect to the number of applied load cycles [2]. Actual determination of the crack growth rate requires an evaluation of the slope of the raw a vs. N data at various discrete points, which results in the derivative of a with respect to N, normally called da/dN. A plot of typical da/dN vs. ΔK data is shown in Figure 2.

The importance of the fatigue crack growth rate as a variable of interest is born out in the fact that the fatigue crack growth rate is nearly independent of the geometry for the same stress intensity level of loading [3]. This allows crack growth behavior prediction based only on the knowledge of the crack growth rate vs. the stress intensity level of loading for a given material for any geometry chosen. Obviously, this would be an important design tool if the crack growth behavior predictions were accurate and reliable. These crack growth behavior predictions can be used to predict the number of load cycles needed to grow a crack from an initial crack length, a_0, to some new crack length, a_i, and the distance a crack propagates, Δa, during a specified number of applied load cycles. In addition, using various prediction techniques, the constant amplitude loading crack growth rate behavior is used to predict variable amplitude loading crack growth rate behavior [4].

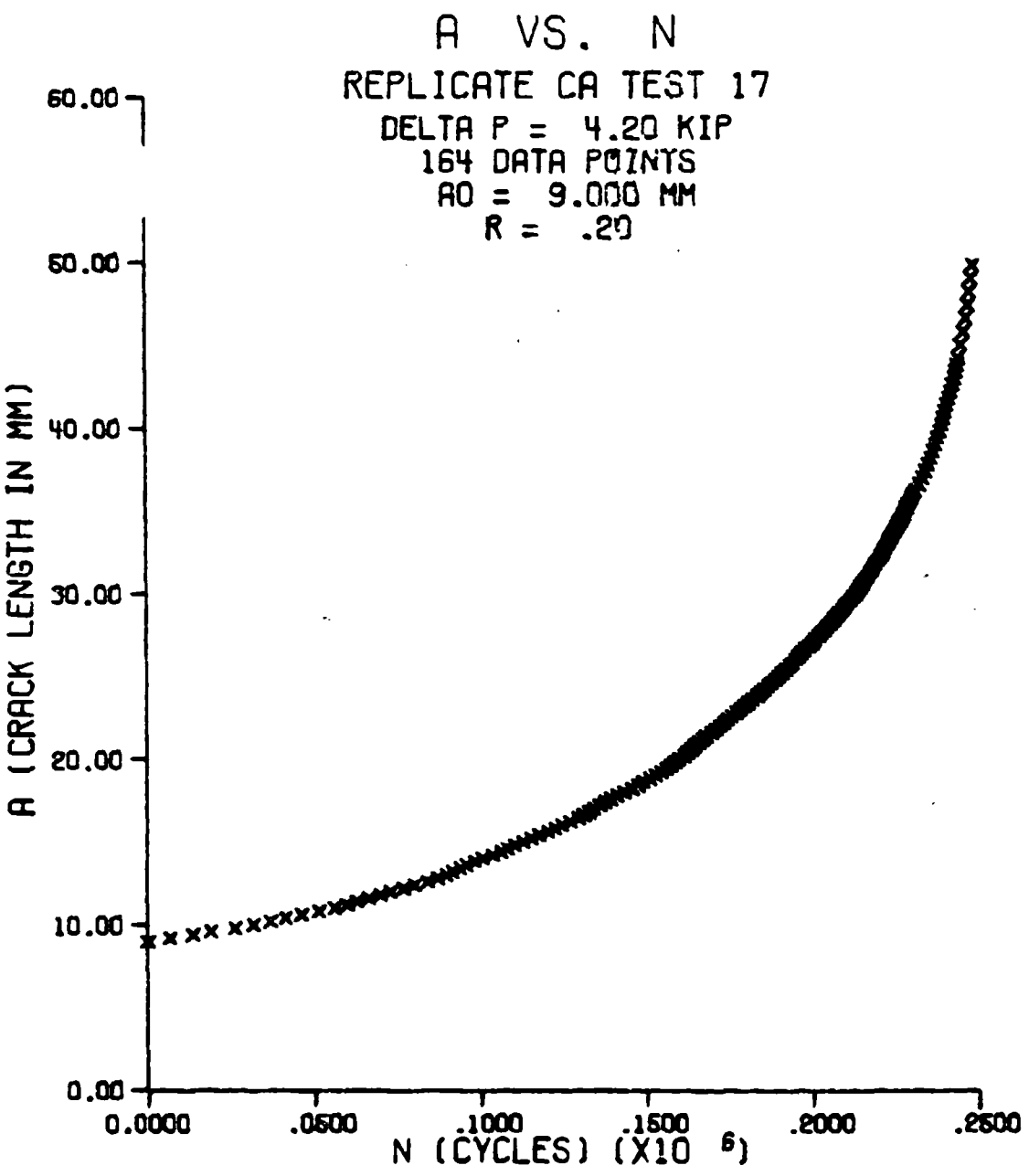

Figure 1. Typical Raw Fatigue Crack Propagation Data

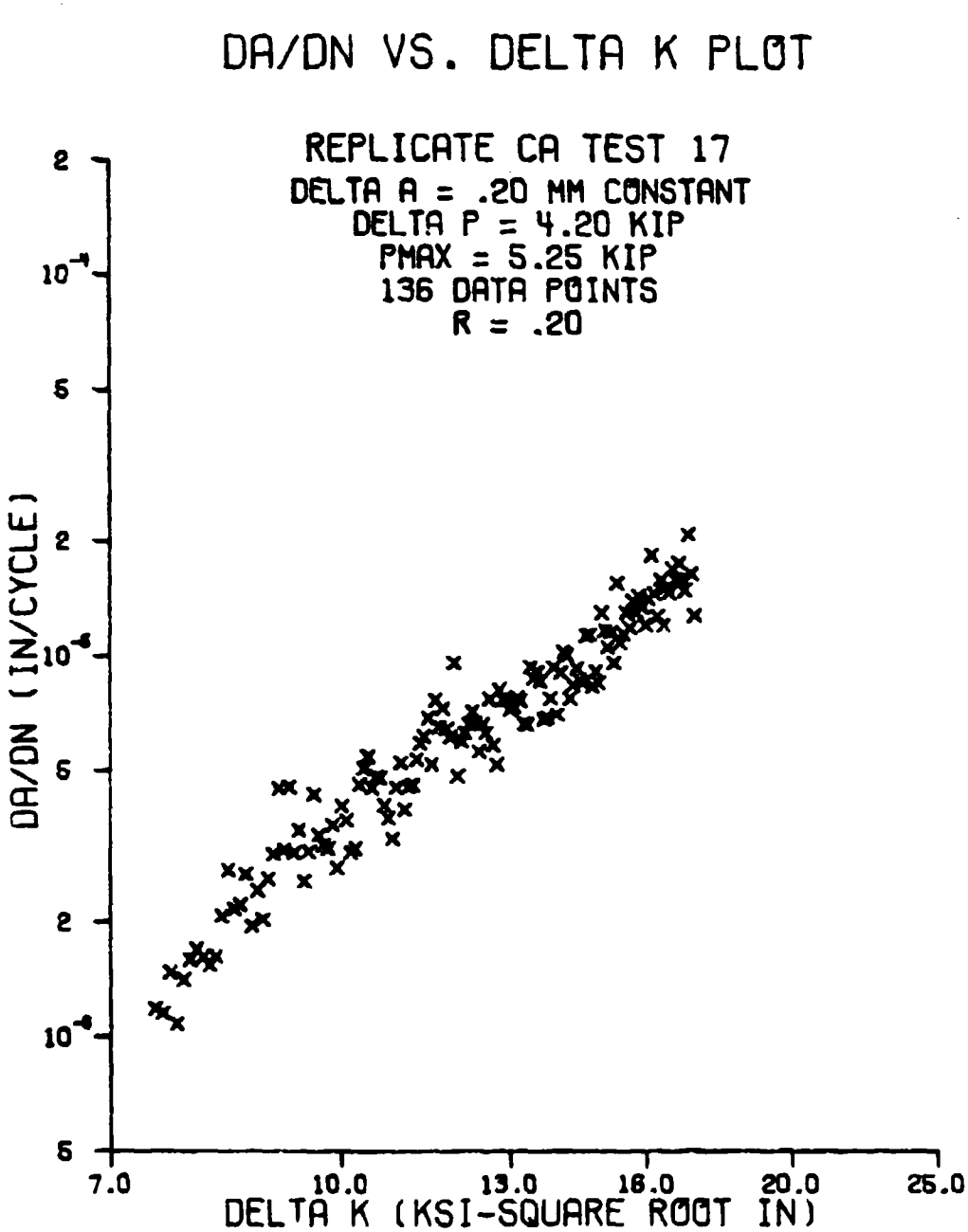

Figure 2. Typical Log_{10} da/dN vs. Log_{10} ΔK Data

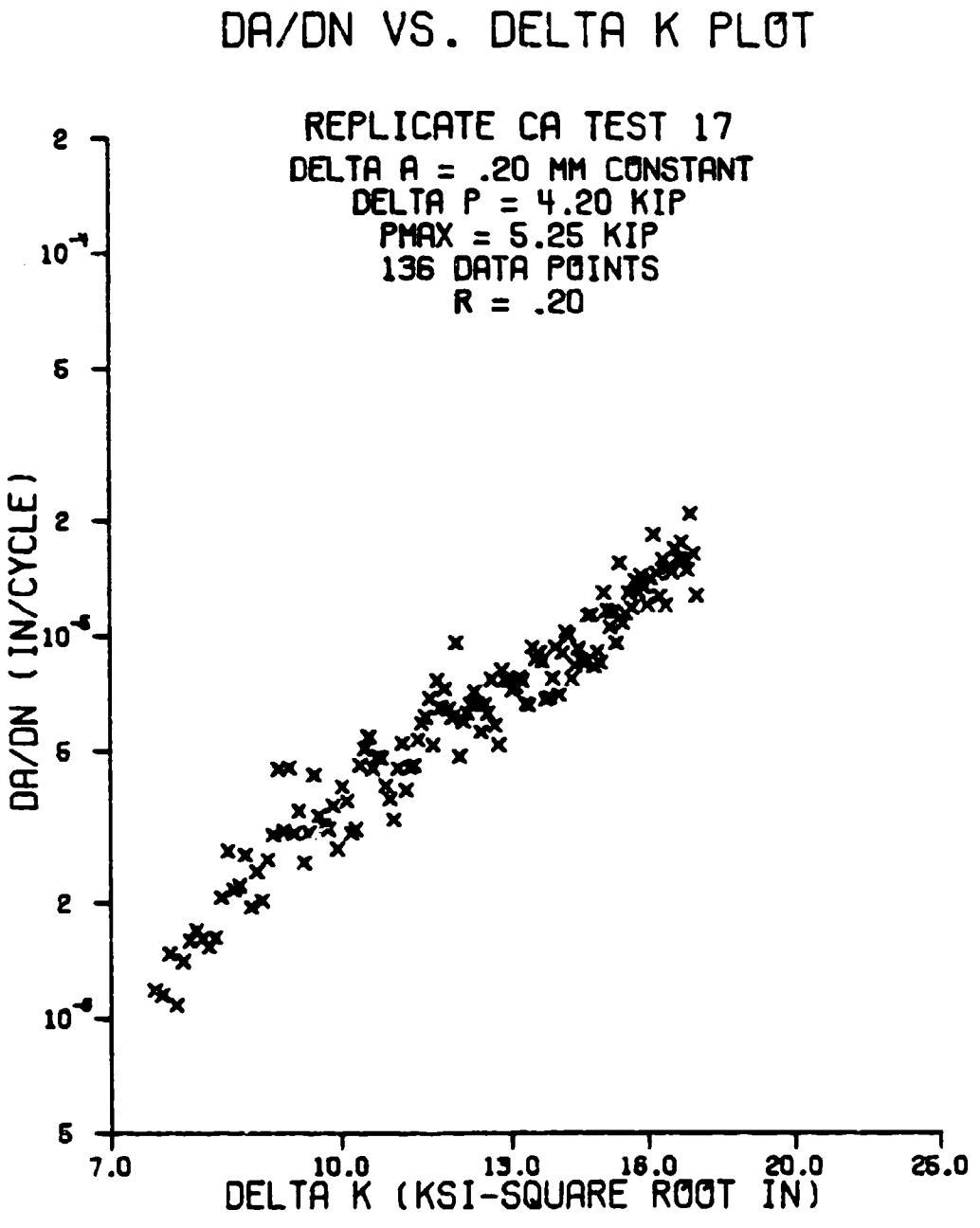

Figure 2. Typical Log_{10} da/dN vs. Log_{10} ΔK Data

There are several methods of numerically determining the crack growth rate from the raw a vs. N data. It has been suspected that the crack growth rate calculation method has a very significant effect on the variance of the resulting growth rate vs. stress intensity parameter data [2,5,6,7].

During the prediction of crack growth behavior, the crack growth rate vs. stress intensity parameter data is integrated back to obtain predicted a vs. N behavior. Considerable variation in this predicted crack growth behavior has been experienced, thus hindering accurate life estimates [2,5,6,7]. This variation is a result of variation in the raw crack growth data, variation due to the crack growth rate calculation method, and material variations.

This investigation will compare several numerical growth rate calculation methods and attempt to find the method which introduces the least amount of error into the growth rate vs. stress intensity parameter data. It will also attempt to describe crack growth behavior in a statistical manner with the expectation that this statistical description of crack growth behavior will reduce the large amount of error currently present in life prediction.

SECTION II

BACKGROUND

Metal fatigue has long been recognized as a random phenomenon [8], but until recently, little effort was devoted to applying statistical tools to fatigue crack propagation behavior. By fitting different equations to the crack growth rate vs. stress intensity parameter data, numerous equations of fatigue crack growth have been suggested [9]. However, due to scatter in the data, it has been impossible to select which equation is the most appropriate. Also, when the original crack growth data are predicted from these equations, the correlation with the original data is generally very poor [8]. Due to the large amount of scatter in the crack growth rate vs. stress intensity parameter data, investigators have started using statistical methods to characterize fatigue crack propagation behavior [5,6,7,8]. It can be easily shown that the amount of data scatter is generally considerably greater than can be accounted for by experimental inaccuracies [8]. It has been pointed out that the remaining scatter is due to the essentially random nature of fatigue crack growth which is a result of the relative nonhomogeneity of the material [8,10].

From a macroscopic viewpoint, it is often convenient to regard a metallic material as a homogeneous continuum, and basing engineering calculations on this assumption does not generally lead to serious error. However, the scatter observed in fatigue testing of a metallic material arises precisely because it is not a homogeneous continuum, when

considered on a microscopic scale [8]. Consequently, it is important to examine fatigue crack growth from a statistical viewpoint. In order to include fatigue crack propagation scatter in the general overall characterization of fatigue crack propagation behavior, this investigation will apply statistical concepts to fatigue crack growth behavior.

In considering the crack growth from some initial crack length, a_0, to a new crack length, a_i, there is a certain mean and variance associated with the number of load cycles required for this amount of crack growth which characterizes the statistical distribution of N at a_i. A schematic representation of this distribution of N is shown in Figure 3. In order to statistically characterize the crack growth behavior, it is necessary to determine the distribution of N from experimental tests.

The variance in N illustrated above can be due to random errors in the measurement of a, N, and ΔK, to systematic errors in these measurements, and to the statistical variation in the material's growth rate properties. Through the use of accurate equipment, the random errors in the measurement of a, N, and ΔK can be reduced to an acceptable level and measured by a separate test. Through a careful experimental set up and procedure, the systematic measurement error can be reduced. From this, the desired statistical behavior of the material's crack growth properties can be determined.

In considering the crack growth rate vs. stress intensity parameter data, there is some statistical distribution associated with the crack growth rate, da/dN, at some stress intensity level, ΔK_i. A schematic representation of this distribution of da/dN is shown in Figure 4. In order to statistically characterize the crack growth rate behavior, it

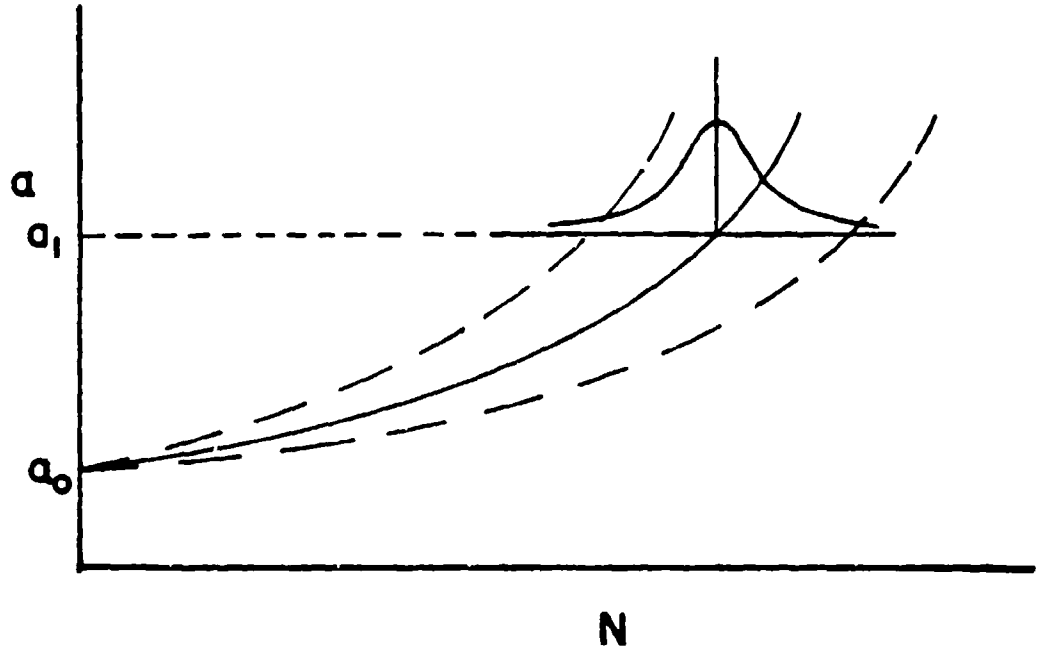

Figure 3. Schematic Representation of the Distribution of N

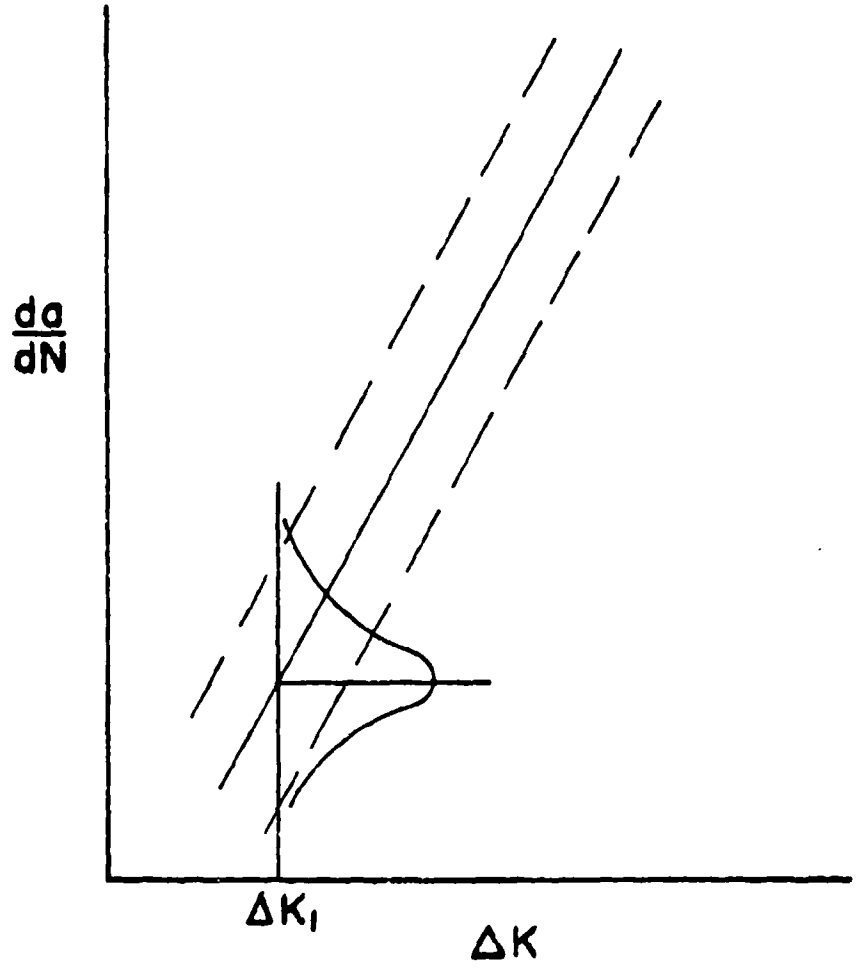

Figure 4. Schematic Representation of the Distribution of da/dN

is also necessary to determine the distribution of the crack growth rate from experimental tests.

The variance of da/dN illustrated above originates in the variance present in the original a vs. N data. The density of the raw data (essentially, the distance between 2 consecutive data points, Δa) and the crack growth rate calculation method both contribute to the overall variance of da/dN. In order to determine the variance of da/dN due to the variance in the original a vs. N data, it is necessary to determine the effect of both data density and the crack growth rate calculation method on the variance of da/dN.

Once the crack growth rate vs. stress intensity parameter data has been obtained, the next step is to be able to predict the change in crack length for a given number of applied load cycles or, inversely, the number of applied load cycles for a given change in crack length. The variance of this prediction is directly related to the variance of the crack growth rate. In order to evaluate the effectiveness of this prediction, it is necessary to predict the original a vs. N data from the crack growth rate data and then compare the predicted a vs. N data with the original a vs. N data.

This a vs. N prediction can be accomplished by either of two methods. The currently popular method is to numerically integrate the mean da/dN vs. ΔK curve to obtain predicted a vs. N data [2,4,5,6,7,9]. However, no adequate method for determining the resulting scatter in a or N exists [5]. An alternate method uses the knowledge of the distribution of da/dN and the fact that da/dN is an independent random variable to obtain a vs. N step by step. This method is discussed in detail in Section 7.3. Using this method, the variances of both a and N can be readily obtained.

SECTION III

OBJECTIVES OF INVESTIGATION

The main purpose of this investigation was to apply statistical concepts and theory to the study of fatigue crack propagation behavior. In doing this, there were four main objectives to be met. They were:

1) Determine the statistical distribution of N (cumulative load cycle count) as a function of a (crack length).
2) Determine which crack growth rate calculation method yields the least amount of error when the crack growth rate curve is integrated back to the original a vs. N data.
3) Determine the statistical distribution of da/dN (crack growth rate) as a function of ΔK (stress intensity parameter.
4) Determine the variance of a set of a vs. N data predicted from the da/dN distribution parameters.

SECTION IV

CRACK GROWTH RATE CALCULATION METHODS

Numerous methods of calculating the crack growth rate from the raw a vs. N data have been used by various investigators [2,5,6]. None of these seem to be universally accepted, but rather each investigator seemed to favor a different method. Since it was virtually impossible to investigate all of these methods, six of the more important methods were selected for examination. These methods are:

1) The secant method,
2) The modified secant method,
3) The linear 7-point incremental polynomial method,
4) The quadratic 7-point incremental polynomial method,
5) The linear log-log 7-point incremental polynomial method, and
6) The quadratic log-log 7-point incremental polynomial method.

4.1 Secant Method

The secant method is a finite difference method and perhaps the simplest of the methods considered [2,5,6]. Basically, the secant method calculates the slope of a straight line between 2 adjacent a vs. N data points. It then approximates this slope as the slope of the tangent line of the a vs. N curve at an average crack length, $\overline{a_i}$, and average cycle count, $\overline{N_i}$. A schematic representation of the secant method is shown in Figure 5.

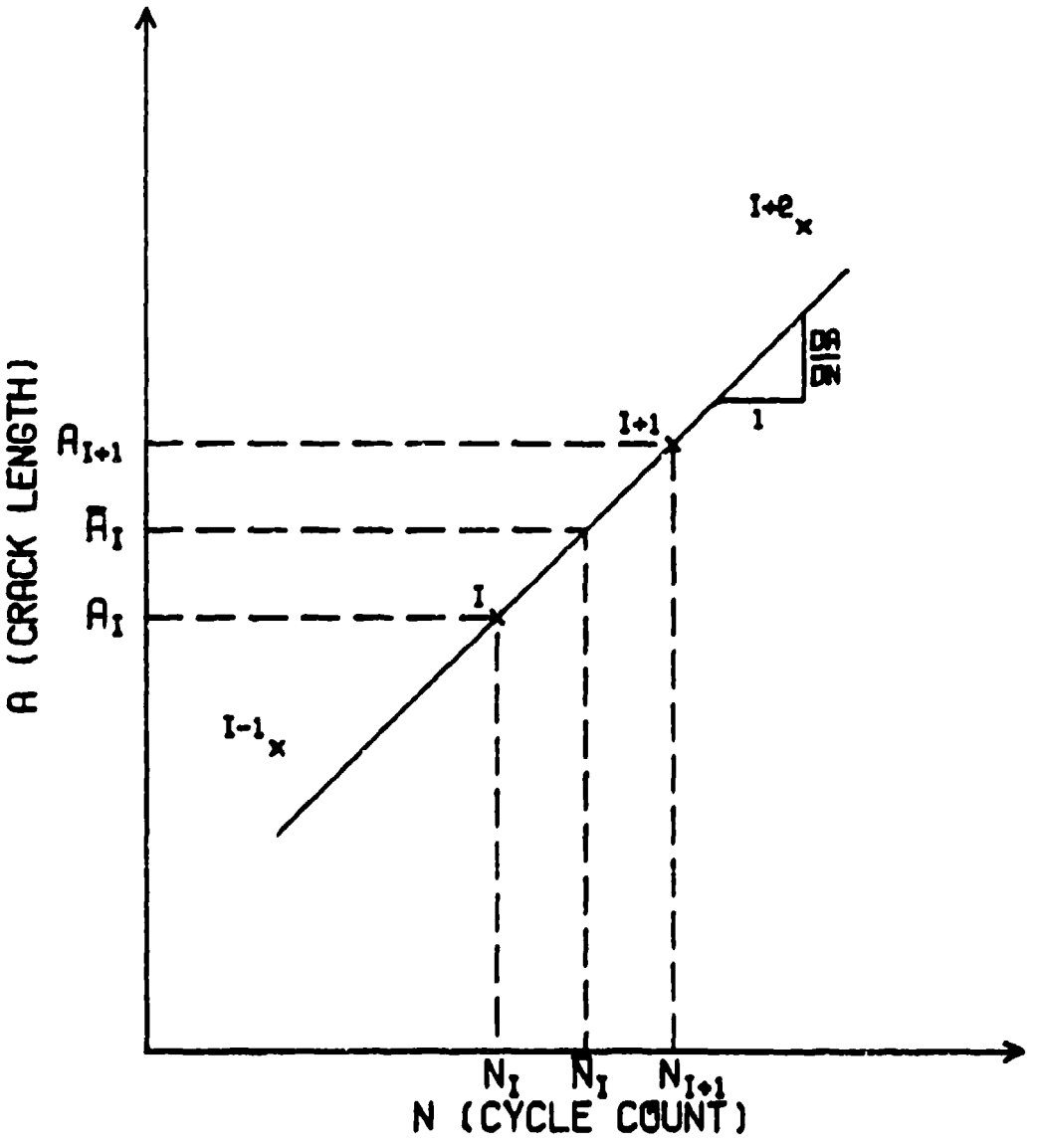

Figure 5. Secant Method

The average crack length, $\overline{a_i}$, is given by

$$\overline{a_i} = \frac{a_i + a_{i+1}}{2} \tag{1}$$

Similarly, the average cycle count, $\overline{N_i}$, is given by

$$\overline{N_i} = \frac{N_i + N_{i+1}}{2} \tag{2}$$

The slope of the line connecting the 2 adjacent data points, which is used to approximate the growth rate, is given by

$$\frac{da}{dN_i} = \frac{(a_{i+1} - a_i)}{(N_{i+1} - N_i)} \tag{3}$$

at $\overline{a_i}$ and $\overline{N_i}$.

4.2 Modified Secant Method

The modified secant method is really an extension of the secant method. Basically, this method averages the growth rates obtained by the secant method so that the da/dN data coincides with the original a vs. N data. The beginning and end points are assumed to be equal to the first and last growth rates, respectively. A schematic representation of the modified secant method is shown in Figure 6.

The growth rate is given by

$$\frac{da}{dN_i} = \frac{\left[\frac{a_i - a_{i-1}}{N_i - N_{i-1}}\right] + \left[\frac{a_{i+1} - a_i}{N_{i+1} - N_i}\right]}{2} \tag{4}$$

at a_i and N_i for i=2 to (n-1) where n is the number of data points in the data set.

The first growth rate data point is given by

$$\frac{da}{dN_1} = \frac{(a_2 - a_1)}{(N_2 - N_1)} \tag{5}$$

at a_1 and N_1.

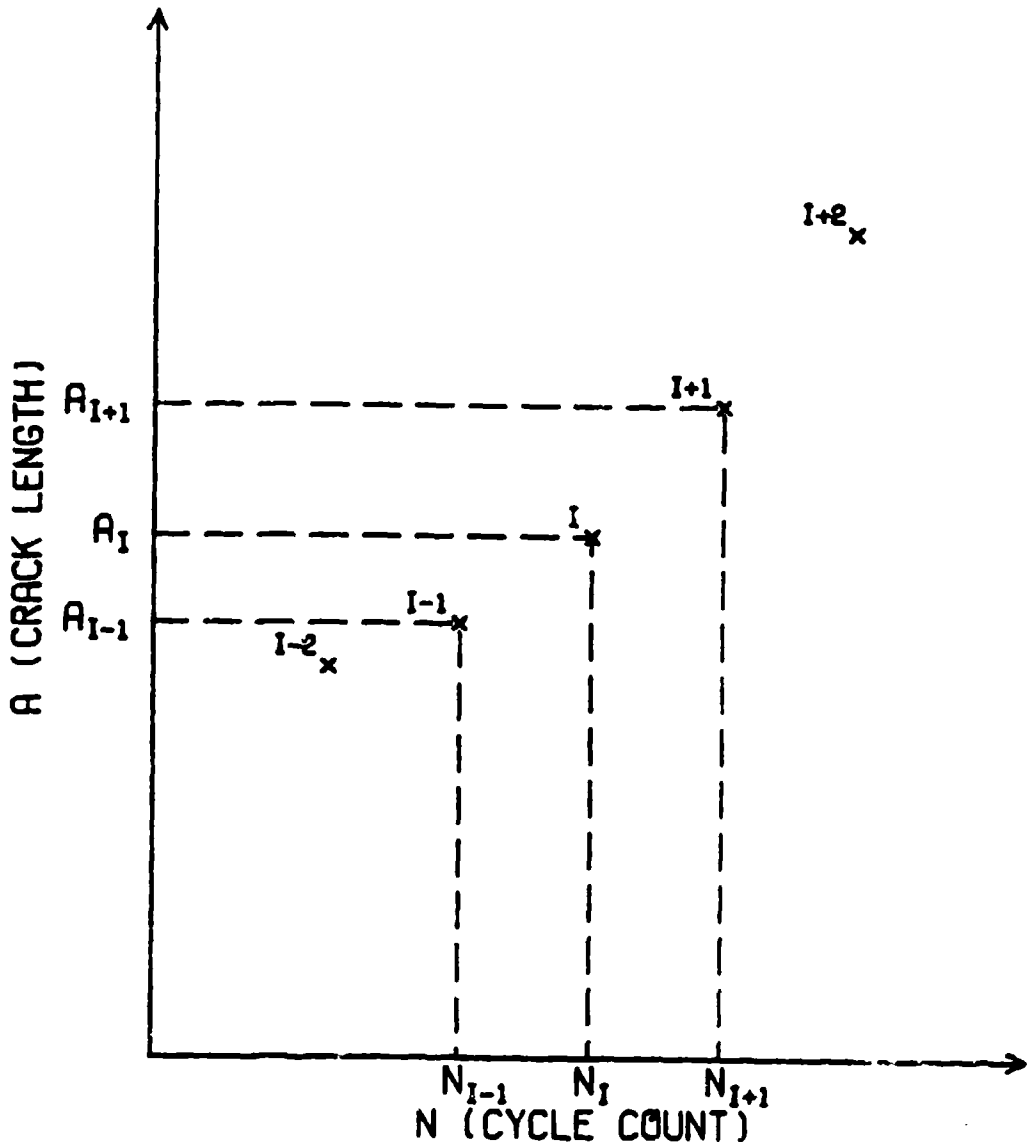

Figure 6. Modified Secant Method

The last growth rate data point is given by

$$\frac{da}{dN_n} = \frac{(a_n - a_{n-1})}{(N_n - N_{n-1})} \tag{6}$$

at a_n and N_n.

4.3 Linear 7-Point Incremental Polynomial Method

The linear 7-point incremental polynomial method is the simplest of the four incremental polynomial methods. In each of the incremental polynomial methods, a polynomial is fit by the method of least squares to a series of data points, called a strip, and the derivative of the polynomial is evaluated at the middle point [2,5,6]. This strip is then incremented by one data point and the curve fitting and evaluation process is repeated. The strip incrementation process is repeated until all of the data points have been used. Any odd number of data points can be used for the incremented strip, although 7 points are usually used. The incremental polynomial methods differ basically in the polynomial which is fit to the data.

Initially the strip data points are scaled in the following manner. Two constants, C_1 and C_2, are calculated as follows [5,6]:

$$C_1 = \frac{N_{i+n_{HS}} + N_{i-n_{HS}}}{2} \tag{7}$$

$$C_2 = \frac{N_{i+n_{HS}} - N_{i-n_{HS}}}{2} \tag{8}$$

where

$$n_{HS} = \frac{n_{strip} - 1}{2} \tag{9}$$

where n_{strip} is the number of data points in the strip. Note that C_1 is the center of the strip cycle count data and C_2 is the range of the strip

cycle count data. The data scaling is then performed as follows:

$$N_S = \frac{N - C_1}{C_2} \tag{10}$$

where N_S is the scaled cycle count data. As a result of this scaling, the strip cycle count data runs from -1 to +1. This insures that when least squares curve fitting occurs, the scale of the data will not influence the curve fitting, which is a constant danger when using least squares as a curve fitting technique.

After the curve fitting has been performed, the derivative of the resulting polynomial is then evaluated at the midpoint of the strip, N_1. This evaluation takes into account the scaling that was performed prior to the curve fitting. A schematic representation of the incremental polynomial method is shown in Figure 7.

In the linear 7-point incremental polynomial method, the fitted polynomial is a first order linear straight line. After fitting by linear least squares, the fitted polynomial takes the following form:

$$a = b_o + b_1 N_S \tag{11}$$

Substituting the scaling equation,

$$a = \left[b_o - \frac{b_1 C_1}{C_2}\right] + \left[\frac{b_1}{C_2}\right] N \tag{12}$$

Taking the derivative of a with respect to N,

$$\frac{da}{dN} = \frac{b_1}{C_2} \tag{13}$$

Obviously, for a straight line, the slope is independent of where the derivative is evaluated at.

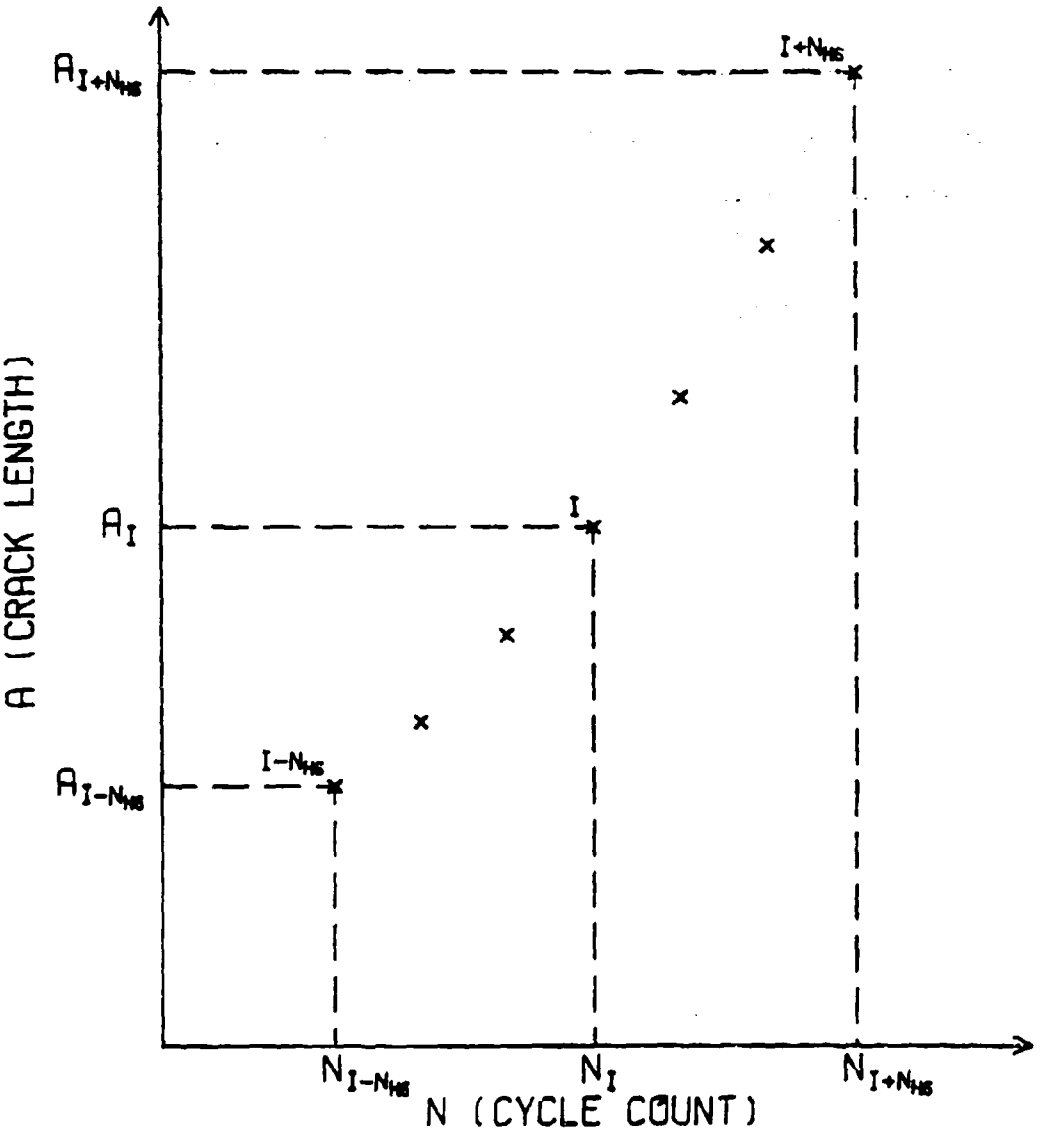

Figure 7. Incremental Polynomial Method

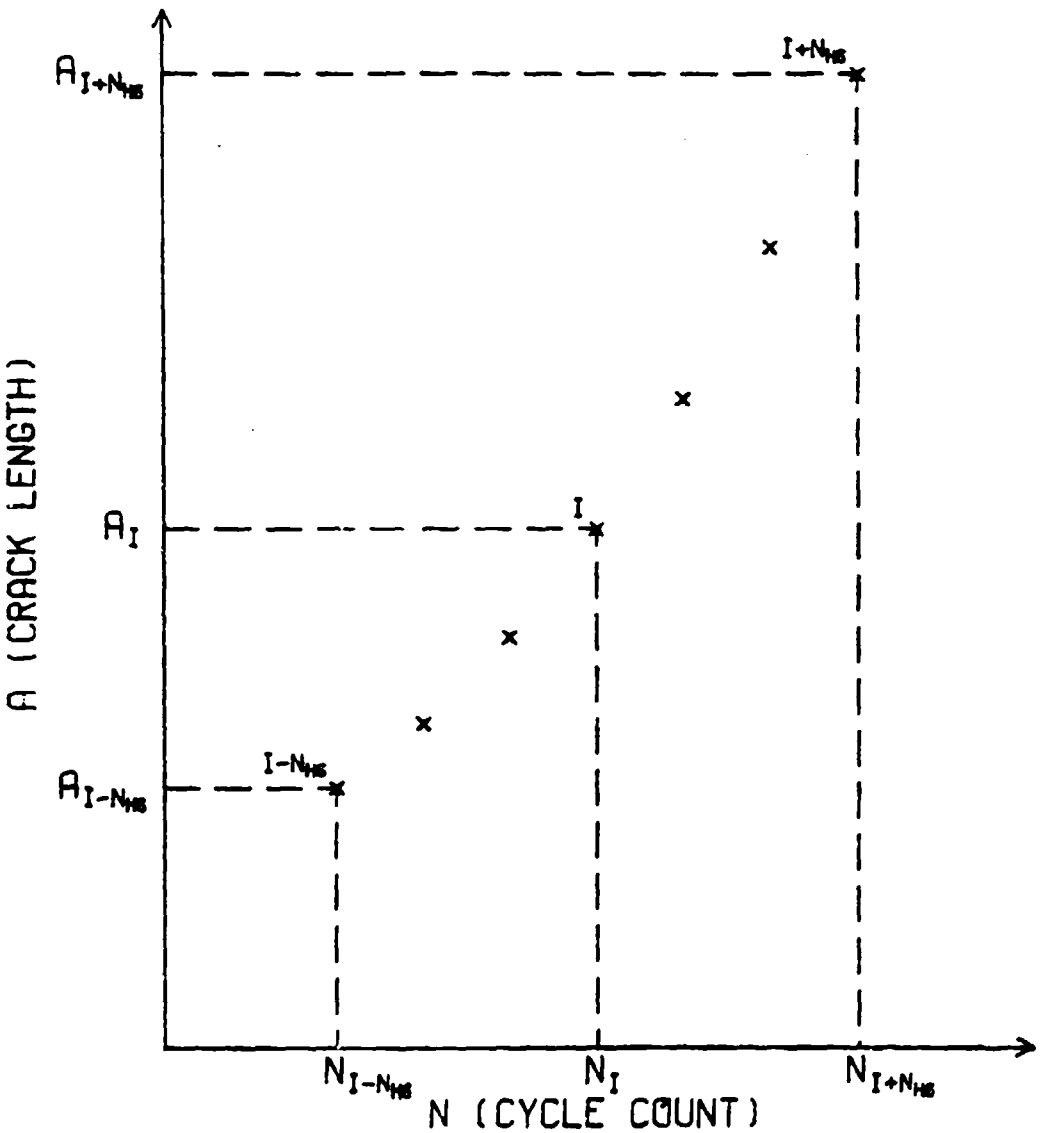

Figure 7. Incremental Polynomial Method

4.4 Quadratic 7-Point Incremental Polynomial Method

The quadratic 7-point incremental polynomial method has gained wide acceptance as a valid crack growth rate calculation method [5,6]. In this method, the fitted polynomial is a second order curve. After fitting by second order least squares, the fitted polynomial takes the following form:

$$a = b_o + b_1 N_S + b_2 N_S^2 \tag{14}$$

Substituting the scaling equation,

$$a = \left[b_o - \frac{b_1 C_1}{C_2} + \frac{b_2 C_1^2}{C_2^2}\right] + \left[\frac{b_1}{C_2} - \frac{2b_2 C_1}{C_2^2}\right] N + \left[\frac{b_2}{C_2^2}\right] N^2 \tag{15}$$

Taking the derivative of a with respect to N and evaluating at the mid-point, N_i,

$$\frac{da}{dN_i} = \left[\frac{b_1}{C_2} - \frac{2b_2 C_1}{C_2^2}\right] + \left[\frac{2b_2}{C_2^2}\right] N_i \tag{16}$$

4.5 Linear Log-Log 7-Point Incremental Polynomial Method

The linear log-log 7-point incremental polynomial method was used to determine if the data could be linearized by a $\log_{10}$ transformation on both the crack length and cycle count data. This method is essentially the same as the linear incremental polynomial method except for the log transformations of the input data just prior to the data scaling.

The fitted polynomial is linear and takes the following form:

$$\log a = b_o + b_1 N_{LS} \tag{17}$$

where N_{LS} is the log scaled cycle count data.

4.4 Quadratic 7-Point Incremental Polynomial Method

The quadratic 7-point incremental polynomial method has gained wide acceptance as a valid crack growth rate calculation method [5,6]. In this method, the fitted polynomial is a second order curve. After fitting by second order least squares, the fitted polynomial takes the following form:

$$a = b_o + b_1 N_S + b_2 N_S^2 \tag{14}$$

Substituting the scaling equation,

$$a = \left[b_o - \frac{b_1 C_1}{C_2} + \frac{b_2 C_1^2}{C_2^2}\right] + \left[\frac{b_1}{C_2} - \frac{2b_2 C_1}{C_2^2}\right] N + \left[\frac{b_2}{C_2^2}\right] N^2 \tag{15}$$

Taking the derivative of a with respect to N and evaluating at the mid-point, N_i,

$$\frac{da}{dN_i} = \left[\frac{b_1}{C_2} - \frac{2b_2 C_1}{C_2^2}\right] + \left[\frac{2b_2}{C_2^2}\right] N_i \tag{16}$$

4.5 Linear Log-Log 7-Point Incremental Polynomial Method

The linear log-log 7-point incremental polynomial method was used to determine if the data could be linearized by a $\log_{10}$ transformation on both the crack length and cycle count data. This method is essentially the same as the linear incremental polynomial method except for the log transformations of the input data just prior to the data scaling.

The fitted polynomial is linear and takes the following form:

$$\log a = b_o + b_1 N_{LS} \tag{17}$$

where N_{LS} is the log scaled cycle count data.

$$\frac{da}{dN_i} = 10^{\left[\frac{b_o - b_1 C_1}{C_2}\right]} \cdot \frac{b_1 N_i}{C_2} \left[\frac{b_1}{C_2} - 1\right] \tag{18}$$

The derivation of this equation is shown in Appendix A.

4.6 Quadratic Log-Log 7-Point Incremental Polynomial Method

The quadratic log-log 7-point incremental polynomial method was used to determine if a second order curve fit could improve the performance of the linear log-log 7-point incremental polynomial method. This method is essentially the same as the linear log-log 7-point incremental polynomial method except that the fitted polynomial is second order instead of first order.

The fitted polynomial takes the following form:

$$\log a = b_o + b_1 N_{LS} + b_2 N_{LS}^2 \tag{19}$$

The growth rate, da/dN, for this method, evaluated at the midpoint, N_1, is given by

$$\frac{da}{dN_i} = \frac{10^{b_o} \cdot 10^{\left[\frac{b_1 \log N_i}{C_2} - \frac{b_1 C_1}{C_2}\right]} \cdot 10^{\left[\frac{b_2 (\log N_i)^2 - 2b_2 C_1 \log N_i + b_2 C_1^2}{C_2^2}\right]}}{C_2 N_i} \cdot \left[\frac{2b_2 \log N_i - 2b_2 C_1}{C_2} + b_1\right] \tag{20}$$

The derivation of this equation is shown in Appendix B.

SECTION V

STATISTICAL CONCEPTS

When used properly, statistics is extremely useful in quantifying the results of many engineering experiments. In many applications, however, statistics is used as a quick substitute for a thorough experimental analysis and often times it is used without checking the underlying assumptions or else the results are misinterpreted. In an attempt to alleviate these problems, the statistical concepts used in this investigation and their use as tools in analyzing fatigue crack growth behavior will be presented and discussed.

5.1 Histograms

The first step in statistically analyzing any set of data is to see what the data looks like. Histograms are statistically derived pictures of a data set. They give a rough idea of the shape of the density function of the data. They also give a rough estimate of the average value and the amount of variability present in the data.

The most common histogram used is a frequency histogram. The data is divided into several classes and the frequency of the data in each class is plotted against the limits of the classes [11]. This type of histogram frequently takes the form of a bar chart. A slight modification of this involves calculating the relative frequencies in each class by dividing the frequency in each class by the total number of data points. The relative frequencies are then plotted against the limits of the classes.

This is called a relative frequency histogram [12]. An example of a relative frequency histogram is shown in Figure 8.

Another convenient form of the histogram is called a cumulative frequency histogram. This histogram shows the frequency of data less than or equal to a specified value. It is calculated by cumulatively adding successive class frequencies of the frequency histogram from the smallest class value to the largest class value. It frequently takes the form of a step chart. Again, the relative cumulative frequencies can be calculated by dividing the cumulative frequencies by the total number of data points so that the last value of the relative cumulative frequency is equal to one. When the relative cumulative frequencies are plotted against the limits of the classes, the resulting plot is called a relative cumulative frequency histogram [12]. An example of a relative cumulative frequency histogram is shown in Figure 9.

5.2 Distributions

Once a rough idea of what the density function of the data looks like based on the histograms, the next step is to try to fit the data to several likely distributions. Eight different distributions were selected as likely candidates for the distribution of fatigue crack propagation variables.

5.2.a Two-Parameter Normal Distribution

The most widely used distribution in statistics is the two-parameter normal distribution [12]. This distribution was selected as a candidate for the distribution of fatigue crack propagation variables mainly for this reason and for the sake of completeness.

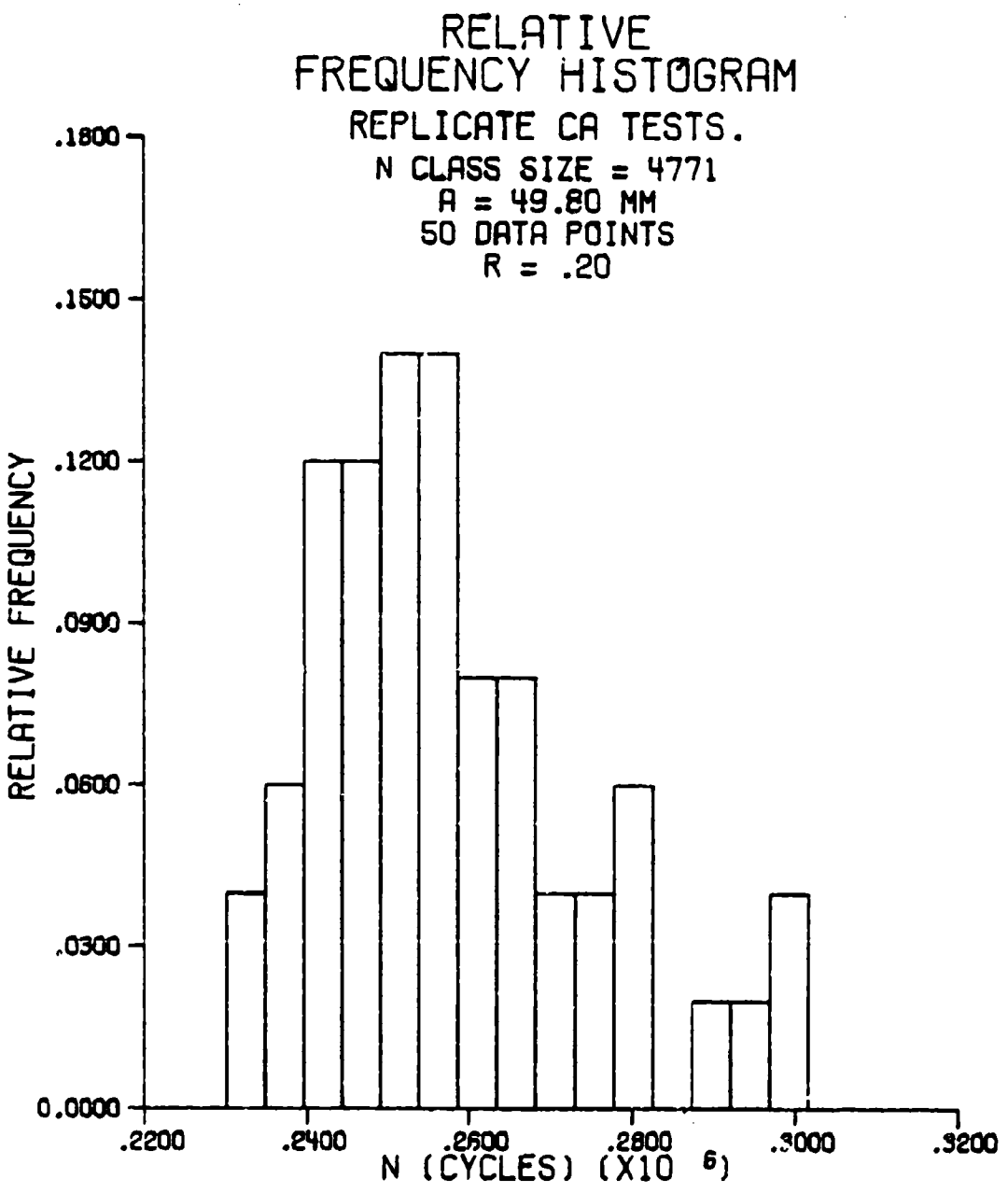

Figure 8. Typical Relative Frequency Histogram

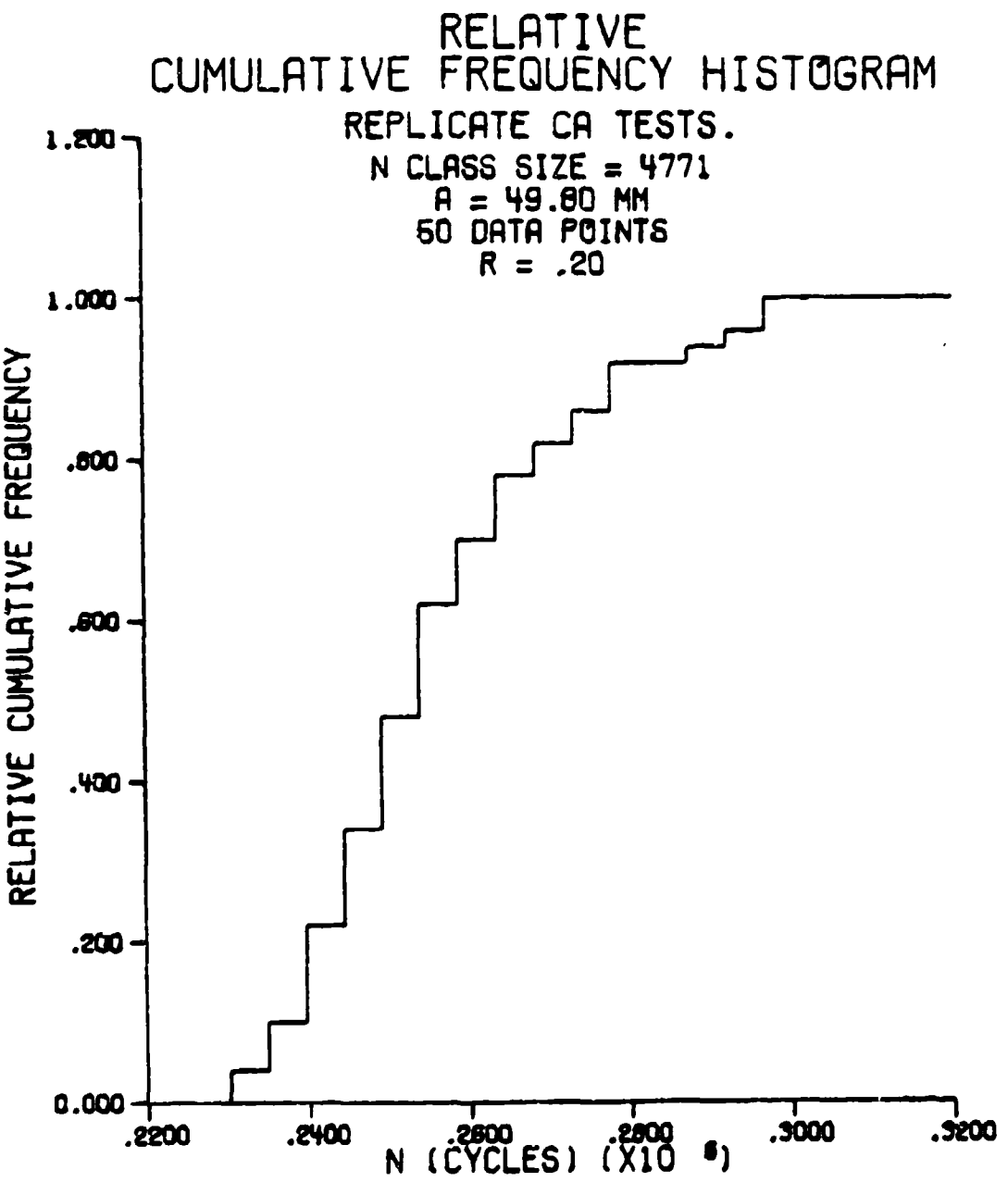

Figure 9. Typical Relative Cumulative Frequency Histogram

The two parameters of the two-parameter normal distribution are the mean, designated by μ, which is the scale parameter, and the standard deviation, designated by σ, which is the shape parameter. The density function, $f(\chi)$, for the two-parameter normal distribution is given by [11,12].

$$f(\chi) = \frac{1}{\sigma\sqrt{2\pi}} \exp\left[-\frac{1}{2}\left(\frac{\chi-\mu}{\sigma}\right)^2\right], \quad \begin{matrix} -\infty < \chi < \infty \\ -\infty < \mu < \infty \\ 0 < \sigma < \infty \end{matrix} \tag{21}$$

The estimates for the mean and standard deviation are computed by [11,12]

$$\hat{\mu} = \frac{\sum_{i=1}^{n} \chi_i}{n} \tag{22}$$

$$\hat{\sigma} = \sqrt{\frac{\sum_{i=1}^{n} (\chi_i - \hat{\mu})^2}{n}} \tag{23}$$

Where n is the number of data points and the symbol $\hat{}$ symbolizes an estimated value.

The standard errors of the estimates provide a measure of how good these estimates are. The standard errors of the estimated mean and standard deviation are given by [13]

$$S.E.\ \hat{\mu} = \sqrt{\frac{\hat{\sigma}^2}{n}} \tag{24}$$

$$S.E.\ \hat{\sigma} = \sqrt{\frac{\hat{\sigma}^2}{n}\left[(n-1) - 2.\left\{\frac{\Gamma\left(\frac{n}{2}\right)}{\Gamma\left(\frac{n-1}{2}\right)}\right\}^2\right]} \tag{25}$$

where Γ represents the gamma function. The covariance of $\hat{\mu}$ with $\hat{\sigma}$ is always equal to zero, due to their orthogonality [13].

5.2.b Two-Parameter Log Normal Distribution

The two-parameter log normal distribution has been suspected of being a likely candidate for the distribution of fatigue crack propagation

variables [5,6]. Essentially, the two-parameter log normal distribution states that the $\log_{10}$ of the random variable χ, i.e., $\log_{10}\chi$, is normally distributed.

The two parameters of the two-parameter log normal distribution are μ, the scale parameter, and β, the shape parameter. The density function for the two-parameter log normal distribution is given by [14,15]

$$f(\chi) = \frac{1}{\chi\sqrt{2\pi\beta}} \exp\left[-\frac{1}{2\beta}\left\{\log_{10}\chi - \mu\right\}^2\right], \begin{array}{l}\chi > 0 \\ -\infty < \mu < \infty \\ 0 < \beta < \infty\end{array} \qquad (26)$$

The estimates for μ and β are computed by using the following equations [14]

$$\hat{\mu} = \frac{\sum_{i=1}^{n} \log_{10}\chi_i}{n} \qquad (27)$$

$$\hat{\beta} = \frac{\sum_{i=1}^{n} (\log_{10}\chi_i - \hat{\mu})^2}{n} \qquad (28)$$

The standard errors of these estimates are given by the following equations [13,14].

$$\text{S. E. } \hat{\mu} = \sqrt{\frac{\hat{\beta}}{n}} \qquad (29)$$

$$\text{S. E. } \hat{\beta} = \sqrt{\frac{2(n-1)\,\hat{\beta}^2}{n^2}} \qquad (30)$$

The covariance of $\hat{\mu}$ with $\hat{\beta}$ is again always equal to zero, due to their orthogonality [13].

5.2.c Three-Parameter Log Normal Distribution

With the expectation of a better fit of the data, the three-parameter log normal distribution was considered as a candidate for the distribution of fatigue crack propagation variables. The main difference between

the two-parameter and the three-parameter log normal distributions is the inclusion of the location parameter in the three-parameter log normal distribution.

The three parameters of the three-parameter log normal distribution are μ, the scale parameter, β, the shape parameter, and the terminus, τ, which is the location parameter. The density function for the three-parameter log normal distribution is given by [14,15]

$$f(\chi) = \frac{1}{(\chi-\tau)\sqrt{2\pi\beta}} \exp\left[-\frac{1}{2\beta}\left\{\log_{10}(\chi-\tau) - \mu\right\}^2\right], \quad \begin{matrix} -\infty < \mu < \infty \\ 0 < \beta < \infty \\ -\infty < \tau < \chi \end{matrix} \tag{31}$$

The difficulty in using distributions containing a location parameter is the estimation of that location parameter. The parameter estimation methods used to obtain the value of the location parameter are presented in Section 5.3.

Once the location parameter, τ, has been estimated, μ and β are estimated using the following equations [15].

$$\hat{\mu} = \frac{\sum_{i=1}^{n} \log_{10}(\chi_i - \tau)}{n} \tag{32}$$

$$\hat{\beta} = \frac{\sum_{i=1}^{n} \left[\log_{10}(\chi_i - \tau) - \hat{\mu}\right]^2}{n} \tag{33}$$

To obtain the standard errors of the estimates and the covariance values, the covariance matrix for the three-parameter log normal distribution is computed. The covariance matrix is a symmetric matrix and is given by [16]

$$V = C_V \begin{bmatrix} \hat{\mu} & \hat{\beta} & \tilde{\tau} \\ (\hat{\beta}+1)\exp(\hat{\beta}) - 2\hat{\beta} & -2\hat{\beta} & -\exp\left[\hat{\mu} - \frac{\hat{\beta}}{2}\right] \\ & 2\hat{\beta}\left[(\hat{\beta}+1)\exp(\hat{\beta}) - 1\right] & 2\hat{\beta}\exp\left[\hat{\mu} - \frac{\hat{\beta}}{2}\right] \\ & & \exp\left[2\hat{\mu} - \hat{\beta}\right] \end{bmatrix} \quad (34)$$

where

$$C_V = \frac{\hat{\beta}}{n\left[(\hat{\beta}+1)\exp(\hat{\beta}) - 2\hat{\beta} - 1\right]} \quad (35)$$

The standard errors of the estimates are given by the diagonal terms and the covariances between the estimates are given by the off-diagonal terms of the 3 by 3 covariance matrix.

5.2.d Three-Parameter Weibull Distribution

The three-parameter Weibull distribution has long been considered in representing fatigue data [17]. For this reason, the three-parameter Weibull distribution was considered as a candidate for the distribution of fatigue crack propagation variables. This distribution also includes the location parameter as one of its three parameters and thus the difficulty of its estimation arises. Two basic methods were used to estimate the parameters (Section 5.3) and each method required different parameters. Thus, two sets of Weibull parameters and their associated equations will be presented.

The first set of the three parameters of the three-parameter Weibull distribution include the characteristic value, θ, which is the scale parameter, the Weibull slope, B, which is the shape parameter, and the expected minimum value of χ, χ_o, which is the location parameter. The density function for these parameters is given by [18]

$$f(\chi) = \left[\frac{B}{\theta-\chi_o}\left(\frac{\chi-\chi_o}{\theta-\chi_o}\right)^{B-1}\right] \exp\left\{-\left(\frac{\chi-\chi_o}{\theta-\chi_o}\right)^{B}\right\}, \quad \begin{matrix} 0 < \theta < \infty \\ 0 < B < \infty \\ -\infty < \chi_o < \chi \end{matrix} \tag{36}$$

In the method of estimating the location parameter used with this set of parameters, all three parameters are estimated simultaneously.

The second set of three parameters of the three-parameter Weibull distribution include b, the scale parameter, c, the shape parameter, and the terminus, τ, which is the location parameter. The two sets of parameters are related as follows.

$$b = \theta - \chi_o \tag{37}$$

$$c = B \tag{38}$$

$$\tau = \chi_o \tag{39}$$

The density function for the second set of parameters is given by [19]

$$f(\chi) = c(\chi-\tau)^{c-1}.b^{-c}.\exp\left\{-\left[\frac{(\chi-\tau)}{b}\right]^{c}\right\}, \quad \begin{matrix} 0 < b < \infty \\ 0 < c < \infty \\ -\infty < \tau < \chi \end{matrix} \tag{40}$$

As with the previous set of parameters, all three parameters are estimated simultaneously when the location parameter is estimated. To obtain the standard errors of the estimates obtained by the method referred to above and the covariance values, the covariance matrix for the three-parameter Weibull distribution is computed. The covariance matrix is a symmetric matrix and is given by [13]

$$V = v^{-1} \tag{41}$$

where

$$V = \begin{bmatrix} & \hat{b} & \hat{c} & \hat{\tau} \\ \hat{b} & \dfrac{\pi^2}{6} - (1-\gamma)^2 & \dfrac{\gamma-1}{\hat{b}} & \dfrac{1}{\hat{b}}\left[\dfrac{1}{\hat{c}}\,\Gamma(1-\dfrac{1}{\hat{c}}) - \psi\,(2-\dfrac{1}{\hat{c}})\right] \\ \hat{c} & \dfrac{\hat{c}^2}{\hat{b}^2} & \dfrac{\hat{c}(\hat{c}-1)}{\hat{b}^2}\,\Gamma(1-\dfrac{1}{\hat{c}}) & \\ \hat{\tau} & & \dfrac{(\hat{c}-1)^2}{\hat{b}^2}\,\Gamma(1-\dfrac{2}{\hat{c}}) & \end{bmatrix} \qquad (42)$$

where γ is Eulers Constant (0.577215) and ψ represents the digamma function.

Once the covariance matrix is obtained, the standard errors of the estimates and the covariances between the estimates are obtained from the same terms in the covariance matrix as outlined above for the three-parameter log normal distribution.

5.2.2 Gamma Distribution

Due to the nature of the fatigue crack propagation process, two important assumptions can be made. The first assumption, called the increasing failure rate assumption, states that because the crack growth rate increases as the crack grows (under constant amplitude conditions), the rate, or probability, of failure increases as the crack grows. The second assumption states that the distribution of a fatigue crack propagation variable is independent of the crack length and is a function of the initial crack length only. If these two assumptions are made, then it can be proven that a generalized gamma distribution is a valid distribution for any fatigue crack propagation variable [13,20].

Generalized Four-Parameter Gamma Distribution. The four parameters of the generalized four-parameter gamma distribution are the location parameter, τ, the power parameter, α, the scale parameter, b, and the shape/power parameter, g. The shape parameter, c, is given simply by [21]

$$c = g\,\alpha \tag{43}$$

The density function for the generalized four-parameter gamma distribution is given by [21]

$$f(\chi) = \frac{\alpha(\chi-\tau)^{g\alpha-1}}{b^{g\alpha}\,\Gamma(g)} \exp\left[-\left\{\frac{\chi-\tau}{b}\right\}^{\alpha}\right], \quad \begin{array}{l}\chi \geq \tau \\ \alpha \geq 1 \\ b \geq 0 \\ g \geq 1\end{array} \tag{44}$$

All four parameters are estimated simultaneously using the parameter estimation methods presented in Section 5.3. To obtain the standard erros of the estimates and the covariances between the estimates the covariance matrix for the generalized four-parameter gamma distribution is computed. The covariance matrix is a symmetric matrix and is given by [13,21,22]

$$V = \frac{1}{n} v^{-1} \tag{45}$$

where

$$v = \begin{bmatrix} \hat{b} & \hat{g} & \hat{\alpha} & \hat{\tau} \\ \frac{\hat{g}\hat{\alpha}^2}{\hat{b}^2} & \frac{\hat{\alpha}}{\hat{b}} & \frac{[1+\hat{g}\,\psi(\hat{g})]}{\hat{b}} & \frac{\hat{\alpha}^2\left(\hat{g}-\frac{1}{\hat{\alpha}}\right)\Gamma\left(\hat{g}-\frac{1}{\hat{\alpha}}\right)}{\hat{b}^2} \\ & \psi'(\hat{g}) & \frac{\psi(\hat{g})}{\hat{\alpha}} & \frac{\hat{\alpha}\,\Gamma\left(\hat{g}-\frac{1}{\hat{\alpha}}\right)}{\hat{b}\,\Gamma(\hat{g})} \\ & & \frac{[1+2\psi(\hat{g})+\hat{g}[\psi'(\hat{g})-\psi^2(\hat{g})]]}{\hat{\alpha}^2} & \frac{\Gamma\left(\hat{g}-\frac{1}{\hat{\alpha}}\right)}{\hat{b}\,\Gamma(\hat{g})}\left[\frac{1}{\hat{\alpha}}-\left(\hat{g}-\frac{1}{\hat{\alpha}}\right)\cdot\psi\left(\hat{g}+1-\frac{1}{\hat{\alpha}}\right)\right] \\ & & & \frac{\Gamma\left(\hat{g}-\frac{2}{\hat{\alpha}}\right)}{\hat{b}^2\,\Gamma(\hat{g})}\left[\hat{g}\hat{\alpha}^2-2\hat{\alpha}+1\right] \end{bmatrix} \tag{46}$$

where ψ' represents the trigamma function.

The standard errors of the estimates are given by the diagonal terms and the covariances between the estimates are given by the off-diagonal terms of the 4 by 4 covariance matrix.

Three-Parameter Gamma Distribution. If the power parameter, α, is assumed to be equal to one, the generalized four-parameter gamma distribution reduces to the three-parameter gamma distribution. The density function for the three-parameter gamma distribution is given by [21,23]

$$f(\chi) = \frac{(\chi-\tau)^{g-1}}{b^g \Gamma(g)} \left[- \frac{(\chi-\tau)}{b} \right] \quad , \quad \begin{matrix} \chi \geq \tau \\ b \geq 0 \\ g \geq 1 \end{matrix} \tag{47}$$

The three parameters are estimated using the same method used for the generalized four-parameter gamma distribution. The standard errors and covariances are found by using the covariance matrix for the generalized four-parameter gamma distribution (equations 45 and 46) and setting α equal to one.

Generalized Three-Parameter Gamma Distribution. If the fatigue crack propagation variable of interest is $\Delta N/\Delta a$, then considering the fatigue crack propagation process it would be expected that ΔN would be zero for Δa zero [24]. From this, it is assumed that the location parameter, γ, is equal to zero which reduces the generalized four-parameter gamma distribution to the generalized three-parameter gamma distribution. The density function for the generalized three-parameter gamma distribution is thus [23]

$$f(\chi) = \frac{a(\chi)^{ga-1}}{b^{ga} \Gamma(g)} \exp\left[-(\frac{\chi}{b})^a \right] \quad , \quad \begin{matrix} \chi \geq 0 \\ a \geq 1 \\ b \geq 0 \\ g \geq 1 \end{matrix} \tag{49}$$

The standard errors of the estimates are given by the diagonal terms and the covariances between the estimates are given by the off-diagonal terms of the 4 by 4 covariance matrix.

Three-Parameter Gamma Distribution. If the power parameter, α, is assumed to be equal to one, the generalized four-parameter gamma distribution reduces to the three-parameter gamma distribution. The density function for the three-parameter gamma distribution is given by [21,23]

$$f(\chi) = \frac{(\chi-\tau)^{g-1}}{b^g \Gamma(g)} \left[-\frac{(\chi-\tau)}{b} \right] \quad , \quad \begin{matrix} \chi \geq \tau \\ b \geq 0 \\ g \geq 1 \end{matrix} \tag{47}$$

The three parameters are estimated using the same method used for the generalized four-parameter gamma distribution. The standard errors and covariances are found by using the covariance matrix for the generalized four-parameter gamma distribution (equations 45 and 46) and setting α equal to one.

Generalized Three-Parameter Gamma Distribution. If the fatigue crack propagation variable of interest is $\Delta N/\Delta a$, then considering the fatigue crack propagation process it would be expected that ΔN would be zero for Δa zero [24]. From this, it is assumed that the location parameter, γ, is equal to zero which reduces the generalized four-parameter gamma distribution to the generalized three-parameter gamma distribution. The density function for the generalized three-parameter gamma distribution is thus [23]

$$f(\chi) = \frac{\alpha(\chi)^{g\alpha-1}}{b^{g\alpha} \Gamma(g)} \exp\left[-\left(\frac{\chi}{b}\right)^{\alpha} \right] \quad , \quad \begin{matrix} \chi \geq 0 \\ \alpha \geq 1 \\ b \geq 0 \\ g \geq 1 \end{matrix} \tag{49}$$

The three parameters are estimated using the same method used for the generalized four-parameter gamma distribution. The standard errors and covariances are found by using the 3 by 3 submatrix for $\hat{b}$, $\hat{g}$, and $\hat{\alpha}$ from the 4 by 4 covariance matrix for the generalized four-parameter gamma distribution (equations 45 and 46).

Two-Parameter Gamma Distribution. If the power parameter, α, is again assumed to be equal to one, the generalized three-parameter gamma distribution reduces to the two-parameter gamma distribution. The density function for the two-parameter gamma distribution is given by [11, 12, 23]

$$f(x) = \frac{x^{g-1}}{b^g \Gamma(g)} \exp\left[-\left(\frac{x}{b}\right)\right], \quad \begin{matrix} x \geq 0 \\ b \geq 0 \\ g \geq 1 \end{matrix} \qquad (50)$$

The two parameters are estimated using the same method used for the generalized four-parameter gamma distribution. The standard errors and covariances are found by using the 3 by 3 submatrix used for the generalized three-parameter gamma distribution and setting α equal to one.

5.3 Parameter Estimation Methods

Since the determination of the estimates of the parameters is critical to a proper fitting of the data to the two, three, and four-parameter distributions, two different parameter estimation methods were used [14, 25]. The first method, a graphical method, was selected for its simplicity [17, 18, 26, 27]. The second method, the method of maximum likelihood estimators (MLE), was selected because of its reliability, accuracy, and widespread acceptance [14, 15, 19, 21-23, 28-32].

5.3.a Graphical Method

This method was the first of the two methods attempted, due mainly to its simplicity in use [17, 18]. This method was tried with both the

three-parameter log normal distribution and the three-parameter Weibull distribution. The graphical method involves plotting the data on special probability paper whose axis scales correspond to special distribution characteristics and then selecting the value of the location parameter such that the resulting plot of data follows a straight line [17,18]. Once the estimate of the location parameter is known, the estimates of the other two parameters are made graphically. Since only three parameters can be estimated graphically, this limits the use of this method to two or three parameter distributions [17].

For the three-parameter log normal distribution, a plot of Y vs. X yields a straight line for data that follows a three-parameter log normal distribution [14] where

$$Y = G(s) \tag{91}$$

$$X = \log_{10}(x_e) \tag{92}$$

where G(s) is the equation for the standard normal probability scale which is given by [11]

$$G(s) = \int_{-\infty}^{s} \frac{1}{\sqrt{2\pi}} \exp\left(-\frac{u^2}{2}\right) du \tag{93}$$

where

$$s = F(x_e) \tag{94}$$

where $F(x_e)$ is the cumulative density function of the corrected data, x_e is the value of the data corrected for the value of the location parameter by the following equation,

$$x_e = x - x_0 \tag{95}$$

three-parameter log normal distribution and the three-parameter Weibull distribution. The graphical method involves plotting the data on special probability paper whose axis scales correspond to special distribution characteristics and then selecting the value of the location parameter such that the resulting plot of data follows a straight line [17,18]. Once the estimate of the location parameter is known, the estimates of the other two parameters are made graphically. Since only three parameters can be estimated graphically, this limits the use of this method to two or three parameter distributions [27].

For the three-parameter log normal distribution, a plot of Y vs. X yields a straight line for data that follows a three-parameter log normal distribution [14] where

$$Y = G(z) \tag{51}$$

$$X = \log_{10}(x_c) \tag{52}$$

where G(z) is the equation for the standard normal probability scale which is given by [11]

$$G(z) = \int_{-\infty}^{z} \frac{1}{2\pi} \exp\left(\frac{-x^2}{2}\right) dx \tag{53}$$

where

$$z = F(x_c) \tag{54}$$

where $F(x_c)$ is the cumulative density function of the corrected data. x_c is the value of the data corrected for the value of the location parameter by the following equation.

$$x_c = x - x_o \tag{55}$$

For the three-parameter Weibull distribution, a plot of Y vs. X where

$$Y = \ln \ln \left(\frac{1}{1-F(\chi_c)} \right) \tag{56}$$

$$X = \ln (\chi_c) \tag{57}$$

yields a straight line for data that follows the three-parameter Weibull distribution [17,18].

For both of these plots, $F(\chi_c)$ corresponds to the median ranks which are calculated by [18]

$$F(\chi_c) = \frac{\chi_c}{n+1} \quad , \quad 1 \leq \chi_c \leq n \tag{58}$$

To determine the value of the location parameter such that the resulting plot yields a straight line, an iterative process which minimizes some variable must be used. For the graphical method, the variable to be minimized is the curvature of a second order curve fit using least squares, thereby assuring a straight line. One of the fastest and most efficient of the many minimization methods available is the Golden Section search method [26].

In the Golden Section search method, the value of the curvature (the variable to be minimized) is calculated at two optimal locations and, based on these values, a certain area where the curvature minimum is known not to exist is excluded from the rest of the search. This process is repeated until the area remaining to be searched is less than some tolerance level. The value of the location parameter in this area is then taken as the estimated value of the location parameter. A schematic representation of the Golden Section search method is shown in Figure 10.

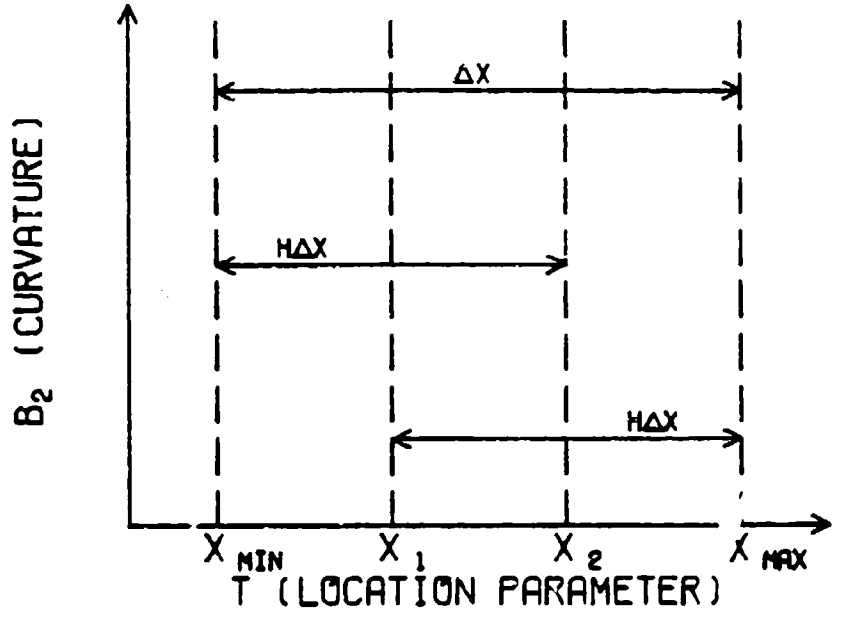

IF $B_2(X_1) < B_2(X_2)$
THEN X_2 BECOMES X_{MAX}

IF $B_2(X_1) > B_2(X_2)$
THEN X_1 BECOMES X_{MIN}

IF $B_2(X_1) = B_2(X_2)$
THEN X_2 BECOMES X_{MAX}
AND X_1 BECOMES X_{MIN}

$H = 0.618033989$

Figure 10. Golden Section Search Method

5.3.b Maximum Likelihood Estimators Method

After the graphical method was perfected and used, the need for a more statistical approach to the estimation of the parameters of the two, three, and four-parameter distributions became evident (Section 8.1). This led to the use of the Maximum Likelihood Estimators method to statistically estimate the distribution parameters.

The Maximum Likelihood Estimators (MLE) method involves solving maximum likelihood equations through the use of a nonlinear programming algorithm [14,15,19,21,22,23,28,30,31,32]. Many forms of the maximum likelihood equations have been determined by investigators for the three-parameter log normal distribution, the three-parameter Weibull distribution, and the two, three, and four-parameter gamma distributions [14,15,19,28-32].

Three-Parameter Log Normal Distribution. The maximum likelihood equation used in this investigation for the three-parameter log normal distribution is [15]

$$\ln L(\tau) = -n\left[\hat{\mu}(\tau) + \frac{1}{2} \ln \hat{\beta}\ (\tau)\right] \tag{59}$$

where

$$\hat{\mu}(\tau) = \frac{\sum_{i=1}^{n} \ln(\chi_i - \tau)}{n} \tag{60}$$

and

$$\hat{\beta}\ (\tau) = \frac{\sum_{i=1}^{n} \left[\ln\ (\chi_i - \tau) - \hat{\mu}(\tau)\right]^2}{n} \tag{61}$$

Three-Parameter Weibull Distribution. The maximum likelihood equation used in this investigation for the three-parameter Weibull distribution is [19]

$$L(b,c,\tau) = n(\ln c - c\ln b) + (c - 1) \sum_{i=1}^{n} \ln(\chi_i - \tau) - b^{-c} \sum_{i=1}^{n} (\chi_i - \tau)^c \tag{62}$$

Note that the maximum likelihood equation is a function of all three parameters whereas for the three-parameter log normal distribution, the maximum

likelihood equation is a function of just the location parameter. However, the scale parameter, b, can be factored out of this equation and estimated separately. The resulting two parameter maximum likelihood equation for the three-parameter Weibull distribution is [13]

$$L(c,\tau) = \ln c - \ln\left[\frac{1}{n}\sum_{i=1}^{n}(\chi_i-\tau)^c\right] + \frac{(c-1)}{n}\left[\sum_{i=1}^{n}\ln(\chi_i-\tau)\right] \qquad (63)$$

where the estimation of the scale parameter is given by [13]

$$\hat{b} = \left[\frac{1}{n}\sum_{i=1}^{n}(\chi_i-\tau)^c\right]^{1/c} \qquad (64)$$

The effect of reducing the number of parameters in the maximum likelihood equation is to reduce the computing time, and thus the cost, of the maximization of the maximum likelihood equation.

Generalized Four-Parameter Gamma Distribution. The maximum likelihood equation for the generalized four-parameter gamma distribution is [21,30, 32]

$$L(b,g,\alpha,\tau) = n\ln\alpha + (g\alpha-1)\left[\sum_{i=1}^{n}\ln(\chi_i-\tau)\right] - gn\ln(b^{\alpha}) - \sum_{i=1}^{n}\left[\frac{(\chi_i-\tau)}{b}\right]^{\alpha} - n\ln\Gamma(g) \qquad (65)$$

The number of parameters in this equation can also be reduced by factoring out the scale parameter, b. The resulting three parameter maximum likelihood equation for the generalized four-parameter gamma distribution is [13]

$$L(g,\alpha,\tau) = n\ln\alpha + (g\alpha-1)\left[\sum_{i=1}^{n}\ln(\chi_i-\tau)\right] - gn\left[1 + \ln\left\{\sum_{i=1}^{n}(\chi_i-\tau)^{\alpha}\right\} - \ln gn\right] - n\ln\Gamma(g) \qquad (66)$$

where the estimation of the scale parameter is given by [13]

$$\hat{b} = \left[\frac{\sum_{i=1}^{n} (x_i-\tau)^{\alpha}}{ng}\right]^{1/\alpha} \tag{67}$$

Three-Parameter Gamma Distribution. The maximum likelihood equation for the three-parameter gamma distribution reduced to eliminate the scale parameter is [13]

$$L(g,\tau) = (g-1)\left[\sum_{i=1}^{n} \ln(x_i-\tau)\right] - gn\left[1 + \ln\left\{\sum_{i=1}^{n} (x_i-\tau)\right\} - \ln(gn)\right] - n \ln\Gamma(g) \tag{68}$$

where the estimation of the scale parameter is given by [13]

$$\hat{b} = \frac{1}{ng}\left[\sum_{i=1}^{n} (x_i-\tau)\right] \tag{69}$$

Generalized Three-Parameter Gamma Distribution. The maximum likelihood equation for the generalized three-parameter gamma distribution is [21,30,32]

$$L(b,g,\alpha) = n \ln\alpha + (g\alpha-1)\left[\sum_{i=1}^{n} \ln(x_i)\right] - gn \ln(b^{\alpha}) - \sum_{i=1}^{n}\left[\frac{x_i}{b}\right]^{\alpha} - n \ln\Gamma(g) \tag{70}$$

This equation can also be reduced to eliminate the scale parameter, b. The resulting two parameter maximum likelihood equation for the generalized three-parameter gamma distribution is [13]

$$L(g,\alpha) = n \ln\alpha + (g\alpha-1)\left[\sum_{i=1}^{n} \ln(x_i)\right] - gn\left[1 + \ln\left\{\sum_{i=1}^{n} (x_i)^{\alpha}\right\} - \ln(gn)\right] - n \ln\Gamma(g) \tag{71}$$

where the estimation of the scale parameter is given by [13]

$$\hat{b} = \left[\frac{1}{ng}\left\{\sum_{i=1}^{n}(x_i)^{\alpha}\right\}\right]^{1/\alpha} \tag{72}$$

Two-Parameter Gamma Distribution. The maximum likelihood equation for the two-parameter gamma distribution reduced to eliminate the scale parameter is [13]

$$L(g) = (g-1)\left[\sum_{i=1}^{n}\ln(x_i)\right] - gn\left[1 + \ln\left\{\sum_{i=1}^{n}(x_i)\right\} - \ln(gn)\right] - n\ln\Gamma(g) \tag{73}$$

where the estimation of the scale parameter is given by [13]

$$\hat{b} = \frac{1}{ng}\left[\sum_{i=1}^{n}(x_i)\right] \tag{74}$$

Interior Point Penalty Function. After some experience using the Graphical method to estimate the location parameter of the three-parameter Weibull distribution, it was found that the iteration tended to go to minus infinity in some cases. Since this was the global (overall) maximum of the function to be maximized, it became necessary to use a method that converged on the local maximum, and not the global maximum. The method used to achieve this requires the use of an interior point penalty function which prevents the value of each of the parameters from reaching either of its global limits [15].

The interior point penalty function, better known as the objective function in nonlinear programming terms, for the three-parameter log normal distribution using the maximum likelihood equation is [15]

$$P(\tau, r) = \ln L(\tau) - r\left[(\tau + c_+ - \epsilon_+)^{-1} + (x_{min} - \tau - \epsilon_+)^{-1}\right] \tag{75}$$

where c_+ is a large positive number ($\approx 10^{25}$),

r is an iteration variable, and

ϵ_+ is a small positive number ($\simeq 10^{-8}$).

The objective function for the three-parameter Weibull distribution using the two parameter maximum likelihood equation is [15]

$$P(\tau,c,r) = L(\tau,c) - r\left[(\tau + c_+ - \epsilon_+)^{-1} + (\chi_{min} - \tau - \epsilon_+)^{-1} + (c - \epsilon_+)^{-1} + (10 - c - \epsilon_+)^{-1}\right] \tag{76}$$

The objective function for the generalized four-parameter gamma distribution using the three parameter maximum likelihood equation is [15]

$$P(g,\alpha,\tau,r) = L(g,\alpha,\tau) - r\left[(g - 1 - \epsilon_+)^{-1} + (100 - g - \epsilon_+)^{-1} + (\alpha - 1 - \epsilon_+)^{-1} + (100 - \alpha - \epsilon_+)^{-1} + (\tau + c_+ - \epsilon_+)^{-1} + (\chi_{min} - \tau - \epsilon_+)^{-1}\right] \tag{77}$$

The objective function for the three-parameter gamma distribution using the two parameter maximum likelihood equation is [15]

$$P(g,\tau,r) = L(g,\tau) - r\left[(g - 1 - \epsilon_+)^{-1} + (100 - g - \epsilon_+)^{-1} + (\tau + c_+ - \epsilon_+)^{-1} + (\chi_{min} - \tau - \epsilon_+)^{-1}\right] \tag{78}$$

The objective function for the generalized three-parameter gamma distribution using the two parameter maximum likelihood equation is [15]

$$P(g,\alpha,r) = L(g,\alpha) - r\left[(g - 1 - \epsilon_+)^{-1} + (100 - g - \epsilon_+)^{-1} + (\alpha - 1 - \epsilon_+)^{-1} + (100 - \alpha - \epsilon_+)^{-1}\right] \tag{79}$$

The objective function for the two-parameter gamma distribution using the one parameter maximum likelihood equation is [15]

$$P(g,r) = L(g) - r\left[(g - 1 - \epsilon_+)^{-1} + (100 - g - \epsilon_+)^{-1}\right] \qquad (80)$$

The algorithm used to converge the objective function towards the local maximum likelihood is as follows [15].

1. Maximize the objective function, $P(\tau,r)$.
2. Check for convergence to the optimum i.e. when

$$|\tau(r_j) - \tau(r_{j-1})| < \epsilon \qquad (81)$$

where ϵ is the convergence criterion constant.

3. If the convergence criterion is not satisfied, reduce r_j by setting

$$r_{j+1} = dr_j, \quad 0 < d < 1 \qquad (82)$$

where d is a convergence constant.

4. Increment j and repeat.

The maximization of the objective function has been done by many non-linear routines [19]. However, the Hooke-Jeeves pattern search method [33] has enjoyed particularly good success in maximizing MLE objective functions and was therefore utilized in maximizing the objective functions for the three-parameter log normal distribution, the three-parameter Weibull distribution and the two, three, and four-parameter gamma distributions [15].

5.4 Goodness of Fit Criteria

Once the statistical parameters for each of the candidate distributions have been estimated, the distribution which the data follows the closest must be selected from the candidate distributions. A statistical

method which is used many times to find out how well data fits a certain distribution is the goodness of fit test. Several goodness of fit tests have been proposed [12], but three of the more reliable and widely used goodness of fit tests have been selected as criteria for the selection of the "best" distribution. These three goodness of fit tests are regression, the chi-square test, and the Kolmogorov-Smirnov test.

5.4.a Regression

Regression in its simplest form involves fitting a polynomial to a set of given data plotted on certain axes [34]. In the case of fitting data to a statistical distribution, the data can be plotted on a plot whose axes correspond to certain characteristics of that particular statistical distribution (Section 5.3.a). It is known that if data follows that particular distribution, then the data will follow a straight line fit when plotted on these special axes. If a linear regression is performed on this plotted data, it can be determined how close the data does fit a straight line. This then provides a measure of the goodness of fit of the data to that particular distribution.

If a set of data follows the two-parameter normal distribution, a plot of the data with the X axis as a linear scale and the Y axis as a normal probability scale will follow a straight line [18]. The normal probability scale is described in detail in Section 5.3.a. A typical plot for the two-parameter normal distribution is shown in Figure 11.

If a set of data follows the two-parameter log normal distribution, a plot of the data with the X axis as a $\log_{10}$ scale and the Y axis as a normal probability scale (Section 5.3.a) will follow a straight line [18]. In this plot, the location parameter is not estimated and is assumed to be

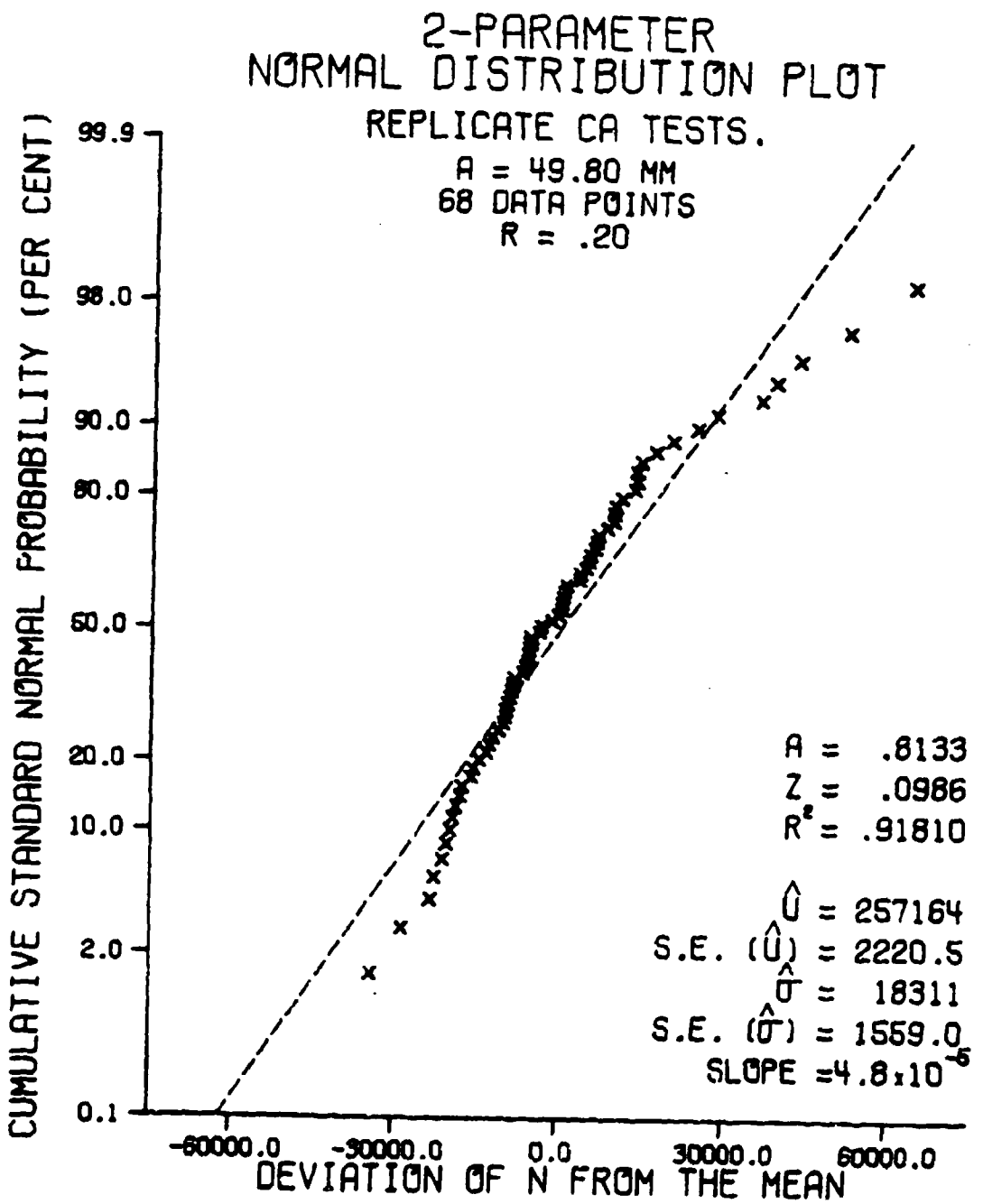

Figure 11. Typical 2-Parameter Normal Distribution Plot

zero. A typical plot for the two-parameter log normal distribution is shown in Figure 12.

Both the plots for the three-parameter log normal distribution and the three-parameter Weibull distribution have been discussed in Section 5.3.a. A typical plot for the three-parameter log normal distribution is shown in Figure 13 and a typical plot for the three-parameter Weibull distribution is shown in Figure 14. The three-parameter gamma distribution plot requires the data to be plotted on a plot where the X axis is a linear scale and the Y axis is a gamma probability scale. The equation for calculating the gamma probability scale, H(z), is [27]

$$F(\chi_c)\,\Gamma(g) = \int_0^{H(z)} t^{-1}\, e^{-t}\, dt \tag{83}$$

where

$$z = F(\chi_c) \tag{84}$$

where $F(\chi_c)$ is the cumulative density function of the corrected data which is given by equation (58). Equation (83) was solved iteratively for H(z) using the interval halving method [27]. A typical three-parameter gamma distribution plot is shown in Figure 15. The two-parameter gamma distribution plot also requires the X axis to be a linear scale and the Y axis to be a gamma probability scale. A typical two-parameter gamma distribution plot is shown in Figure 16. In each of the above plots, the data are plotted on the X axis against the corresponding median ranks on the Y axis.

Linear regression uses linear least squares which uses the matrix approach to linear regression to fit a best fit straight line to the data [34]. As a result of this matrix approach to linear regression, a goodness

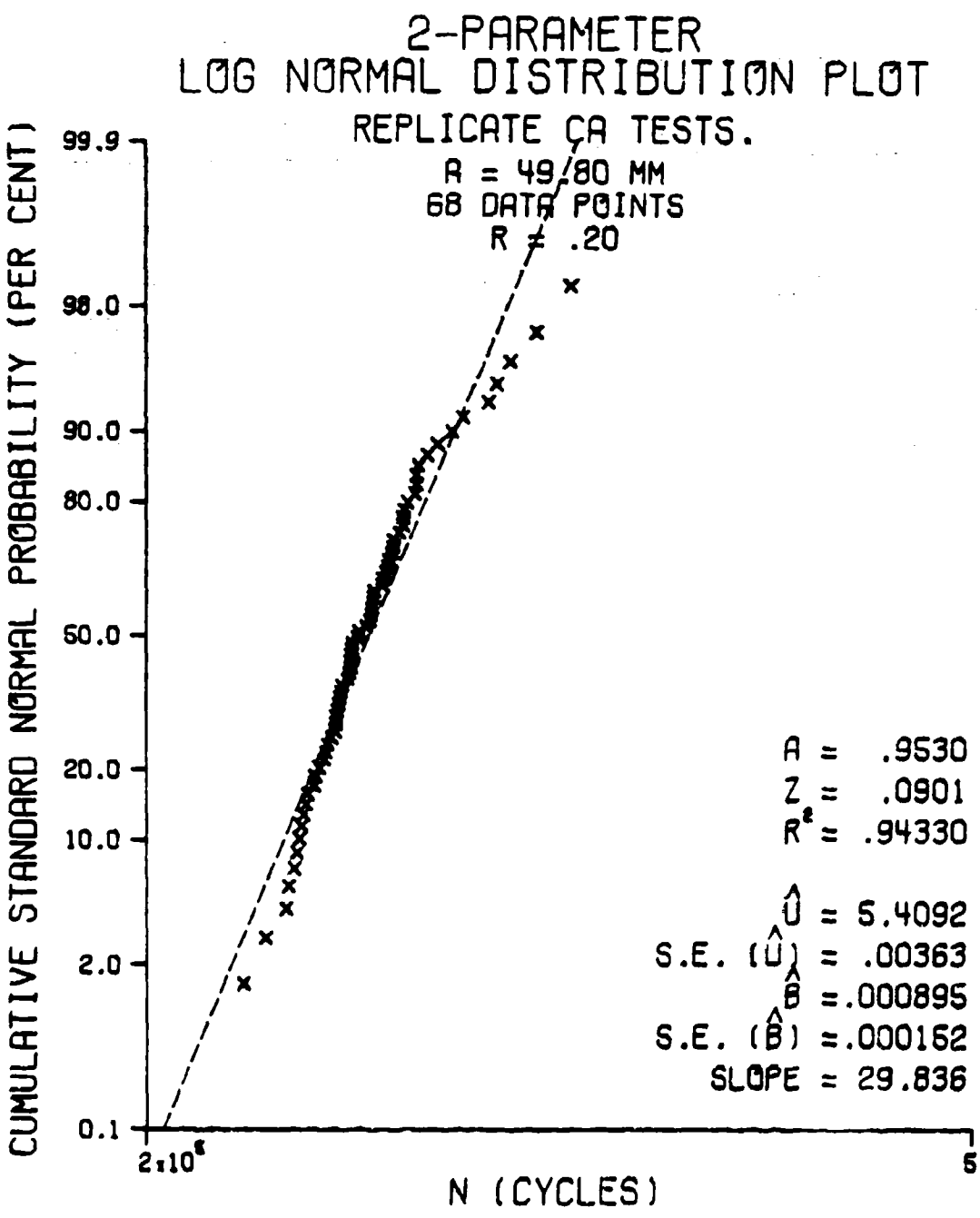

Figure 12. Typical 2-Parameter Log Normal Distribution Plot

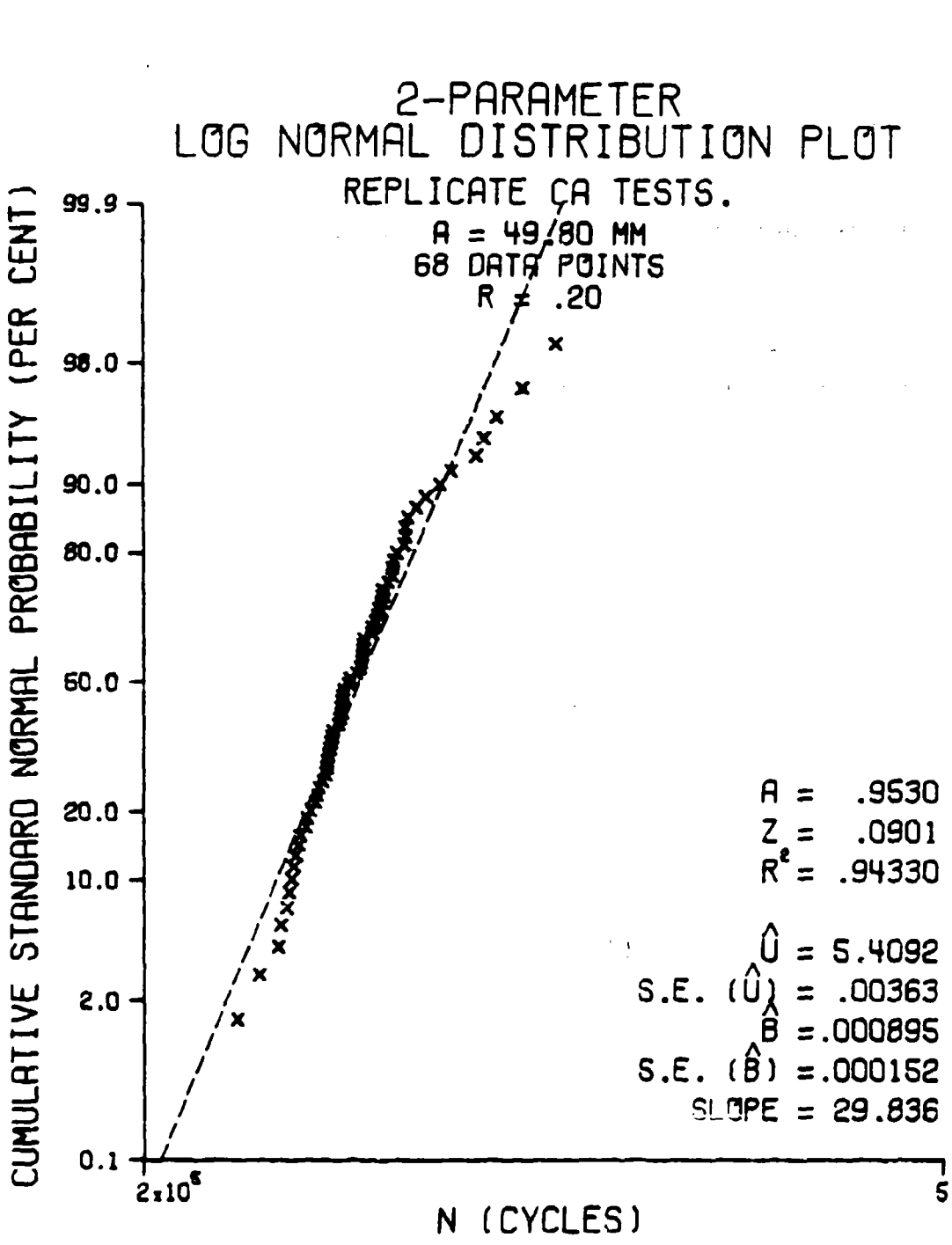

Figure 12. Typical 2-Parameter Log Normal Distribution Plot

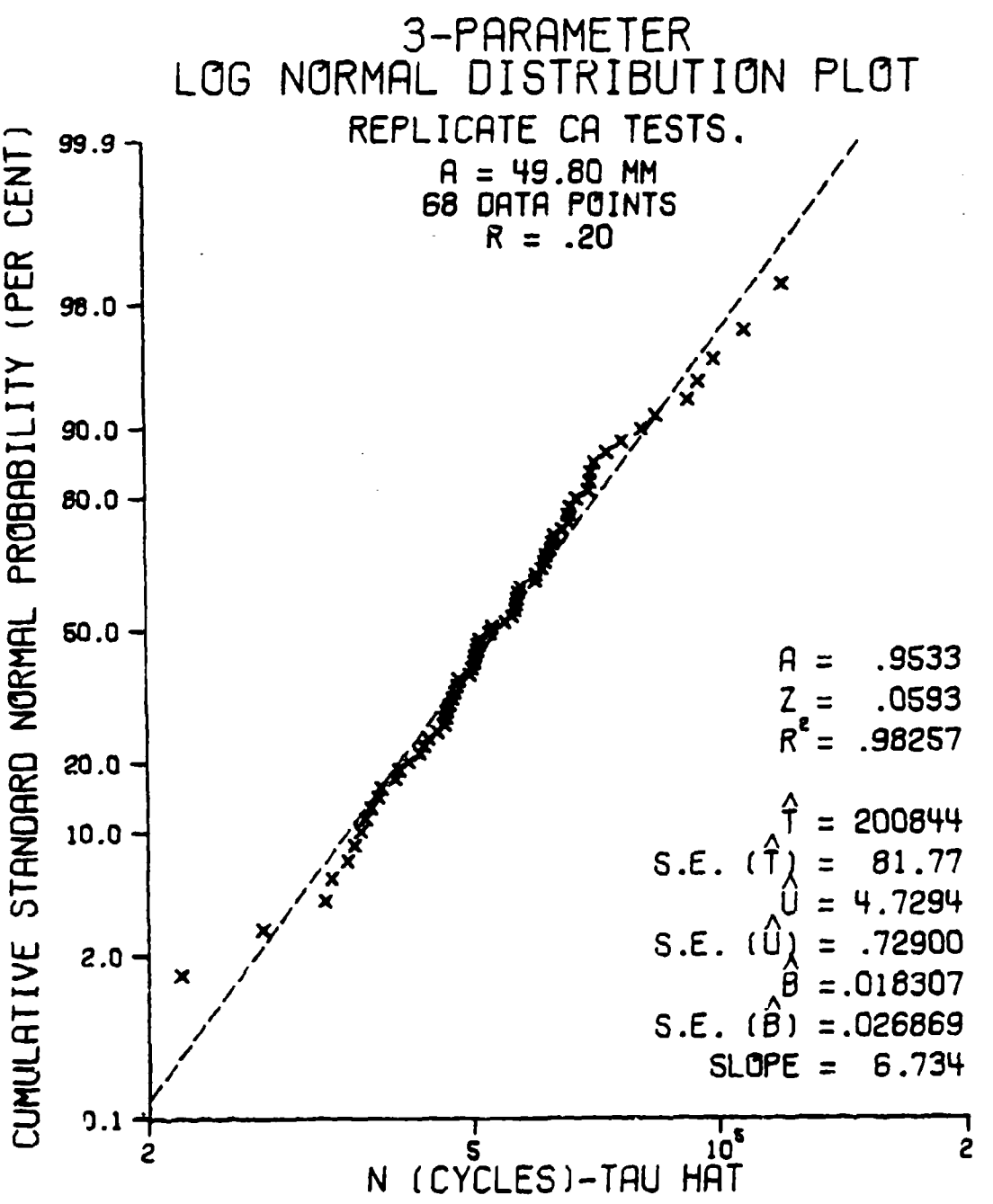

Figure 13. Typical 3-Parameter Log Normal Distribution Plot

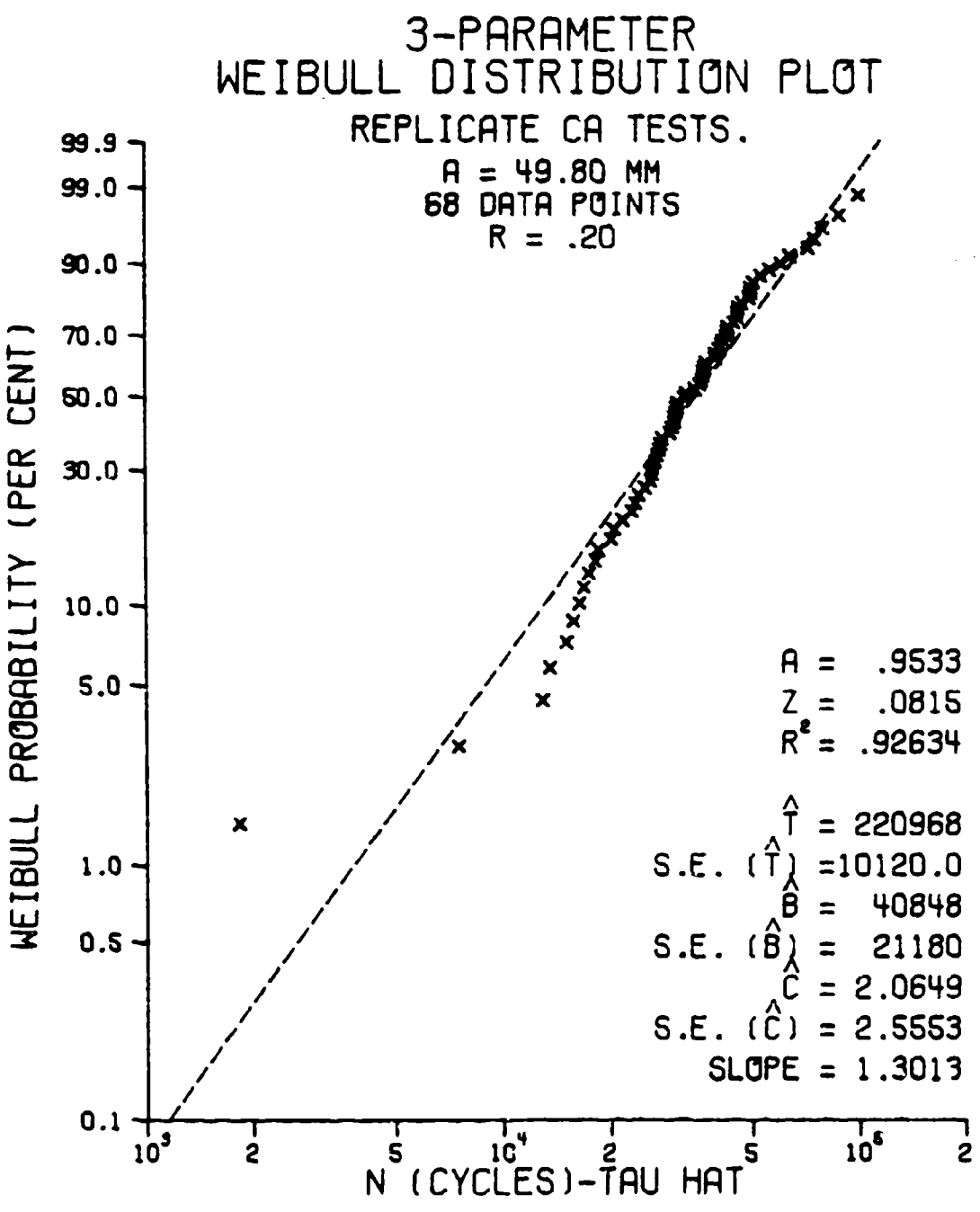

Figure 14. Typical 3-Parameter Weibull Distribution Plot

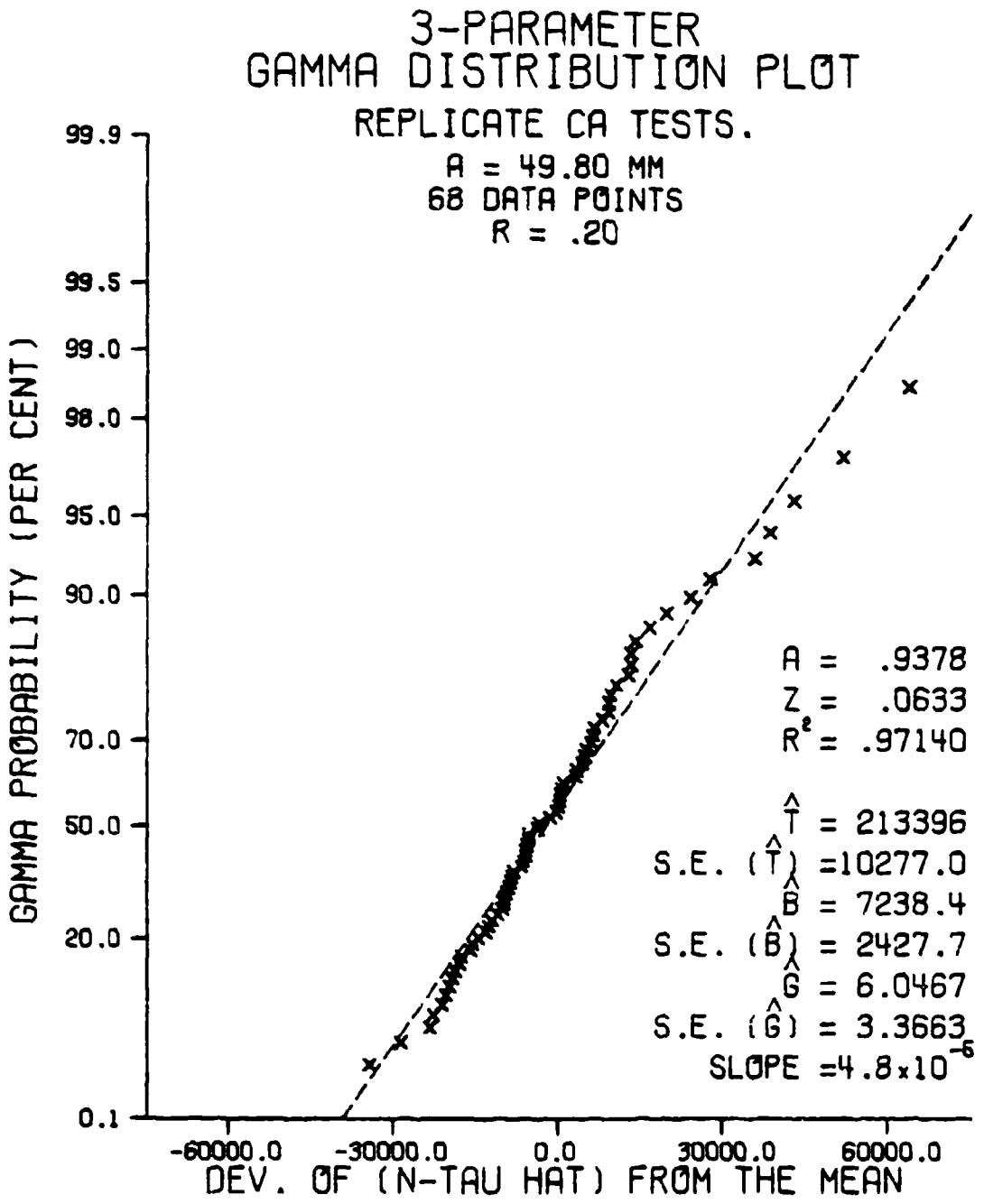

Figure 15. Typical 3-Parameter Gamma Distribution Plot

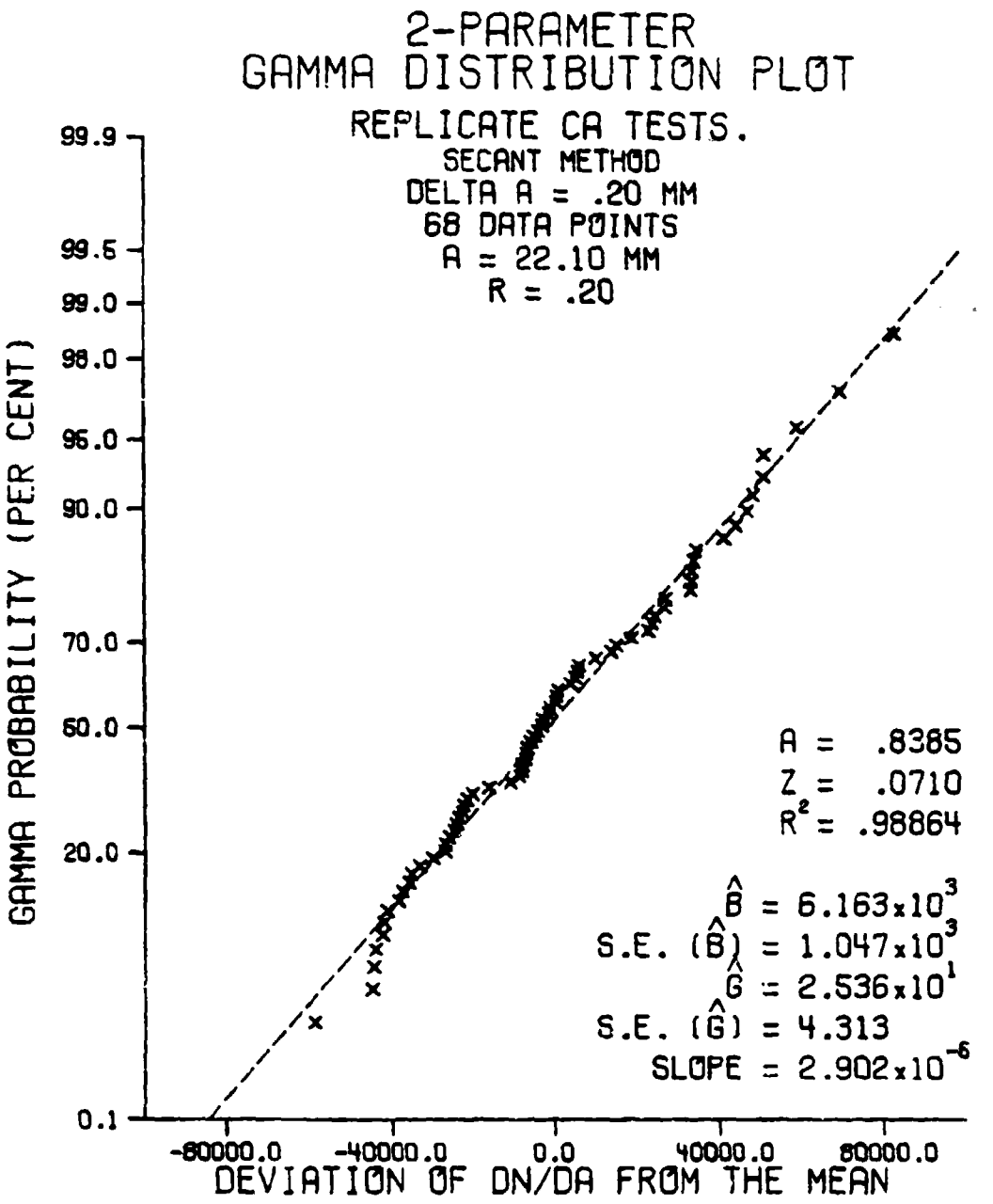

Figure 16. Typical 2-Parameter Gamma Distribution Plot

of fit statistic, called the coefficient of multiple determination, R^2, can be calculated. The value of R^2 is always between zero and one. The closer the value of R^2 is to one, the closer the fit of the data is to a straight line. Therefore, by comparing the values of R^2 for each of the distributions, the distribution with the highest value of R^2 is the distribution which the data follows the closest.

This value of R^2 can be corrected for the slope of the least squares line in an attempt to achieve a more precise measure of the closeness of the data to the straight line. This corrected value of R^2 is called the closeness and is given the symbol C^2. The derivation of C^2 is given in Appendix C.

5.4.b Chi-Square Test

The chi-square goodness of fit test is a statistical method for determining how close given data follow a certain distribution. Basically, it

1) divides the data into an optimum number of equiprobable intervals,
2) counts the number of data points in each interval (called the observed frequencies),
3) calculates the number of data points that should be in each interval based on the estimated distribution parameters (called the expected frequencies), and
4) compares the observed frequencies with the expected frequencies [11,12].

The test statistic, χ^2, is a measure of how close the observed frequencies are to the expected frequencies, and thus how close the data follows the given distribution. χ^2 is given by

$$\chi^2 = \sum_{i=1}^{k} \frac{(o_i - e_i)^2}{e_i} \tag{85}$$

where k is the number of equiprobable intervals,

o_i are the observed frequencies, and

e_i are the expected frequencies.

The lower the value of the chi-square statistic, the closer the observed frequencies match the expected frequencies and thus the closer the data follows the given distribution. However, the chi-square statistic can not be compared between distributions that do not have the same number of distribution parameters, n_p, because the degrees of freedom for the chi-square statistic for distributions not having the same number of distribution parameters is not constant [13]. Therefore, the tail area of the chi-square distribution to the right of the chi-square statistic, called A, is computed for each distribution by [13]

$$A = \frac{\int_{\chi^2/2}^{\infty} \exp(-u) \cdot u^{(\frac{\nu}{2} - 1)} \, du}{\Gamma(\frac{\nu}{2})} \tag{86}$$

where ν is the number of degrees of freedom and u is a variable of integration. The value of A is always between zero and one, with A equal to one being a perfect fit. The lower the value of the chi-square statistic, the higher the value of the tail area, all other things being equal. Therefore, the distribution to be chosen as the distribution which the data follows the closest is the one which has the highest value of A.

The chi-square statistic may be compared with a critical value which follows the chi-square distribution at an acceptance level of α_a with ν degrees of freedom, $\chi^2_{\alpha_a,\nu}$ [12], where

$$\nu = k - n_p - 1 \tag{87}$$

Acceptance of the proposed distribution as the distribution which the data follows should occur when [12]

$$\chi^2 \leq \chi^2_{\alpha_a,\nu} \tag{88}$$

The tail area, A, may be compared with the acceptance level to test acceptance of the proposed distribution. Acceptance should occur when [13]

$$A \geq \alpha_a \tag{89}$$

The end points for the classes for the two and three-parameter normal distributions were found by dividing a standard normal curve into different numbers of equiprobable intervals [35]. The end points for the equiprobable intervals for the three-parameter Weibull distribution were given by [19]

$$q_i = \hat{\tau} + \hat{b}\left[-\ln\left\{1 - \left(\frac{i}{k}\right)\right\}^{1/\hat{c}}\right] \tag{90}$$

The end points for the equiprobable intervals for the two, three, and four-parameter gamma distribution were given by [21]

$$q_i = \hat{\tau} + \hat{b}\left[\left\{F_{\hat{g}}^{-1}\left(\frac{i}{k}\right)\right\}^{1/\hat{\alpha}}\right] \tag{91}$$

where $F_{\hat{g}}^{-1}$ is the inverse cumulative density function for the generalized four-parameter gamma distribution.

5.4.c Kolmogorov-Smirnov Test

The Kolmogorov-Smirnov test is another statistical goodness of fit test similar to the chi-square goodness of fit test. Basically, it calculates the sample cumulative density function and compares it with the theoretical cumulative density function of the given distribution by calculating the maximum deviation, D, between the two cumulative density

functions [11]. The test statistic, Z, is a measure of how close the two cumulative density functions are and thus how close the data follows the given distribution and is actually equal to D.

The lower the value of the Kolmogorov-Smirnov statistic, the closer the sample cumulative density function lies to the theoretical cumulative density function, and thus the closer the data follows the given distribution. Therefore, the distribution to be chosen as the distribution which the data follows the closest is the one which has the lowest value of the Z statistic. The Kolmogorov-Smirnov statistic may be compared with a table of critical values to determine if the proposed distribution should be accepted as the distribution which the data follows [36].

SECTION VI

DETERMINATION OF THE DISTRIBUTION

Several computer programs were written to determine the distribution of the desired fatigue crack propagation variables using the previously mentioned statistical concepts. The four programs written to determine statistical distributions of fatigue crack propagation variables are:

1) Delta N Distribution Determination Program (Golden), or DNDDPG,
2) Cycle Count Distribution Determination Program, or CCDDP,
3) Crack Growth Rate Distribution Determination Program, or CGRDDP, and
4) Delta N Distribution Determination Program (MLE), or DNDDP.

6.1 Delta N Distribution Determination Program (Golden)

This program, called DNDDPG, was written to determine the distribution of the $\Delta N/\Delta a$ variable computed from the input a vs. N data which is supplied by program DELTCP (Section 7.1). Basically, it fits the data to four distributions and computes a goodness of fit statistic for the comparison of the distributions. The four distributions fitted are:

1) the two-parameter normal distribution,
2) the two-parameter log normal distribution,
3) the three-parameter log normal distribution, and
4) the three-parameter Weibull distribution.

It uses the graphical method, including the Golden Section search method, to estimate the location parameter for both the three-parameter log normal distribution and the three-parameter Weibull distribution. The goodness of fit criterion used is C^2 (Section 5.4.a).

This program produces output which includes the input a vs. N data, the computed a vs. N data, some of the test conditions, some of the internal program parameters, the frequency distribution array, the $\Delta N/\Delta a$ data, and the distribution parameters and a partial analysis of variance table for each distribution. The plots generated by this program are a relative frequency histogram, a relative cumulative frequency histogram, and a distribution plot for each of the distributions. Further documentation of this program is shown in Appendix D.

6.2 Cycle Count Distribution Determination Program

This program, called CCDDP, was written to determine the distribution of the N (cycle count) variable from a set of replicate cycle count data at one crack length level. Identical load and test conditions are required for the replicate data. This program fits the data to six distributions. These distributions are:

1) the two-parameter normal distribution,
2) the two-parameter log normal distribution,
3) the three-parameter log normal distribution,
4) the three-parameter Weibull distribution,
5) the three-parameter gamma distribution, and
6) the generalized four-parameter gamma distribution.

It uses the Maximum Likelihood Estimators method to estimate the parameters of each of the above distributions except the two-parameter normal

distribution and the two-parameter log normal distribution. Three goodness of fit criteria are calculated for the comparison of the distributions. They are:

1) the chi-square tail area,

2) the Kolmogorov-Smirnov statistic, and

3) R^2 from regression.

This program produces output which includes the input replicate cycle count data, the test conditions, some of the internal program parameters, the frequency distribution array, and 1) the estimated distribution parameters, 2) a partial analysis of variance table, and 3) the goodness of fit criteria for each distribution except the generalized four-parameter gamma distribution, for which only the estimated distribution parameters and the goodness of fit criteria are printed. It also prints a comparison of the distributions and the resulting "best" distribution based on the goodness of fit criteria. The plots generated by this program are the original cycle count data plot, a relative frequency histogram, a relative cumulative frequency histogram, and a distribution plot for each of the distributions except the generalized four-parameter gamma distribution. Further documentation of this program is shown in Appendix E.

6.3 Crack Growth Rate Distribution Determination Program

This program, called CGRDDP, was written to determine the distribution of the crack growth rate (da/dN) variable from a set of replicate da/dN data at one crack length level. This da/dN data is calculated by the DADNCP program (Section 7.2). Identical load and test conditions are required for the replicate data.

This program is nearly identical to the CCDDP program (Section 6.2), using the same distributions, the same parameter estimation method, the same goodness of fit criteria, and having nearly the same output. The main difference is the variable of interest being da/dN instead of cycle count. Thus the required input is different and some of the output is different in this respect. Further documentation of this program is shown in Appendix F.

6.4 Delta N Distribution Determination Program (MLE)

This program, called DNDDP, was written to determine the distribution of the $\Delta N/\Delta a$ variable from a set of replicate da/dN data at one crack length level. The da/dN data used is the same as that used by the CGRDDP program (Section 6.3).

This program is based on the CGRDDP program. One main difference between them is that the input da/dN data is inverted to create the variable $\Delta N/\Delta a$. The second main difference is the assumption that $\hat{\tau}$ for the gamma distributions is equal to zero, thus reducing the 3-parameter gamma distribution and the generalized 4-parameter gamma distribution by one parameter (Section 5.2.3). Along with the change in variable, there are appropriate changes in the output. Further documentation of this program is shown in Appendix G.

SECTION VII

GROWTH RATE AND GROWTH PREDICTION

Since this investigation was not just interested in the distribution of fatigue crack propagation variables alone, it became necessary to write several other programs to aid in the analysis of the experimental data. These supporting programs inclued 1) Delta N Calculation Program, or DELTCP, 2) da/dN Calculation Program, or DADNCP, and 3) a vs. N Prediction Program, or AVNPRD. Several others not mentioned here were used to aid in the analysis and manipulation of the experimental data.

7.1 Delta N Calculation Program

This program, called DELTCP, was written to calculate intermediate Δa vs. ΔN data to be used by program DNDDPG (Section 6.1). Basically, it calculates Δa vs. ΔN data from a set of constant amplitude a vs. N data by one of five different methods. These methods are;

1) the secant method,
2) reject certain selectable data points and use the secant method, thereby increasing Δa,
3) the quadratic 7-point incremental polynomial method,
4) reject certain selectable data points, recreate new a vs. N data, and then use the quadratic 7-point incremental polynomial method, and
5) use the quadratic 7-point incremental polynomial method, recreate new a vs. N data, reject certain selectable data points, and then use the secant method.

Further documentation of this program is shown in Appendix H.

7.2 da/dN Calculation Program

This program, called DADNCP, was written to calculate the crack growth rate, da/dN, by the six different methods presented in Section 4. These methods are;

1) the secant method,

2) the modified secant method,

3) the linear 7-point incremental polynomial method,

4) the quadratic 7-point incremental polynomial method,

5) the linear log-log 7-point incremental polynomial method, and

6) the quadratic log-log 7-point incremental polynomial method.

For each of these methods, the calculated da/dN data is integrated back into estimated a vs. N data, which is compared with the original a vs. N data, resulting in an average incremental error. By comparing these errors, the da/dN calculation method which results in the lowest error can be selected.

The required input for this program is a set of constant Δa a vs. N data. This program produces output which includes the input a vs. N data, the test conditions, da/dN vs. ΔK and actual cycle count data vs. estimated cycle count data for each da/dN calculation method, and a summary of the errors from each method with the resulting "best" da/dN calculation method. Further documentation of this program is shown in Appendix I.

7.3 a vs. N Prediction Program

This program, called AVNPRD, predicts a vs. N data from the distribution of da/dN (or dN/da) as a function of crack length and compares it

with the original a vs. N data. The required input is the knowledge of the distribution of da/dN (or dN/da) as a function of crack length as determined by the CGRDDP (or DNDDP) program. This program selects a growth rate at each crack length using a random number generator and the distribution parameters. This growth rate is then used to calculate ΔN as a function of crack length, which is used to predict replicate sets of a vs. N data. These predicted sets of a vs. N data are then compared with the original a vs. N data sets.

This program produces output which includes the test conditions, the predicted a vs. N data, and a plot of all of the predicted a vs. N data. Further documentation of this program is shown in Appendix J.

with the original a vs. N data. The required input is the knowledge of the distribution of da/dN (or dN/da) as a function of crack length as determined by the CGRDDP (or DNDDP) program. This program selects a growth rate at each crack length using a random number generator and the distribution parameters. This growth rate is then used to calculate ΔN as a function of crack length, which is used to predict replicate sets of a vs. N data. These predicted sets of a vs. N data are then compared with the original a vs. N data sets.

This program produces output which includes the test conditions, the predicted a vs. N data, and a plot of all of the predicted a vs. N data. Further documentation of this program is shown in Appendix J.

SECTION VIII

STATISTICAL ANALYSIS OF PREVIOUSLY GENERATED DATA

A considerable amount of crack propagation data in the form of a vs. N data have recently been generated at Purdue University for center crack specimens of 2024-T3 aluminum alloy [37]. From this set of data, there were 30 different overload/underload tests which were conducted under constant stress intensity conditions and at constant Δa. From each of these tests, approximately 19 to 155 data points, for a total of 2076 data points, were collected after the crack had grown through the region influenced by the overload/underload sequence. The data typically chosen for analysis is shown in Figure 17. This large amount of data was collected following the overload affected region to establish a final steady state growth rate as well as establishing the steady state growth rate for the next test [37,38,39]. From this set of test results, there are 2 to 7 sets of data at each of five different loading conditions.

The value of these data for statistical evaluation centers on the accuracy with which the original a vs. N data were collected. In these tests, the crack length was monitored and measured with a 100X microscope mounted on a digital measurement traverse. The traverse has a resolution of 0.001 mm (0.00004 in.) with a direct digital read-out. A printer activated by a push button was connected to the cycle counter and the digital traverse. In collecting the data, the microscope was advanced an increment of 0.01 mm, 0.02 mm, or 0.05 mm (depending on the

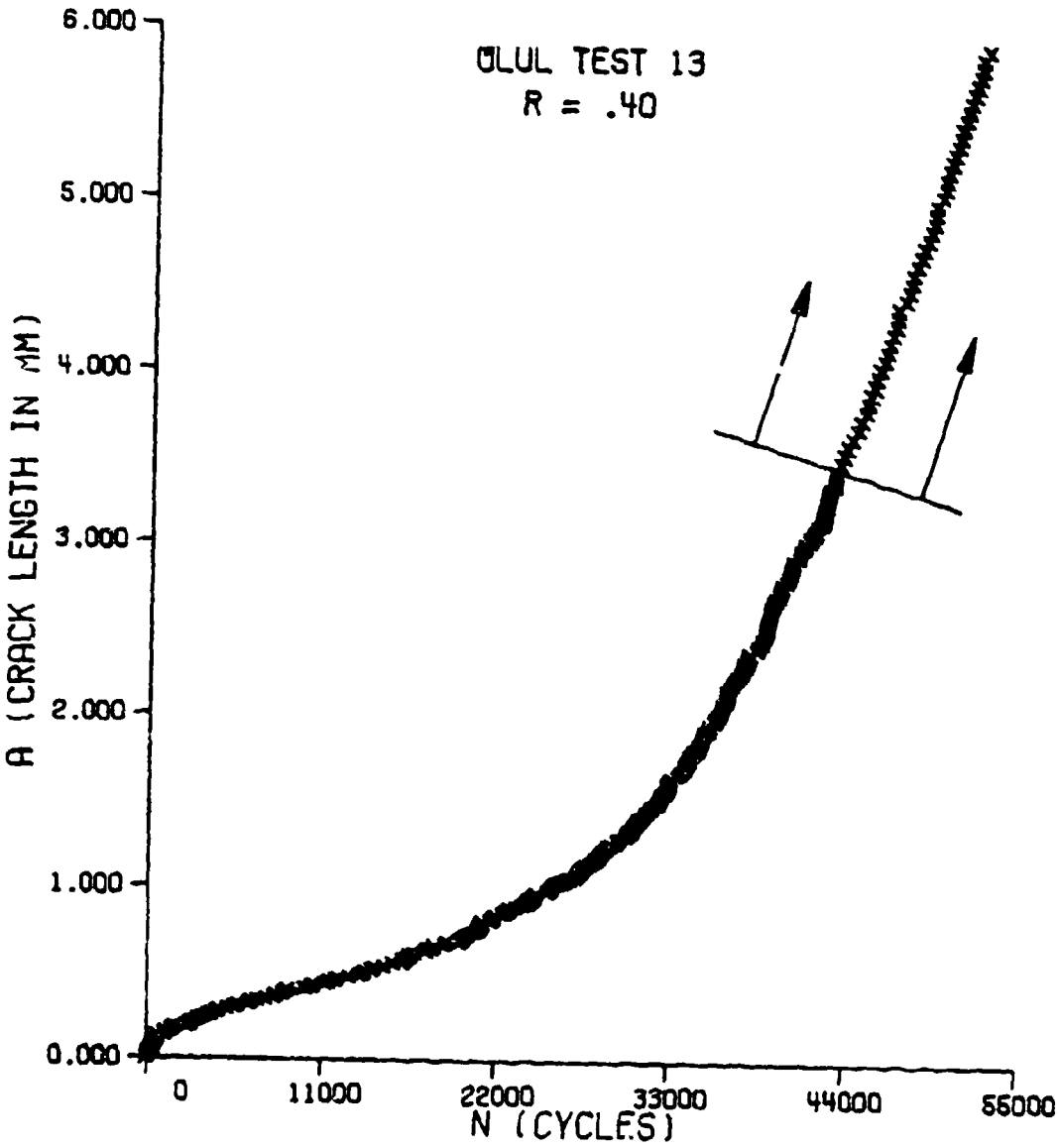

Figure 17. Typical Data Chosen for Analysis from Overload/Underload Test Data

growth rate). When the crack had grown this increment as observed with the cross hair in the microscope, the printer was activated with the push button and the crack length and number of cycles were printed. The resulting data are very dense and appear to be fairly accurate. This large amount of data was used to make a preliminary statistical analysis to aid in the direction and scope of this investigation [40].

8.1 Distribution of $\Delta N/\Delta a$

The first step of the analysis was to determine the distribution of the variable $\Delta N/\Delta a$ which was calculated by the secant method. This was done by writing a pair of programs using many of the statistical concepts presented in Section 5. These programs, called Delta N Calculation Program, or DELTCP (Section 7.1), and Delta N. Distribution Determination Program (Golden), or DNDDPG (Section 6.1), were run on each of the data sets. The distributions were ranked from 1 to 4 (1 being the best) based on the goodness of fit criterion, C^2 (Section 5.4.a). The rankings were averaged over all of the tests and the results are shown in Table I. The best distribution was the three-parameter log normal distribution followed closely by the two-parameter log normal distribution. A plot of the fit of the $\Delta N/\Delta a$ data to the three-parameter log normal distribution is shown in Figure 18.

Based on these results and the use of the DELTCP and DNDDPG programs, the following conclusions were made.

1) The 2-parameter Weibull distribution was tried and rejected from all further analysis because of its poor performance in providing a fit for the $\Delta N/\Delta a$ data due to it's lack of a location parameter.

Table I

Distribution of $\Delta N/\Delta a$

DISTRIBUTION	$\overline{C^2}$	S_{C^2}	AVE. RANK
2-PARAMETER NORMAL	0.9668	0.0190	3.95
2-PARAMETER LOG NORMAL	0.9969	0.0025	1.87
3-PARAMETER LOG NORMAL	0.9984	0.0014	1.31
3-PARAMETER WEIBULL	0.9932	0.0055	2.67

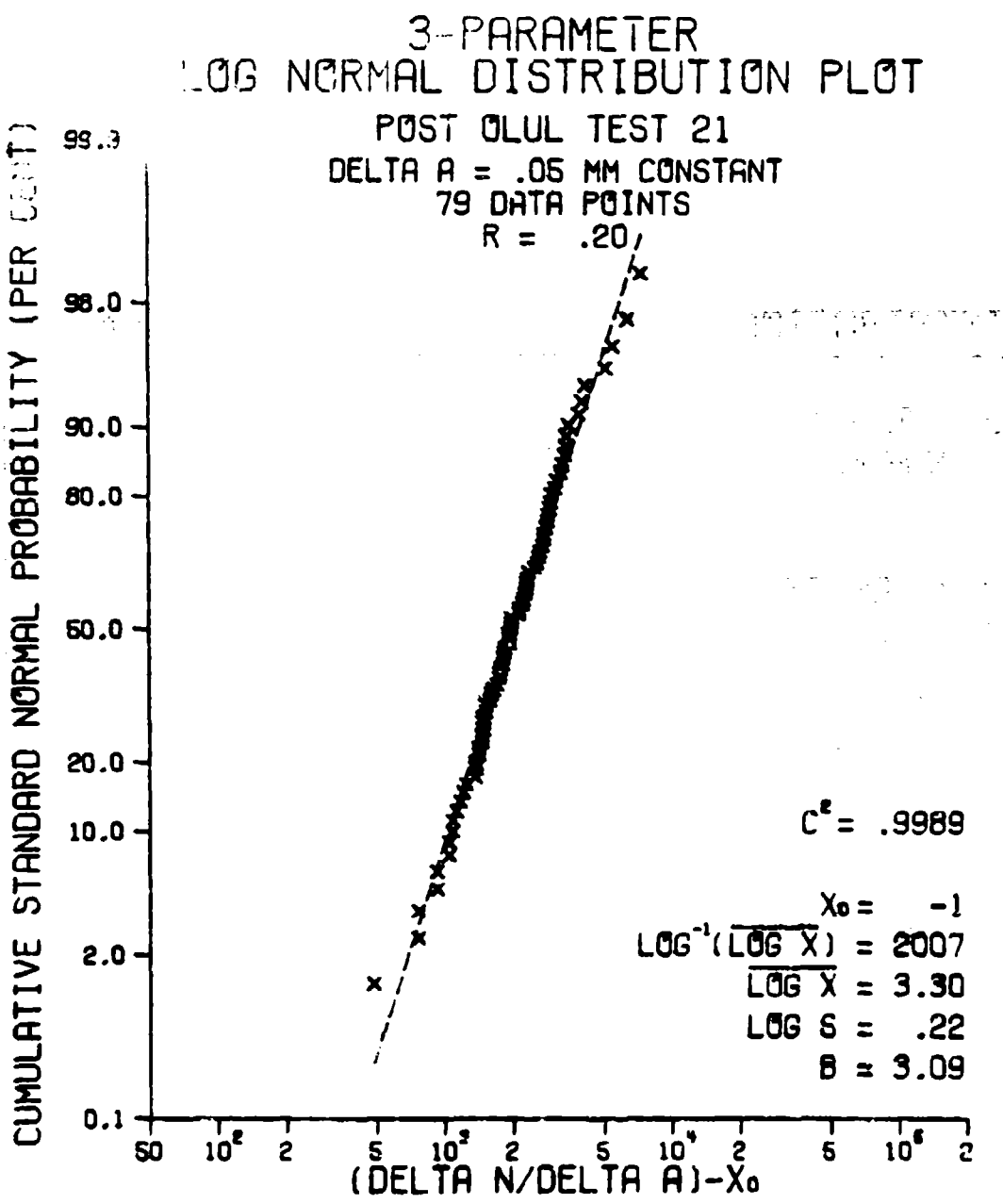

Figure 18. Fit of the ΔN/Δa Data to the 3-Parameter Log Normal Distribution

2) Include the other four distributions in the analysis of other fatigue crack propagation variables.

3) Using the constant amplitude portion of overload/underload data does not lead to a satisfactory statistical analysis. Therefore, a statistically designed test program was needed.

4) The graphical method of parameter estimation tended to be unstable and unreliable for the data used. Therefore, the Maximum Likelihood Estimators method of parameter estimation was tried and used.

5) The use of C^2 as a goodness of fit criterion was poor because it failed to distinguish between the distributions very well. Therefore, the chi-square and Kolmogorov-Smirnov goodness of fit tests were tried and used.

8.2 Effect of Quadratic 7-Point Incremental Polynomial Method

The second step of the analysis was to examine the effect using the quadratic 7-point incremental polynomial method vs. using the secant method in calculating the variable $\Delta N/\Delta a$. This was done by running the DELTCP program and changing the ΔN calculation method for each of the data sets. Once the $\Delta N/\Delta a$ data was calculated for each data set, it was run on the DNDDPG program to determine the effect of the ΔN calculation method on the distribution parameters. The most noticeable effect was the decrease in the variance using the quadratic 7-point incremental polynomial method as shown in Table II. From this, it is evident that the quadratic 7-point incremental polynomial method introduces quite a smoothing effect in reducing the amount of data scatter and thus the data variance.

Table II

Smoothing Effect of the Incremental Polynomial Method

DISTRIBUTION	AVERAGE $\frac{\text{VAR. (I.P.)}}{\text{VAR. (SECANT)}}$	STD. DEV. OF $\frac{\text{VAR. (I.P.)}}{\text{VAR. (SECANT)}}$
2-PARAMETER NORMAL	0.419	0.0820
2-PARAMETER LOG NORMAL	0.444	0.1273
3-PARAMETER LOG NORMAL	0.647	0.2817
3-PARAMETER WEIBULL	0.871	0.4185

8.3 Life Prediction Using Estimated Distribution Parameters

The next step in the analysis was to see if the estimated distribution parameters could be used for life prediction. Using the mean of the $\Delta N/\Delta a$ data (for the two-parameter normal distribution) and the overall change in crack length $(a_f - a_o)$, the final cycle count, N_f, was predicted and compared with the observed value of N_f for each set of data and then averaged over all the data sets. The results are shown in Table III. From the relatively low amount of error, it is evident that statistical methods using estimated distribution parameters could prove invaluable for life prediction.

Table III

Life Prediction Based on the Mean

AVERAGE $\frac{N_{F\ PREDICTED}}{N_{F\ OBSERVED}}$	PERCENT ERROR
1.011	2.93

8.4 Effect of Δa

The final step in the analysis of the previously generated data was to determine the effect of the size of Δa. This was done by using the DELTCP program to generate ΔN data with different values of Δa. By

rejecting certain successive data points (i.e. every 1 out of 2, every 2 out of 3, etc.), data with increasing values of Δa were generated. The DNDDPG program was then run on each different Δa set of data for each of the data sets. Also, several tests at the same load conditions were combined to give a large amount of data and then Δa was increased as described above. The results are shown in Figure 19 and Table IV. From these results, it is obvious that the larger Δa is, the smaller the resulting variance of the data will be.

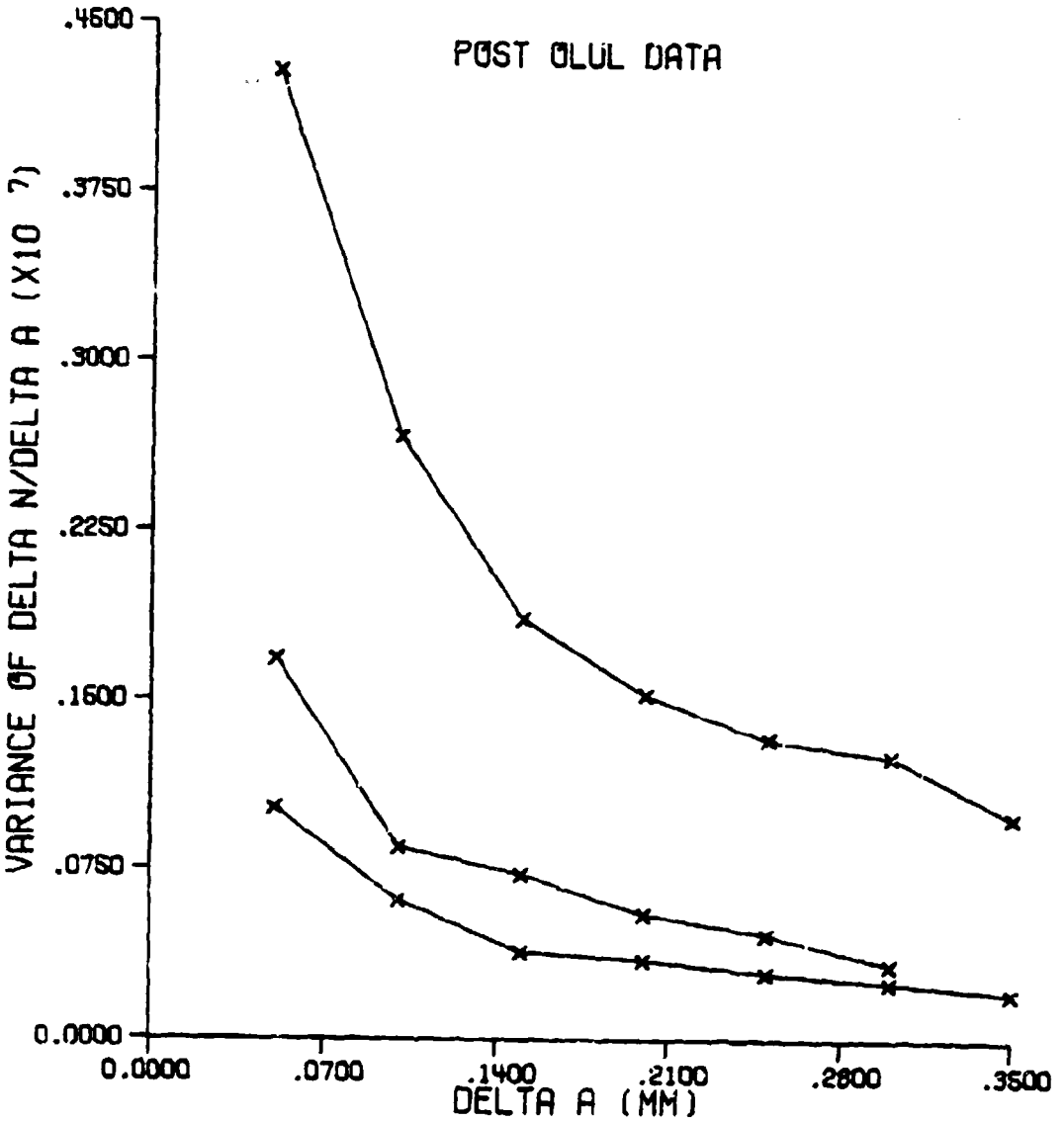

Figure 19. Effect of Increasing Δa

Table IV

Effect of Increasing Δa

DISTRIBUTION	AVERAGE VAR. (ΔA=.10 MM) / VAR. (ΔA=.05 MM)	AVERAGE VAR. (ΔA=.15 MM) / VAR. (ΔA=.05 MM)
2-PARAMETER NORMAL	0.617	0.513
2-PARAMETER LOG NORMAL	0.660	0.539
3-PARAMETER LOG NORMAL	0.851	0.412
3-PARAMETER WEIBULL	0.883	0.761

SECTION IX

EXPERIMENTAL INVESTIGATION

In an effort to answer the investigation objectives, it became necessary to conduct an experimental investigation to provide adequate data for subsequent analysis. Through the use of previously collected data (Section 8), it became increasingly clear that any experimental investigation that would be expected to provide meaningful results would have to be statistically designed. Through the use of some preliminary theoretical and experimental testing, a test program was designed.

9.1 Experimental Test Program

Given the objectives of the investigation (Section 3), it was evident that replicate tests under identical load and environmental conditions had to be conducted. It was also obvious that constant amplitude loading should be used rather than constant ΔK (load shed) loading since it would be much easier to control and replicate and also give a range of ΔK levels. To be able to find the distributions of N and da/dN, the data from each test had to be taken at consistent discrete a levels.

To determine the actual load levels to be used, several preliminary tests using the same lot of the same material were conducted. To obtain the desired growth rates ($da/dN_{min} \cong 1 \times 10^{-6}$ in./cycle and $da/dN_{max} \cong 5 \times 10^{-5}$ in./cycle) and keep the testing time within reason, it was found that ΔP should be 4200 lbs. It was also determined to use an R ratio of 0.2 to stay well out of the compression region.

A preliminary theoretical investigation was conducted to determine where the data was to be taken. It was found that to get the desired range of growth rates, the data would have to be taken over at least 40.0 mm. It was determined that steady state conditions would not exist until 9.0 mm due to the crack initiation load shedding process. In an effort to reduce data error as much as possible and still obtain a reasonable amount of data, the initial Δa was chosen to be 0.20 mm based on the statistical analysis of previous data (Section 8.4). Since the growth rate would be too fast to operate the optical system and the printer at the end of the test for the load levels chosen, Δa would be increased to 0.40 mm and finally to 0.80 mm. The number of data points taken at $\Delta a = 0.40$ mm and $\Delta a = 0.80$ mm were arranged so that when successive data points were rejected (to find the effect of increasing Δa), there would be no large gaps in the data. A schematic representation of the test program is shown in Figure 20.

In order to obtain enough data to conduct a meaningful statistical analysis, it was determined that there should be at least 50 replicate tests [13]. However, since more specimens were available, a total of 68 tests were conducted, thereby increasing the confidence of the statistical analysis results. The test conditions are listed below.

a_0 = 9.00 mm.

a_f = 49.80 mm.

R = 0.20

P_{min} = 1050 lbs.

P_{max} = 5250 lbs.

ΔP = 4200 lbs.

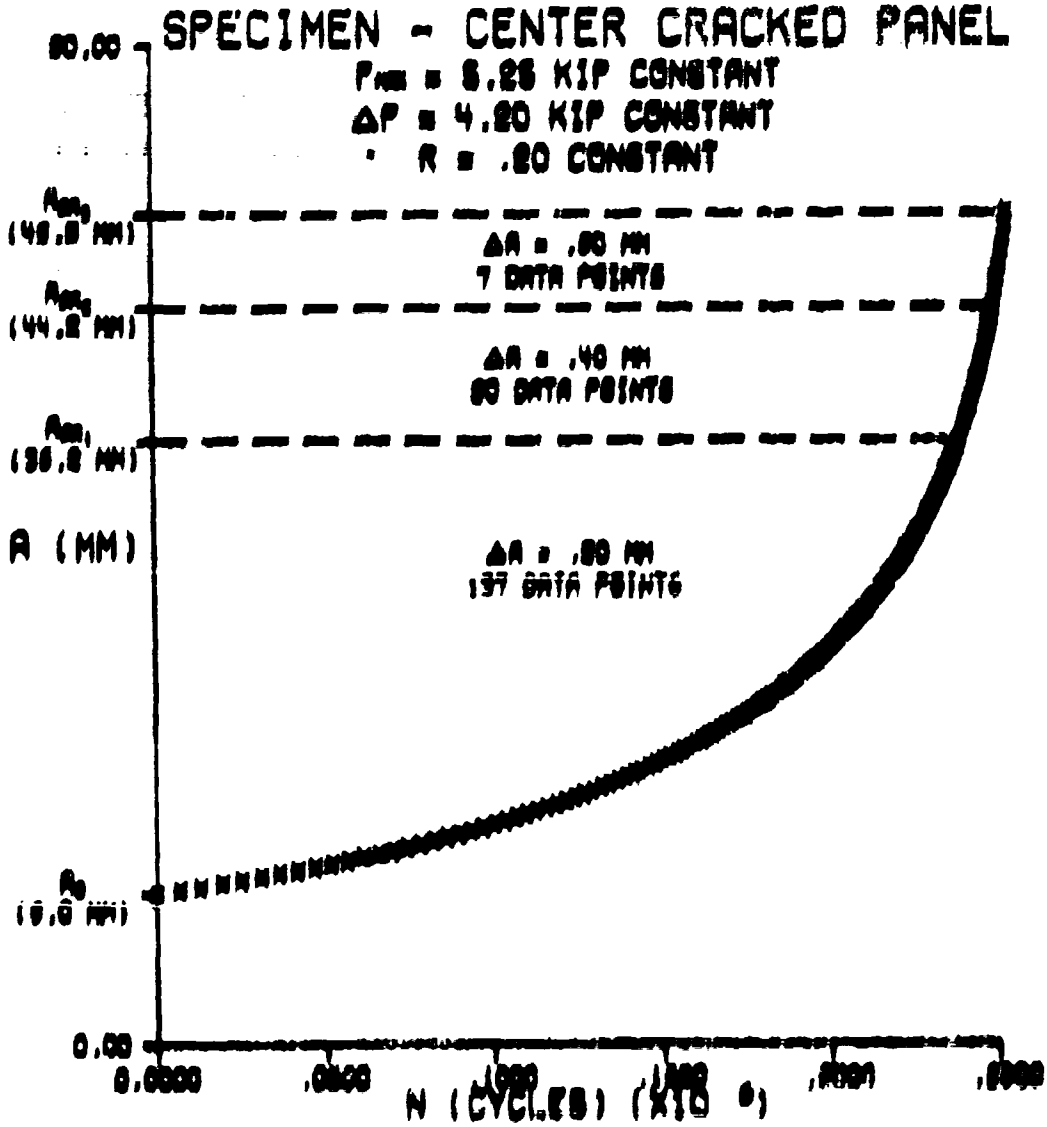

Figure 10. Test Program

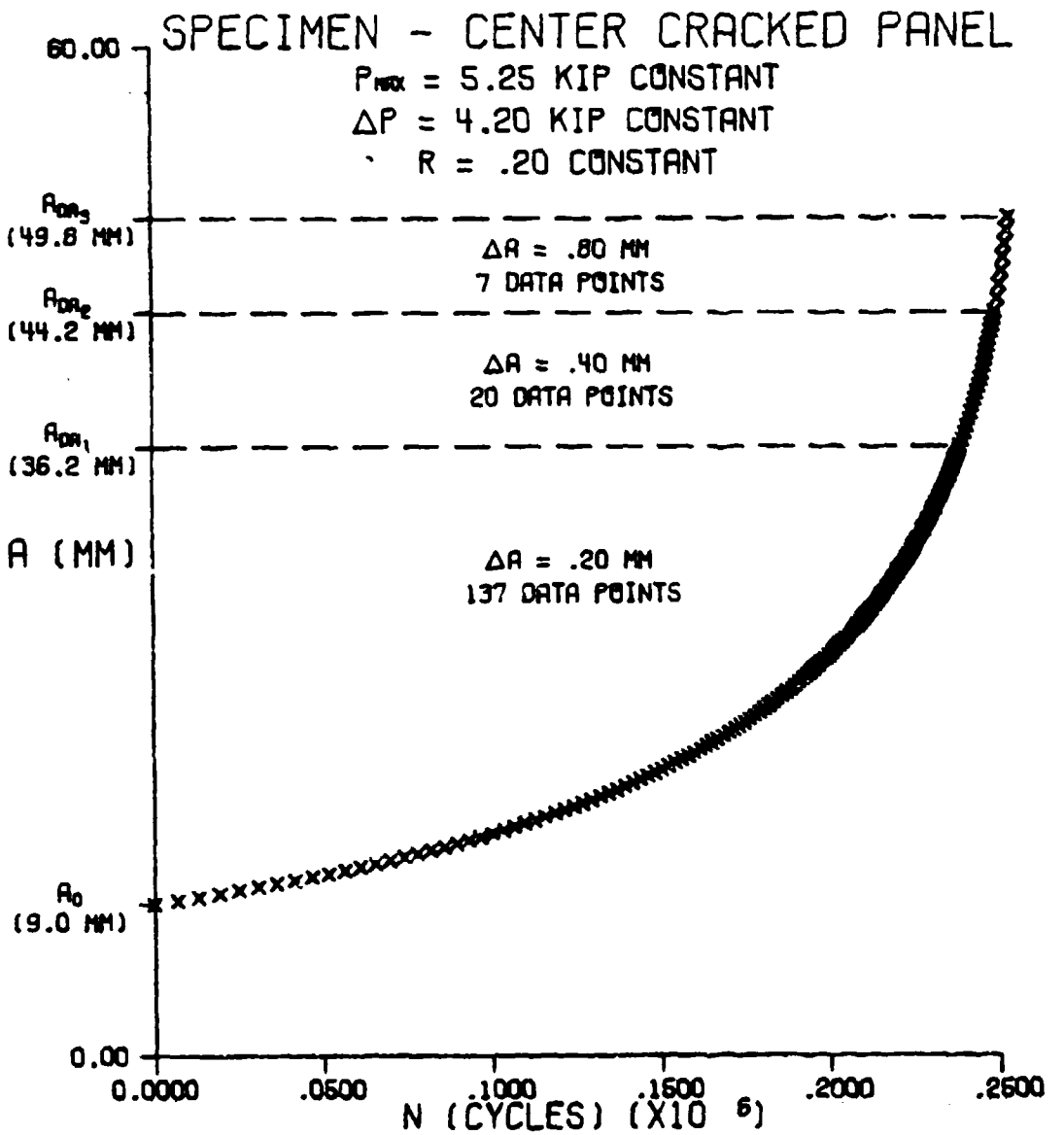

Figure 20. Test Program

9.2 Test Specimen

The test specimens used in this investigation were 0.100 inch thick center crack panels of 2024-T3 aluminum alloy. The specimen geometry is shown in Figure 21.

Test specimens were obtained with a mill finish and polished to a mirror finish in the vicinity of the crack path to facilitate optical observation of the crack tip during crack growth measurement. The lot of specimens was numbered in order as they were taken out of the shipping crate so that true randomization of the samples could be accomplished. The fixture plate holes were drilled and reamed to the desired dimensions. The stress raiser shown in detail in Figure 21 was machined with an electro-discharge machine.

Before loading each specimen, the centerline of the specimen was scribed at the stress raiser and a silica gel desiccant was applied at the stress raiser. The entire expected crack path was then sealed with clear polyethylene to insure desiccated air at the crack tip. Loading was then applied parallel to the direction of rolling of the material.

9.3 Test Equipment

The test machine was a 20 Kip electro-hydraulic closed-loop system operated in load control. A function generator was used to generate a sinusoidal voltage signal which, when superimposed on a d.c. set point voltage, constituted the desired input to the system. During testing, an oscilloscope was used to monitor the feedback signal (load) and the output of the amplitude measurement system of the testing machine to insure correct load levels and sinusoidal loading. A digital cycle counter was used to count the number of applied load cycles. Crack growth was monitored with a zoom stereo microscope operated at a magnification of 150x

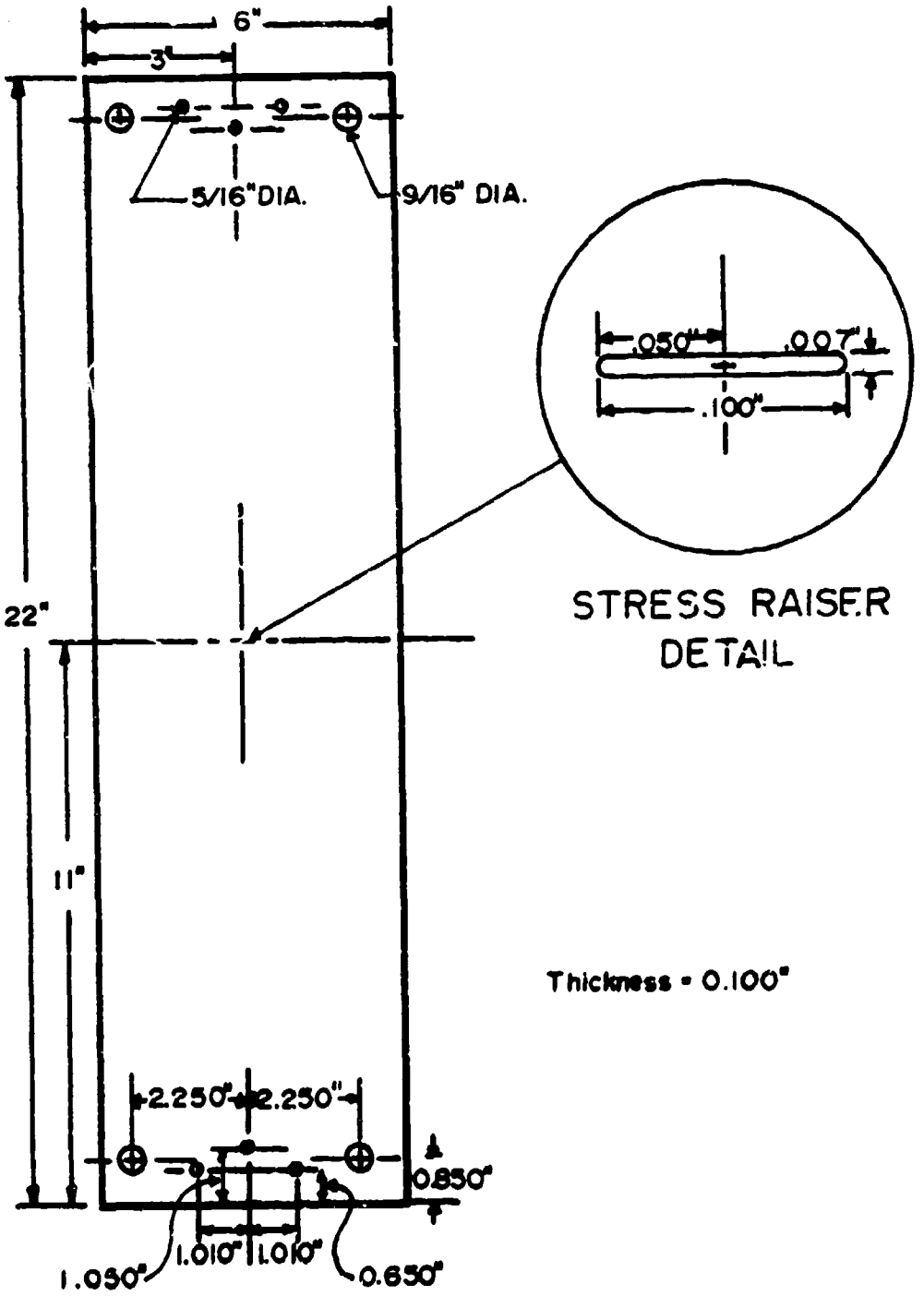

Figure 21. Test Specimen

rigidly mounted on a horizontal and vertical digital traversing system. A crosshair mounted in the microscope was used as a reference line during data acquisition. A digital resolver system on the horizontal traverse produced a digital output with a resolution of 0.001 mm (.00004 in.). The direction of travel of the optical system prior to data acquisition was never changed during a test to eliminate any hysteresis effects in the traverse system. Both the digital traverse and cycle counter outputs (crack length and number of cycles) were connected to a mechanical printer. The printer printed both the crack length and the cumulative cycle count by the operation of a push button. A strobe light synchronized with the feedback signal was triggered at the point in the load cycle when the crack was most fully open to illuminate the crack tip. More detailed discussions of the test equipment can be found in references [37,38,39].

9.4 Test Procedure

Since the scope of this investigation strictly involved the determination of the effect of material properties on fatigue crack propagation, care was taken to control as many other variables as possible. All tests were subject to nearly identical environmental conditions of room temperature (24°C) and desiccated air. Loads were controlled to within 0.2% of the desired load using the test machine's amplitude measurement system. To prevent any effects from the order in which the specimens were run, the specimens were randomized using a computer program which utilized a random number generator. The tests were run in the random order determined by this program. The order of tests is shown in Appendix K.

Crack initiation starting at the stress raiser was performed starting at ΔP = 15000 lbs. and shedding the load 10% no sooner than every 0.5 mm (12.5 times the change in plastic zone radius due to the load shed) to the desired test load level. Fatigue cycling was done initially at 10 hz up to 5.4 mm (due to reduced frequency response of the testing machine at high loads) and then at 20 hz. To make certain that no load effects were present in the data, the test load level was reached 1.0 mm before data acquisition (58 times the change in plastic zone radius due to the last load shed). The load level was held constant throughout the test (thus increasing ΔK with increasing crack length). All tests were started at the same initial crack length ($2a$ = 18.00 mm). The location of the centerline of the specimen was noted as a reference to insure consistent crack length measurements throughout the test. Cycling was continuous throughout the test to eliminate any time or underload effects on subsequent fatigue crack growth.

The crack length and number of cycles were monitored continuously for each test and discrete data points were taken as determined by the test program. Data were actually taken by advancing the optical system by the specified increment and pressing the printer push button when the crack tip had grown to the incremented position as determined by the crosshair in the stereo microscope. The amount of error in the data acquisition process is given in Section 9.5.

9.5 Measurement Accuracy

In an attempt to isolate the data variance due to the material properties, a measure of the experimental error was needed. This experimental error results from the random error in measuring the cycle count and the crack length.

By using the test machine's amplitude measurement system which compares a known input signal with the feedback signal (applied load), the loads can be controlled to within 0.2%.

Error in the crack length measurement is due to two sources. If the spatial relationship between the microscope crosshair and the scribed reference line on the specimen is not constant, then an undetermined amount of measurement error is present. This usually occurs when the microscope is accidentally moved with respect to the specimen and can be avoided by a careful experimental procedure.

The second source of crack length measurement error is the alignment of the crack tip with the microscope crosshair. This alignment process consists of 1) defining the crack tip location, 2) defining the crosshair location, and 3) comparison of the two locations to see if they are identical. If they are, then the printer button is pushed and a data point is taken.

To determine how well the observer's eye performs this alignment process, the following test was devised. A crack was initiated and the cycling was stopped when the observer determined that the crack had reached 9.00 mm. He then took 10 repeat measurements of the crack length, being careful to always approach the crack tip from the same direction to prevent any hysteresis effects. This series of 10 repeat measurements was repeated at 9 other predetermined crack lengths. The mean and standard deviation of each set of 10 repeat measurements was computed and the error of the original data point was then calculated in terms of the standard deviation. The results of the 10 sets of repeat measurements are as follows.

$\overline{X_E}$ = 0.001414 mm.

S_E = 0.001390 mm.

where

$\overline{X_E}$ is the mean of the errors,

S_E is the standard deviation of the errors.

Therefore, the average experimental error for each data point is 0.001414 mm. The average experimental error as a function of the crack length measurement interval, Δa, is shown in Table V. It should be noted here that the larger Δa is, the smaller the average experimental error is.

Table V

Average Experimental Error

ΔA INCREMENT (MM)	AVERAGE ERROR (PERCENT)
0.20	0.71
0.40	0.35
0.80	0.17

SECTION X

DATA ANALYSIS AND RESULTS

As a result of the experimental investigation conducted as described in Section 9, 68 replicate a vs. N data sets were obtained. These data are shown in Figure 22. Using these data, an analysis was performed to meet the objectives of the investigation (Section 3).

10.1 Distribution of N

The first objective to be met was to determine the distribution of N as a function of crack length. The replicate N data used was readily obtained from the original replicate a vs. N data. Typical replicate cycle count data are shown in Figure 23. The distribution of the replicate cycle count data was determined at each crack length level through the use of the CCDDP program (Section 6.2). At each crack length level, this program calculated the distribution parameters and goodness of fit criteria for the six distributions and then compared the goodness of fit criteria between five of the distributions in order to establish the distribution rankings. The generalized 4-parameter gamma distribution was not considered for the distribution rankings because it was expected to have an excellent fit to the cycle count data due to it's power parameter (Section 5.2.e). The distribution parameters, goodness of fit criteria, and the distribution rankings were then combined over all of the crack length levels.

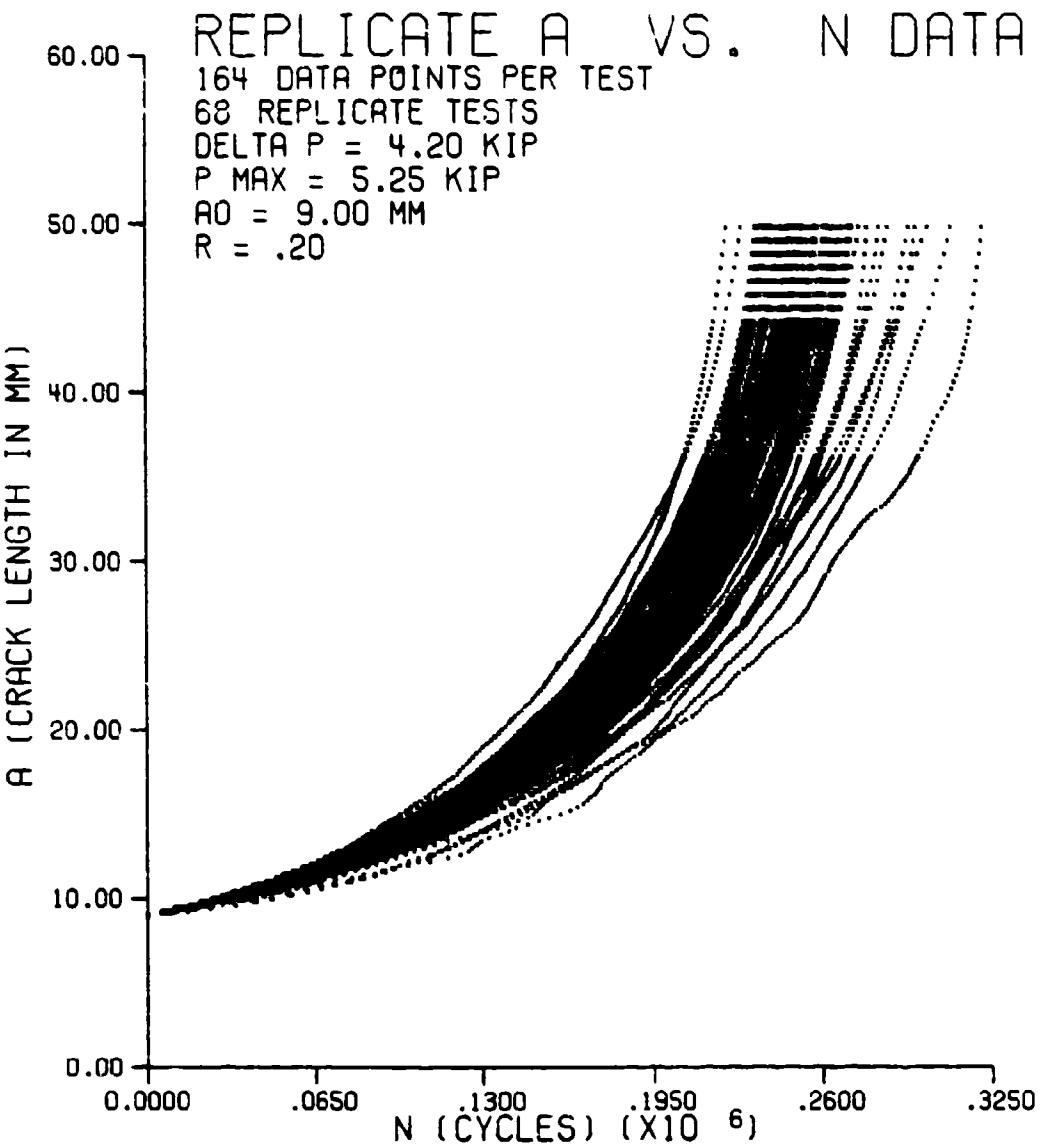

Figure 22. Original Replicate a vs. N Data

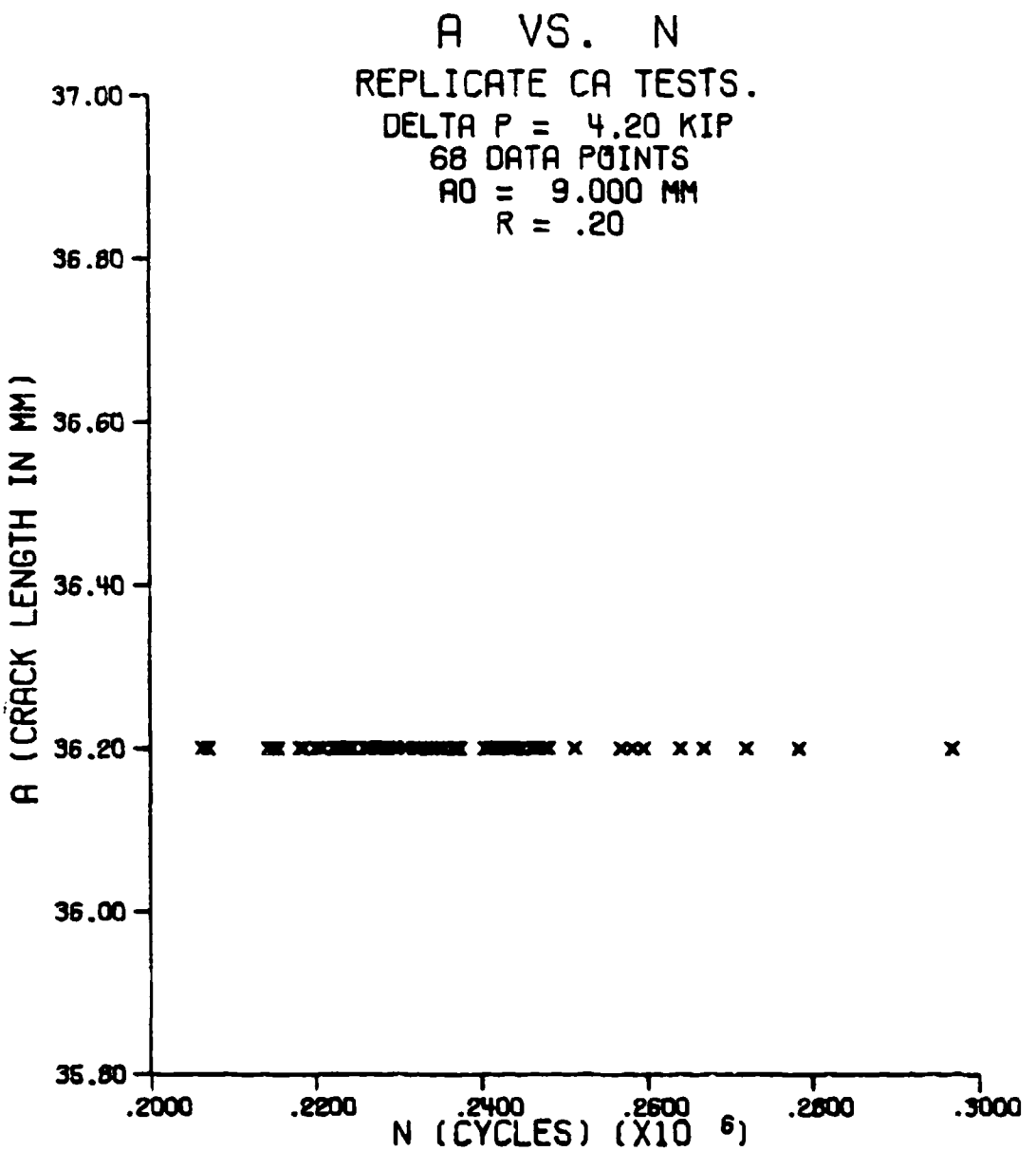

Figure 23. Typical Replicate Cycle Count Data

The distribution parameters of the cycle count data as a function of crack length were plotted for each of the six distributions and are shown in Figures 24 through 29. The distribution parameters are normalized so that their minimum and maximum values are equal to zero and one, respectively. As a result of this normalization, these figures do not show the actual values of the distribution parameters but are intended to reflect trends present in these parameters.

The goodness of fit criteria for each distribution were averaged over all of the crack length levels. These results are shown in Table VI. For these goodness of fit criteria, the best fit of the data to a distribution occurs when the chi-square tail area is a maximum, the Kolmogorov-Smirnov statistic is a minimum, and the closeness, R^2, is a maximum. Using these relationships, an understanding of which distributions provide the best fit for the cycle count data can be obtained.

The distribution rankings at each crack length level were combined over all of the crack length levels. By convention, the lower the value of the distribution ranking, the better the fit of the data to the given distribution. The mean rank and it's standard deviation for each of the distributions and the number of times each distribution was selected as the best distribution were calculated during this combining process. These results are shown in Table VII.

The 3-parameter log normal distribution provided the best fit for the cycle count data by a wide margin, as evidenced by the low distribution ranking value, the low Kolmogorov-Smirnov test statistic value, and the very large number of times it was selected as the best distribution. The 3-parameter gamma distribution provided the next best fit, while the 2-parameter log normal distribution and the 3-parameter Weibull distribution

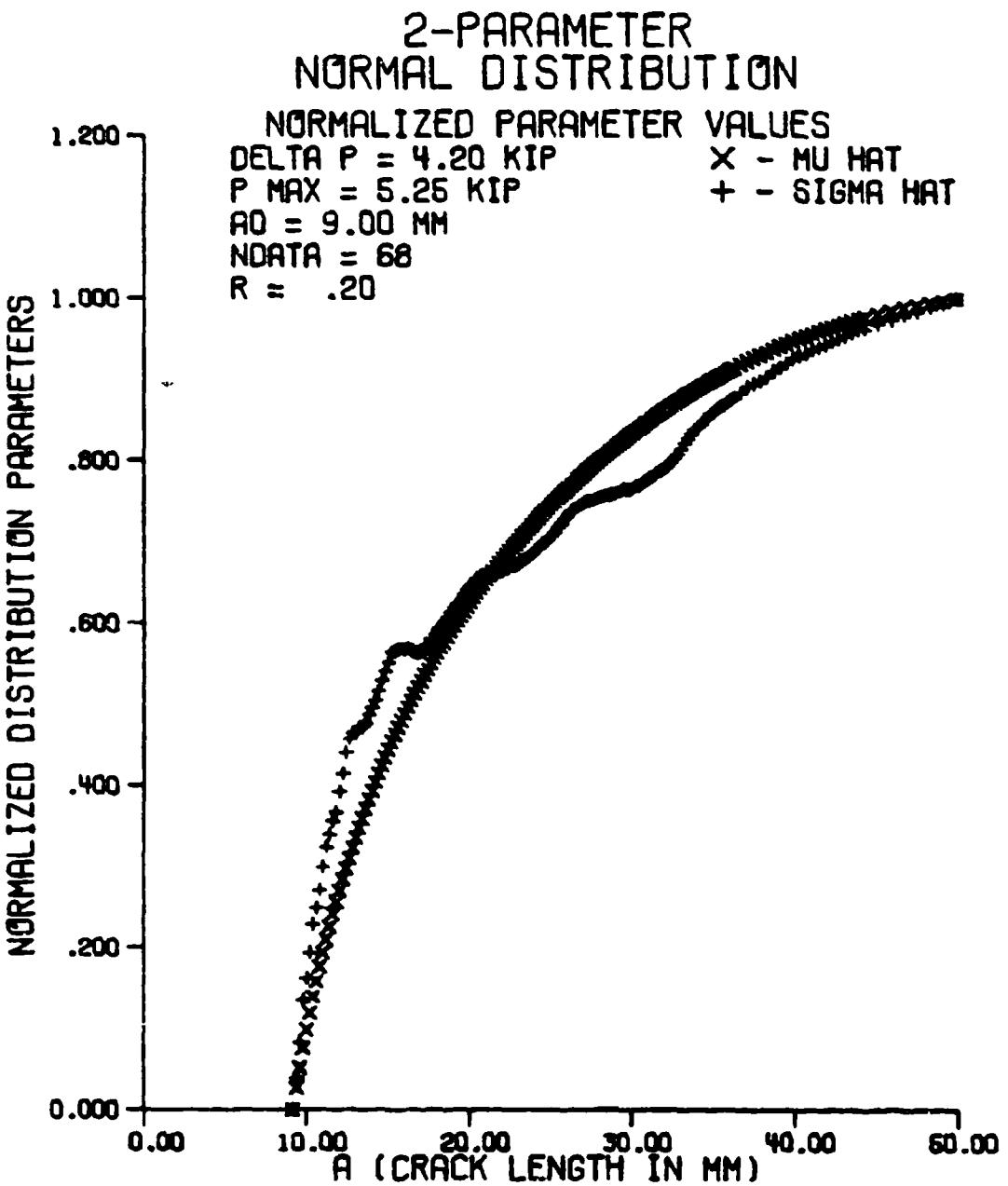

Figure 24. 2-Parameter Normal Distribution Parameters of Cycle Count Data as a Function of Crack Length

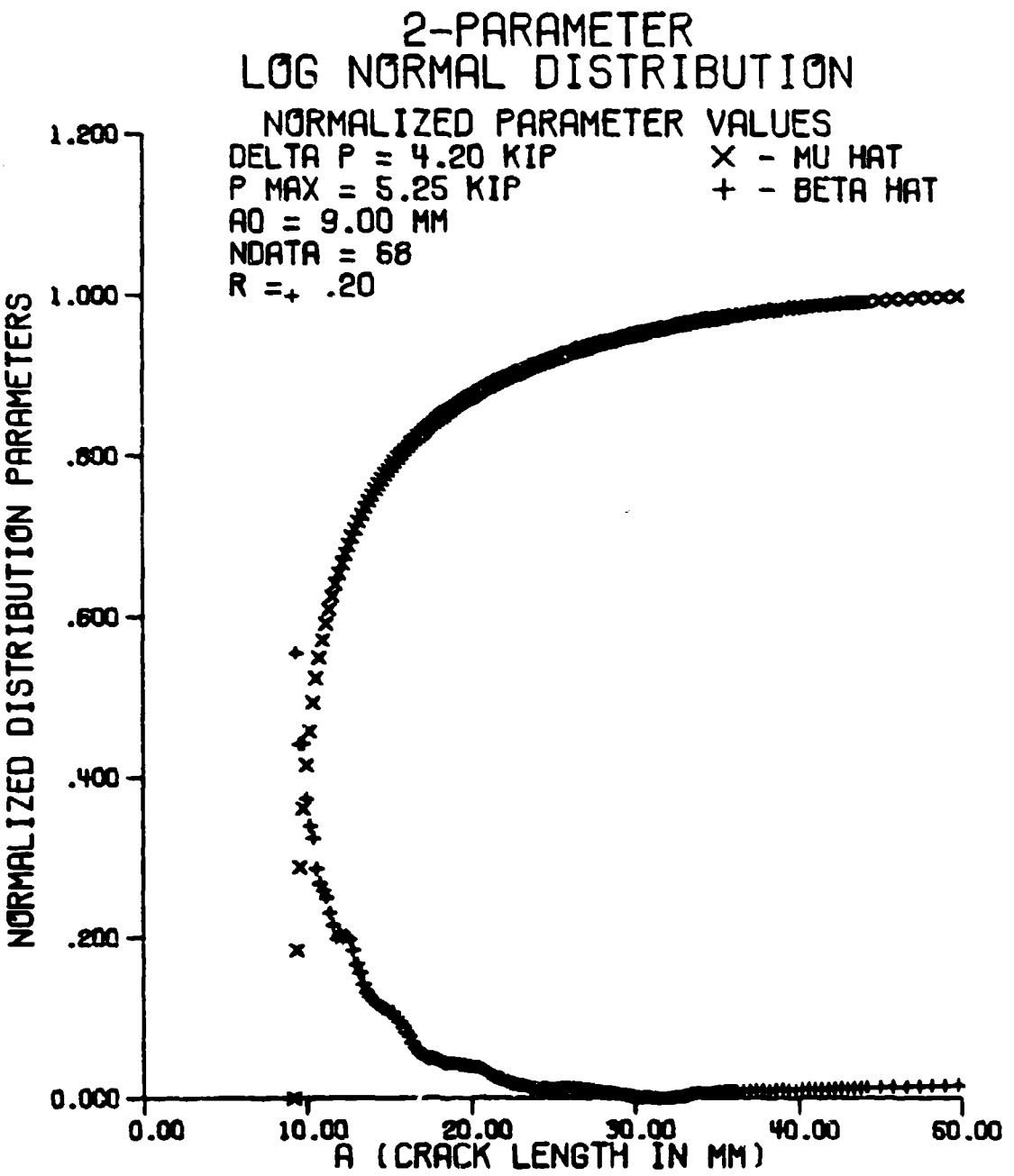

Figure 25. 2-Parameter Log Normal Distribution Parameters of Cycle Count Data as a Function of Crack Length

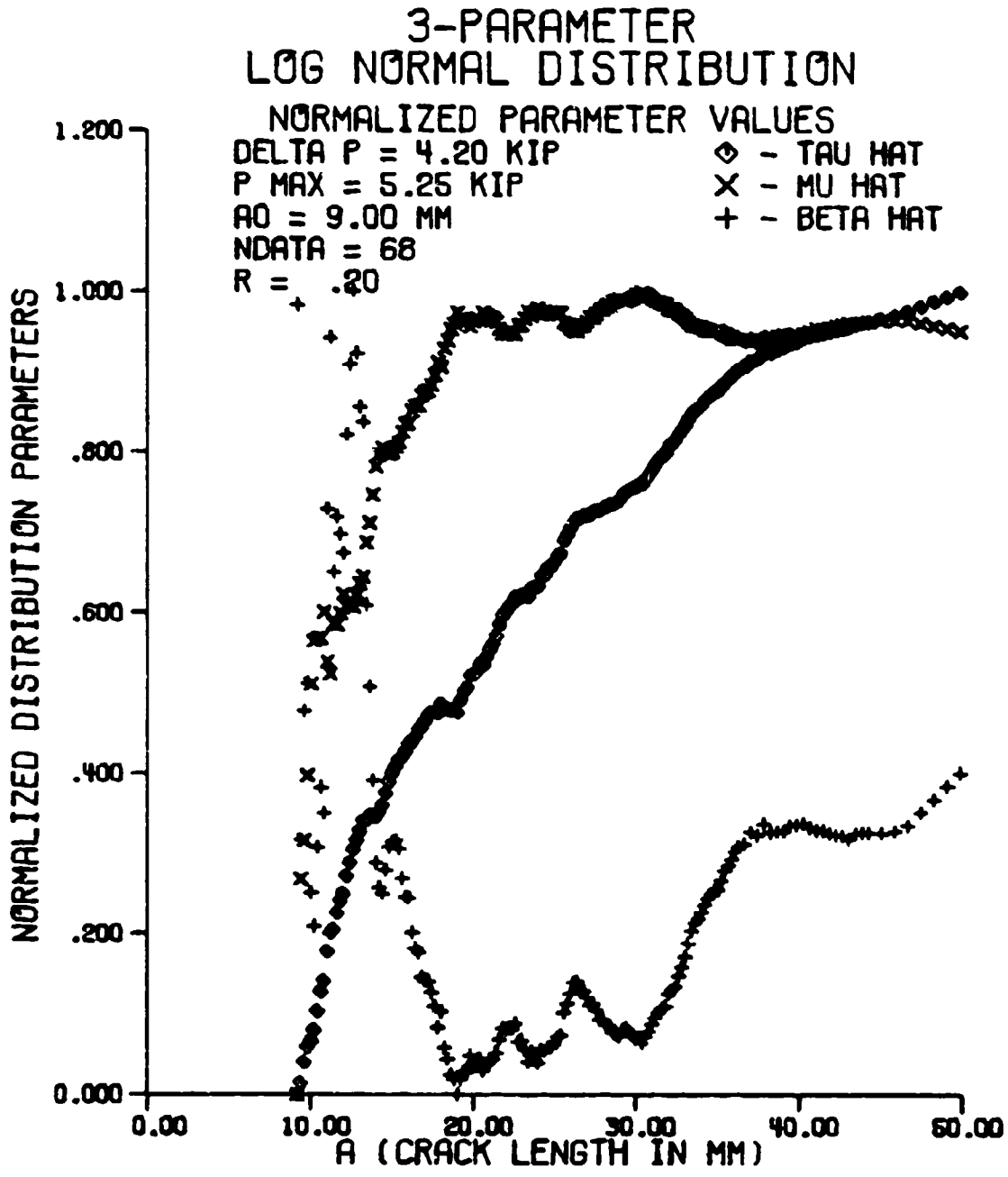

Figure 26. 3-Parameter Log Normal Distribution Parameters of Cycle Count Data as a Function of Crack Length

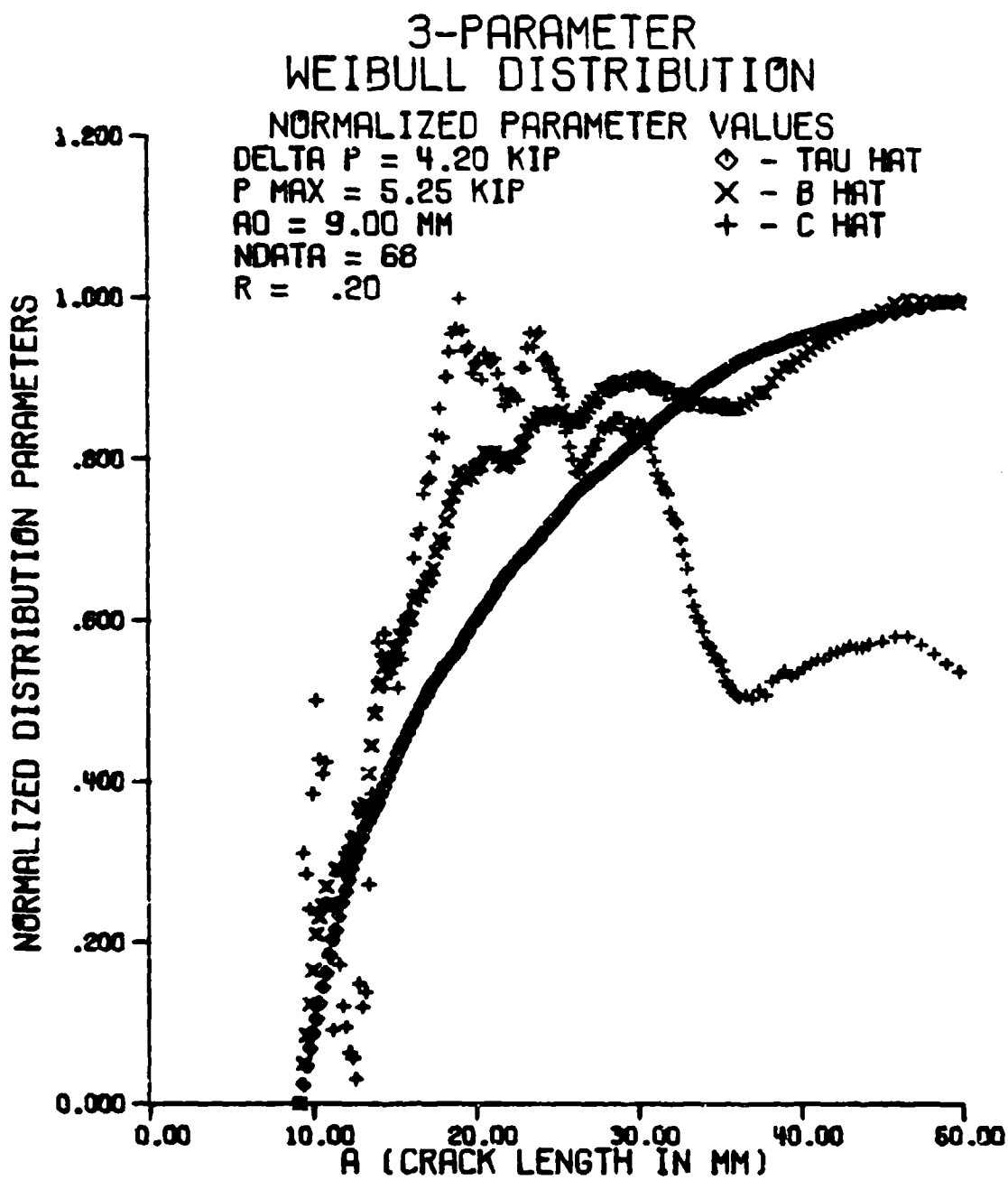

Figure 27. 3-Parameter Weibull Distribution Parameters of Cycle Count Data as a Function of Crack Length

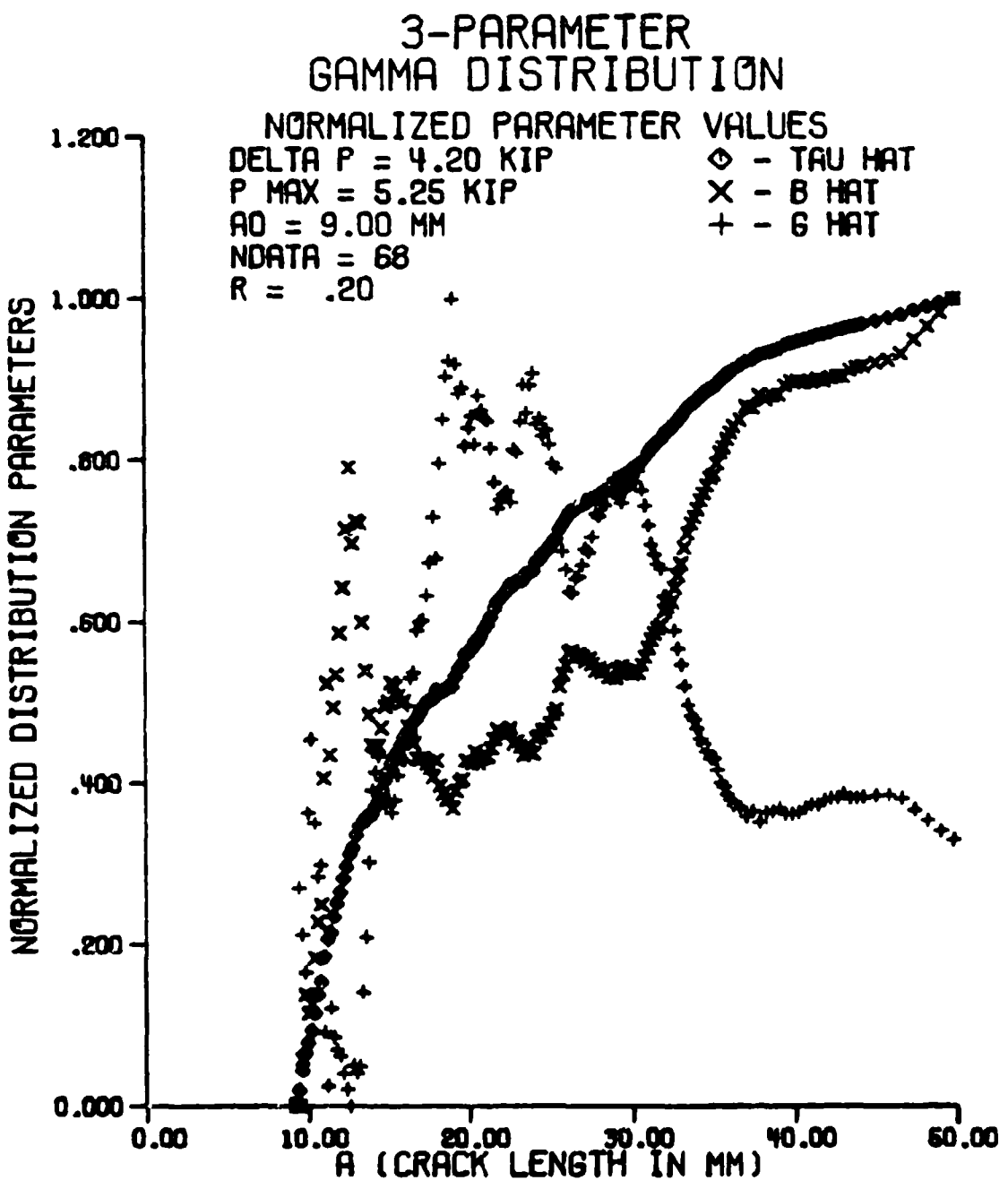

Figure 28. 3-Parameter Gamma Distribution Parameters of Cycle Count Data as a Function of Crack Length

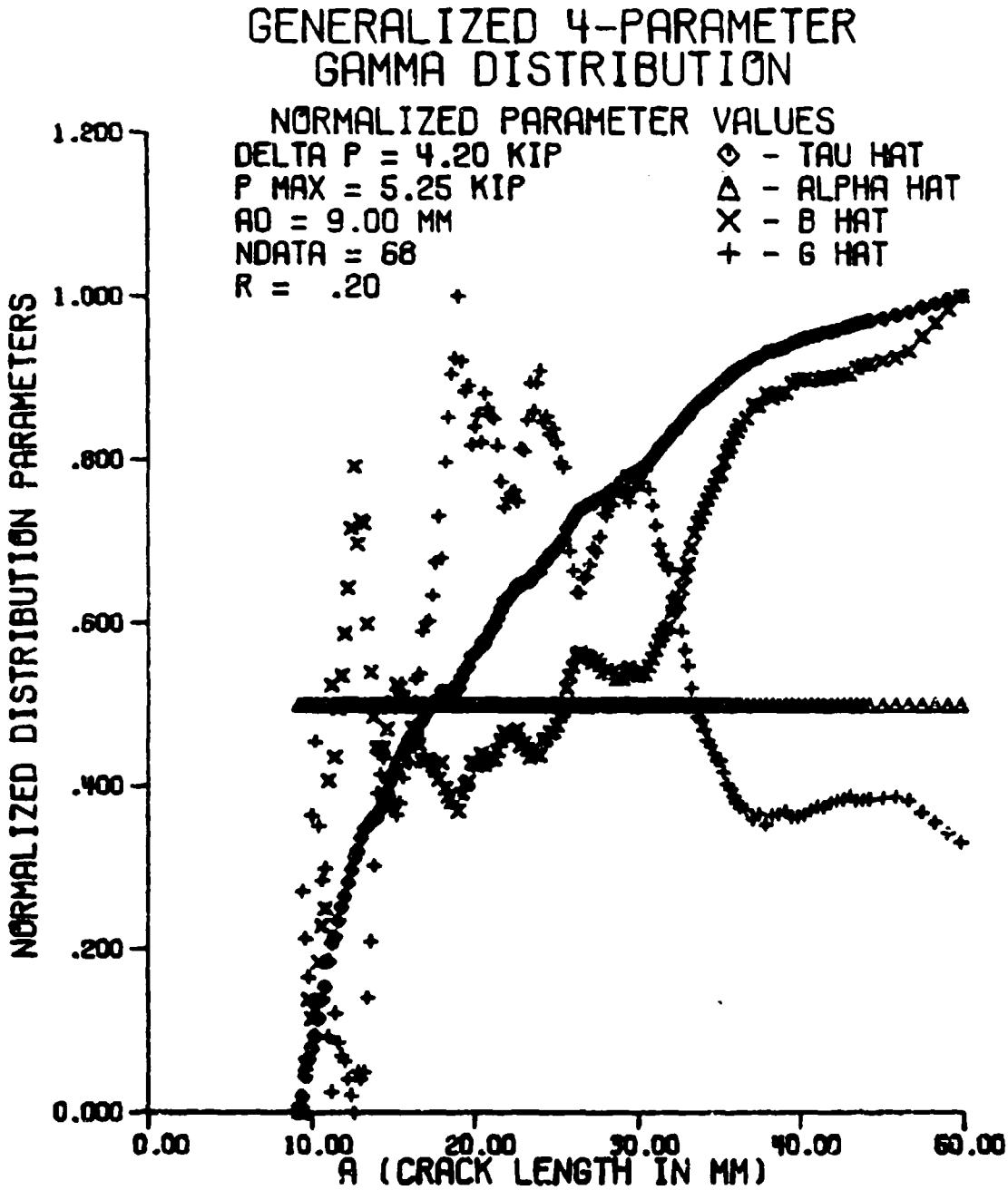

Figure 29. Generalized 4-Parameter Gamma Distribution Parameters of Cycle Count Data as a Function of Crack Length

Table VI

Average Goodness of Fit Criteria for the Distribution of Cycle Count Data

DISTRIBUTION	CHI-SQUARE TAIL AREA	KOLMOGOROV-SMIRNOV TEST	CLOSENESS (R SQUARED)
2-PARAMETER NORMAL	0.8365	0.0995	0.93310
2-PARAMETER LOG NORMAL	0.8842	0.0857	0.95799
3-PARAMETER LOG NORMAL	0.8594	0.0699	0.98223
3-PARAMETER WEIBULL	0.8340	0.0882	0.93658
3-PARAMETER GAMMA	0.8602	0.0722	0.97160
GENERALIZED 4-PARAMETER GAMMA	0.8075	0.0722	

Table VII

Distribution Rankings for the Distribution of Cycle Count Data

DISTRIBUTION	MEAN	STANDARD DEVIATION	NUMBER OF TIMES BEST DISTRIBUTION
2-PARAMETER NORMAL	4.982	0.1348	0
2-PARAMETER LOG NORMAL	3.147	0.6780	7
3-PARAMETER LOG NORMAL	1.221	0.5882	137
3-PARAMETER WEIBULL	3.650	0.6338	3
3-PARAMETER GAMMA	2.000	0.4969	16

tied for the third best fit for the data. The 2-parameter normal distribution finished last in the distribution ranking as it provided a very poor fit for the data.

10.2 Crack Growth Rate Calculation Methods

The second objective to be met was to determine which crack growth rate calculation method introduced the least amount of error into the da/dN data. This was to be done by integrating the da/dN data calculated by each crack growth rate calculation method back into a vs. N data and then calculating the error between the new a vs. N data and the original a vs. N data.

The DADNCP program (Section 7.2) was run on each of the 68 original a vs. N data sets. This program calculates the da/dN vs. ΔK data, integrates the da/dN data back into a vs. N data using Simpson's one-third rule and the trapezoidal rule, and then calculates a step by step average incremental error, as outlined by Frank and Fisher [2], for each of the six da/dN calculation methods. The da/dN calculation method which results in the lowest average incremental error is then selected as the best da/dN calculation method for that data set. The $\log_{10}$ da/dN vs. $\log_{10} \Delta K$ data are plotted for each of the da/dN calculation methods and typical plots of these data are shown in Figures 30 through 35.

The average incremental error from each da/dN calculation method was averaged over all of the data sets and the number of times each da/dN calculation method was selected as the best method was computed. These results are shown in Table VIII. The modified secant method had the lowest average incremental error, followed closely by the secant method. The modified secant method and the secant method were both selected as best

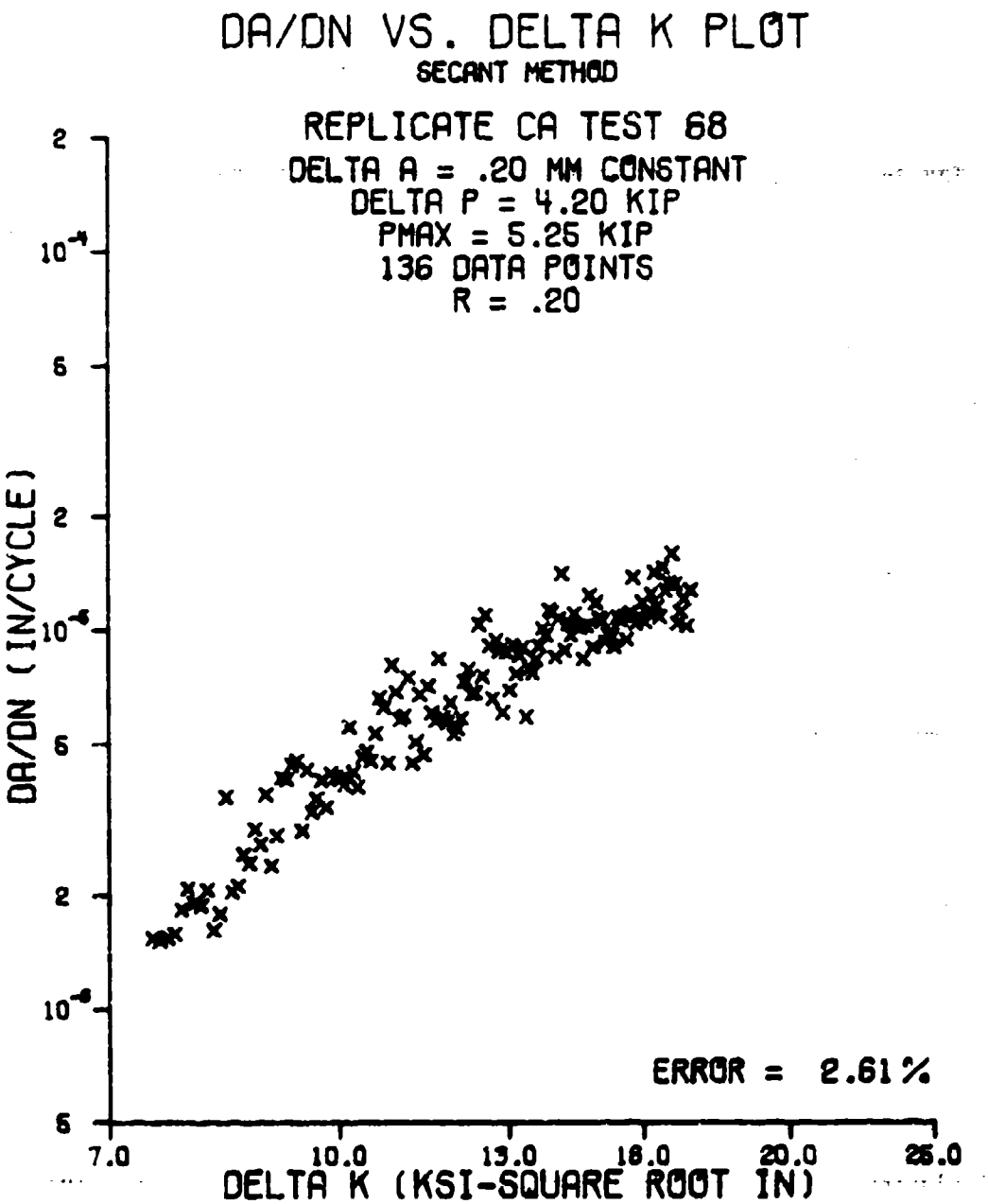

Figure 30. Typical Log_{10} da/dN vs. Log_{10} ΔK Data Calculated by the Secant Method

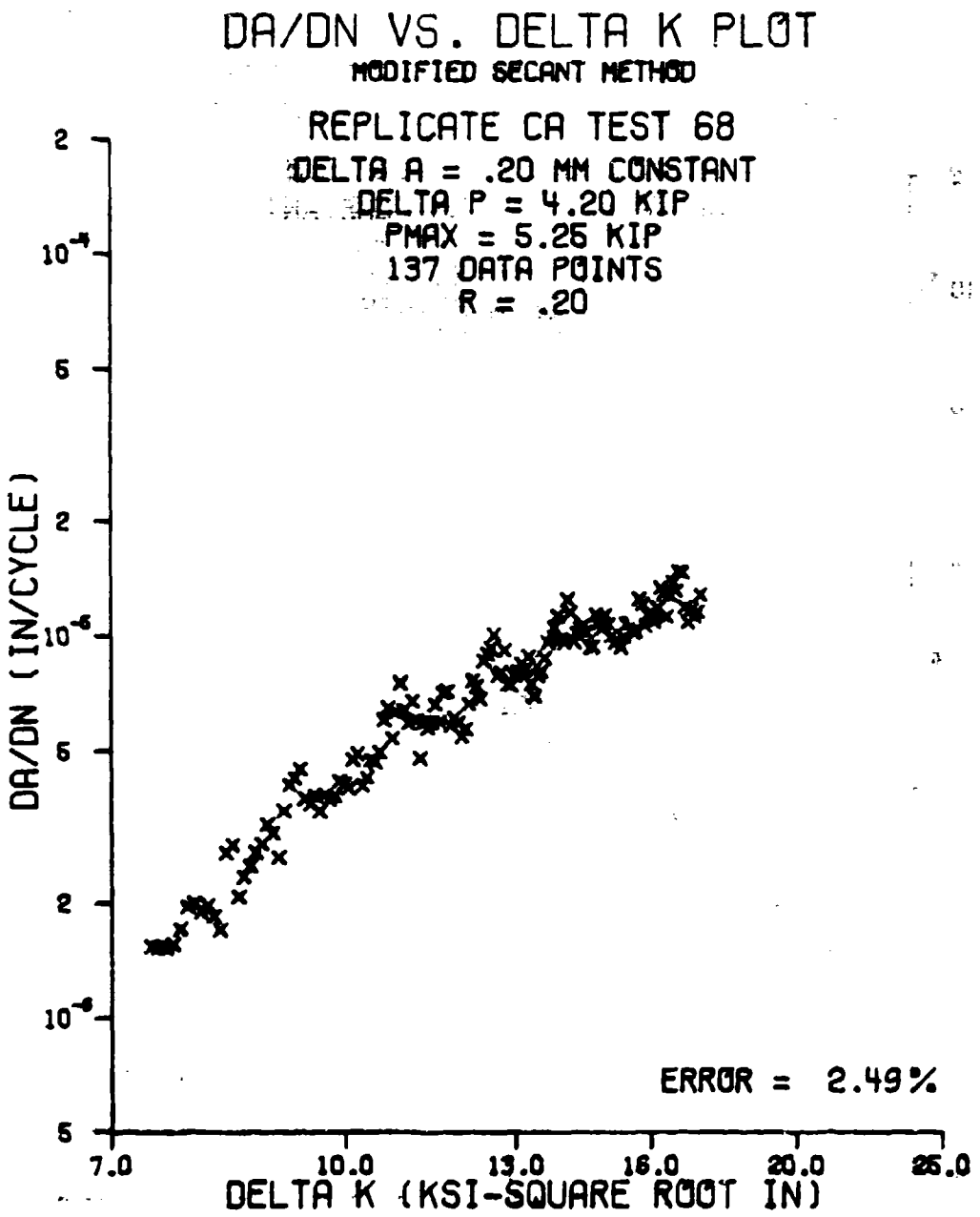

Figure 31. Typical Log_{10} da/dN vs. Log_{10} ΔK Data Calculated by the Modified Secant Method

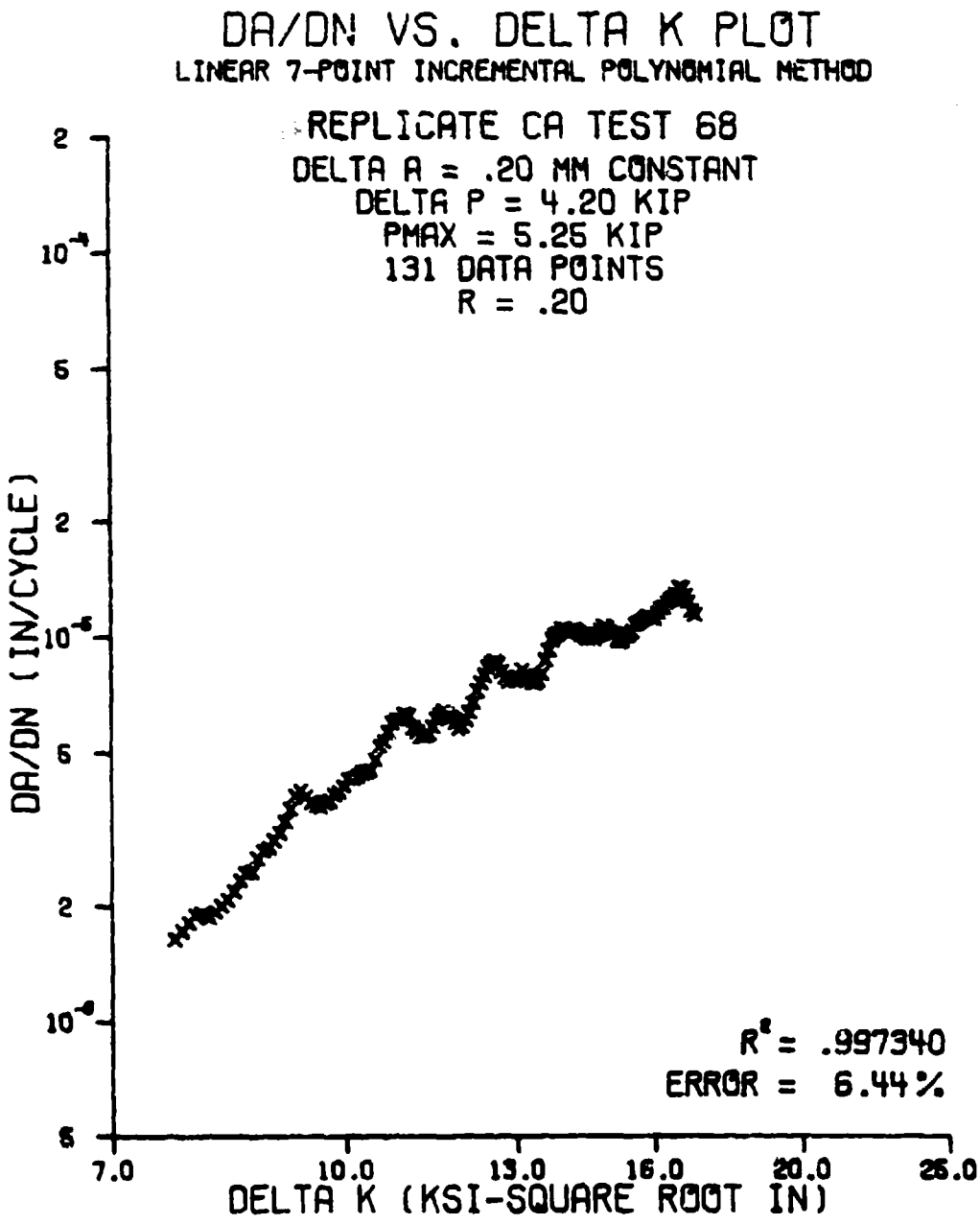

Figure 32. Typical Log_{10} da/dN vs. Log_{10} ΔK Data Calculated by the Linear 7-Point Incremental Polynomial Method

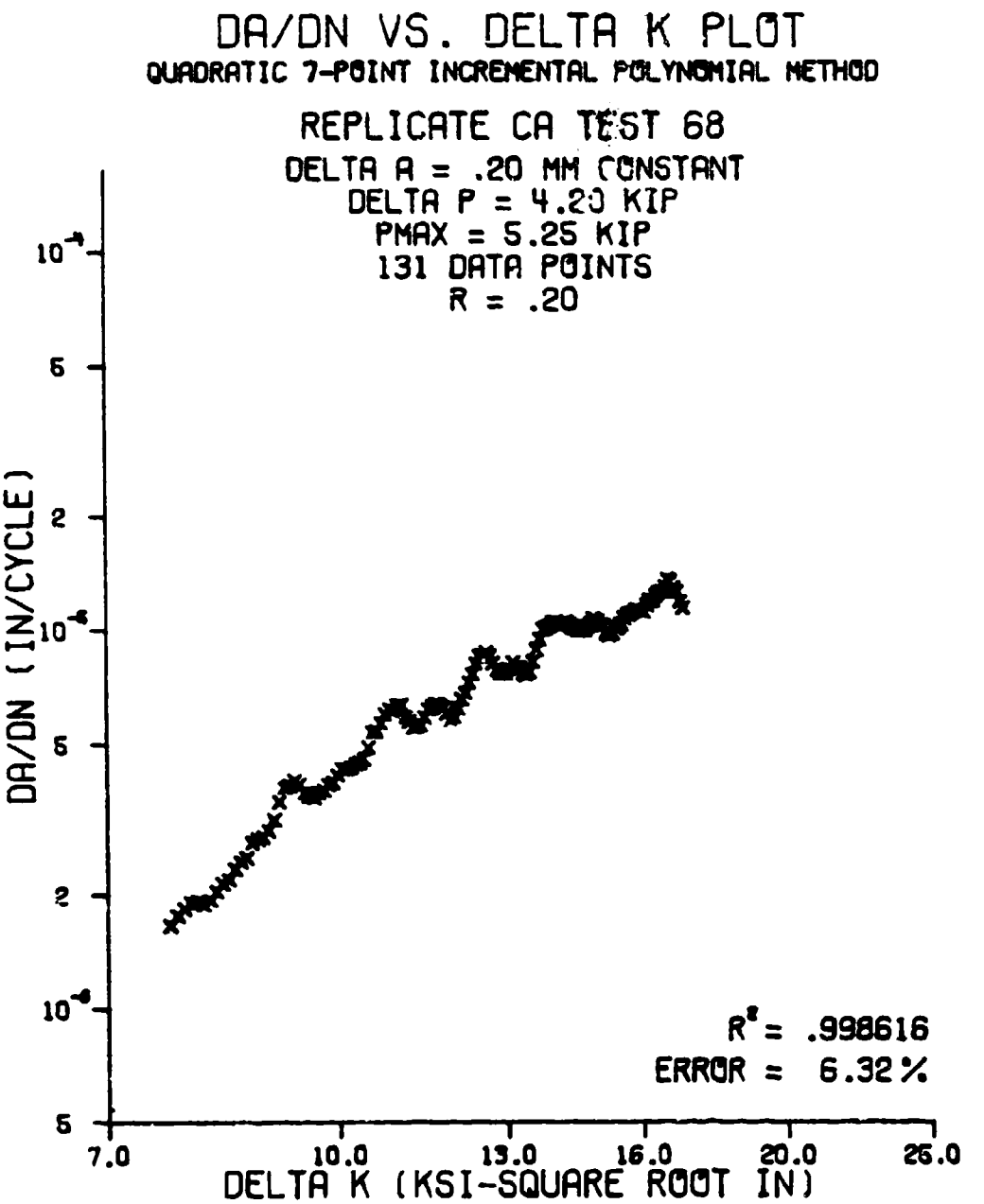

Figure 33. Typical Log_{10} da/dN vs. Log_{10} ΔK Data Calculated by the Quadratic 7-Point Incremental Polynomial Method

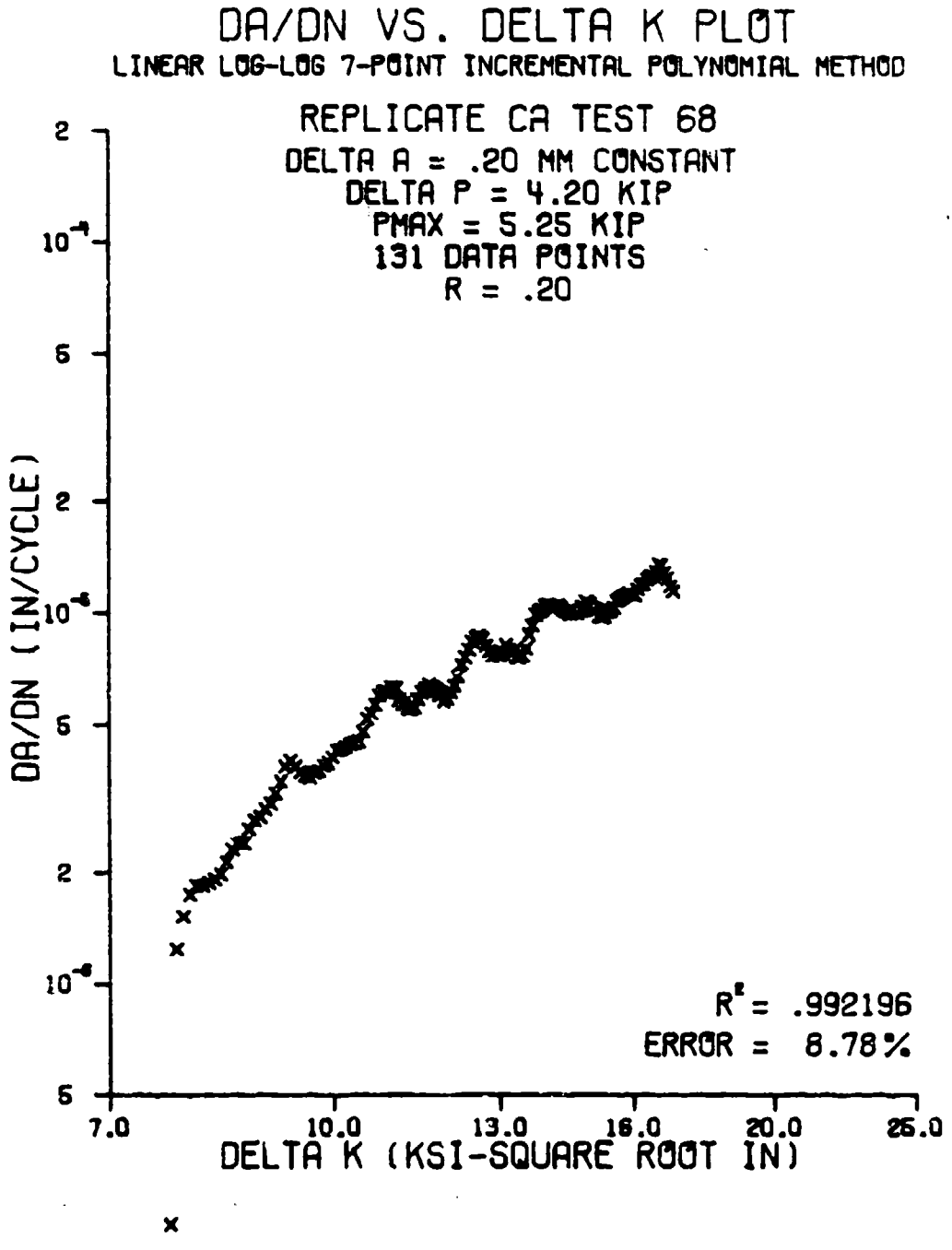

Figure 34. Typical Log_{10} da/dN vs. Log_{10} ΔK Data Calculated by the Linear Log-Log 7-Point Incremental Polynomial Method

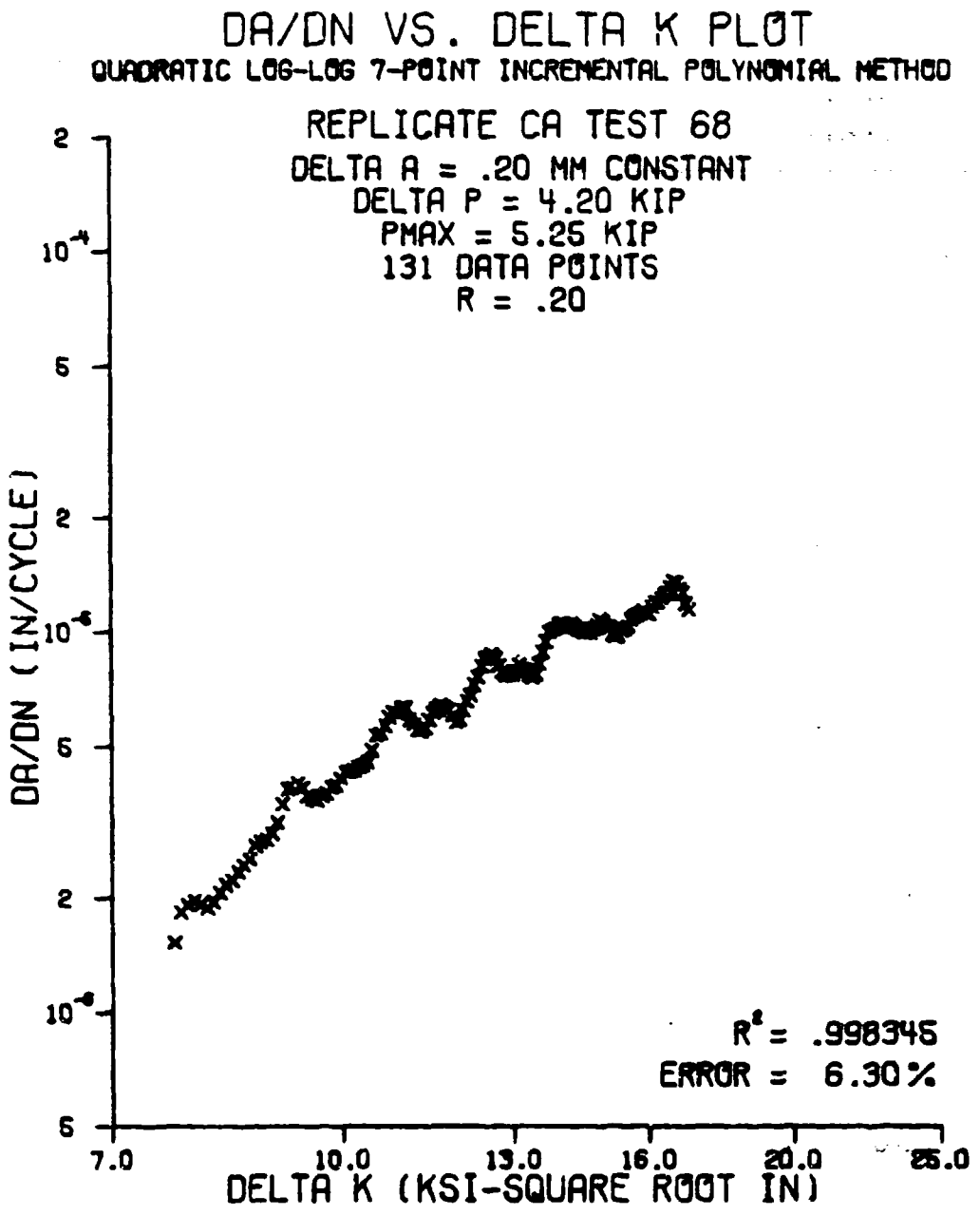

Figure 35. Typical Log_{10} da/dN vs. Log_{10} ΔK Data Calculated by the Quadratic Log-Log 7-Point Incremental Polynomial Method

Table VIII

da/dN Calculation Method Results

DA/DN CALCULATION METHOD	OVERALL AVERAGE INCREMENTAL ERROR (PER CENT)	NUMBER OF TIMES BEST METHOD
SECANT METHOD	2.70	17
MODIFIED SECANT METHOD	2.58	51
LINEAR 7-POINT INCREMENTAL POLYNOMIAL METHOD	6.96	0
QUADRATIC 7-POINT INCREMENTAL POLYNOMIAL METHOD	6.83	0
LINEAR LOG-LOG 7-POINT INCREMENTAL POLYNOMIAL METHOD	9.41	0
QUADRATIC LOG-LOG 7-POINT INCREMENTAL POLYNOMIAL METHOD	6.65	0

methods, with the modified secant method selected three times as often as the secant method. From these results, it can be stated that the modified secant method introduces the lowest amount of error into the da/dN data of the six da/dN calculation methods selected.

10.3 Distribution of da/dN

The third objective to be met was to determine the distribution of da/dN as a function of ΔK. The first set of da/dN data selected for analysis was da/dN data calculated by the secant method, with the anticipation of also finding the distribution of da/dN data calculated by the modified secant method and the quadratic 7-point incremental polynomial method. Data were selected from the first two da/dN calculation methods because of their ability to re-create the original a vs. N data and the quadratic 7-point incremental polynomial method because of its widespread use. The combined data from each of these three methods are shown in Figures 36, 37, and 38.

The steps of analysis for the distribution of da/dN are very similar to the steps of analysis used for the distribution of N. First, the replicate da/dN data used was obtained from the da/dN vs. ΔK data generated by the DADNCP program (Section 7.2) using the secant method. Typical replicate da/dN data are shown in Figure 39. The distribution of the replicate da/dN data was determined at each ΔK level through the use of the CGRDDP program (Sectio 6.3). At each ΔK level, this program calculated the distribution parameters and goodness of fit crit ia for the six distributions and then compared the goodne s of fit crite. . between the different distributions to give the distribution rankings. Again, the generalized 4-parameter gamma distribution was not included in the

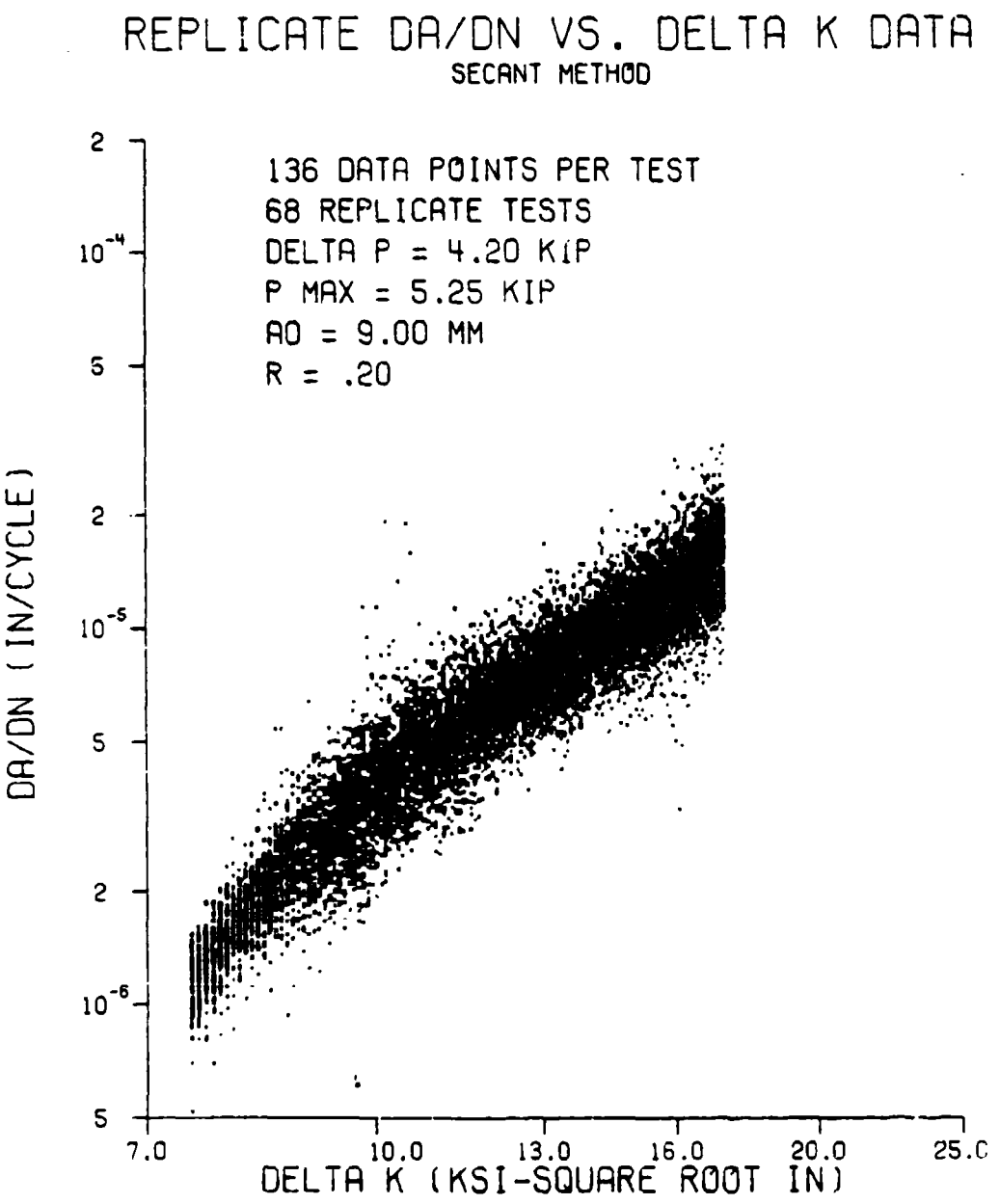

Figure 36. Combined Log_{10} da/dN vs. Log_{10} ΔK Data Calculated by the Secant Method

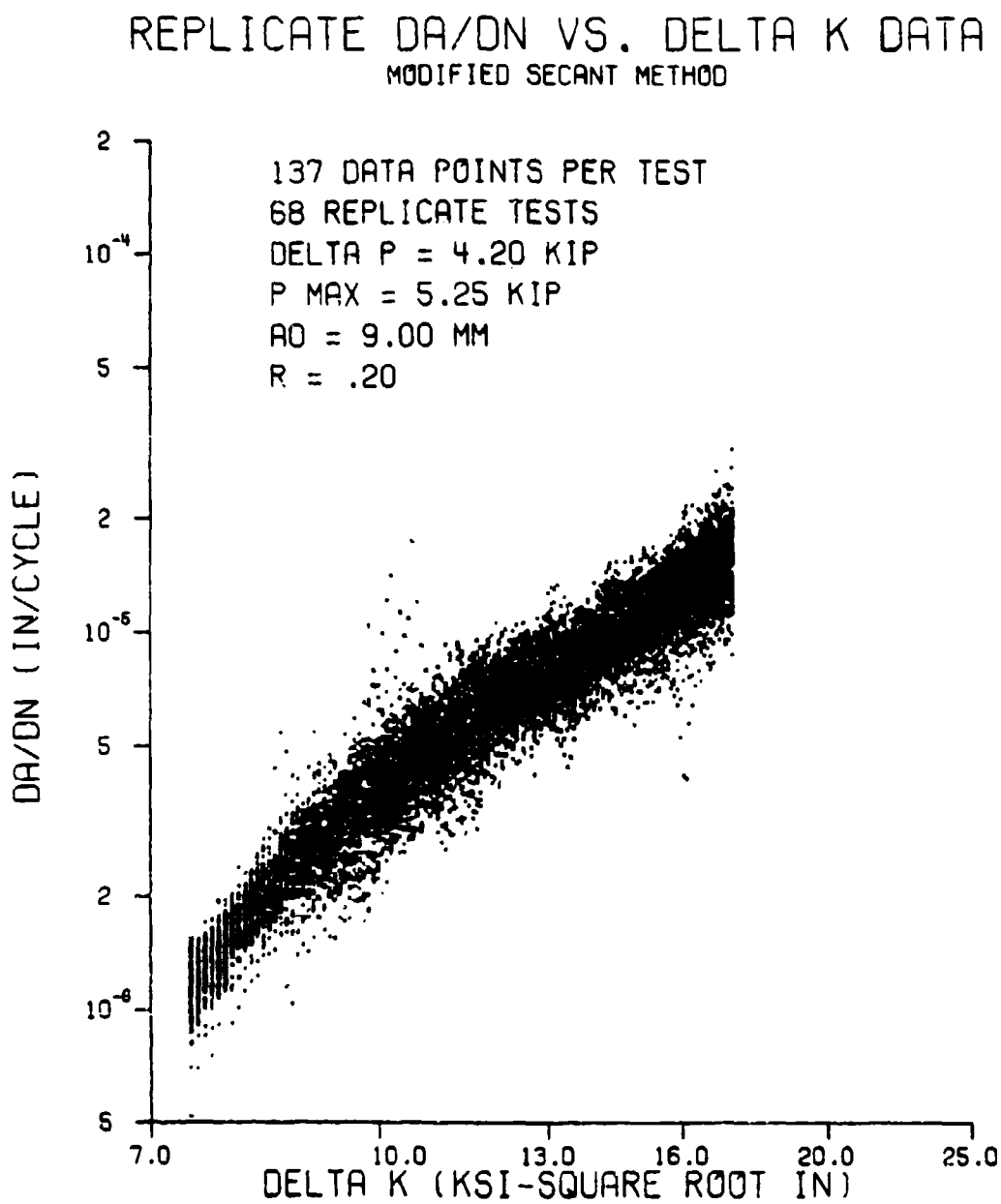

Figure 37. Combined Log_{10} da/dN vs. Log_{10} ΔK Data Calculated by the Modified Secant Method

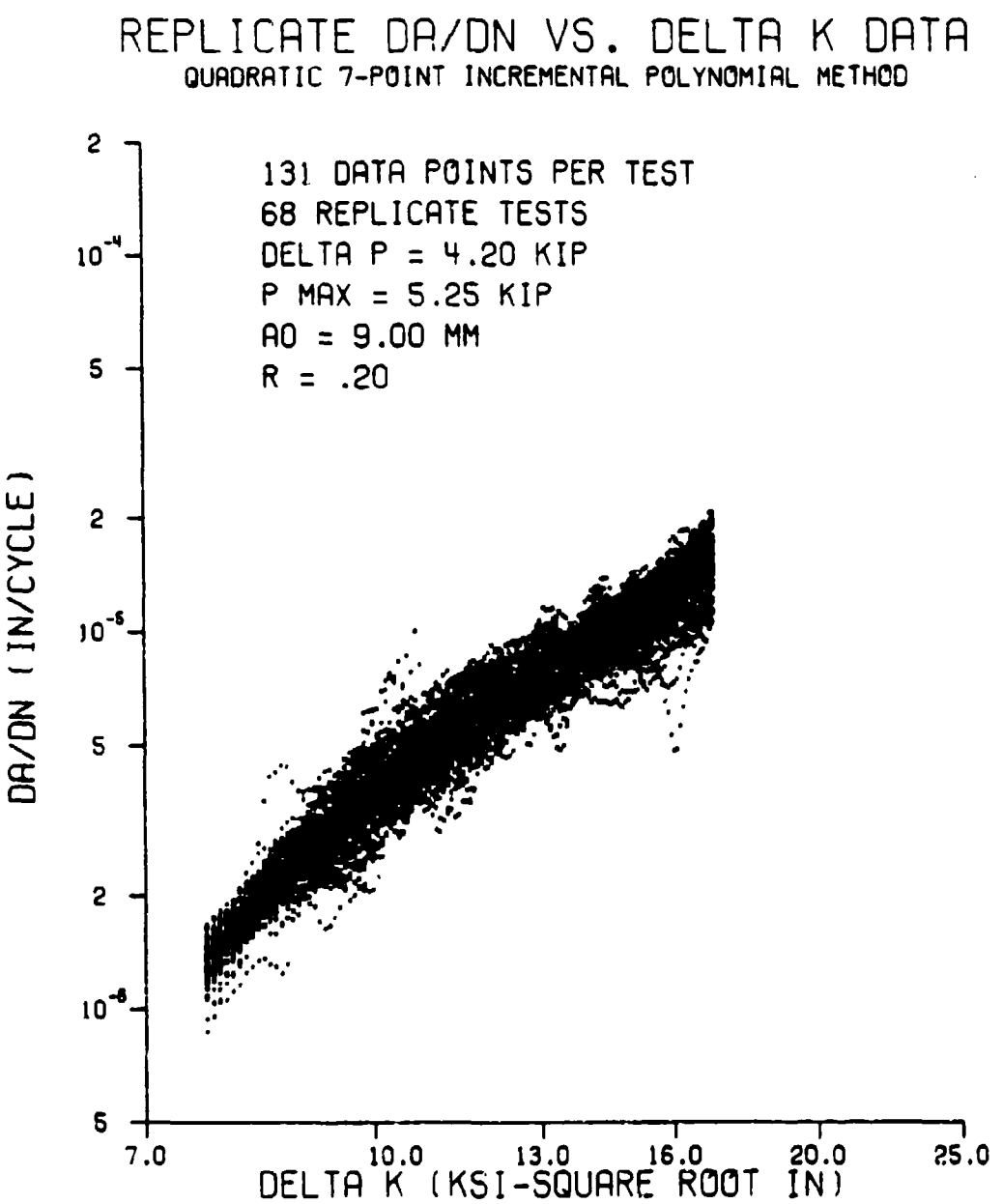

Figure 38. Combined Log_{10} da/dN vs. Log_{10} ΔK Data Calculated by the Quadratic 7-Point Incremental Polynomial Method

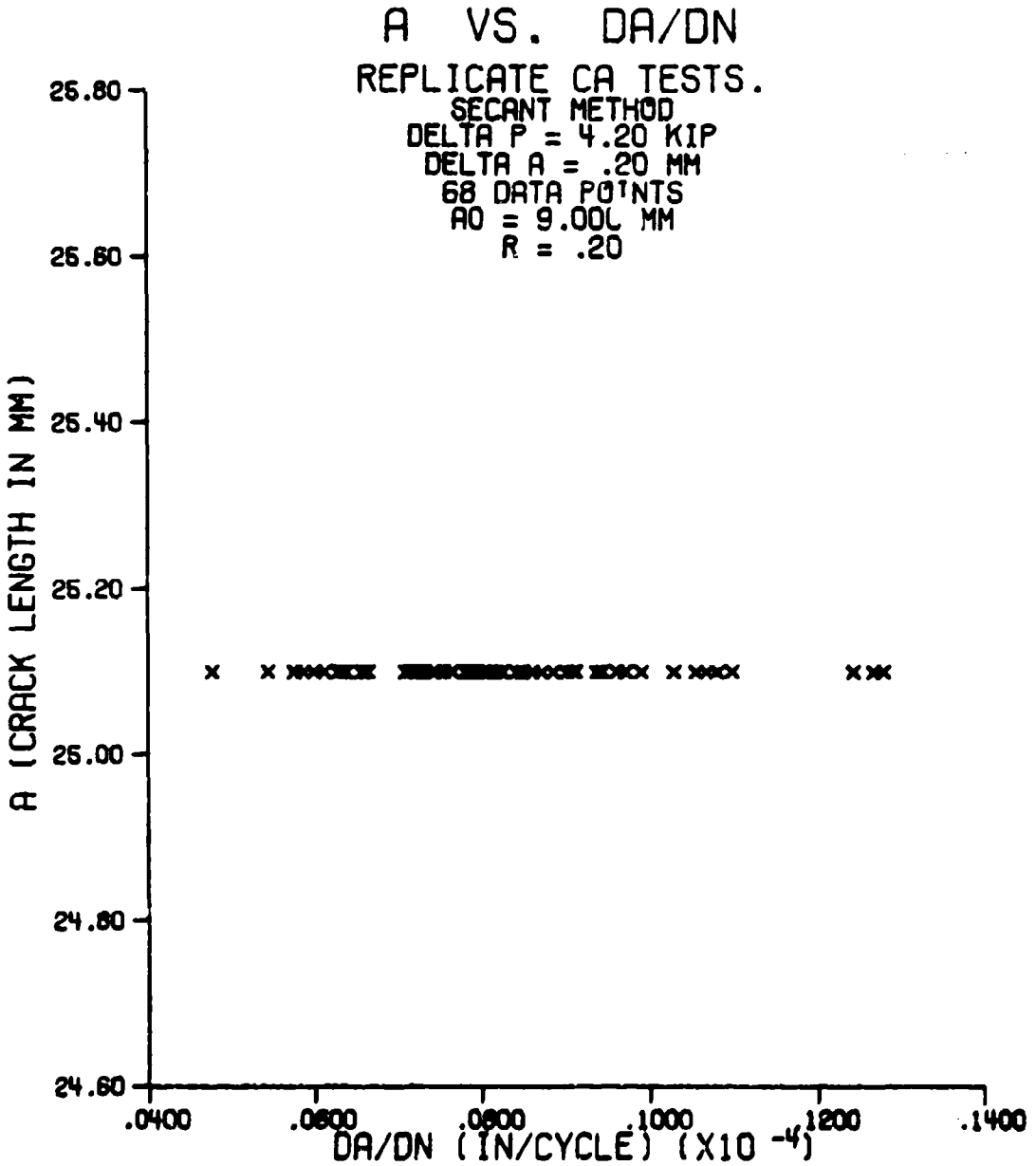

Figure 39. Typical Replicate da/dN Data

distribution rankings. The distribution parameters, goodness of fit criteria, and the distribution rankings were then combined over all of the ΔK levels.

The distribution parameters of the da/dN data as a function of crack length (essentially ΔK) were plotted for each of the six distributions and are shown in Figures 40 through 45. The distribution parameters are again normalized to show the trends present in the parameters.

The goodness of fit criteria for each distribution were averaged over all of the ΔK levels. These results are shown in Table IX. From these results, an understanding of which distributions provide the best fit for the da/dN data can be obtained.

The distribution rankings at each ΔK level were combined over all of the ΔK levels and again the mean rank and its standard deviation for each of the distributions and the number of times each distribution was selected as the best distribution were calculated. These results are shown in Table X.

Each of the distributions gives a fair but not outstanding performance in providing a fit for the da/dN data. There were no significant differences between the means of any of the five distributions, especially considering the high values of standard deviation about the mean. The 3-parameter gamma distribution did have a slightly lower mean than the other distributions and it also had the lowest value of the Kolmogorov-Smirnov statistic. However, the 2-parameter log normal distribution was the best distribution slightly more often than the other four distributions, but again there were no significant differences between the five distributions. These results lead to the conclusion that the 3-parameter gamma distribution provides a better fit for the da/dN data than the other

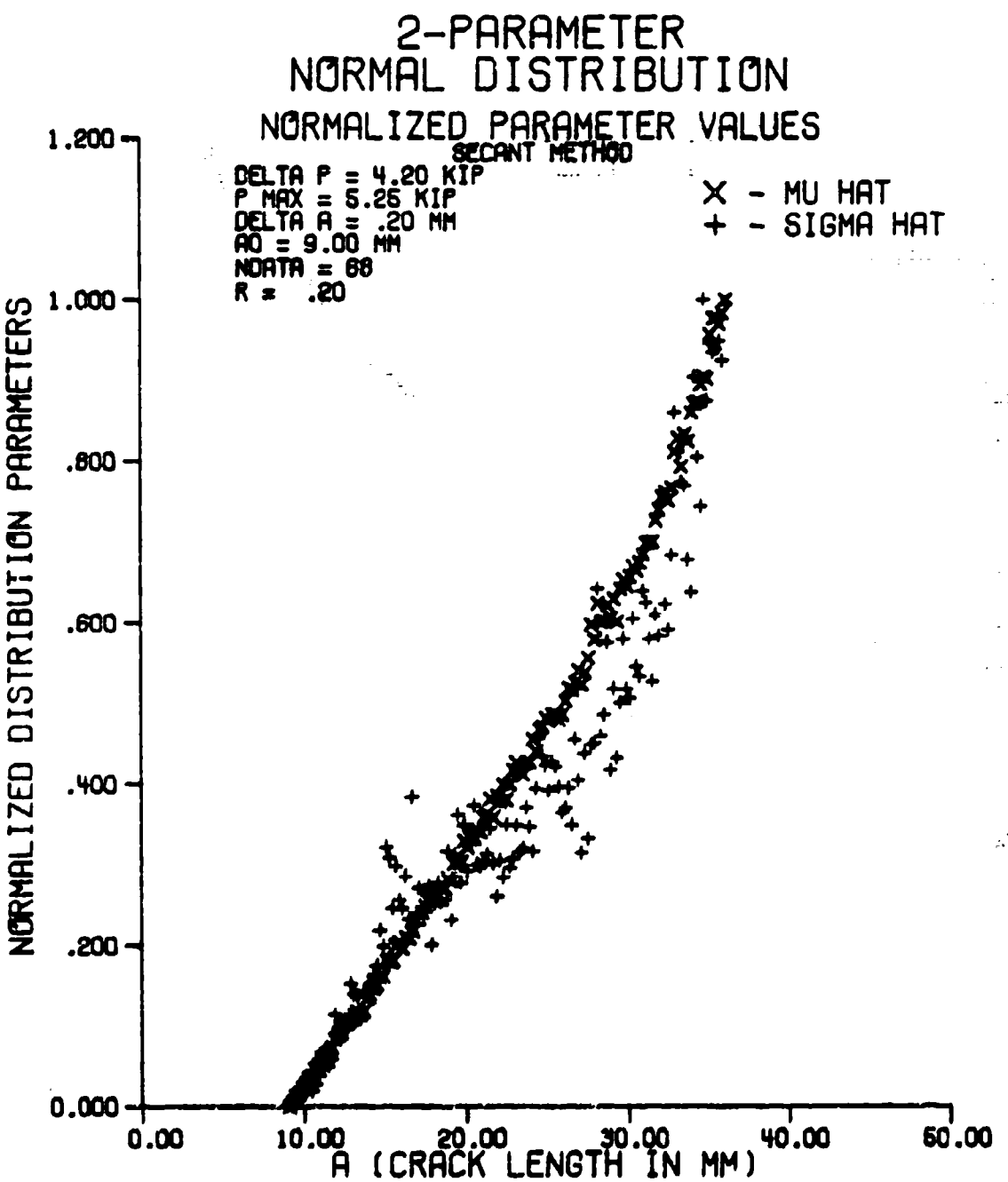

Figure 40. 2-Parameter Normal Distribution Parameters of da/dN Data as a Function of Crack Length

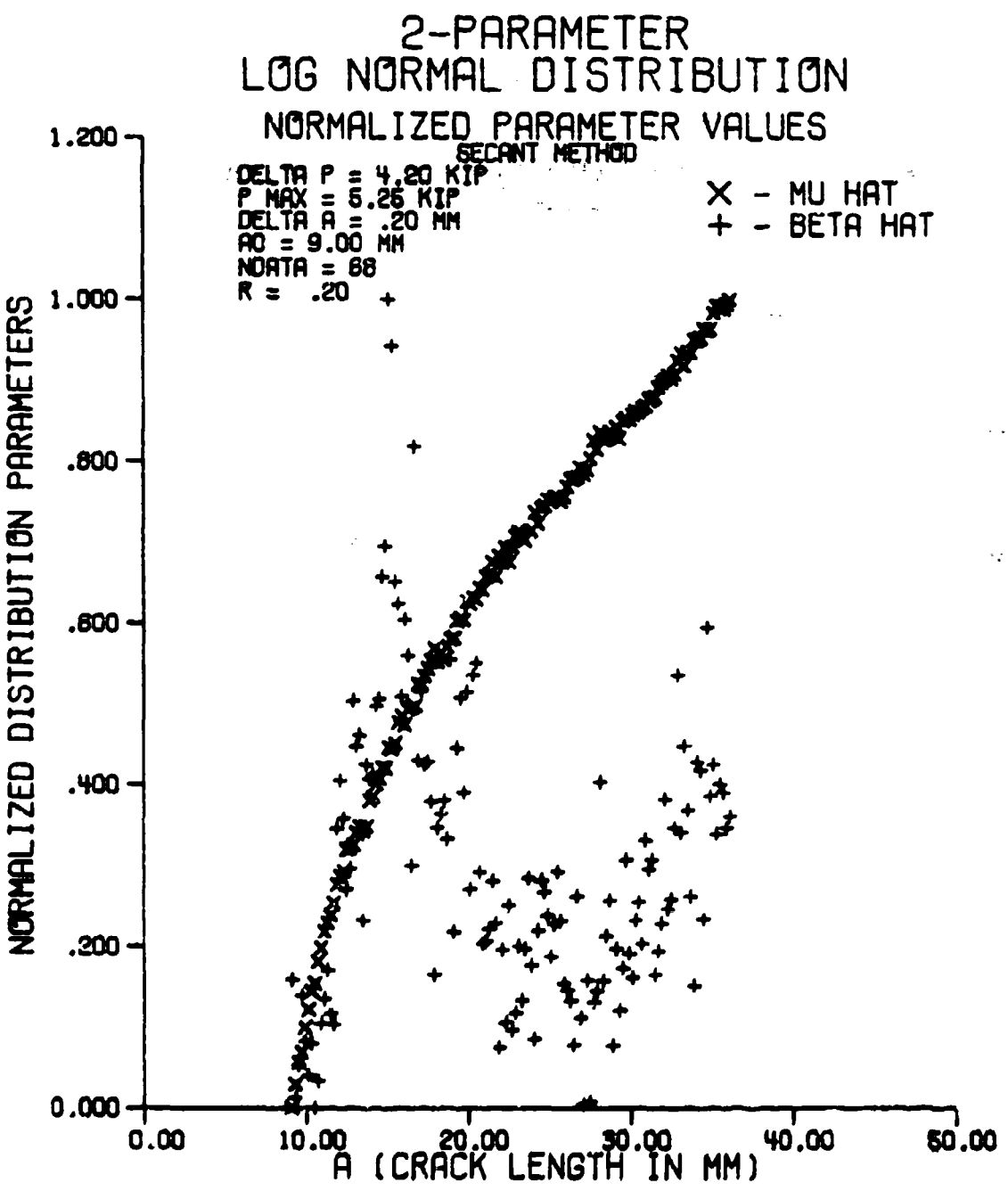

Figure 41. 2-Parameter Log Normal Distribution Parameters of da/dN Data as a Function of Crack Length

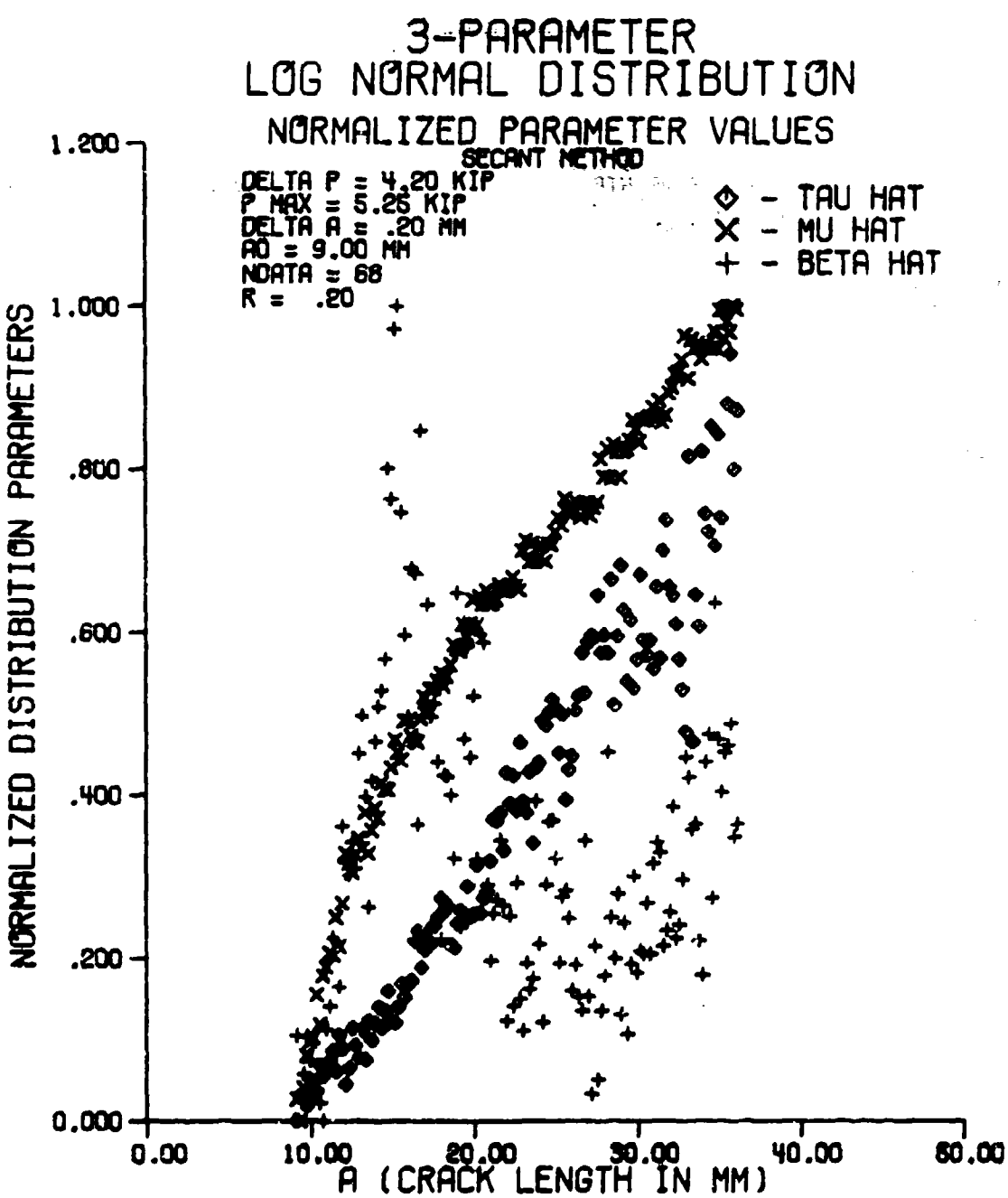

Figure 42. 3-Parameter Log Normal Distribution Parameters of da/dN Data as a Function of Crack Length

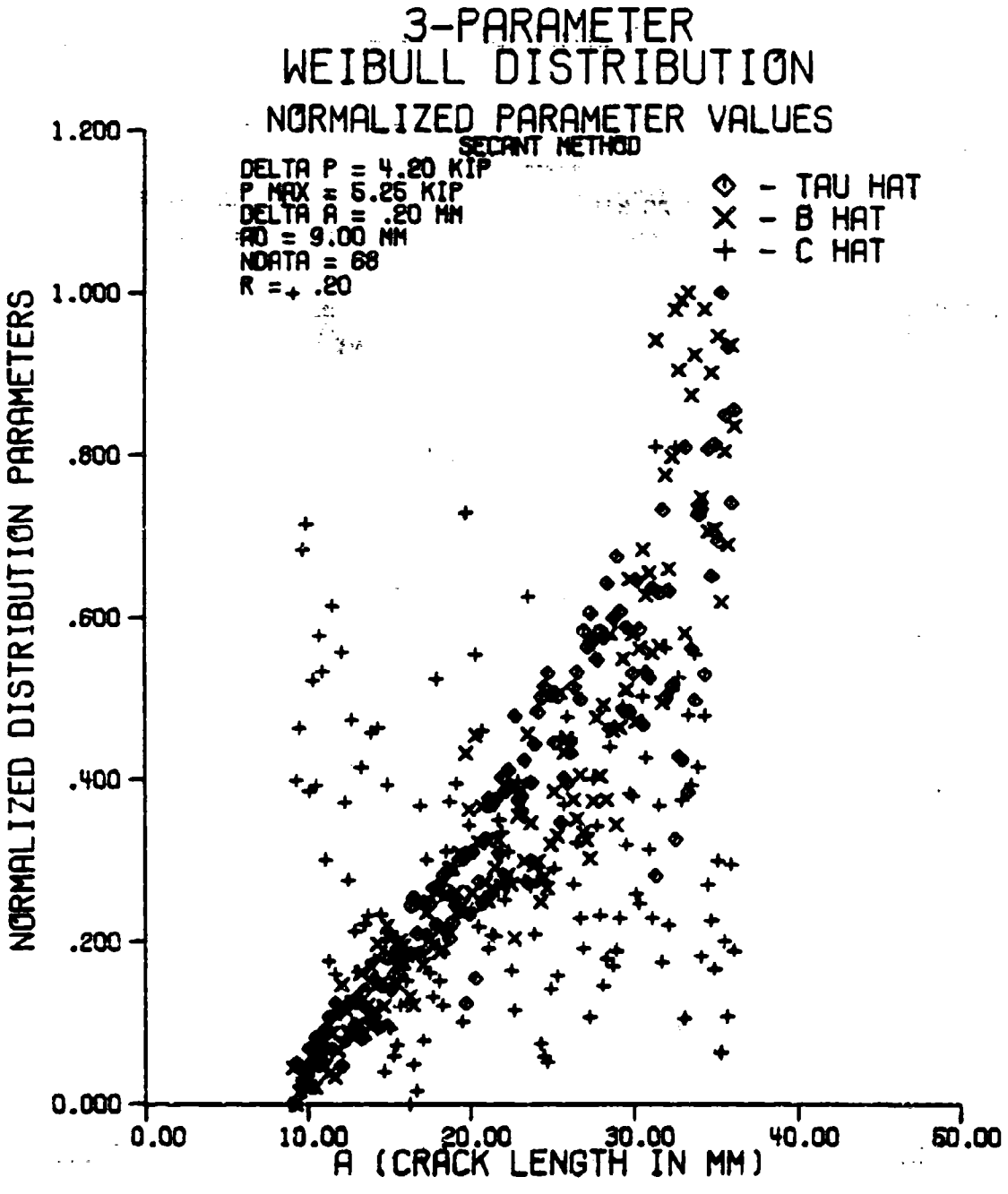

Figure 43. 3-Parameter Weibull Distribution Parameters of da/dN Data as a Function of Crack Length

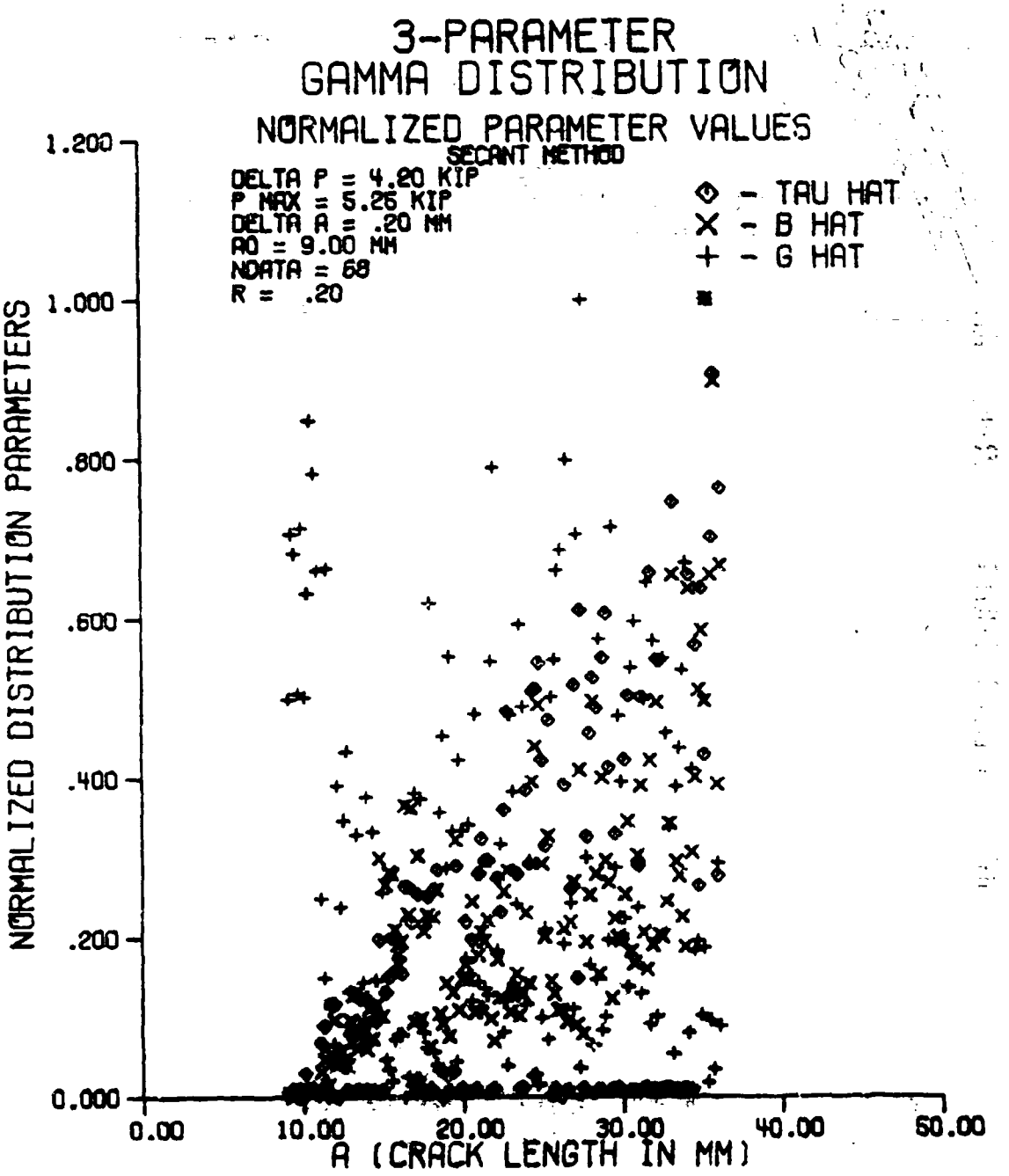

Figure 44. 3-Parameter Gamma Distribution Parameters of da/dN Data as a Function of Crack Length

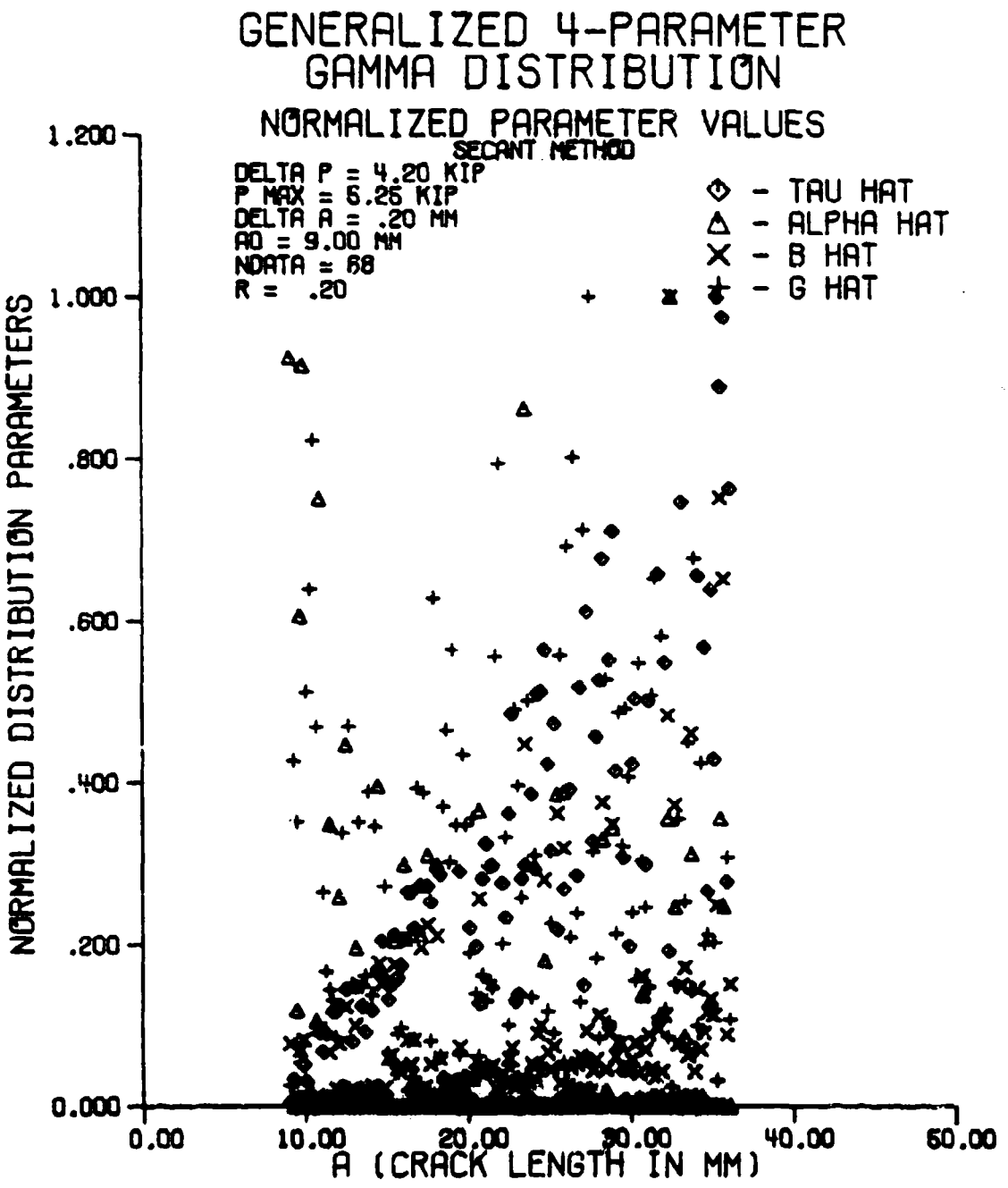

Figure 45. Generalized 4-Parameter Gamma Distribution Parameters of da/dN Data as a Function of Crack Length

Table IX

Average Goodness of Fit Criteria for the Distribution of da/dN Data

DISTRIBUTION	CHI-SQUARE TAIL AREA	KOLMOGOROV-SMIRNOV TEST	CLOSENESS (R SQUARED)
2-PARAMETER NORMAL	0.8494	0.0915	0.94997
2-PARAMETER LOG NORMAL	0.9011	0.0779	0.97647
3-PARAMETER LOG NORMAL	0.8442	0.0834	0.96966
3-PARAMETER WEIBULL	0.8474	0.0777	0.95942
3-PARAMETER GAMMA	0.8389	0.0737	0.96662
GENERALIZED 4-PARAMETER GAMMA	0.7946	0.0726	

Table X

Distribution Rankings for the Distribution of da/dN Data

DISTRIBUTION	MEAN	STANDARD DEVIATION	NUMBER OF TIMES BEST DISTRIBUTION
2-PARAMETER NORMAL	3.684	1.6497	27
2-PARAMETER LOG NORMAL	2.603	1.1943	37
3-PARAMETER LOG NORMAL	3.360	1.5524	26
3-PARAMETER WEIBULL	2.985	1.1925	19
3-PARAMETER GAMMA	2.368	0.9646	27

four distributions, but its performance relative to the other distributions is not strong at all. Due to this poor performance by the da/dN data in fitting a distribution, no analysis of da/dN data calculated by either the modified secant method or the quadratic 7-point incremental polynomial method was conducted.

10.4 Prediction of a vs. N Data from the Distribution of da/dN

The fourth objective to be met was to determine the variance of a set of a vs. N data predicted from the da/dN distribution parameters. The da/dN distribution parameters were estimated by the CGRDDP program (Section 6.3) as described in Section 10.3. The AVNPRD program (Section 7.3) was run on the da/dN distribution parameters and 68 replicate a vs. N data sets were predicted. These data sets are shown in Figure 46.

To obtain the variance of this predicted data, the CCDDP program (Section 6.2) was run at 14 crack length levels of the predicted data. The distribution parameters, goodness of fit criteria, and the distribution rankings were then combined over all of the crack length levels run.

For this predicted data, neither the 3-parameter gamma distribution nor the generalized 4-parameter gamma distribution would converge on parameter estimates, implying that neither distribution would provide a fit for the data. The distribution parameters as a function of crack length obtained for the other four distributions are shown in Figures 47 through 50. The average goodness of fit criteria for the four distributions for the predicted data are shown in Table XI. The distribution rankings results for the four distributions for this data are shown in Table XII.

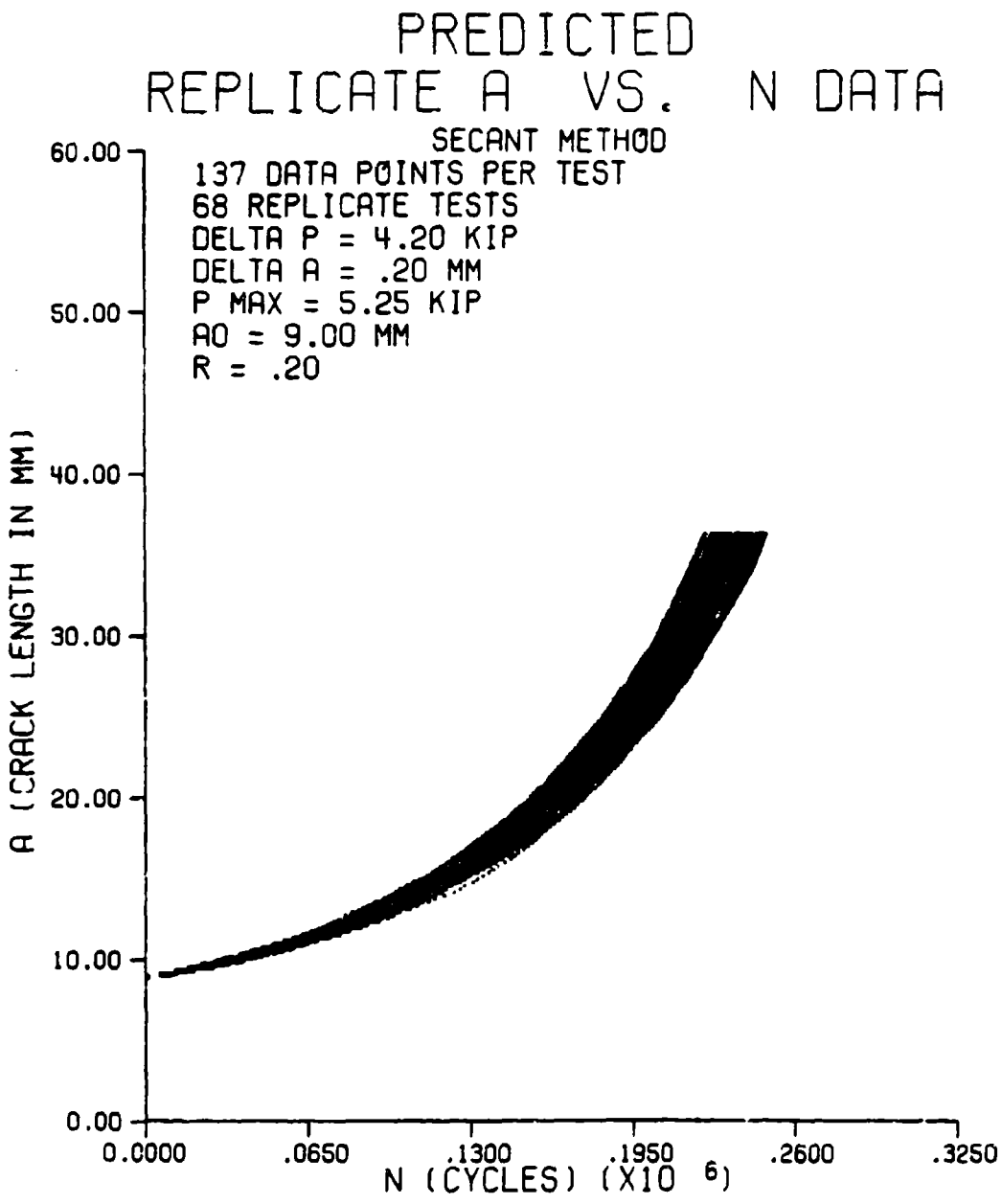

Figure 46. Replicate a vs. N Data Predicted from the Distribution of da/dN

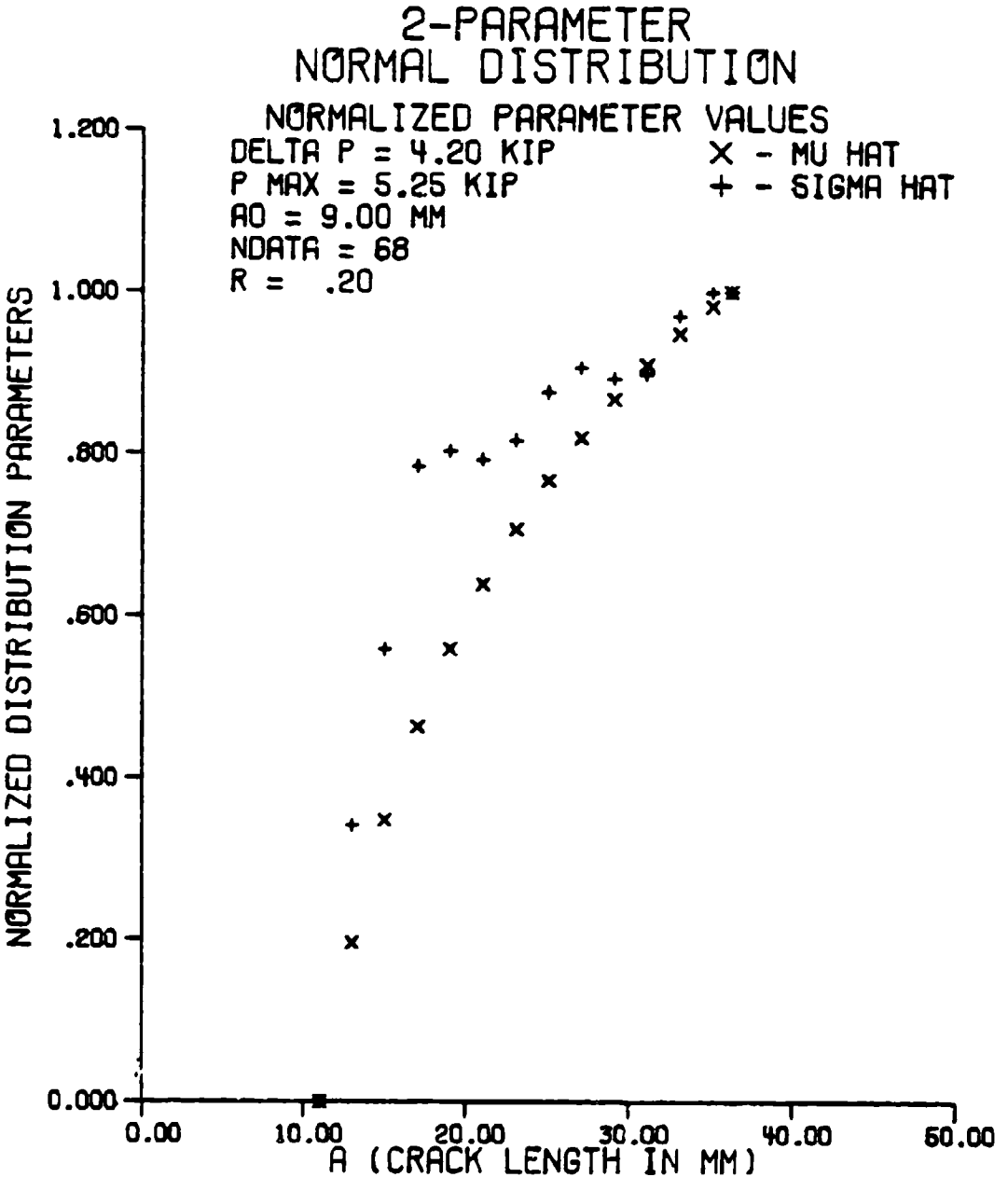

Figure 47. 2-Parameter Normal Distribution Parameters as a Function of Crack Length for Cycle Count Data Predicted from the Distribution of da/dN

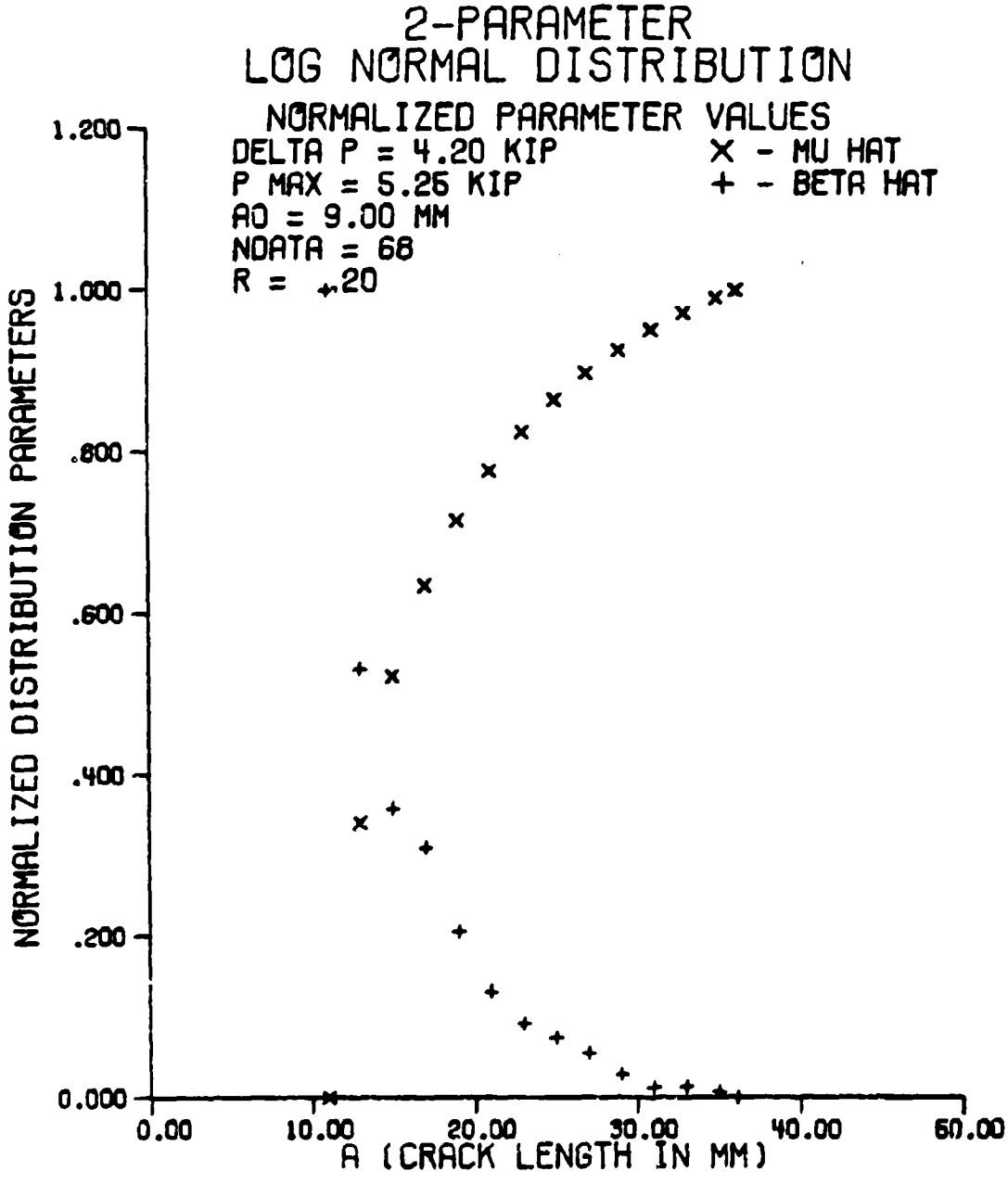

Figure 48. 2-Parameter Log Normal Distribution Parameters as a Function of Crack Length for Cycle Count Data Predicted from the Distribution of da/dN

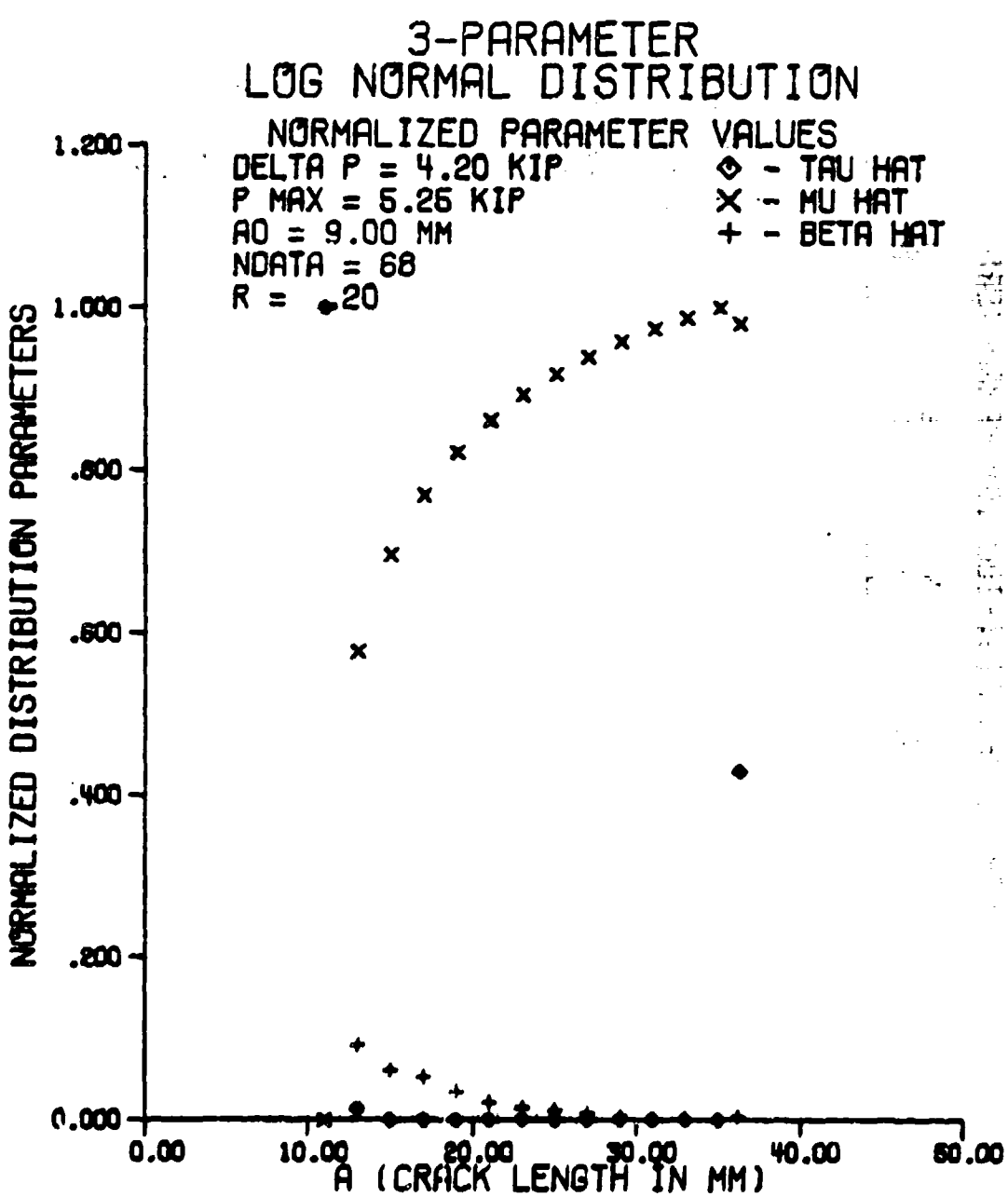

Figure 49. 3-Parameter Log Normal Distribution Parameters as a Function of Crack Length for Cycle Count Data Predicted from the Distribution of da/dN

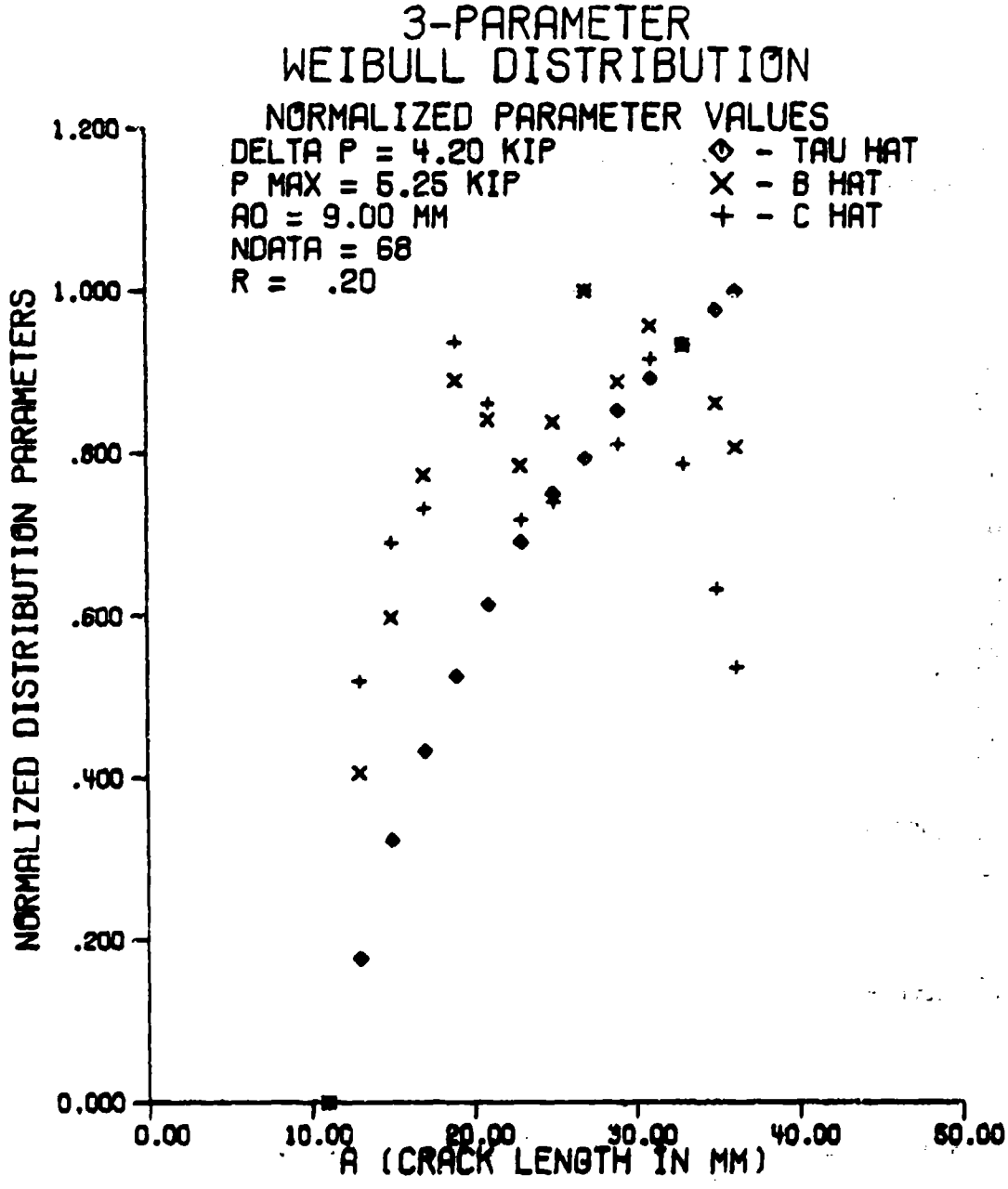

Figure 50. 3-Parameter Weibull Distribution Parameters as a Function of Crack Length for Cycle Count Data Predicted from the Distribution of da/dN

Table XI

Average Goodness of Fit Criteria for the Distribution of Cycle Count Data Predicted from the Distribution of da/dN

DISTRIBUTION	CHI-SQUARE TAIL AREA	KOLMOGOROV-SMIRNOV TEST	CLOSENESS (R SQUARED)
2-PARAMETER NORMAL	0.9087	0.0735	0.98515
2-PARAMETER LOG NORMAL	0.9128	0.0722	0.98497
3-PARAMETER LOG NORMAL	0.8828	0.0730	0.98515
3-PARAMETER WEIBULL	0.8919	0.0818	0.96884

Table XII

Distribution Rankings for the Distribution of Cycle Count Data Predicted from the Distribution of da/dN

DISTRIBUTION	MEAN	STANDARD DEVIATION	NUMBER OF TIMES BEST DISTRIBUTION
2-PARAMETER NORMAL	2.643	0.7449	2
2-PARAMETER LOG NORMAL	1.214	0.5789	12
3-PARAMETER LOG NORMAL	2.286	0.6112	0
3-PARAMETER WEIBULL	3.857	0.5345	0

The 2-parameter log normal distribution provided the best fit for the predicted replicate cycle count data, followed by the 3-parameter log normal distribution and then the 2-parameter normal distribution. The 3-parameter Weibull distribution provided the worst fit for the data of the four distributions which the data fit.

The next step in the analysis was the comparison of the distributions of N between the actual cycle count data and the cycle count data predicted from the distribution of da/dN. The mean and standard deviation of both distributions at the crack length levels used above were computed and the results are shown in Table XIII. At every crack length level, there was no significant difference between the means but there was a very significant difference between the standard deviations of the two distributions. In every case, the standard deviation of the predicted cycle count data is much smaller than the standard deviation of the actual cycle count data.

As a check on the analysis above, a vs. N data were predicted from the distribution of da/dN in a slightly different manner than for the predicted replicate cycle count data. The mean and $\pm$ 1, 2, and 3 sigma values of da/dN at each crack length level were obtained from the distribution of da/dN. Using these 7 lines of da/dN data, a vs. N data was predicted. The results are shown in Figure 51. A comparison between the actual cycle count mean and $\pm$ 1, 2, and 3 sigma values and the cycle count values predicted from the mean and $\pm$ 1, 2, and 3 sigma da/dN lines at a single crack length level is shown in Table XIV.

From the above analysis, it can be concluded that predicting a vs. N data from the distribution of da/dN using the method described in Section 7.2 yields low error in predicting mean crack propagation behavior, but

Table XIII

Comparison of the Distributions Between Actual Cycle Count Data and Cycle Count Data Predicted from the Distribution of da/dN

	MEAN		STANDARD DEVIATION	
CRACK LENGTH (MM)	ACTUAL	PREDICTED	ACTUAL	PREDICTED
11.000	55681	55735	6956	1951
13.000	90128	91222	5832	2512
15.000	117486	118700	6719	4348
17.000	139352	139571	10903	4898
19.000	158382	156915	11849	3288
21.000	170786	171379	12489	3249
23.000	182198	183670	8204	3284
25.000	192578	194504	8547	3380
27.000	202538	204083	8944	3432
29.000	211030	212612	9123	3407
31.000	218688	220323	9325	3416
33.000	226459	227186	9637	3530
35.000	231416	233249	10037	3575
36.200	234573	236533	10191	3574

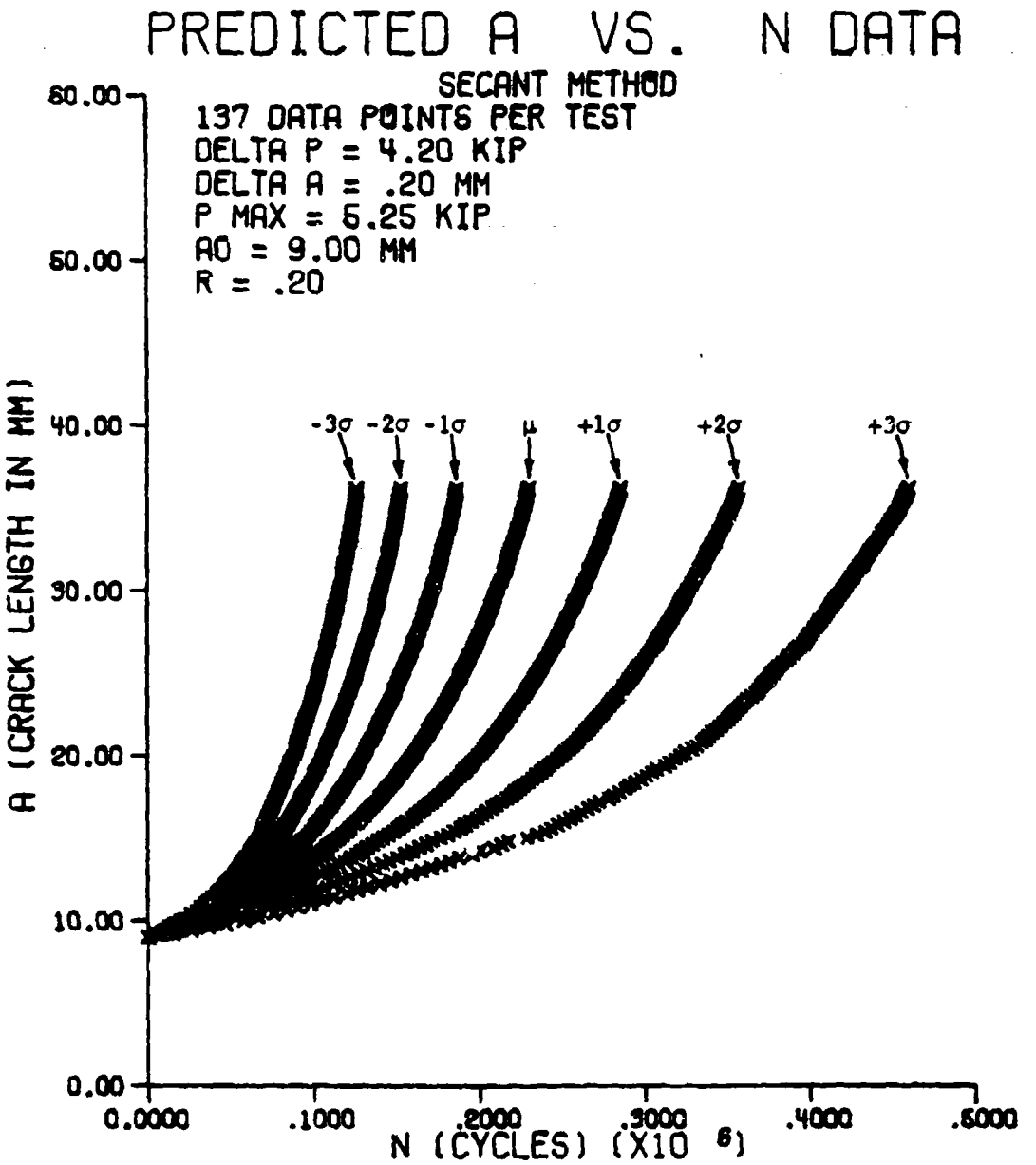

Figure 51. a vs. N Data Predicted from the Mean and ± 1, 2, and 3 Sigma da/dN Lines

Table XIV

Comparison of Actual Cycle Count Data with Cycle Count Data Predicted from Constant Variance da/dN Lines

A = 31.000 MM	ACTUAL	PREDICTED
-3 SIGMA	187829	117430
-2 SIGMA	195882	141941
-1 SIGMA	205562	173192
MEAN	217891	213318
+1 SIGMA	233627	264068
+2 SIGMA	253289	330341
+3 SIGMA	278046	434530

yields high error in predicting crack propagation behavior at the extremes of the distribution of N.

10.5 Inverse Growth Rate

Due to the failure of the da/dN data to fit any of the given distributions satisfactorily, it was decided that the growth rate variable warranted a further investigation. Looking back at the original experimental investigation (Section 9), it can be seen that the dependent variable of the data was N while the independent variable was a (i.e. N was measured as a was varied). Since the dependent variable, N, provided a very nice fit to the 3-parameter log normal distribution, it was strongly suspected that changes in the dependent variable, ΔN, would also provide a good fit to one of the given distributions. Since Δ a was constant it was decided to use $\Delta N/\Delta a$, or in differential terms, dN/da, as a variable of interest for further analysis.

The analysis conducted using dN/da as the variable of interest was the same analysis used for da/dN. The first part of this analysis was to determine the distribution of dN/da. Replicate dN/da data were obtained by inverting the replicate da/dN data calculated by the secant method using the DADNCP program (Section 7.2). Typical replicate dN/da data are shown in Figure 52. The distribution of the replicate dN/da data was determined at each ΔK level through the use of the DNDDP program (Section 6.4). At each ΔK level, this program calculated the distribution parameters and goodness of fit criteria for six distributions and then compared the goodness of fit criteria between the different distributions to give the distribution rankings. The location parameter for the 3-parameter gamma distribution and the generalized 4-parameter gamma

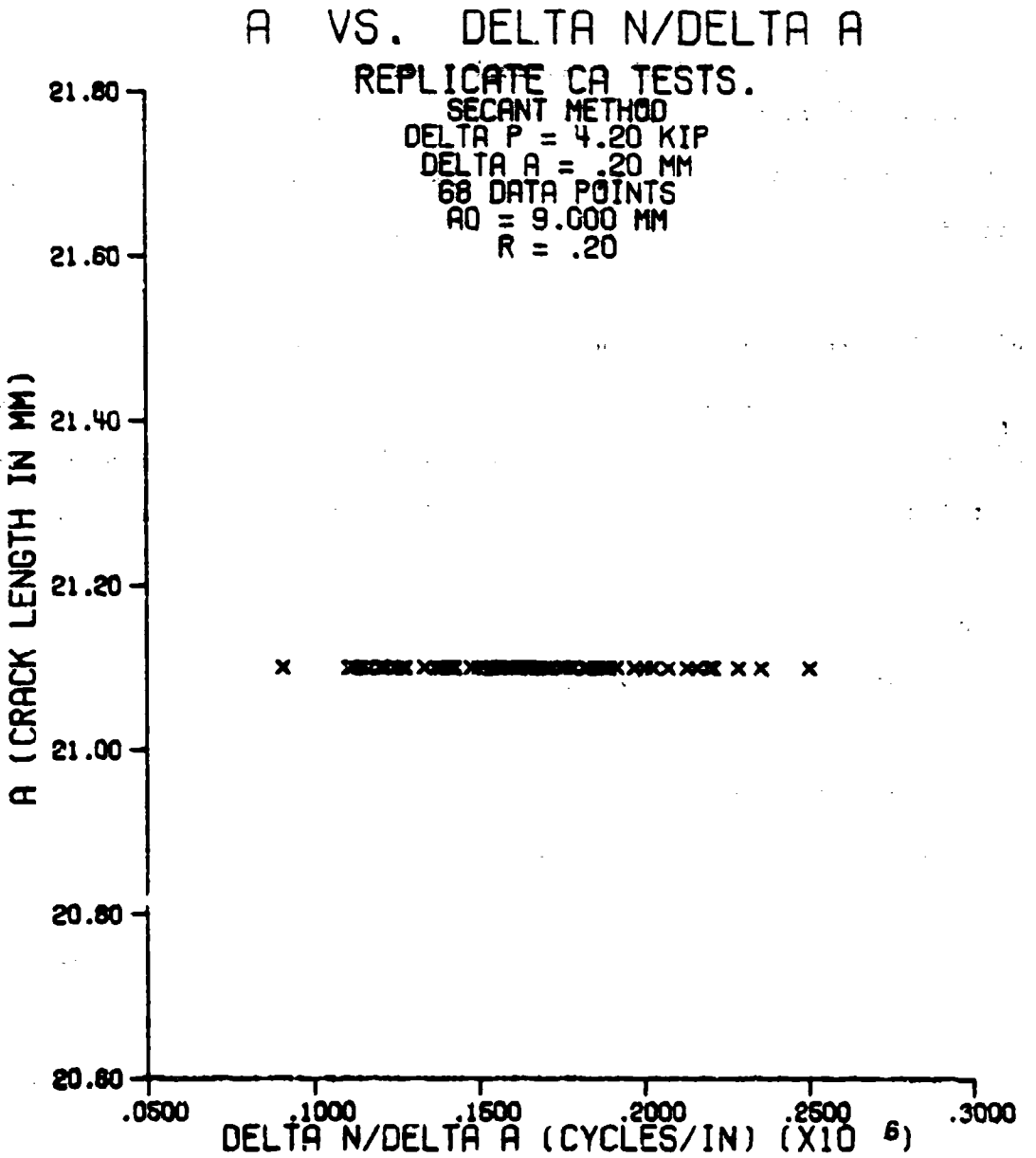

Figure 52. Typical Replicate dN/da Data

distribution was assumed to be zero by this program, thus reducing these two distributions to the 2-parameter gamma distribution and the generalized 3-parameter gamma distribution, respectively. As before, the generalized 3-parameter gamma distribution was not included in the distribution rankings. The distribution parameters, goodness of fit criteria, and the distribution rankings were then combined over all of the ΔK levels.

The distribution parameters of the dN/da data as a function of crack length were plotted for each of the six distributions and are shown in Figures 53 through 58. The distributions parameters are again normalized to show the trends present in the parameters.

The goodness of fit criteria for each distribution were averaged over all of the ΔK levels. These results are shown in Table XV. From these results, an understanding of which distributions provide the best fit for the dN/da data can be obtained.

The distribution rankings at each ΔK level were combined over all of the ΔK levels and the mean rank and its standard deviation for each of the distributions and the number of times each distribution was selected as the best distribution were calculated. These results are shown in Table XVI.

The 3-parameter log normal distribution provided the best fit for the dN/da data, as evidenced by the low distribution ranking, the low Kolmogorov-Smirnov test statistic value, and the large number of times it was selected as the best distribution. The 2-parameter log normal and the 3-parameter Weibull distribution tied for the second best fit for the dN/da data, both having roughly the same distribution ranking and Kolmogorov-Smirnov test statistic value and the same number of times it was

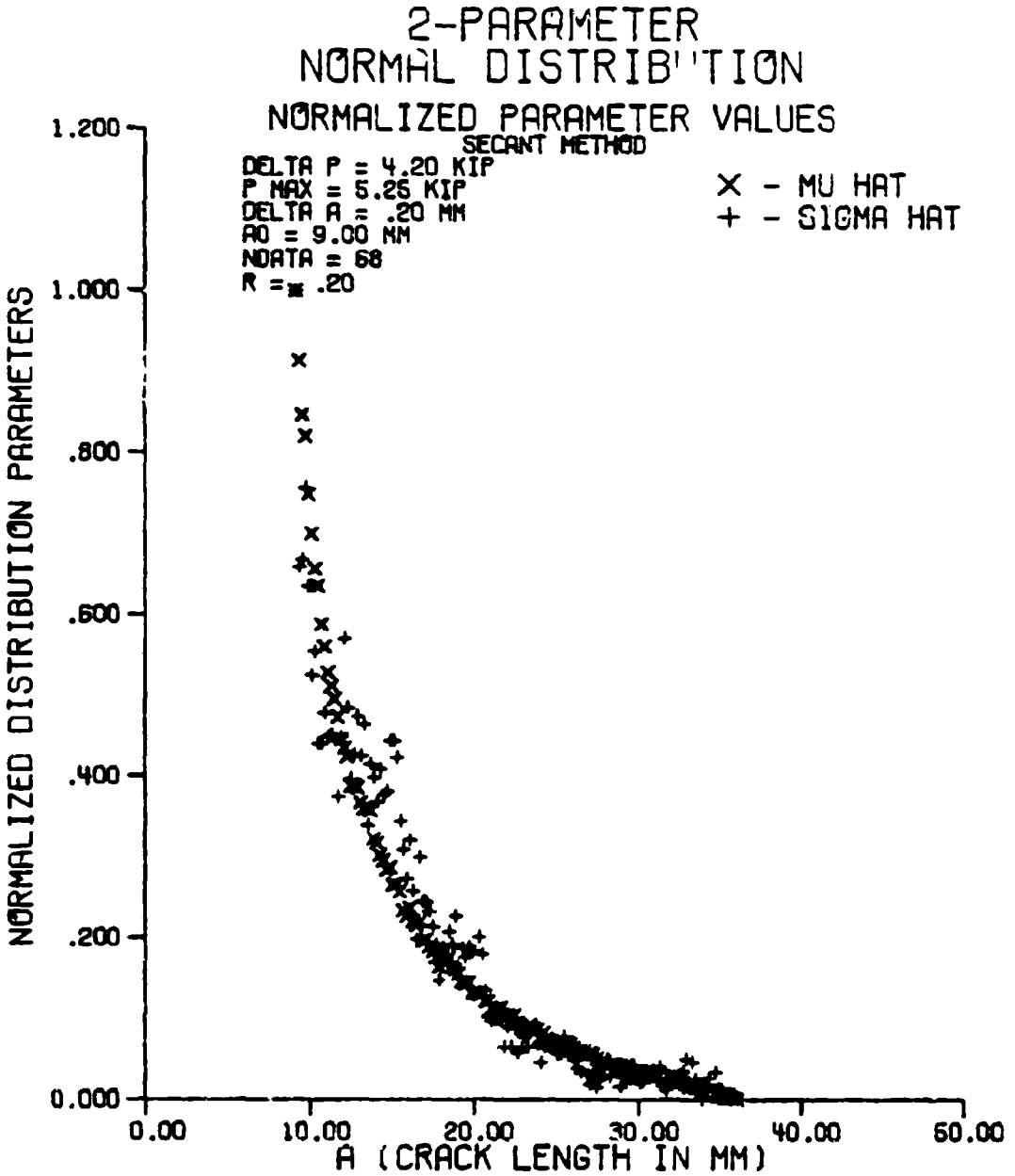

Figure 53. 2-Parameter Normal Distribution Parameters of dN/da Data as a Function of Crack Length

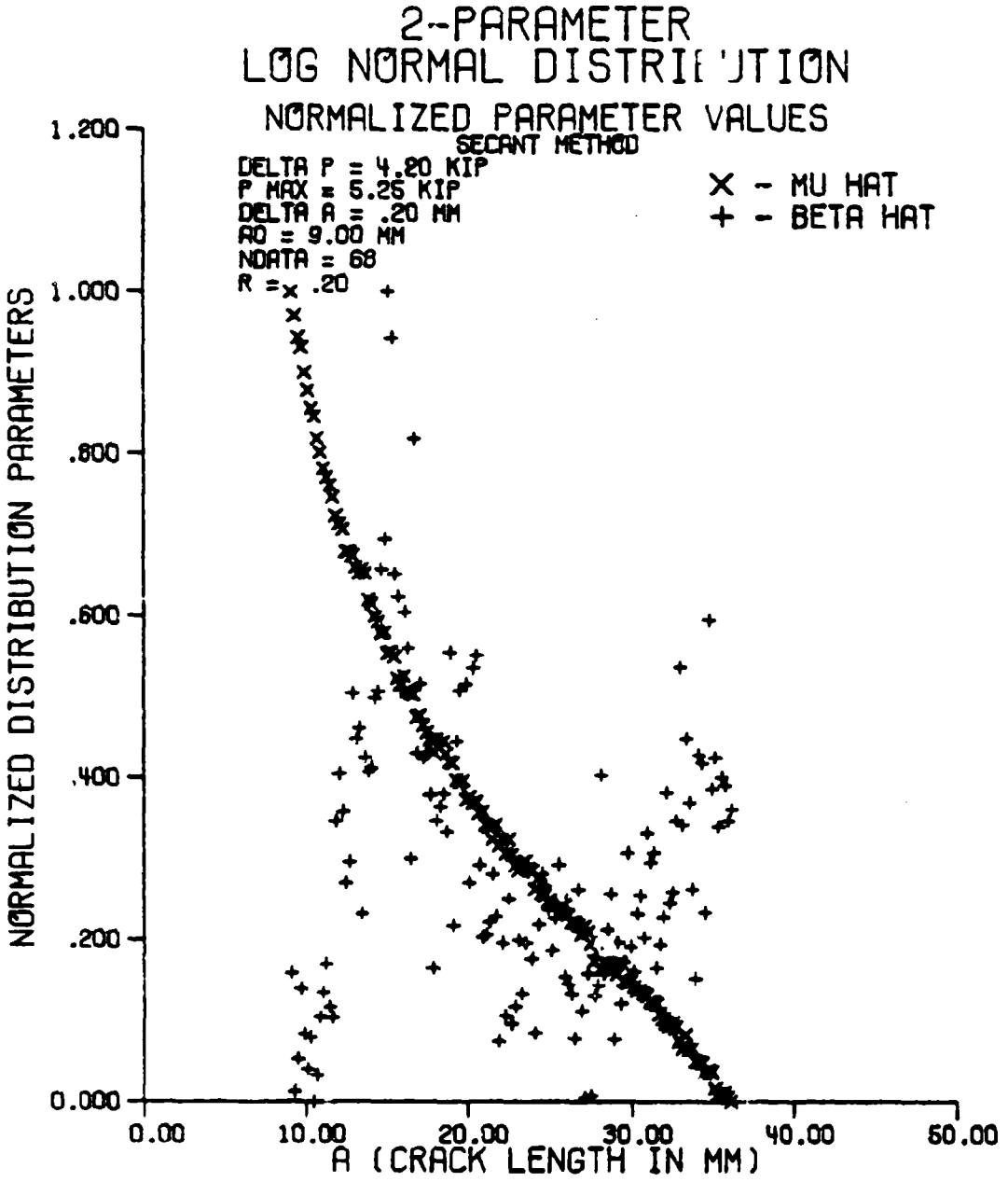

Figure 54. 2-Parameter Log Normal Distribution Parameters of dN/da Data as a Function of Crack Length

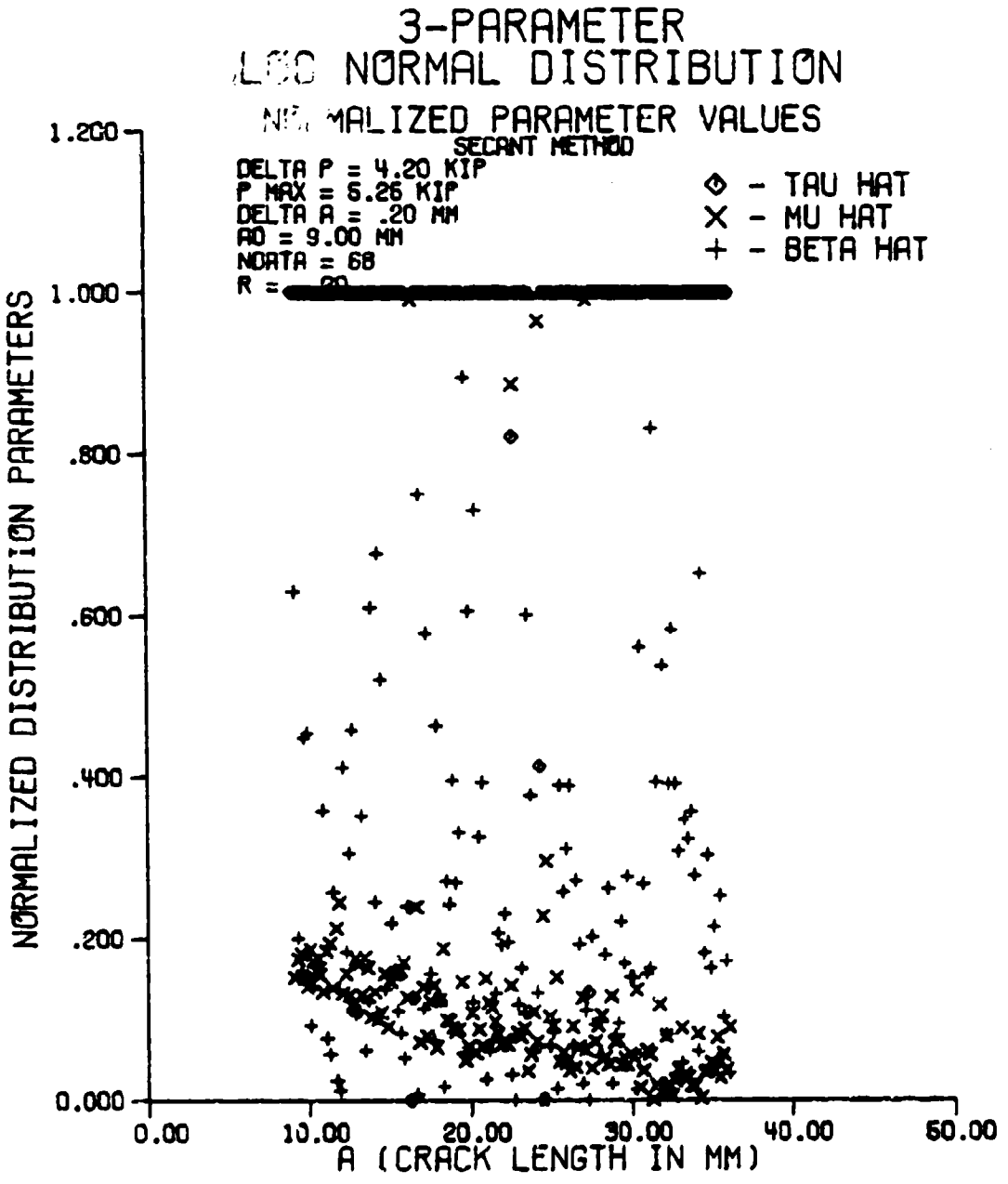

Figure 55. 3-Parameter Log Normal Distribution Parameters of dN/da Data as a Function of Crack Length

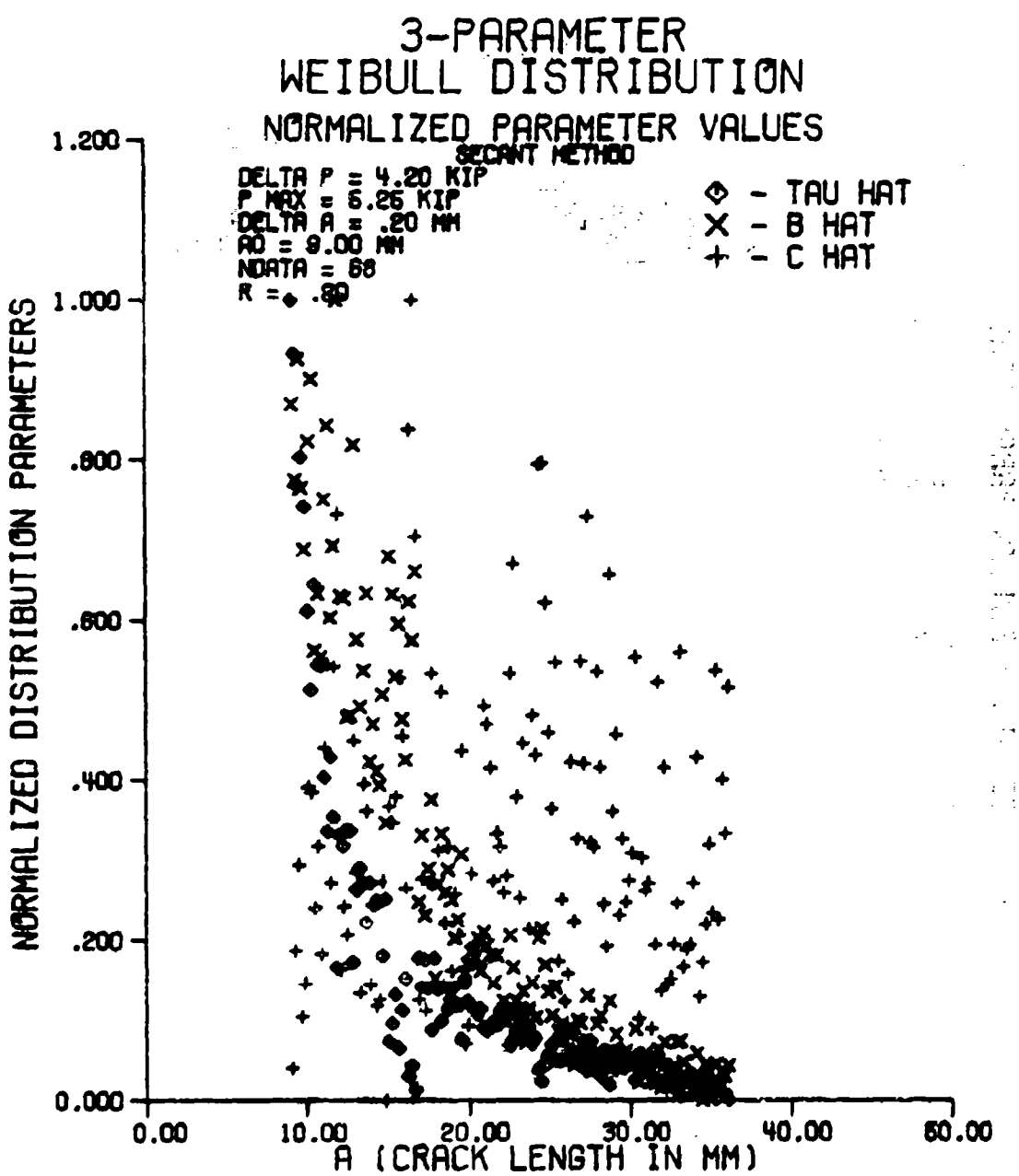

Figure 56. 3-Parameter Weibull Distribution Parameters of dN/da Data as a Function of Crack Length

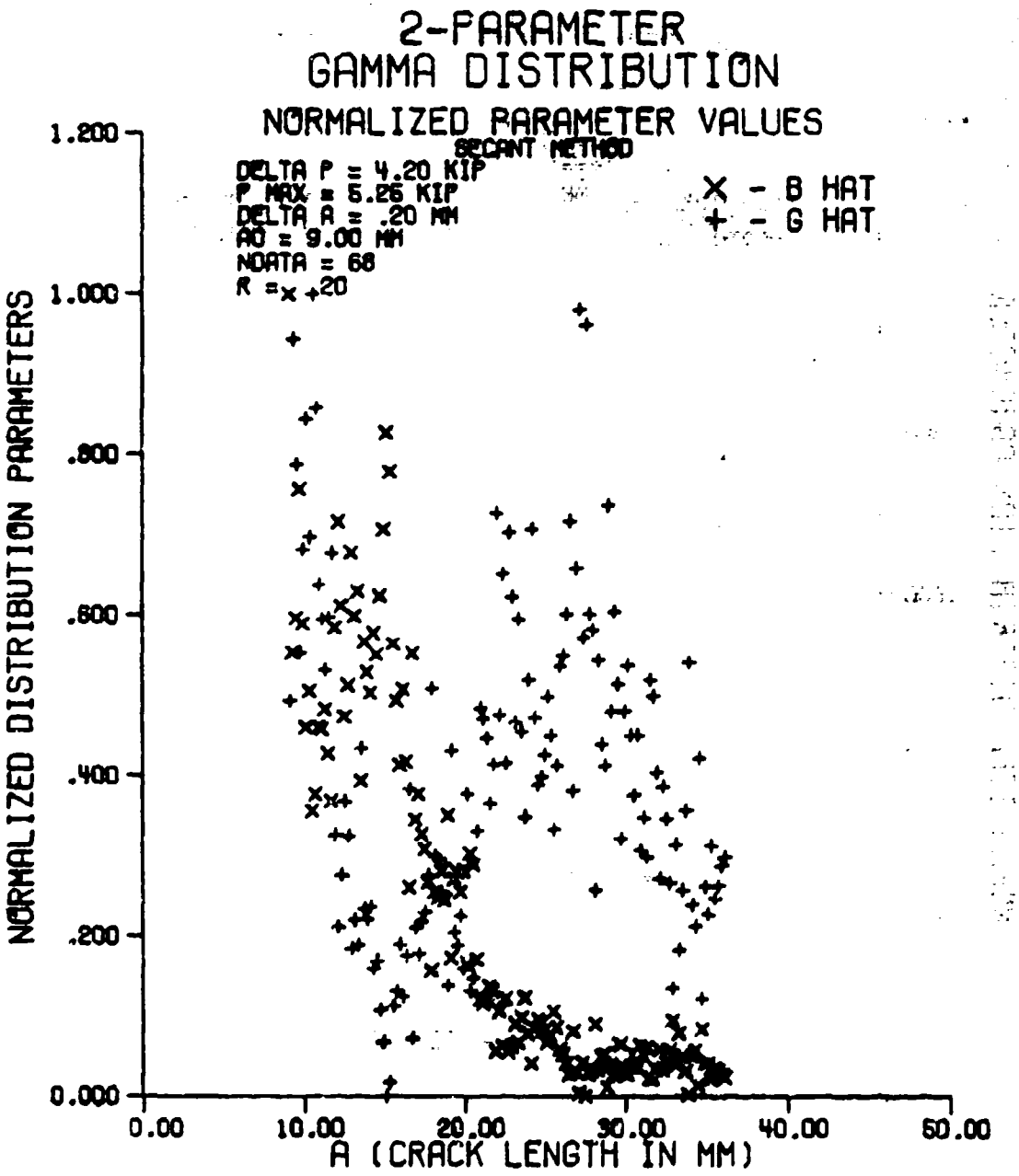

Figure 57. 2-Parameter Gamma Distribution Parameters of dN/da Data as a Function of Crack Length

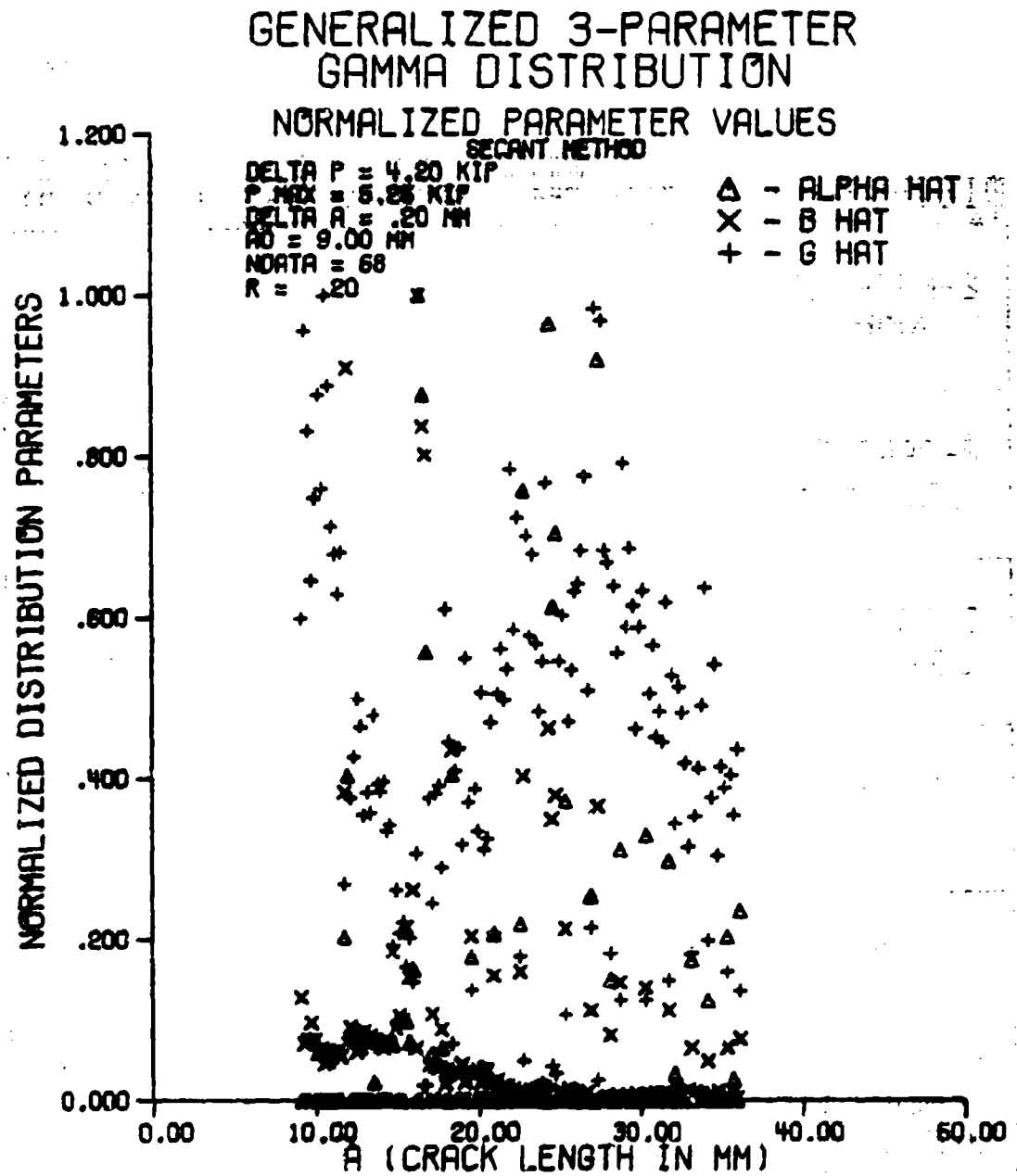

Figure 58. Generalized 3-Parameter Gamma Distribution Parameters of dN/da Data as a Function of Crack Length

Table XV

Average Goodness of Fit Criteria for the Distribution of dN/da Data

DISTRIBUTION	CHI-SQUARE TAIL AREA	KOLMOGOROV-SMIRNOV TEST	CLOSENESS (R SQUARED)
2-PARAMETER NORMAL	0.8383	0.0992	0.94912
2-PARAMETER LOG NORMAL	0.9011	0.0779	0.97647
3-PARAMETER LOG NORMAL	0.8877	0.0695	0.97622
3-PARAMETER WEIBULL	0.8409	0.0790	0.95477
2-PARAMETER GAMMA	0.7640	0.0813	0.93431
GENERALIZED 3-PARAMETER GAMMA	0.7507	0.0800	

Table XVI

Distribution Rankings for the Distribution of dN/da Data

DISTRIBUTION	MEAN	STANDARD DEVIATION	NUMBER OF TIMES BEST DISTRIBUTION
2-PARAMETER NORMAL	4.338	1.1815	10
2-PARAMETER LOG NORMAL	2.610	1.2363	28
3-PARAMETER LOG NORMAL	1.860	0.8621	56
3-PARAMETER WEIBULL	2.882	1.2594	27
2-PARAMETER GAMMA	3.309	1.2019	15

selected as the best distribution. The 2-parameter gamma distribution provided the fourth best fit and the 2-parameter normal distribution provided the worst fit for the dN/da data.

The next step of the analysis was to see if the improved fit of the dN/da data to a distribution would improve the prediction of a vs. N data from the distribution of dN/da. The AVNPRD program (Section 7.3) was slightly modified for the dN/da variable and run on the dN/da distribution parameters, resulting in 68 predicted replicate a vs. N data sets. These data sets are shown in Figure 59.

The CCDDP program (Section 6.2) was run at a few crack length levels of the predicted data. The distribution parameters, goodness of fit criteria, and the distribution rankings were then combined over all of the crack length levels run.

For this set of predicted data, the generalized 4-parameter gamma distribution would not converge on parameter estimates, implying that it could not provide a fit for the dN/da data. The distribution parameters as a function of crack length obtained for the other five distributions are shown in Figures 60 through 64. The average goodness of fit criteria for the five distributions for the predicted data are shown in Table XVII. The distribution rankings results for the five distributions for this data are shown in Table XVIII.

The 3-parameter log normal distribution provided the best fit for the predicted replicate cycle-count data, followed in order by the 2-parameter log normal distribution, the 3-parameter Weibull distribution, the 2-parameter normal distribution, and the 3-parameter gamma distribution.

The next step in the analysis was the comparison of the distributions of N between the actual cycle count data and the cycle count data predicted

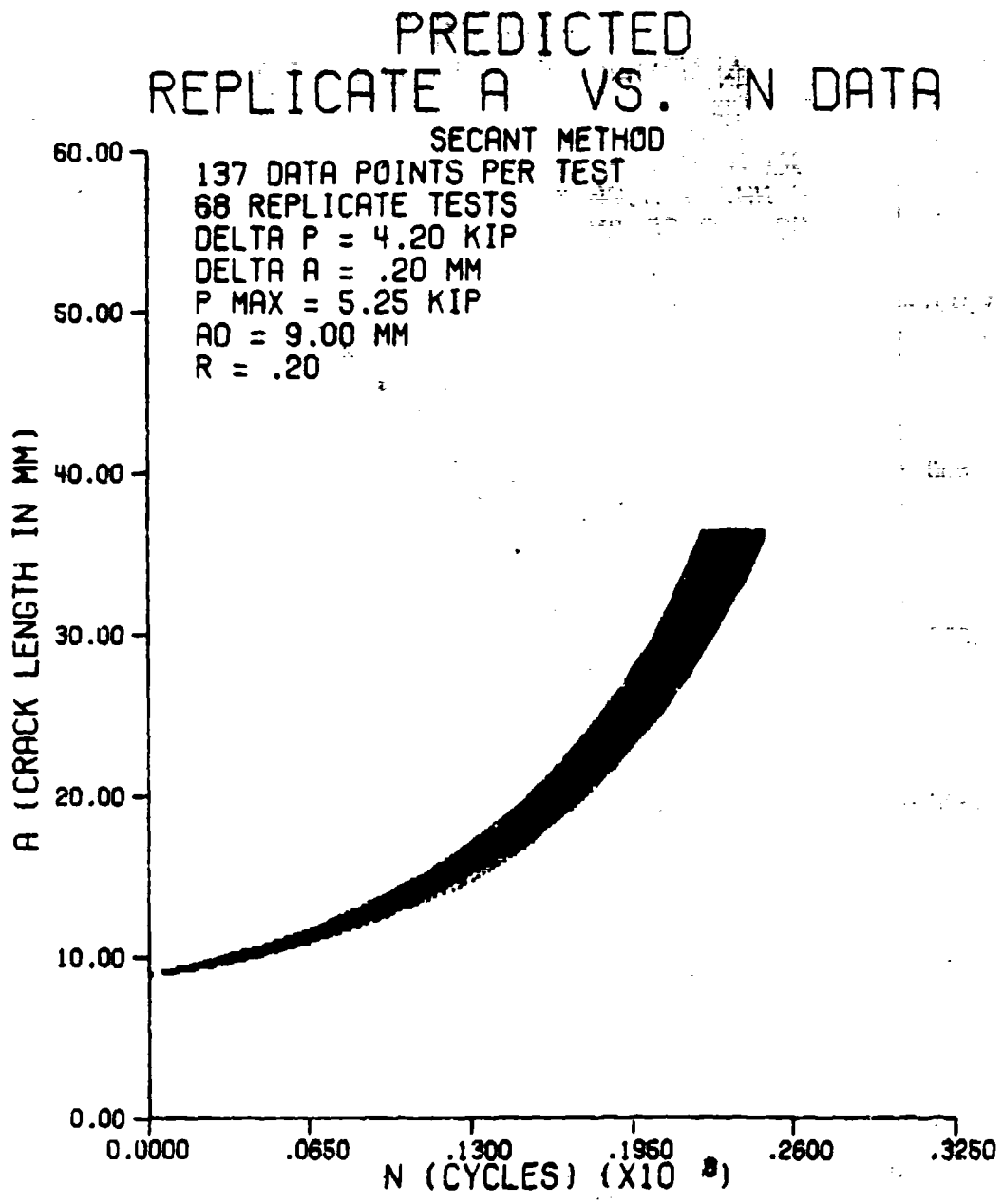

Figure 59. Replicate a vs. N Data Predicted from the Distribution of dN/da

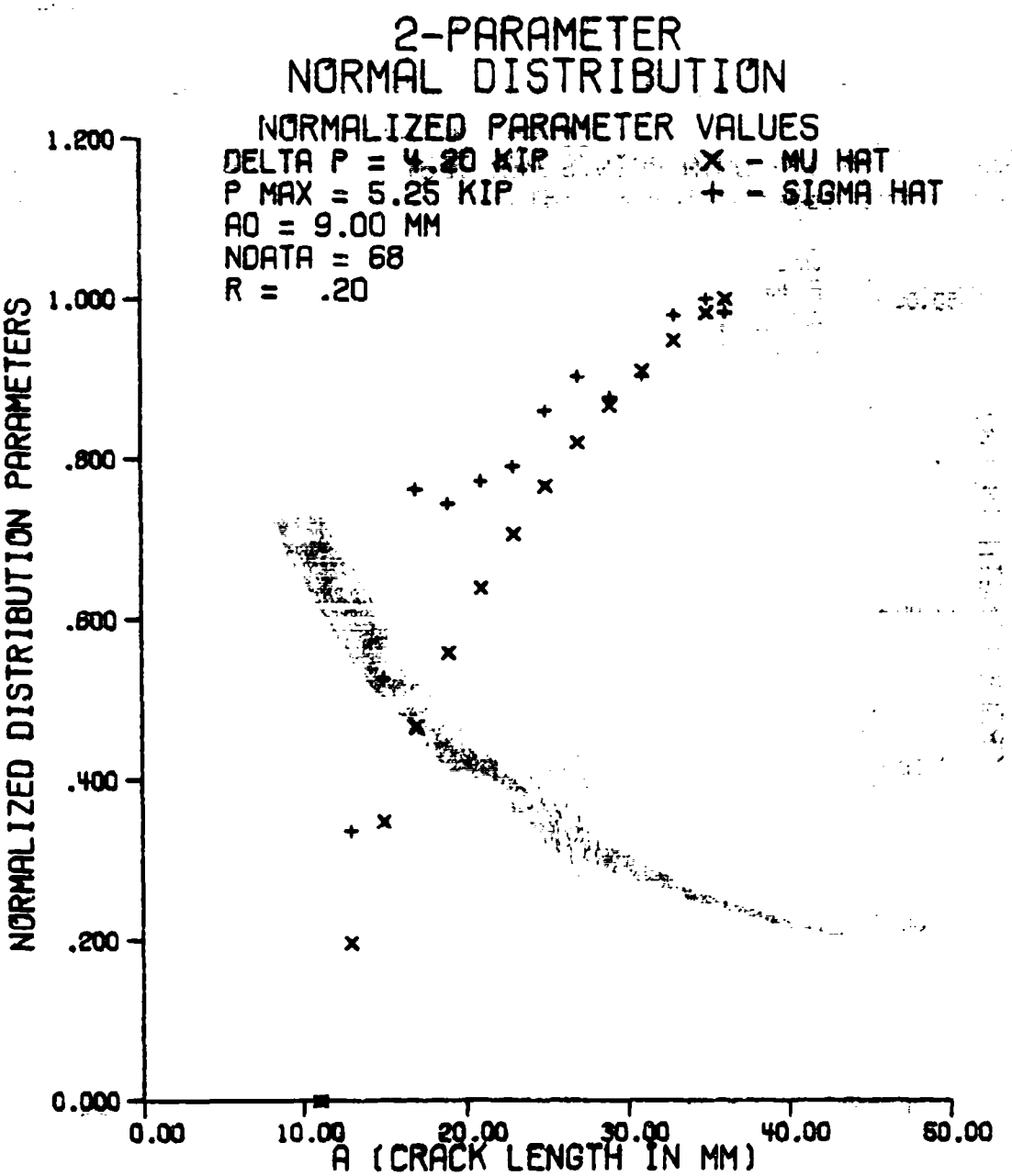

Figure 60. 2-Parameter Normal Distribution Parameters as a Function of Crack Length for Cycle Count Data Predicted from the Distribution of dN/da

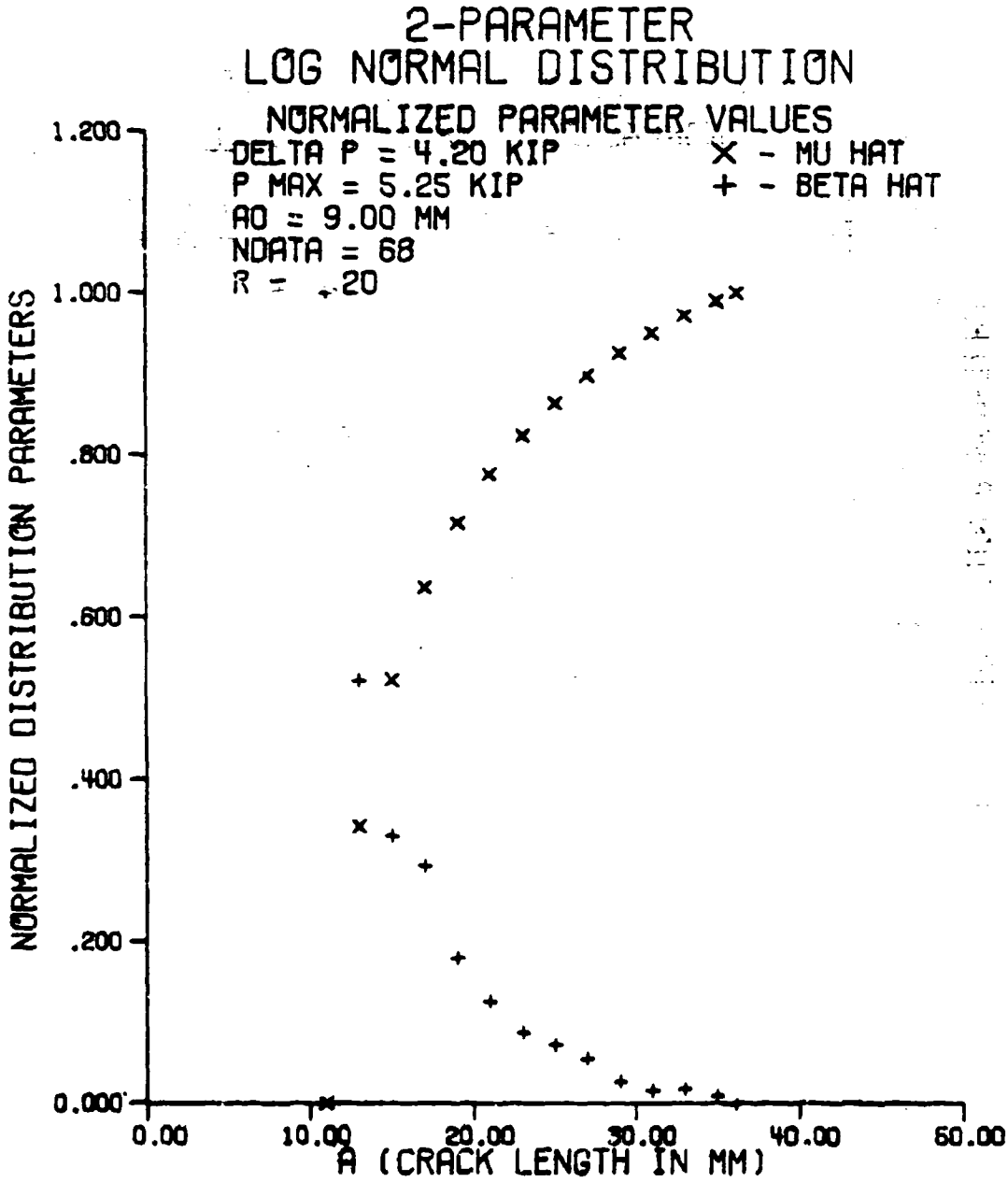

Figure 61. 2-Parameter Log Normal Distribution Parameters as a Function of Crack Length for Cycle Count Data Predicted from the Distribution of dN/da

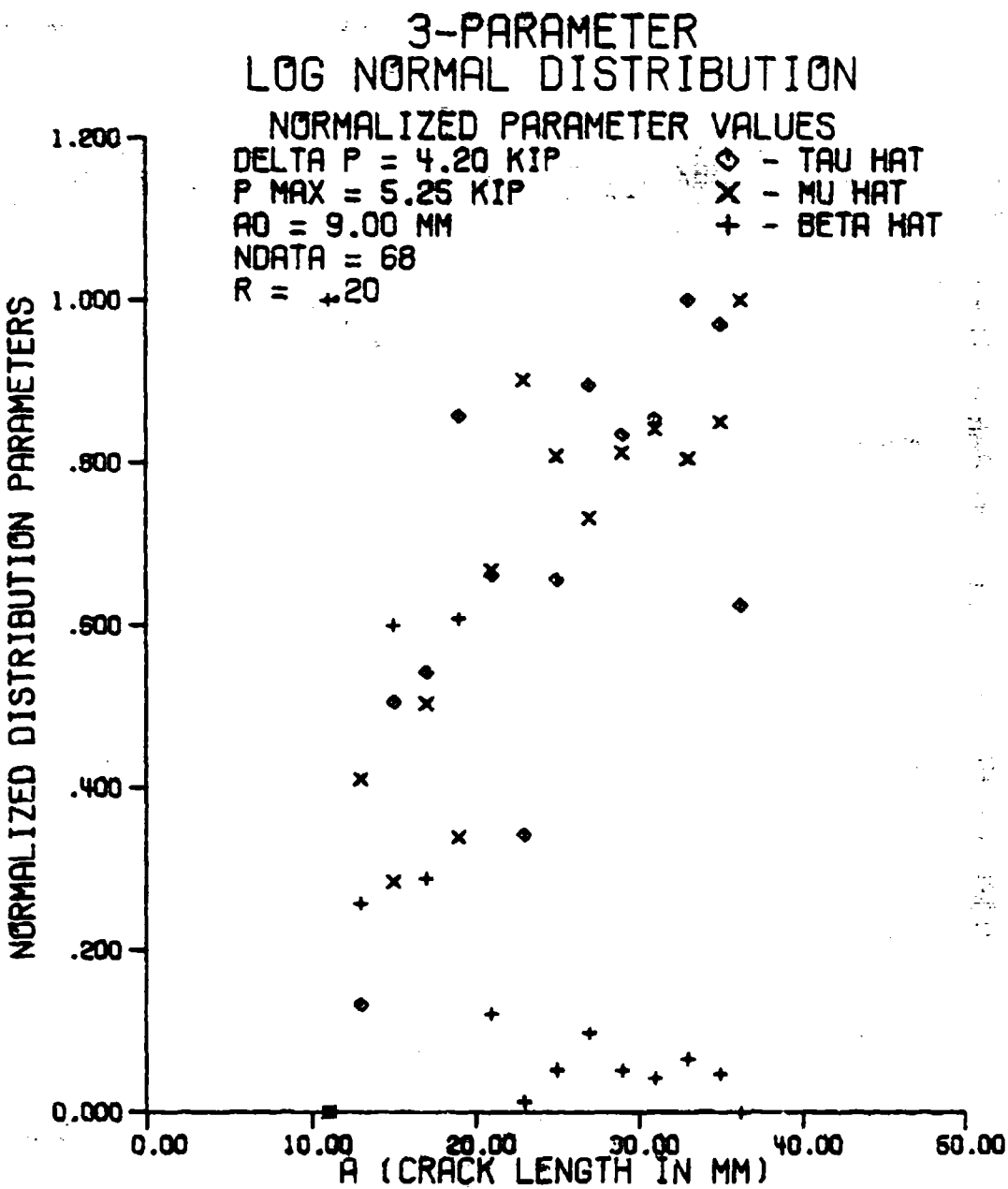

Figure 62. 3-Parameter Log Normal Distribution Parameters as a Function of Crack Length for Cycle Count Data Predicted from the Distribution of (W/da

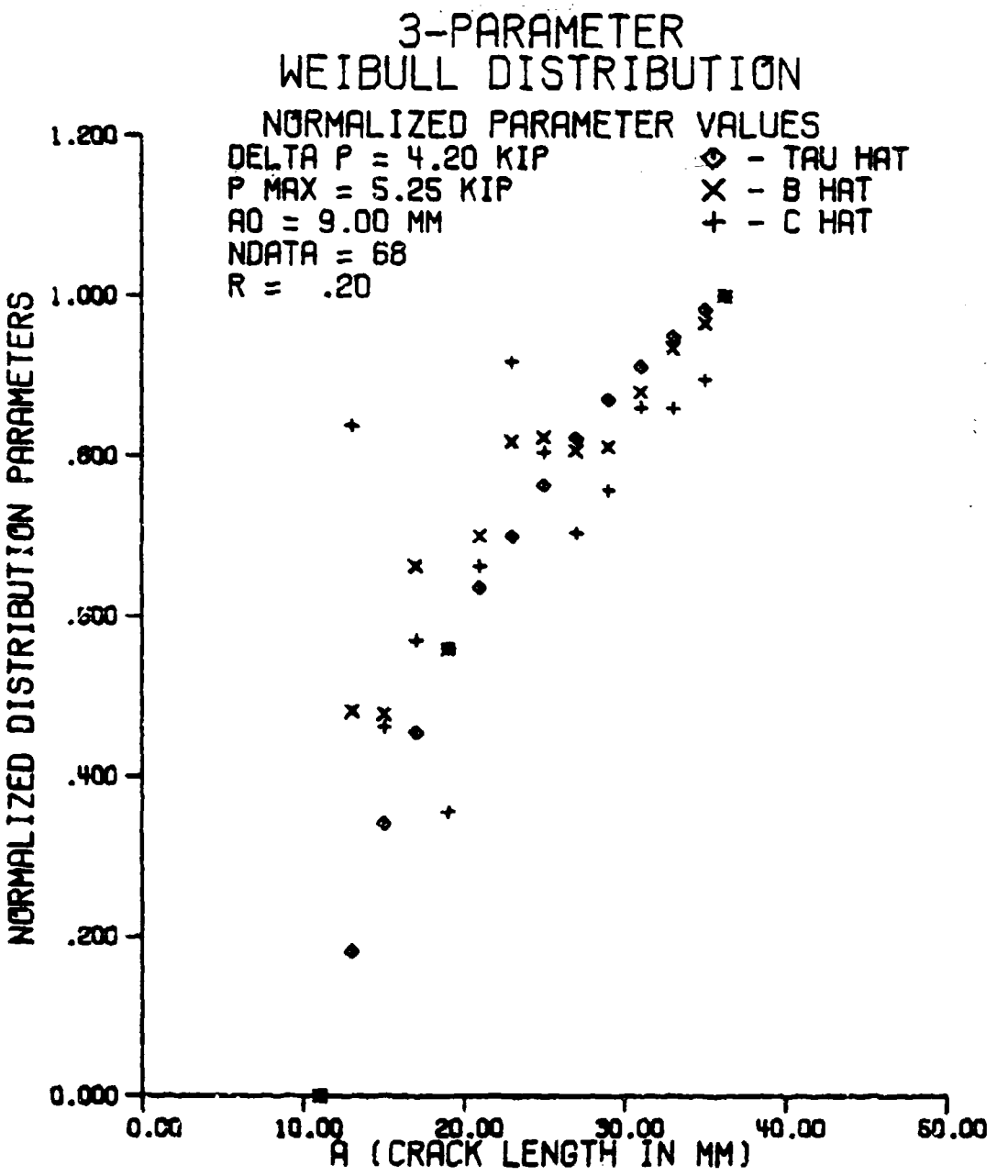

Figure 63. 3-Parameter Weibull Distribution Parameters as a Function of Crack Length for Cycle Count Data Predicted from the Distribution of dN/da

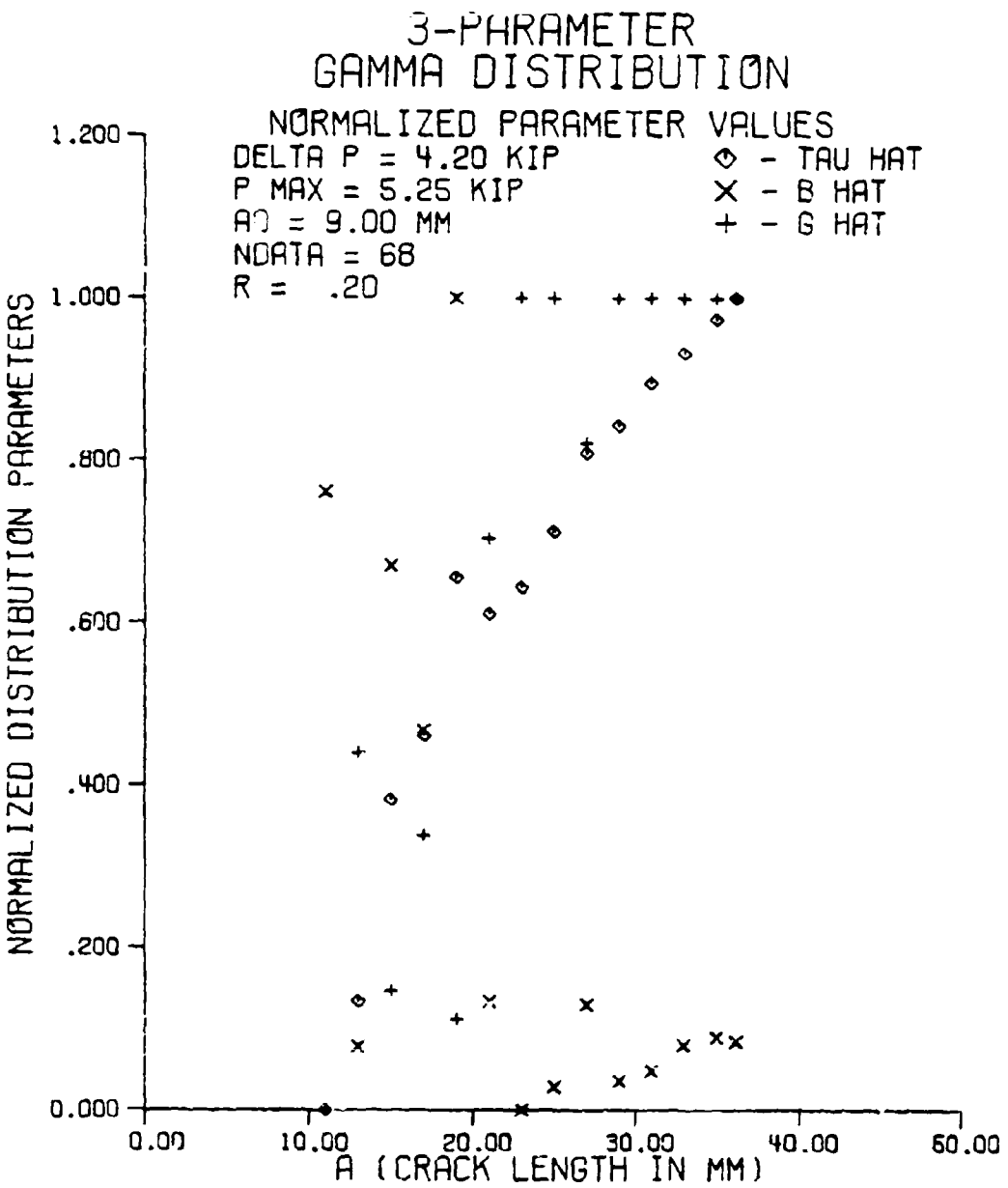

Figure 64. 3-Parameter Gamma Distribution Parameters as a Function of Crack Length for Cycle Count Data Predicted from the Distribution of dN/da

Table XVII

Average Goodness of Fit Criteria for the Distribution of Cycle Count Data Predicted from the Distribution of dN/da

DISTRIBUTION	CHI-SQUARE TAIL AREA	KOLMOGOROV-SMIRNOV TEST	CLOSENESS (R SQUARED)
2-PARAMETER NORMAL	0.9816	0.0652	0.98765
2-PARAMETER LOG NORMAL	0.9640	0.0614	0.98990
3-PARAMETER LOG NORMAL	0.9319	0.0567	0.99169
3-PARAMETER WEIBULL	0.9135	0.0617	0.98100
3-PARAMETER GAMMA	0.2040	2.4493	0.85993

Table XVIII

Distribution Rankings for the Distribution of Cycle Count Data Predicted from the Distribution of dN/da

DISTRIBUTION	MEAN	STANDARD DEVIATION	NUMBER OF TIMES BEST DISTRIBUTION
2-PARAMETER NORMAL	3.714	1.0690	1
2-PARAMETER LOG NORMAL	2.571	0.9376	2
3-PARAMETER LOG NORMAL	1.571	0.7559	8
3-PARAMETER WEIBULL	2.857	1.0995	1
3-PARAMETER GAMMA	2.857	1.4033	2

from the distribution of dN/da. The mean and standard deviation of both distributions at the crack length levels used above were computed and the results are shown in Table XIX. At every crack length level, there was no significant difference between the means but there was a very significant difference between the standard deviations of the two distributions. In every case, the standard deviation of the predicted cycle count data was much smaller than the standard deviation of the actual cycle count data.

Just as for the data predicted from the distribution of da/dN, a vs. N data were predicted from the mean and $\pm$ 1, 2, and 3 sigma dN/da lines. The results are shown in Figure 65. A comparison between the actual cycle count mean and $\pm$ 1, 2, and 3 sigma values and the cycle count values predicted from the mean and $\pm$ 1, 2, and 3 sigma dN/da lines at a single crack length level is shown in Table XX.

From the above analysis, it can be concluded again that predicting a vs. N data from the distribution of dN/da using the method described in Section 7.3 yields low error in predicting mean crack propagation behavior, but yields high error in predicting crack propagation behavior at the extremes of the distribution of N.

Table XIX

Comparison of the Distributions Between Actual Cycle Count Data and Cycle Count Data Predicted from the Distribution of dN/da

	MEAN		STANDARD DEVIATION	
CRACK LENGTH (MM)	ACTUAL	PREDICTED	ACTUAL	PREDICTED
11.000	55681	55987	6556	2000
13.000	90126	91067	5832	2560
15.000	117486	118326	6719	4367
17.000	139352	139578	10903	4977
19.000	156382	156402	11849	4941
21.000	170786	170694	12489	3289
23.000	182198	182852	8204	3323
25.000	192978	193730	8547	5219
27.000	202538	203416	8944	3506
29.000	211030	211809	9123	3465
31.000	218688	219505	9325	3508
33.000	225459	226408	9637	3633
35.000	231416	232528	10037	3667
36.200	234573	235717	10191	3641

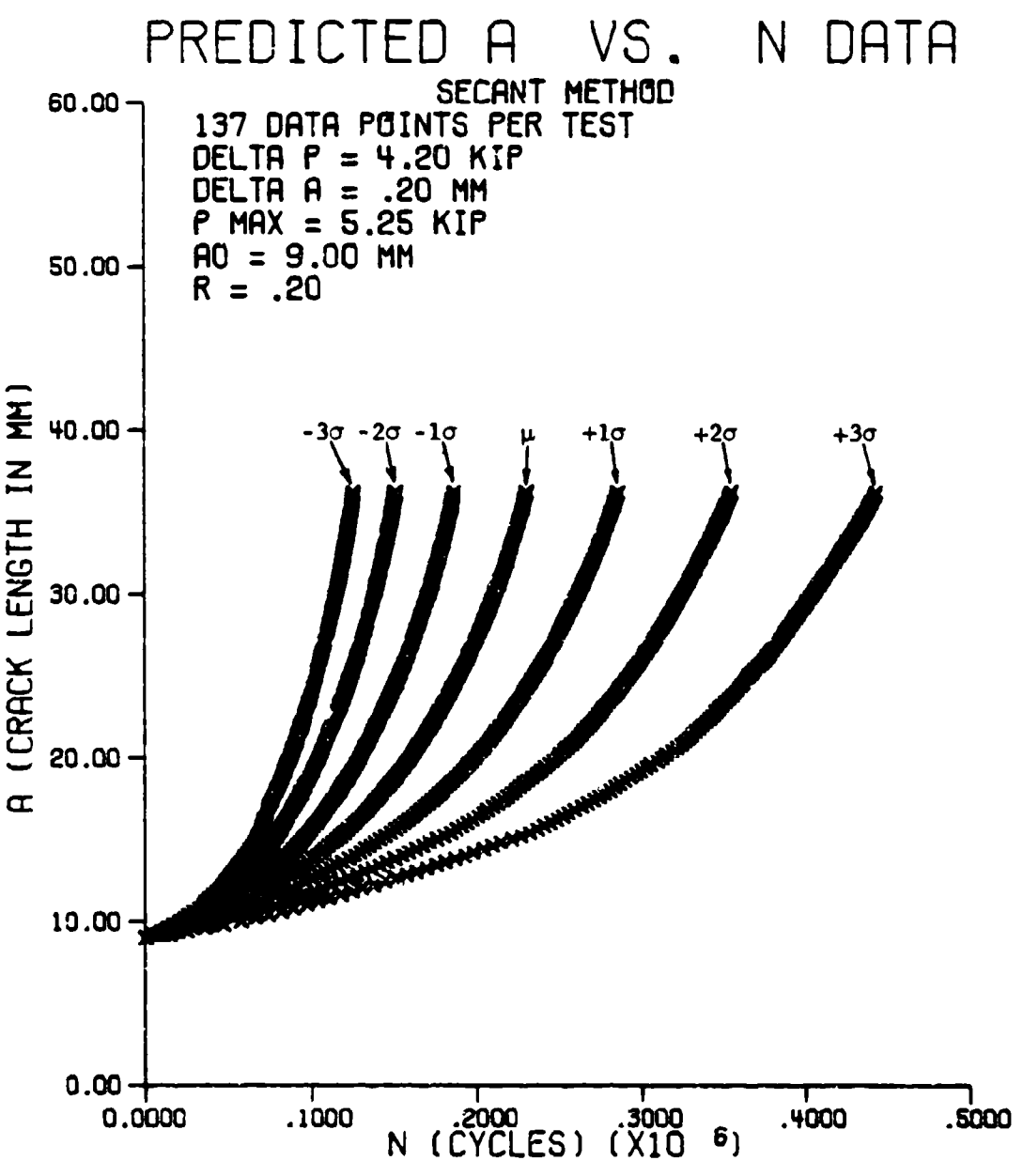

Figure 65. a vs. N Data Predicted from the Mean and ± 1, 2, and 3 Sigma dN/da Lines

Table XX

Comparison of Actual Cycle Count Data with Cycle Count Data Predicted from Constant Variance dN/da Lines

A = 31.000 MM	ACTUAL	PREDICTED
-3 SIGMA	187828	116635
-2 SIGMA	195682	140299
-1 SIGMA	205562	173118
MEAN	217991	213635
+1 SIGMA	233627	264538
+2 SIGMA	253299	328255
+3 SIGMA	278046	409051

SECTION XI

DISCUSSION

Throughout the course of this investigation, a few unique events took place and many interesting observations were made. Some of these have rather simple explanations while others require a quite detailed discussion. Hopefully, some important conclusions can be made as a result.

11.1 Experimental Investigation

The behavior of fatigue crack propagation experienced during this investigation was much different than first anticipated. The most surprising event that took place in almost every test was the sudden changes in the magnitude of the crack growth rate. Both sudden increases in the growth rate, as if the crack had just come upon some unusually weak aluminum, and sudden decreases in the growth rate, as if the crack was experiencing some unusually tough material, were observed repeatedly, many times one or two millimeters after a previous event of similar nature. One of the more outstanding examples of this type of behavior is shown in Figure 66.

It appears that the material is made up mostly of a fairly homogeneous material with many smaller areas located in a random fashion which characteristically have vastly different crack propagation properties than the majority of the material. The size of these small areas seems to vary considerably from as small as less than 1 millimeter in length to perhaps as large as 5 or 10 millimeters in length. These small areas obviously have a very large effect on the overall smoothness of an a vs. N data set

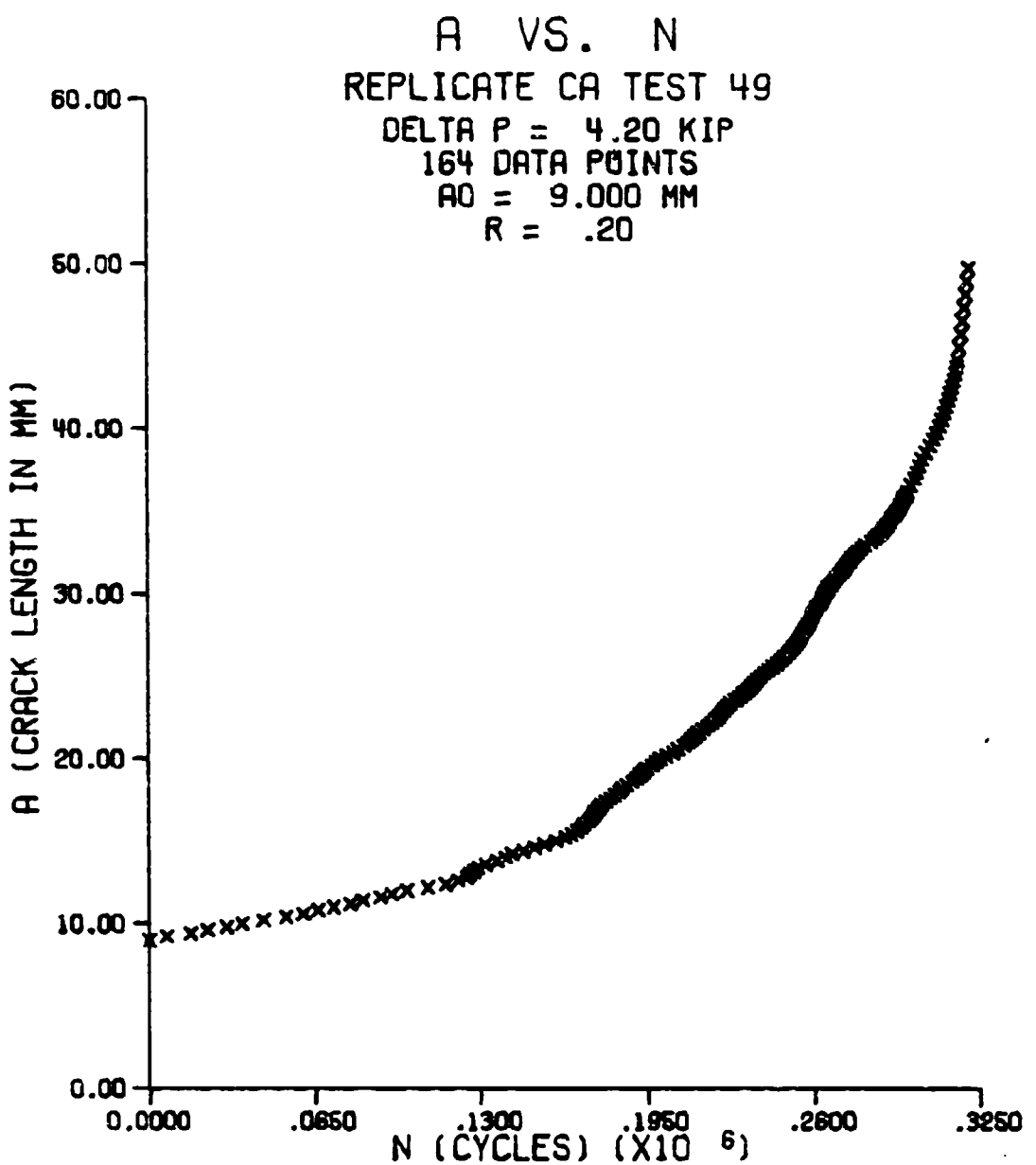

Figure 66. a vs. N Data Showing Abrupt Growth Rate Changes

and on the total amount of scatter, especially in the growth rate data.

The average growth rate also seemed to vary somewhat from test to test, with some tests running slow throughout the whole test, while other tests ran fairly fast throughout the whole test. This phenomenon is the cause of the outlying data sets in Figure 22. As also noted by other investigators [5,6,7], the variation in growth rate at the beginning of the test during the slow growth rates leads to most of the variation in N at the final crack length.

As a result of these observations, the conclusion is made that this alloy is a very non-homogeneous material, especially considering the random nature of crack propagation behavior. It very rarely obeys the smooth growth rate equations often used to describe its behavior and does so only when it's behavior is considered at a very macroscopic level.

11.2 Distribution of N

The conclusion stating that the cycle count data follows a 3-parameter log normal distribution can be considered very strong. The only occurrences where this was not so was at short crack lengths where the need for the location parameter used in the 3-parameter log normal distribution was not near as strong as at long crack lengths.

From Figures 24 through 29, the distribution parameters tend to vary quite a bit at short crack lengths but tend to follow smooth curves after a $\simeq$ 15 mm. The scale parameter in the first two distributions where no location parameter is estimated have very smooth curves, showing that mean crack propagation behavior does follow smooth growth rate equations. The same smooth shape of the location prameter in the last four distributions also supports this statement. Essentially these location parameter

curves define an area where crack propagation will never occur. In other words, the number of load cycles needed to reach a given crack length will never be less than the estimate of the location parameter at that crack length. This is shown in Figure 67. On this plot, crack propagation data will never occur to the left of the location parameter line. Note from Figure 26 that the scale parameter, $\hat{\mu}$, tends to remain constant after a $\simeq$ 20 mm., allowing the location parameter to completely account for the increase of N with increasing crack length. From Figure 24, note the smooth increase of the shape parameter, $\hat{\sigma}$, as a function of crack length, thus supporting the expectation of higher variances at longer crack lengths. Another interesting event is shown in Figure 29. The power parameter, $\hat{\alpha}$, of the generalized 4-parameter gamma distribution was always estimated to be equal to one, thus reducing this distribution to the 3-parameter gamma distribution. It should be noted here that over half of the computer time used to obtain all of the distribution parameters was used to estimate the parameters of the generalized 4-parameter gamma distribution. By eliminating this distribution from the CCDDP program, much time and money can be saved.

Another interesting occurrence which appeared very often is shown in Table VI. Many times the distribution rankings implied by one goodness of fit criterion could not be supported by another goodness of fit criterion and often three different distribution rankings were implied by the three goodness of fit criteria. In other words, the goodness of fit criteria were not consistent between themselves. This necessitated a somewhat subjective analysis of the goodness of fit criteria. The closeness, R^2, tended to be very sensitive to the scales of the plot and the slope of the linear least squares line. Thus, the closeness was rarely used

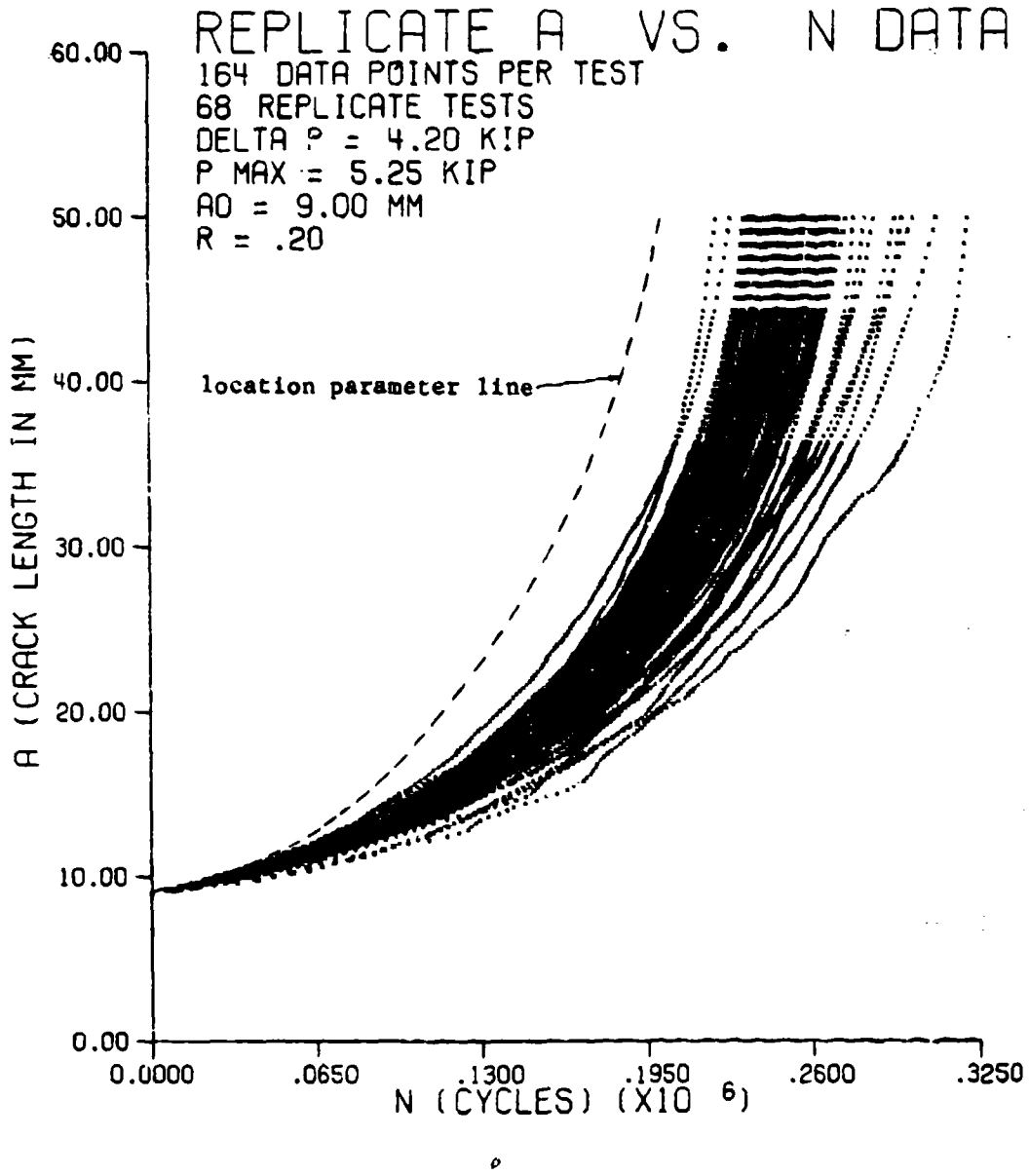

Figure 67. Estimate of the Location Parameter of the 3-Parameter Log Normal Distribution as a Function of Crack Length

unless the slopes were approximately the same between the different distributions. The chi-square tail area tended to be undiscerning between distributions that provided fairly equal fits to the data. Thus, the chi-square goodness of fit criterion was used only when there were fairly large differences between the distributions. The Kolmogorov-Smirnov goodness of fit test provided a fairly reliable and sensitive test and was used heavily in establishing distribution rankings.

A typical fit provided by each of the five distributions for the cycle count data is shown in Figures 68 through 72. As state previously, the 3-parameter log normal distribution provided a reliable tight fit for the cycle count data as shown in Figure 70. The 3-parameter gamma distribution did surprisingly well and although it was not selected as the best distribution very often, it consistently placed a close second to the 3-parameter log normal distribution. The 2-parameter log normal distribution did not do well due to the lack of a location parameter. For the 3-parameter Weibull distribution, the location parameter seemed to work alright, but the shape of the density function did not match the data very well as shown in Figure 71. The 2-parameter normal distribution provided a very poor fit for the cycle count data and should not be included in any further investigations of the dictribution of N.

11.3 Crack Growth Rate Calculation Methods

Of the six da/dN calculation methods selected, both the secant method and the modified secant method contributed low amounts of error into the da/dN data as shown in Table VIII. The modified secant method calculated da/dN data which could be integrated back closer to the original a vs. N data than the secant method could, perhaps because it calculates da/dN

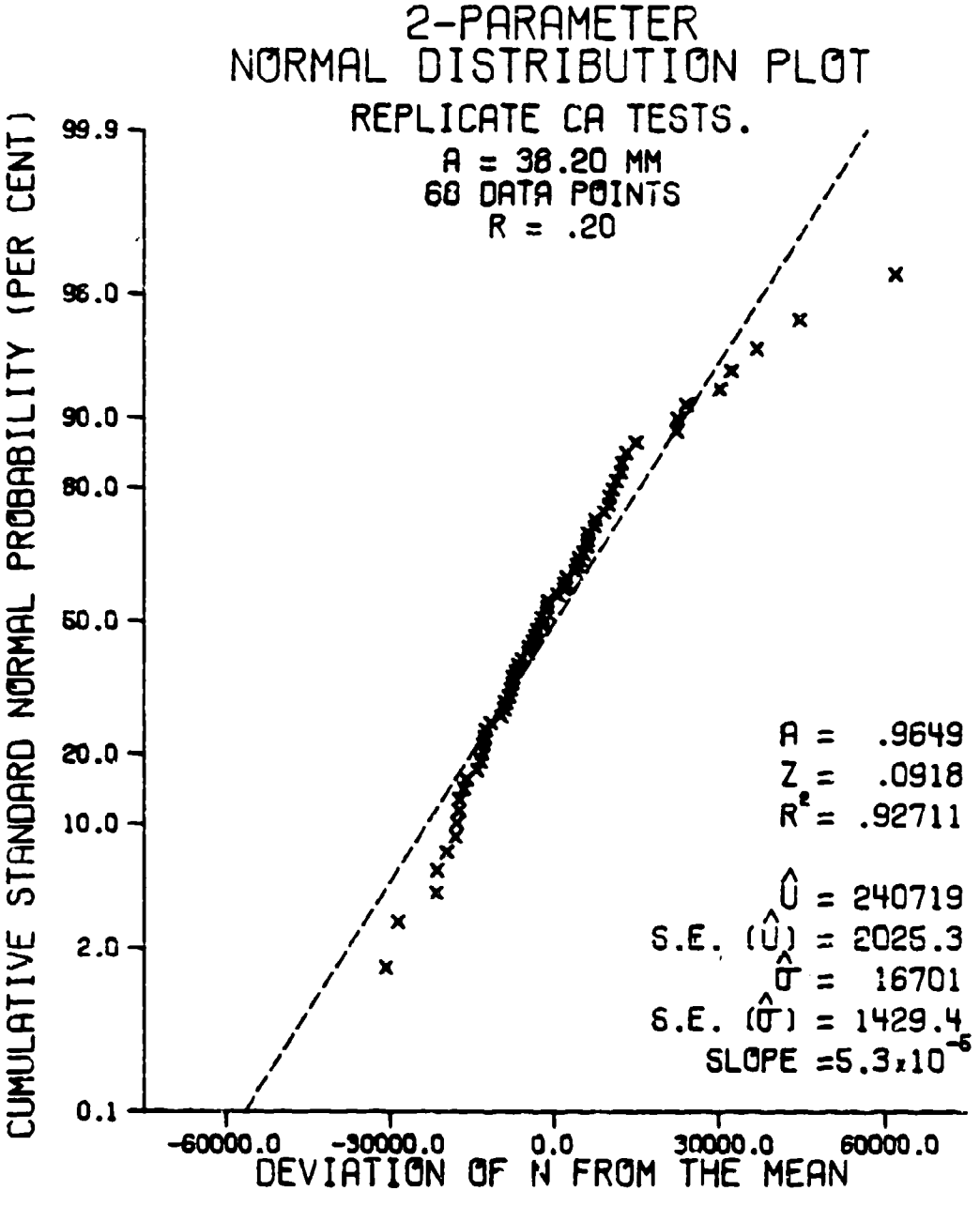

Figure 68. Typical Fit of the Cycle Count Data to the 2-Parameter Normal Distribution

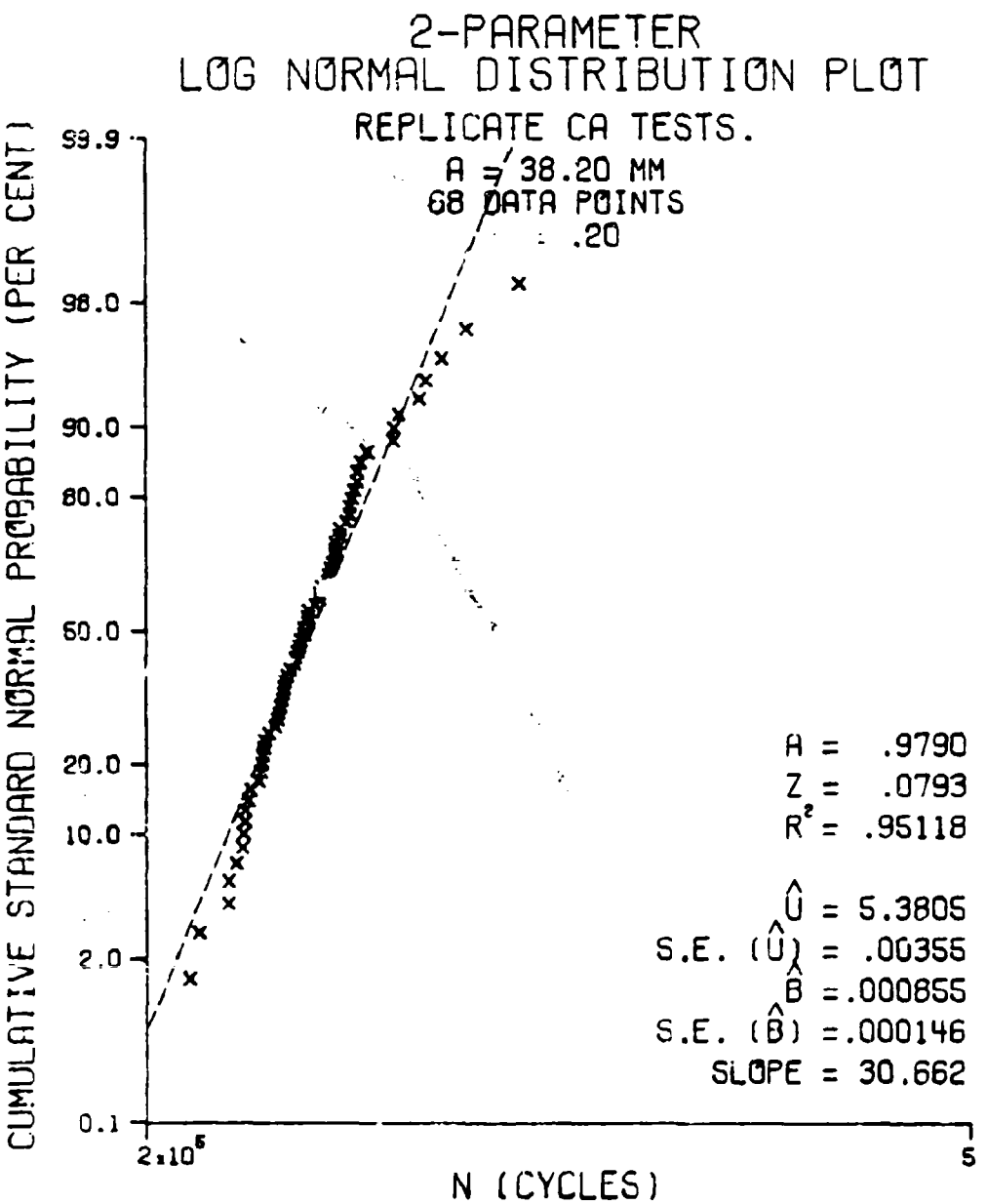

Figure [illegible]. Typical Fit of the Cycle Count Data to the 2-Parameter Log Normal Distribution

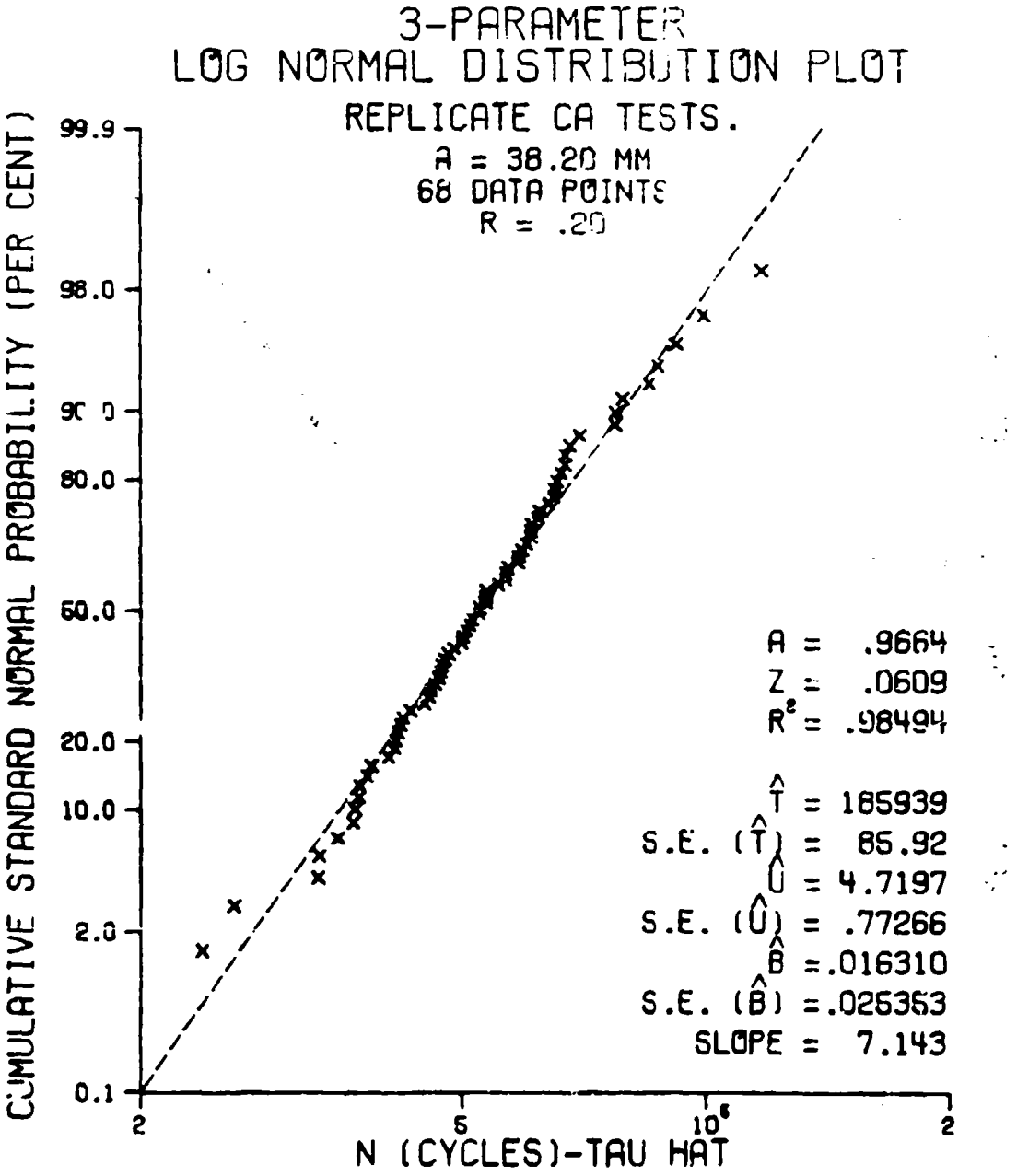

Figure 70. Typical Fit of the Cycle Count Data to the 3-Parameter Log Normal Distribution

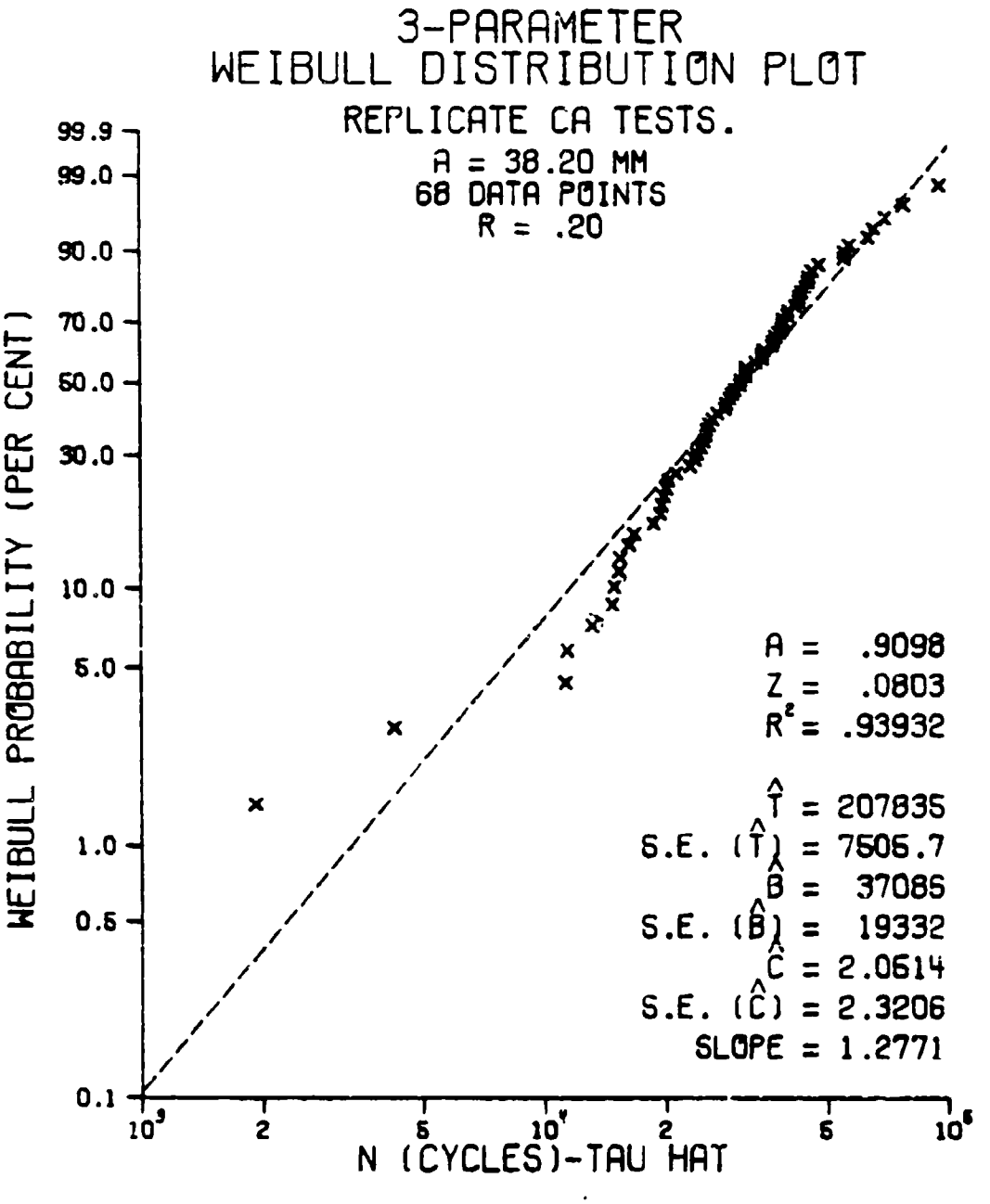

Figure 71. Typical Fit of the Cycle Count Data to the 3-Parameter Weibull Distribution

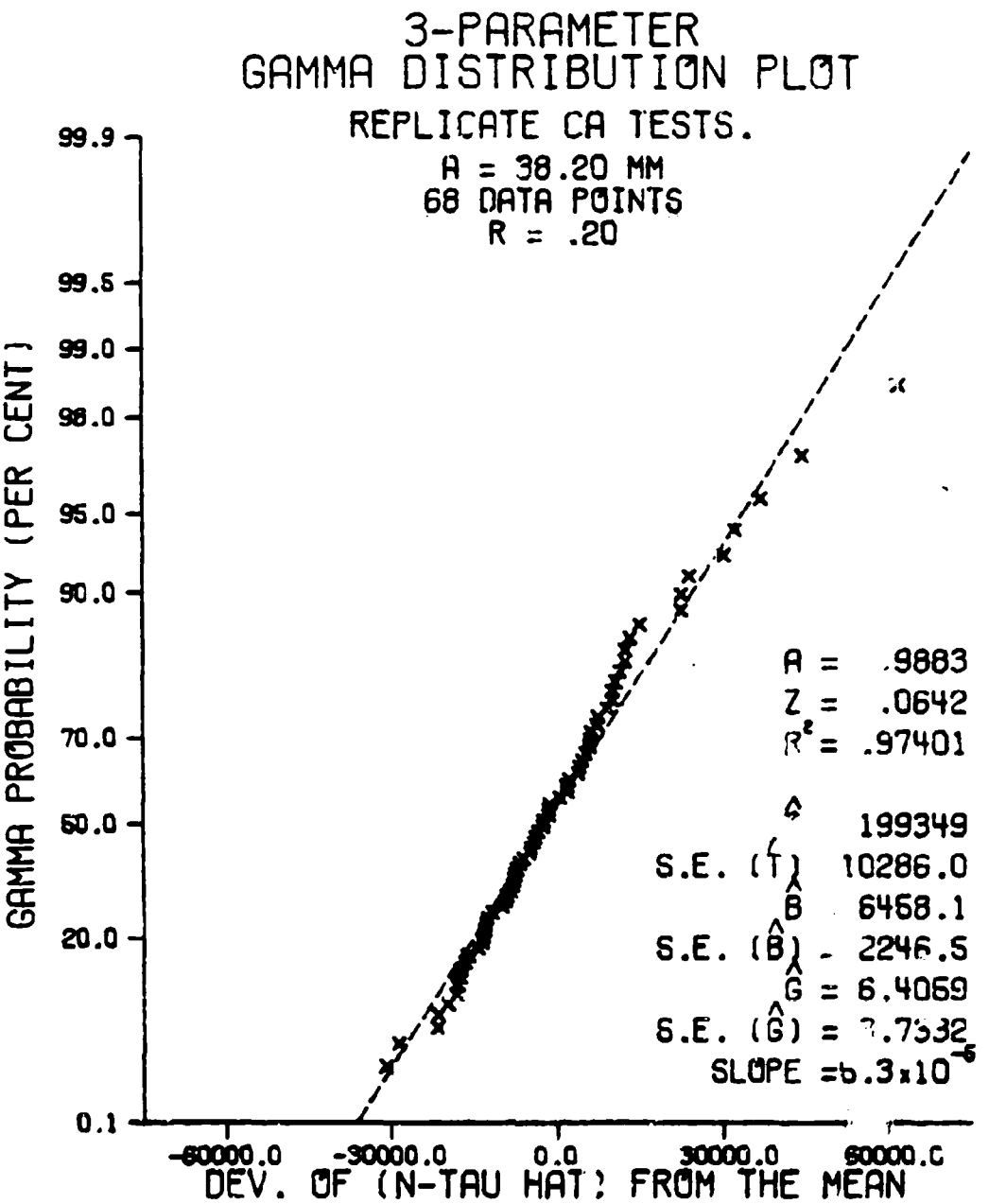

Figure 72. Typical Fit of the Cycle Count Data to the 3-Parameter Gamma Distribution

data at the original crack length levels instead of between the original crack length levels.

None of the incremental polynomial methods calculated da/dN data which could be integrated back even close to the original a vs. N data. This is no doubt due to the smoothing effect of these methods which tends to reduce the sudden changes in growth rates. This is shown in Figure 38 where the number of extreme da/dN data points for the quadratic 7-point incremental polynomial method is much less than the number of extreme da/dN data points for either the secant method of the modified secant method (Figures 36 and 37). This is also shown in Figures 30 through 35 where the incremental polynomial method data follow a narrow band line while the secant method and modified secant method data follow a more broad band line. Note also from Figures 32 through 35 the waviness of the data showing the large changes in growth rate noticed during data acquisition.

If crack propagation data were always very smooth data, then the incremental polynomial methods would introduce a very small amount of error into the da/dN data. But as stated previously, the sudden changes in growth rate are inherent in the crack propagation process, and any attempt at modifying these changes will distort the resulting data and prevent it from becoming a true representation of crack propagation behavior.

Of the four incremental polynomial methods used, both the quadratic 7-point version and the quadratic log-log 7-point version do the best job, followed closely by the linear 7-point version. The linear log-log 7-point version does a very poor job as shown in Figure 34 and Table VIII. The use of the log-log transformation failed to give any improvement over the conventional incremental polynomial methods in the ability to reproduce

the original a vs. N data. The use of the second order polynomial fit over a straight line polynomial fit improves the performance of the incremental polynomial methods, especially when using the log-log transformation.

The amount of variation in the average incremental per cent error over all of the tests was fairly small, usually less than ± 1.5 per cent error, indicating fairly consistent results over all of the experimental tests.

11.4 Distribution of da/dN

No outstanding positive results were achieved for the distribution of da/dN. Each of the distributions provided roughly the same quality of fit for the data, with the 3-parameter gamma distribution doing a slightly better job than the other four distributions.

The da/dN data varied quite a bit as a function of ΔK as shown in Figure 36. As a result, different distributions would provide a fit for the da/dN data at different ΔK levels, depending on the general shape and skewness of the data at a given ΔK level. There were several occasions when the da/dN data was skewed left, as shown in Figure 73, symmetric, as shown in Figure 74, or skewed right, as shown in Figure 75.

When the data was either skewed left or symmetric, the 2-parameter normal distribution provided the best fit for the da/dN data, as shown in Figures 76 and 77. When the data was skewed right, either of the log normal distributions, the 3-parameter Weibull distribution, or the 3-parameter gamma distribution provided a fit for the da/dN data. Typical fits of the skewed right da/dN data to these four distributions are shown in Figures 78 through 81. Due to the large variations in the da/dN data, each of the distributions is needed to provide a fit for the wide range of density

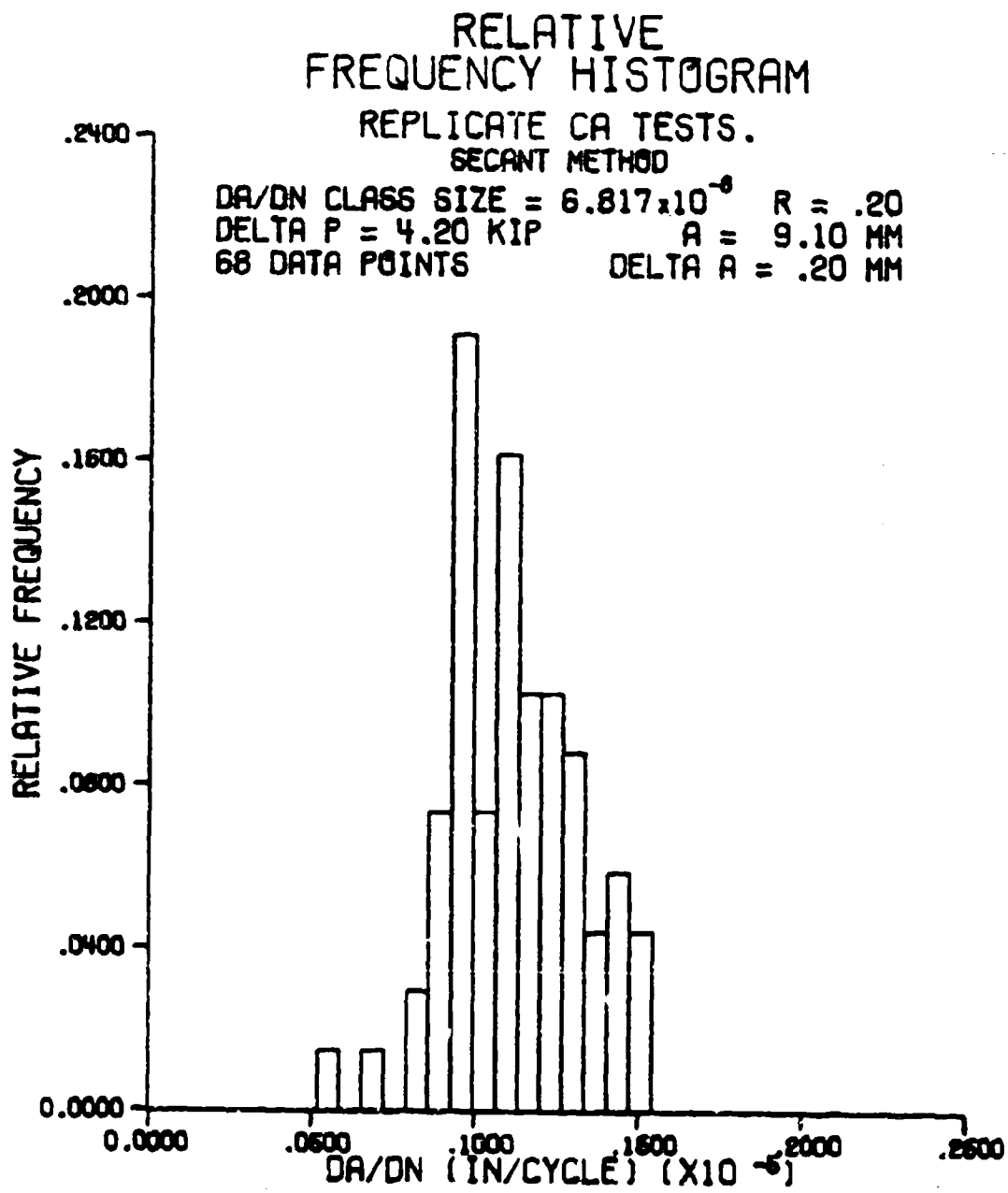

Figure 73. Typical Skewed Left da/dN Data

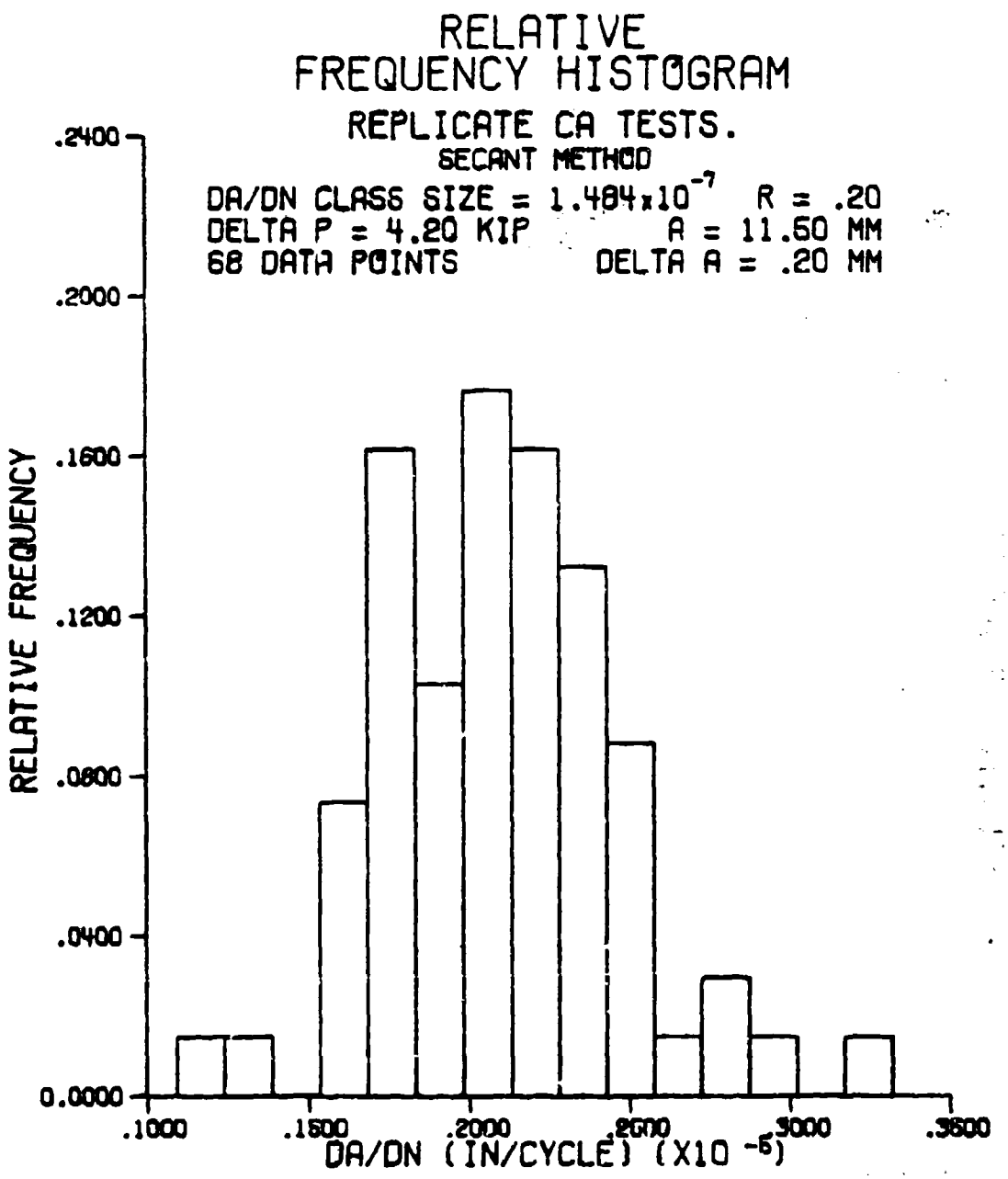

Figure 74. Typical Symmetric da/dN Data

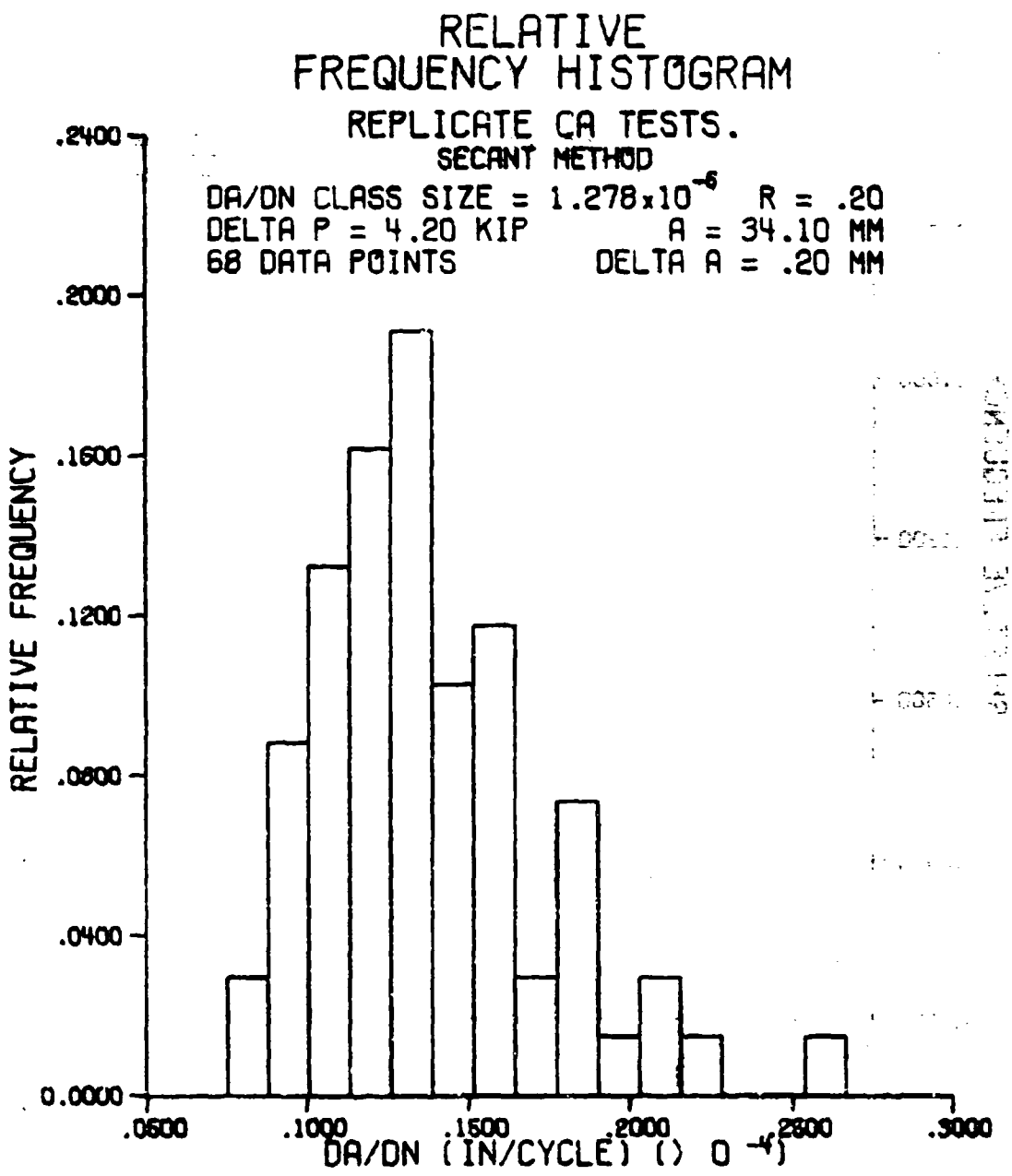

Figure 75. Typical Skewed Right da/dN Data

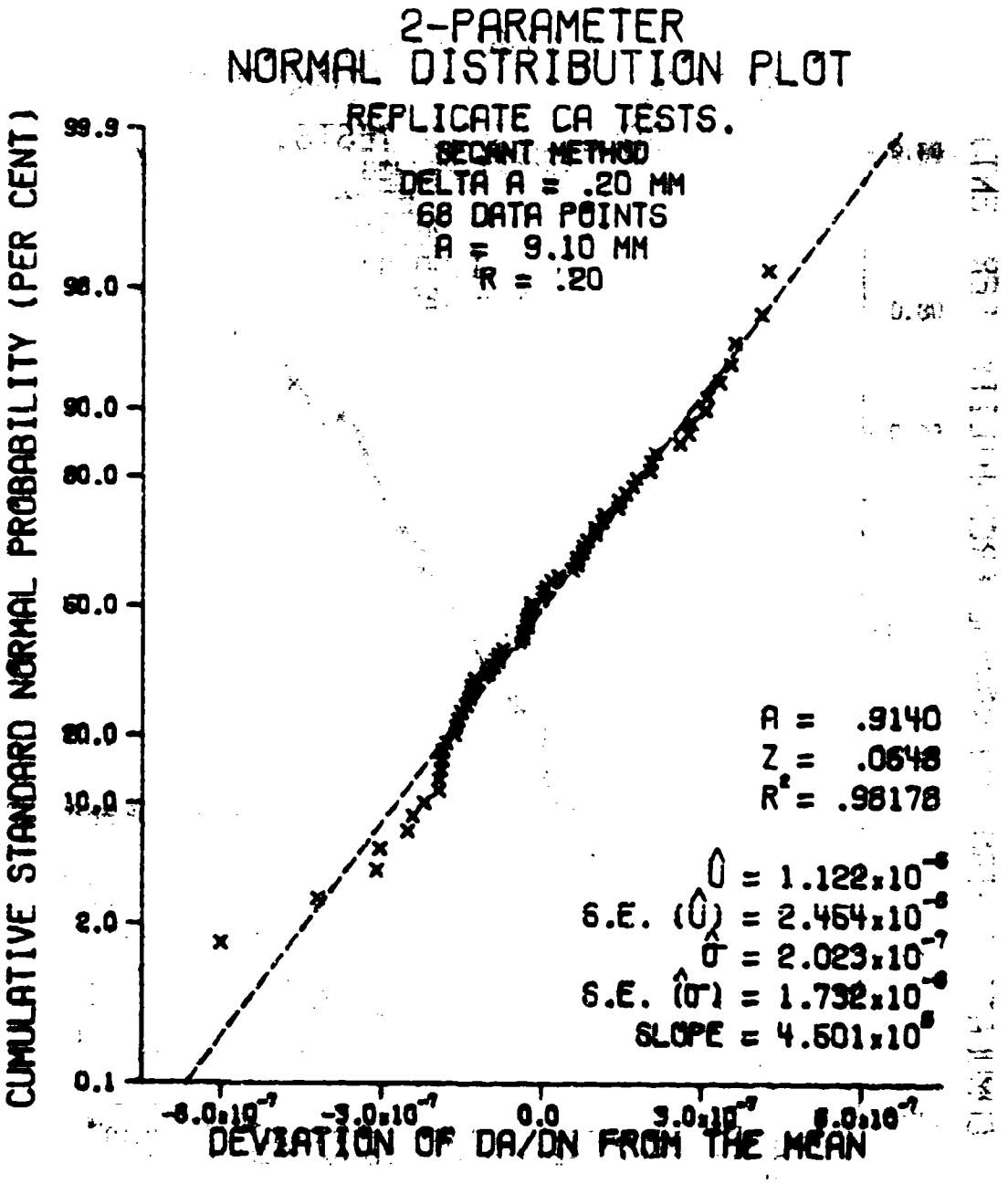

Figure 76. Typical Fit of Skewed Left da/dN Data to the 2-Parameter Normal Distribution

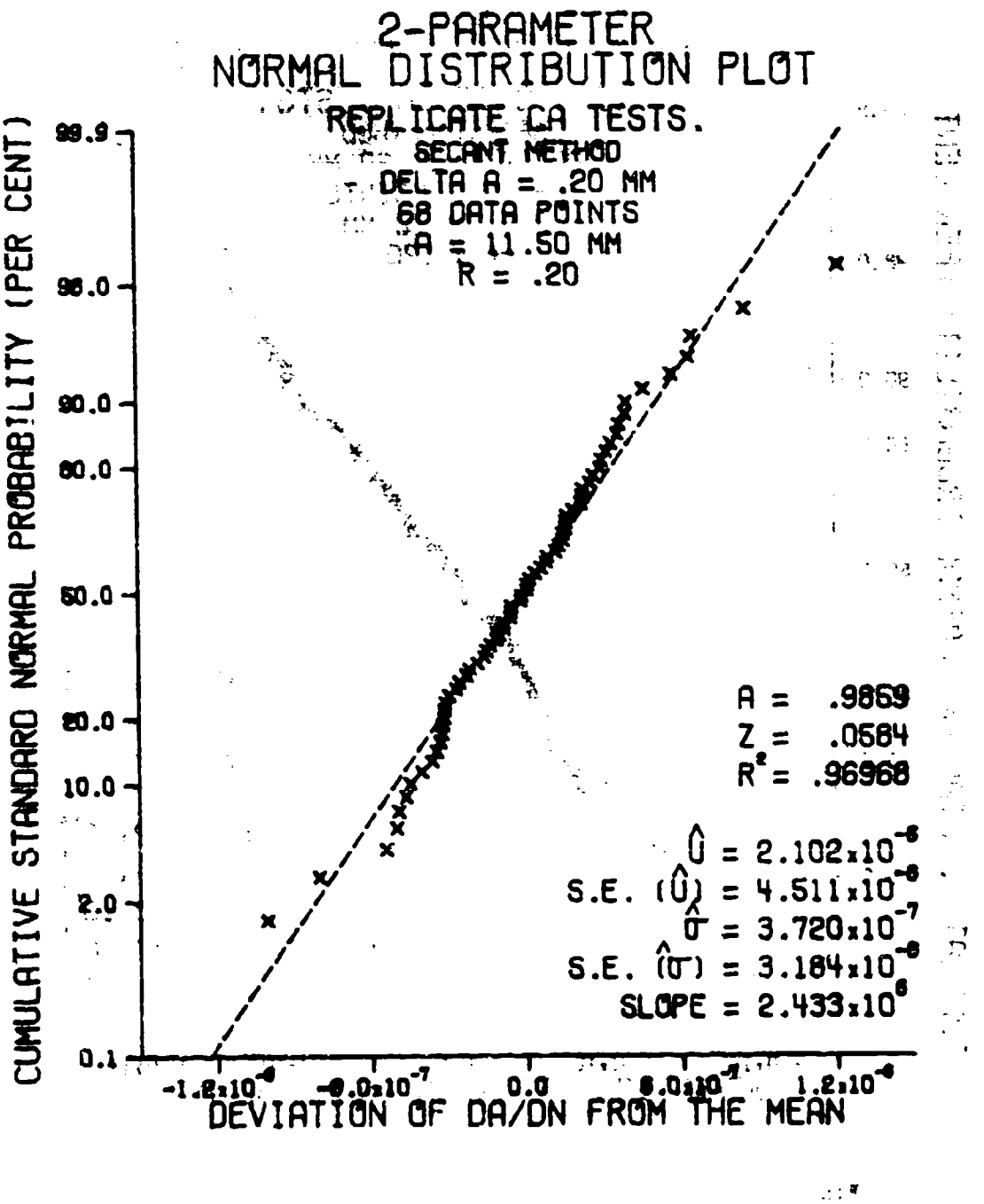

Figure 77. Typical Fit of Symmetric da/dN Data to the 2-Parameter Normal Distribution

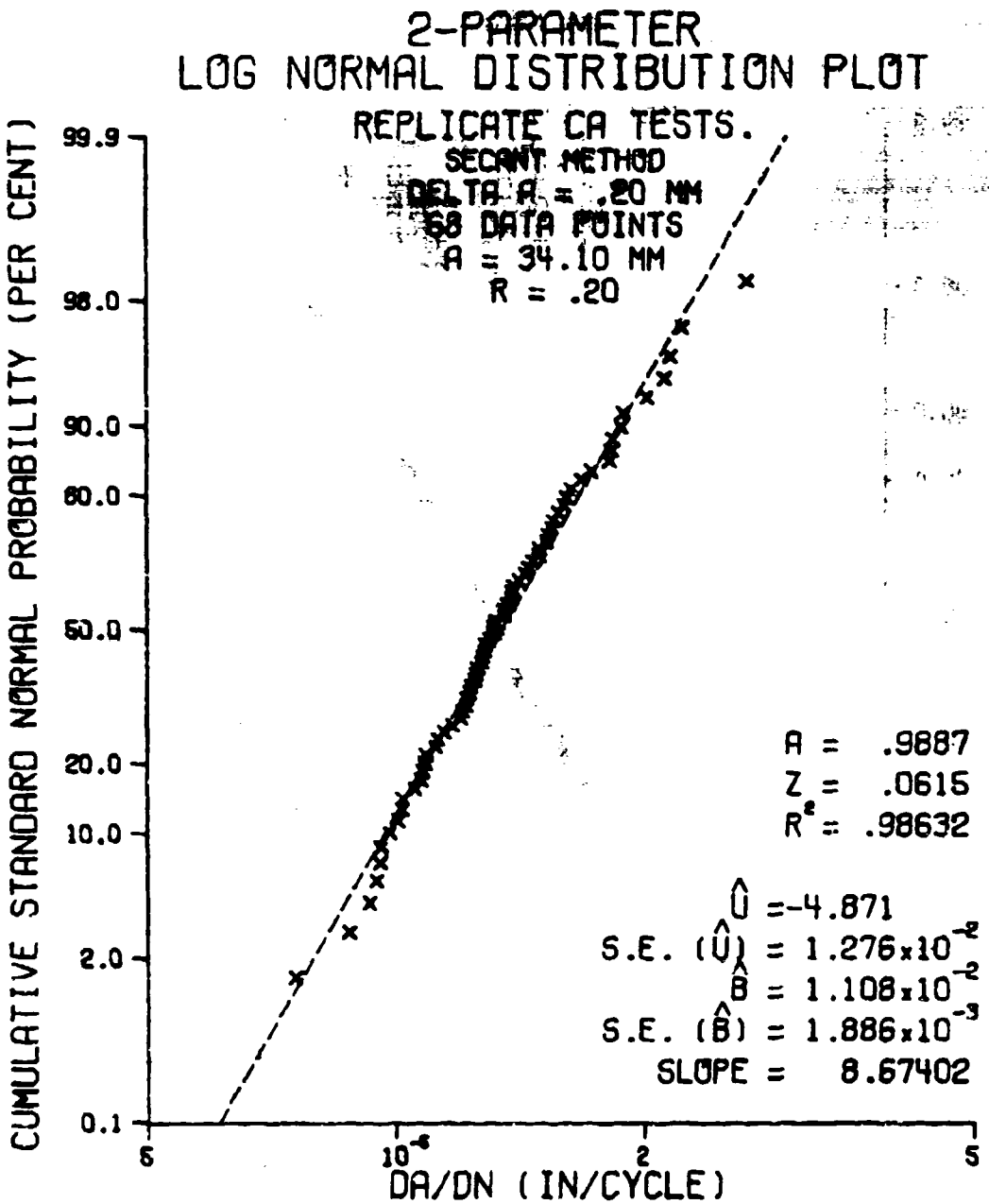

Figure 78. Typical Fit of Skewed Right da/dN Data to the 2-Parameter Log Normal Distribution

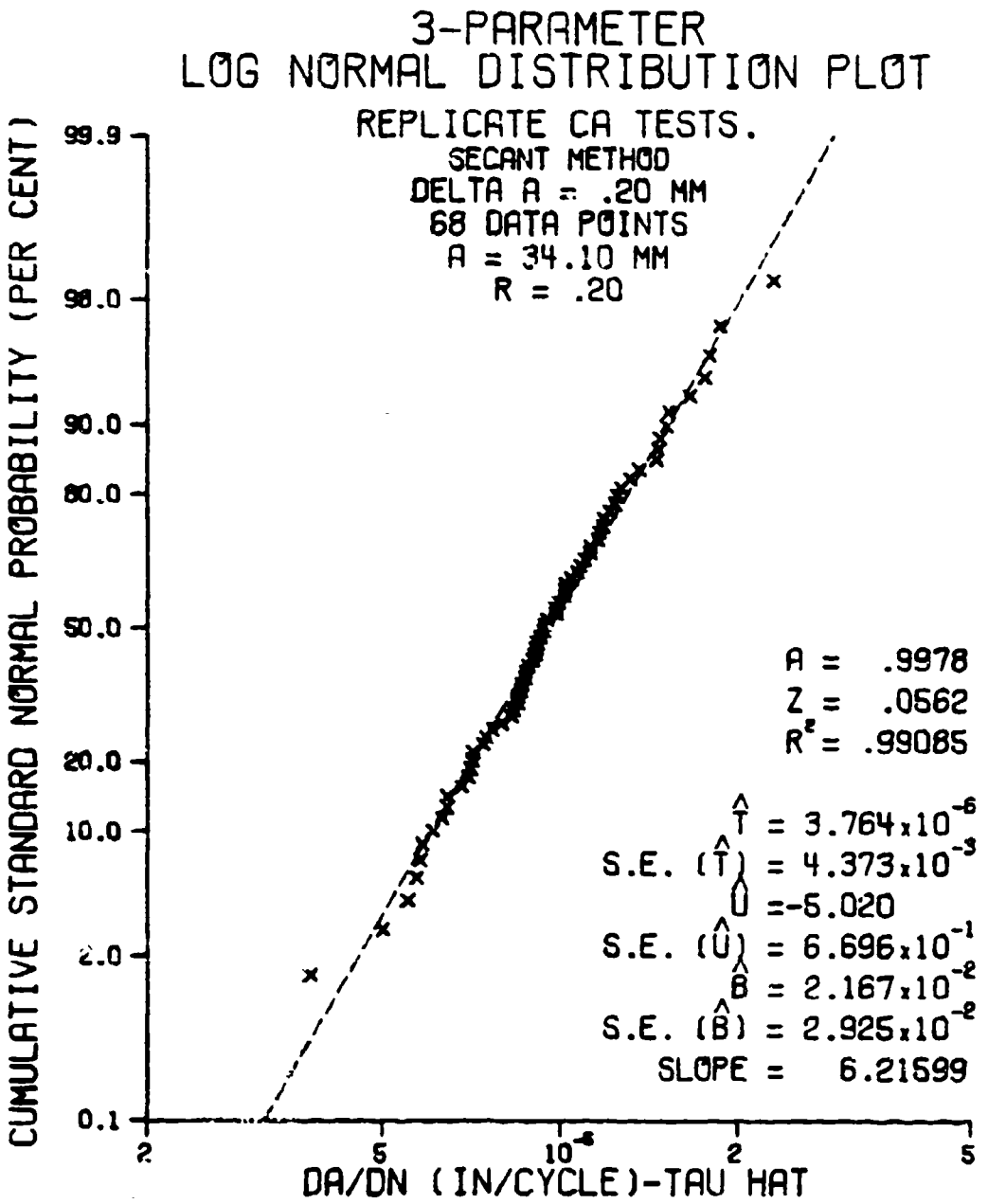

Figure 79. Typical Fit of Skewed Right da/dN Data to the 3-Parameter Log Normal Distribution

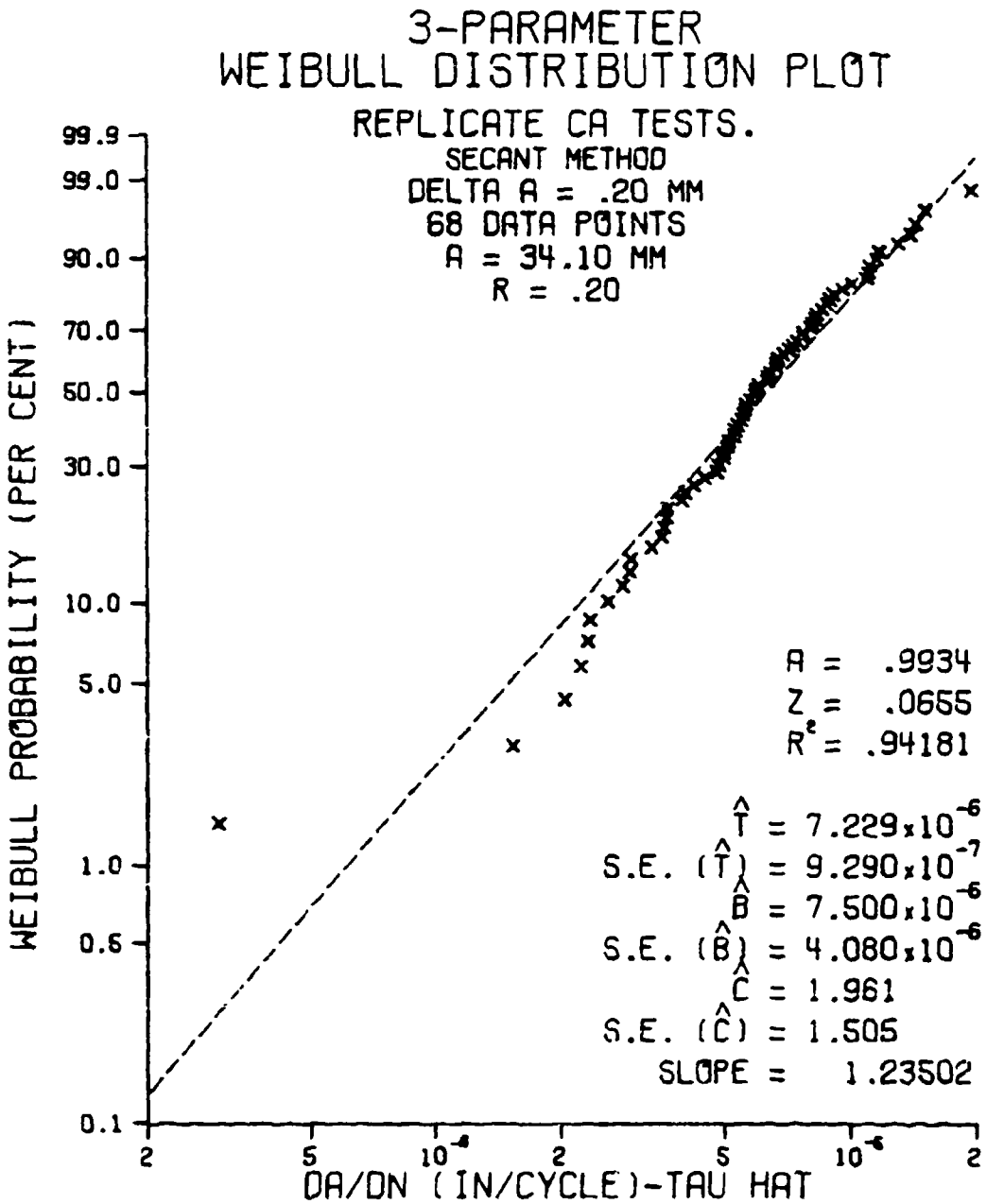

Figure 80. Typical Fit of Skewed Right da/dN Data to the 3-Parameter Weibull Distribution

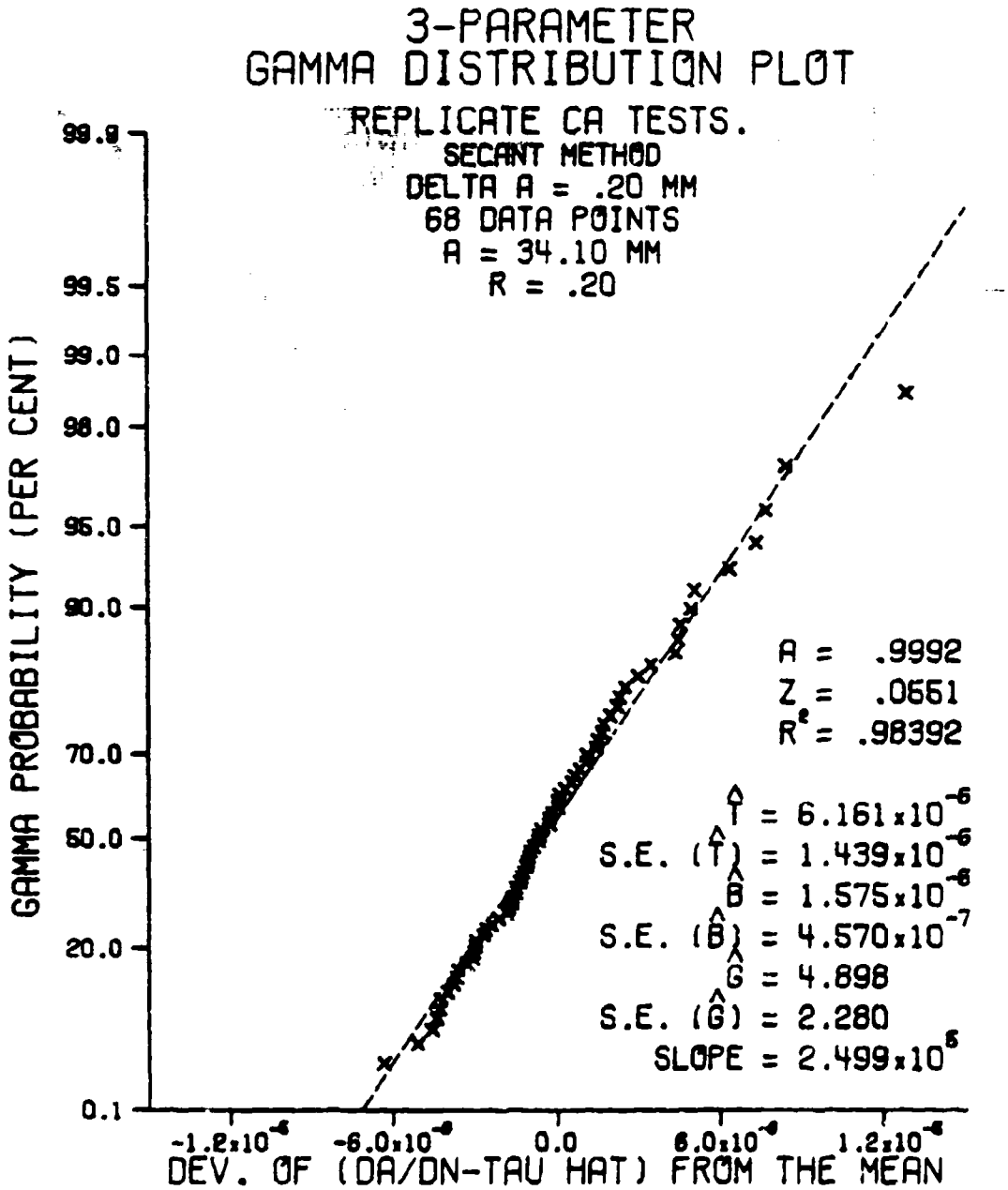

Figure 81. Typical Fit of Skewed Right da/dN Data to the 3-Parameter Gamma Distribution

function shapes.

The large amount of variation in the shape of the da/dN data as a function of ΔK is shown in the plots of the distribution parameters as a function of crack length (Figures 40 through 45). Note that there is a lot of variation in the shape parameter (the pluses) and the location parameter (the diamonds). The variation of the shape parameter reflects the changes in the amount of variance and the shape of the data. The variation of the location parameter reflects the changing skewness of the data. As the skewness goes from right to left, the estimate of the location parameter decreases rapidly. Also, from Figure 45, it can be seen that there are many occurrences where the estimate of $\hat{\alpha}$ was not equal to one, thus implying the necessity of the inclusion of the generalized 4-parameter gamma distribution when analyzing da/dN data so that a wide range of density function shapes can be accommodated for the da/dN data.

11.5 Prediction of a vs. N Data from the Distribution of da/dN

The results of the prediction of replicate a vs. N data from the distribution of da/dN were less revealing than anticipated. When comparing Figure 46 with Figure 22, it becomes apparent that the variance of the predicted a vs. N data is much less than the variance of the actual a vs. N data. However, the mean of the predicted a vs. N data is very close to the mean of the actual a vs. N data. The implication of this is that crack propagation behavior is not being accurately modeled by a randomly selected value of da/dN from the distribution of da/dN. In crack propagation behavior, as discussed in Section 11.1, the growth rate at a given ΔK level is not independent of the growth rates at previous ΔK levels, as evidenced by periods of up to 10 mm. of uncharacteristically fast or slow

growth rates. However, the independence of growth rates is assumed in the prediction of a vs. N data from the da/dN distribution parameters, resulting in very smooth a vs. N data. This smooth a vs. N data lacks the areas of sudden fast and slow growth rates discussed in Section 11.1 which occurs frequently in actual a vs. N data. Thus, the combination of many smooth a vs. N lines of the same mean behavior results in the reduction of variance noted above. To accurately predict crack propagation behavior, some means of quantitatively describing the interdependence of adjacent growth rates must be found.

When the distribution of the cycle count data predicted from the distribution of da/dN was analyzed, neither gamma distribution would converge on its parameters as the estimate of the shape/power parameter, $\hat{g}$, tended to approach its upper global limit. The 2-parameter log normal distribution provided the best fit for this data because the location parameter of the 3-parameter log normal distribution was estimated to be zero at most crack length levels.

When the distribution of the predicted cycle count data is compared with the distribution of the actual cycle count data, as shown in Table XIII, it can again be seen how the mean of the predicted cycle count data is very close to the mean of the actual cycle count data while the standard deviation of the predicted cycle count data is much less than the standard deviation of the actual cycle count data.

When a vs. N data are predicted from constant variance da/dN lines, the spread of the predicted data is much wider than the spread of the actual data, as shown in Table XIV. This occurs because either all very slow or very fast growth rate data is used at the $\pm$ 3 sigma da/dN lines, thus causing either a very long or very short number of cycles. The

actual data, however, rarely has any growth rates on the order of $\pm$ 3 sigma, and even more rarely has repeated growth rates on the order of $\pm$ 3 sigma. On the average, actual data tend to have repeated growth rates within $\pm$ 1 sigma.

From Figure 51, it can be seen that the constant variance lines tend to get further apart when going from left to right, indicating that the distribution of N is skewed right. Since the distribution of N has been determined as the 3-parameter log normal distribution which is a skewed right distribution, the prediction of a vs. N data from constant variance da/dN lines supports this conclusion.

11.6 Inverse Growth Rate

As anticipated, an improvement in the fit provided for the dN/da data over the fit provided for the da/dN data was obtained. The 3-parameter log normal distribution was able to provide the best fit for the dN/da data without serious competition from the other four distributions. This improvement is partially due to the inversion of the growth rate variable. Since N was strongly log normally distributed, it was anticipated that ΔN would be log normally distributed also. Another reason for this improvement was the exclusion of the location parameter from the gamma distributions, thereby severly decreasing their ability to provide an adequate fit for the dN/da data. The fit provided by those distributions which estimated a location parameter was significantly better than the fit provided by the gamma distributions. Quite a large range of values were estimated for the location parameter (from -1.6×10^{-11} to 4.9×10^{5}) and the absolute value of the estimate of the location parameter was always greater than 900, indicating no tendency to approach

zero as acsumed in equation 48 (Section 5.2.e). Thus, this assumption has not proven valid.

The value of the location parameter of the 3-parameter log normal distribution assumed negative values in many instances, indicating that skewed left and symmetric dN/da data was present as well as skewed right dN/da data. This was expected since the simple inversion of the da/dN variable does nothing to change the skewness of the density function of the data. The only effect of this inversion is to change the direction of the skewness and to alter the shape of the density function slightly. A histogram of typical symmetric dN/da data is shown in Figure 82 and plots of the fit of the dN/da data to each of the distributions are shown in Figures 83 through 87. Note in Figure 85 the ability of the 3-parameter log normal distribution to handle symmetric as well as skewed right data. Again, due to the large variation in the dN/da data, each of the distributions is needed in order to provide a fit for the data.

There is a large variation in the shape parameter and location parameter again for the dN/da data, as shown in the plots of the distribution parameters as a function of crack length (Figures 53 through 58). The use of dN/da does not remove these variations from the data, although it does reverse the basic trend of the mean as shown by comparing Figure 40 with Figure 53. The mean value of da/dN increases as a function of crack length while the mean value of dN/da decreases as a function of crack length, both being expected for constant amplitude loading.

The use of dN/da distribution parameters in the prediction of replicate a vs. N data did not change the predicted data noticeably. As suggested previously, the problem of predicting a vs. N data accurately lies

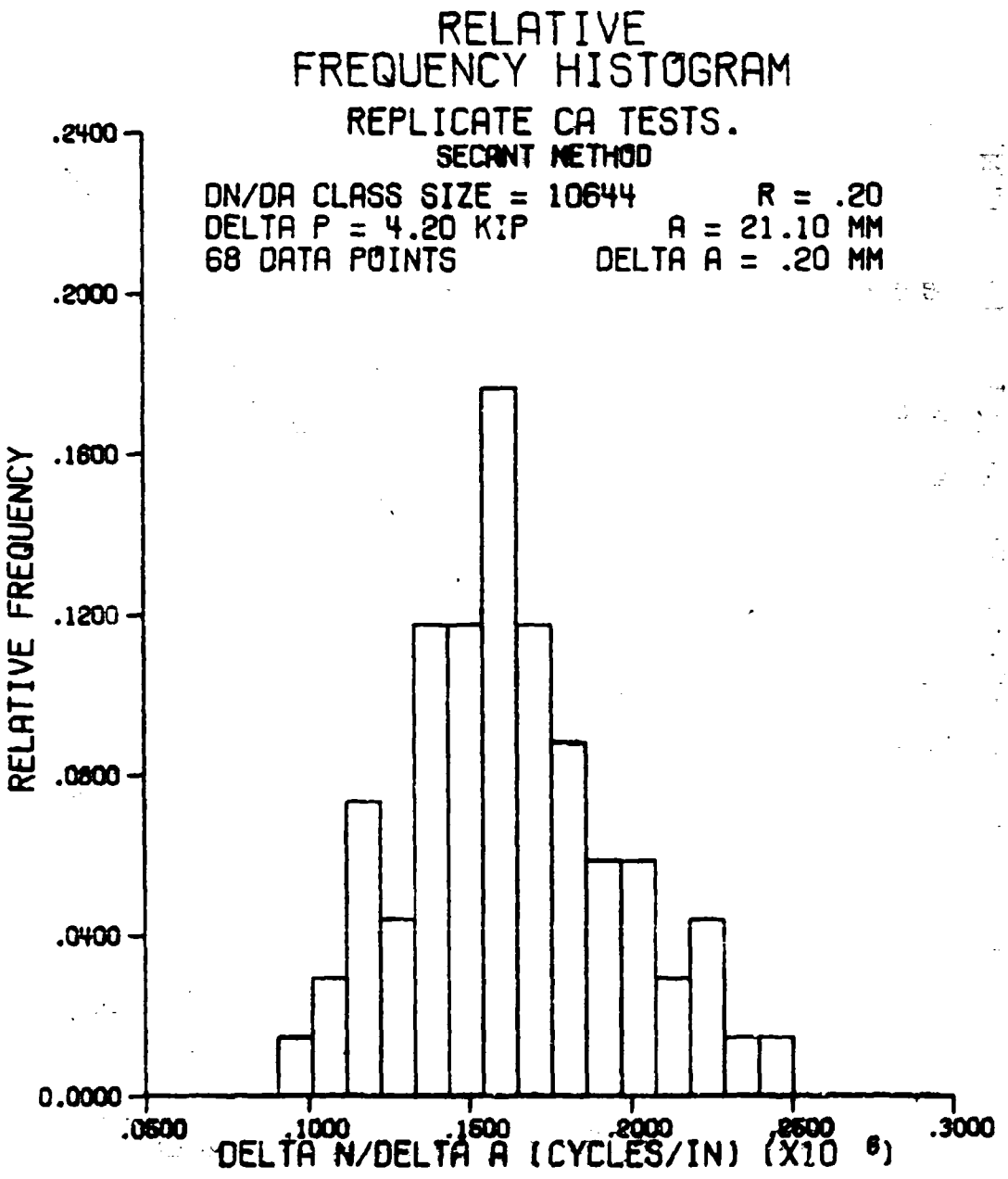

Figure 62. Typical Symmetric dN/da Data

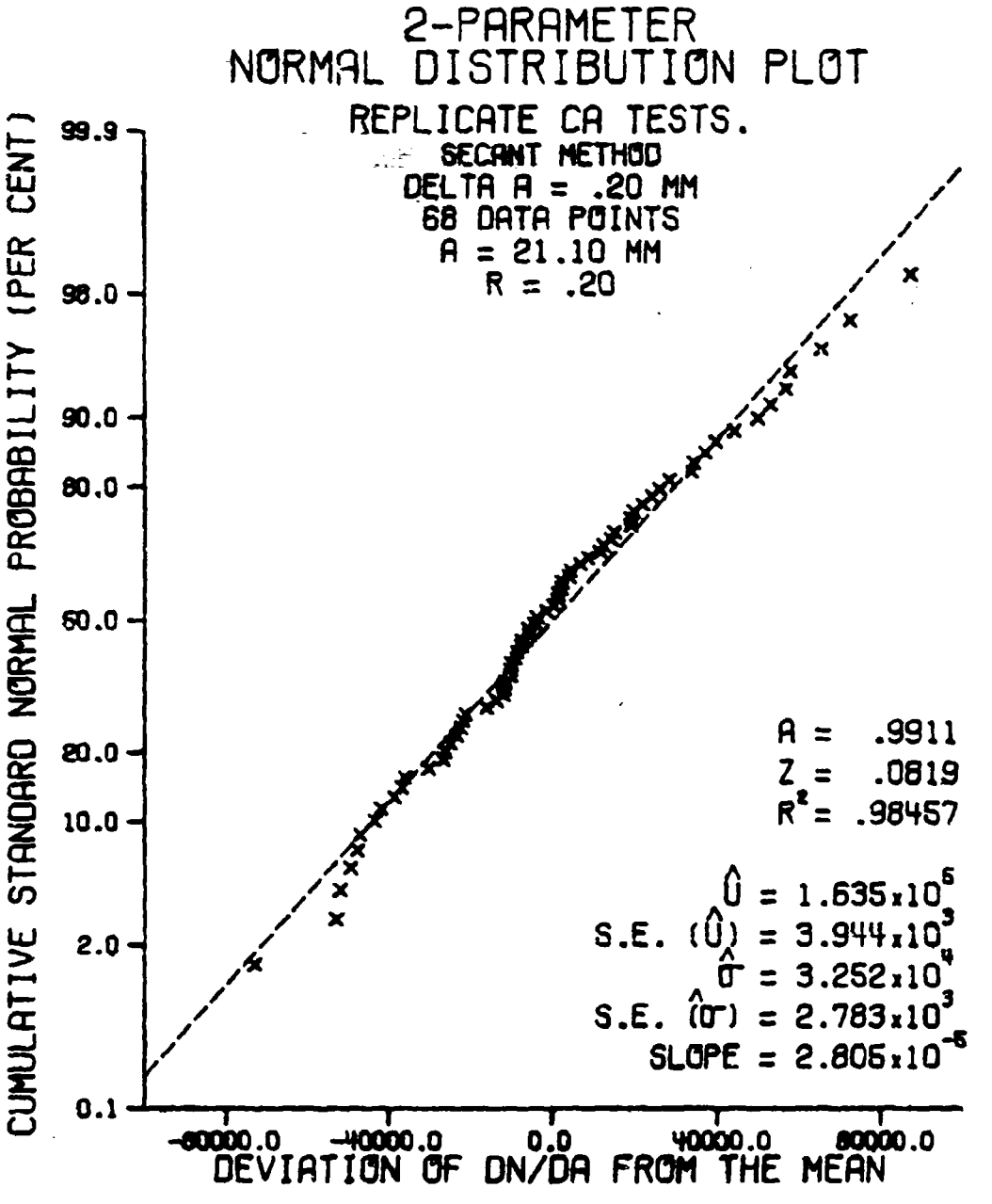

Figure 83. Typical Fit of Symmetric dN/da Data to the 2-Parameter Normal Distribution

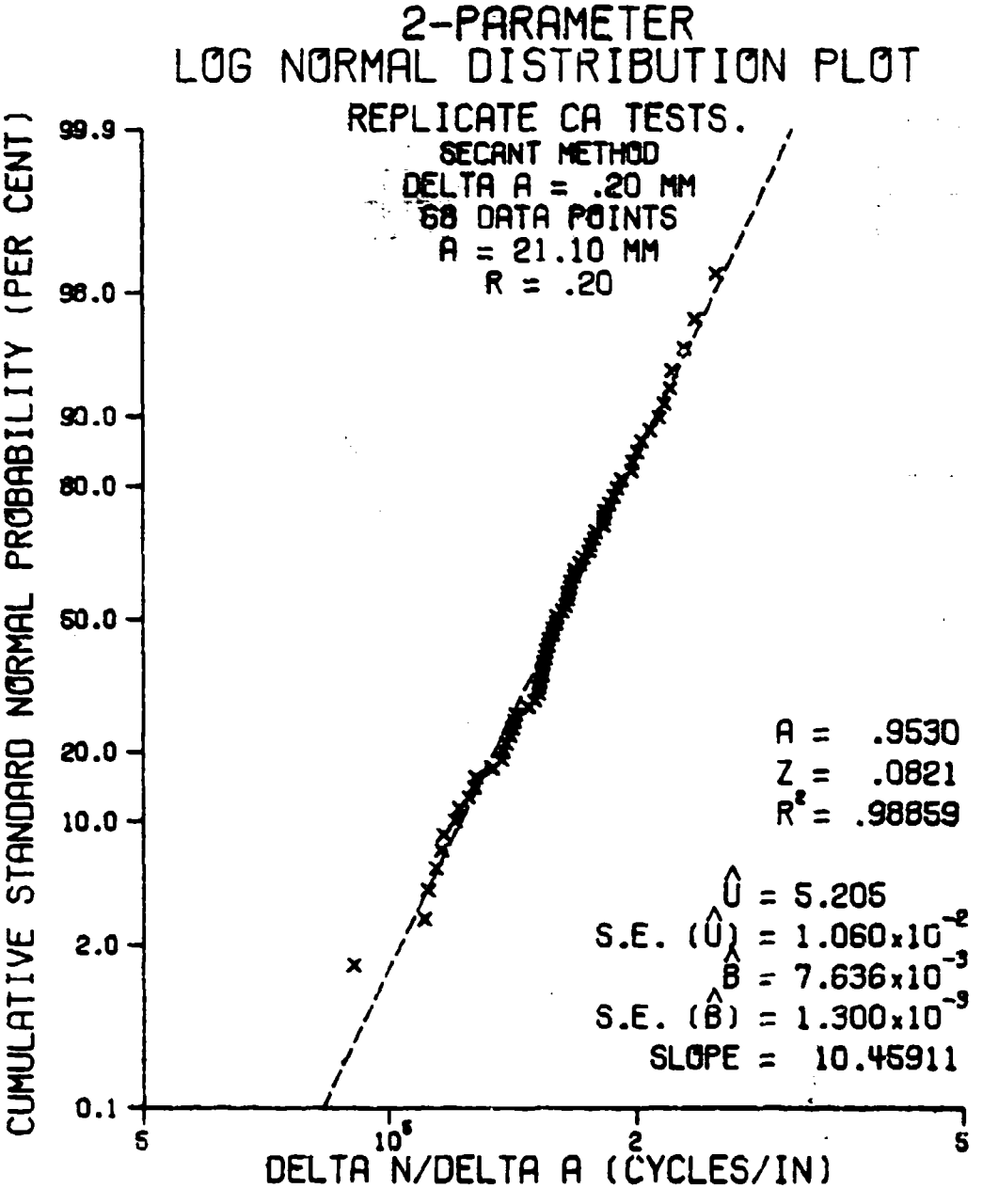

Figure 84. Typical Fit of Symmetric dN/da Data to the 2-Parameter Log Normal Distribution

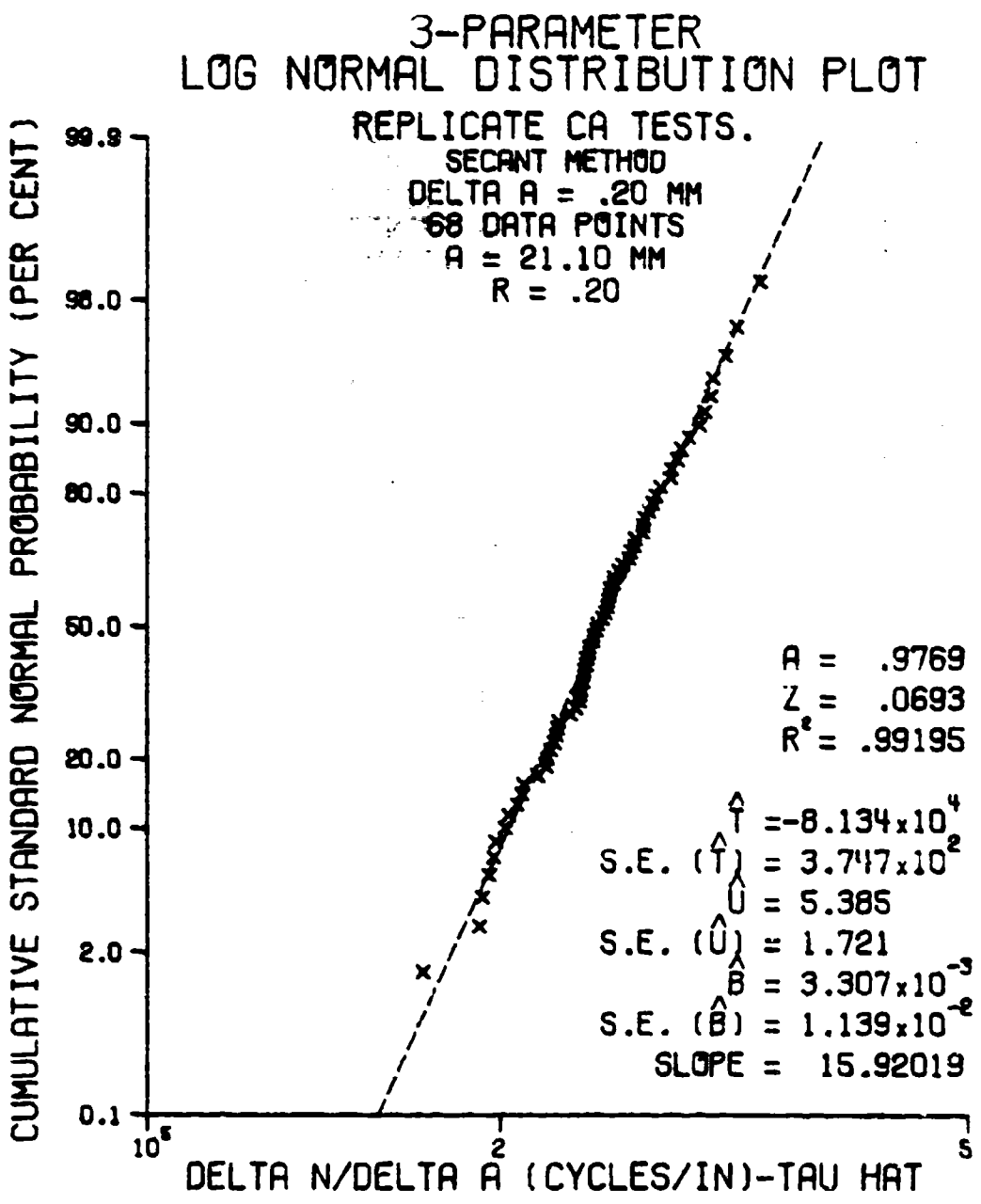

Figure 85. Typical Fit of Symmetric dN/da Data to the 3-Parameter Log Normal Distribution

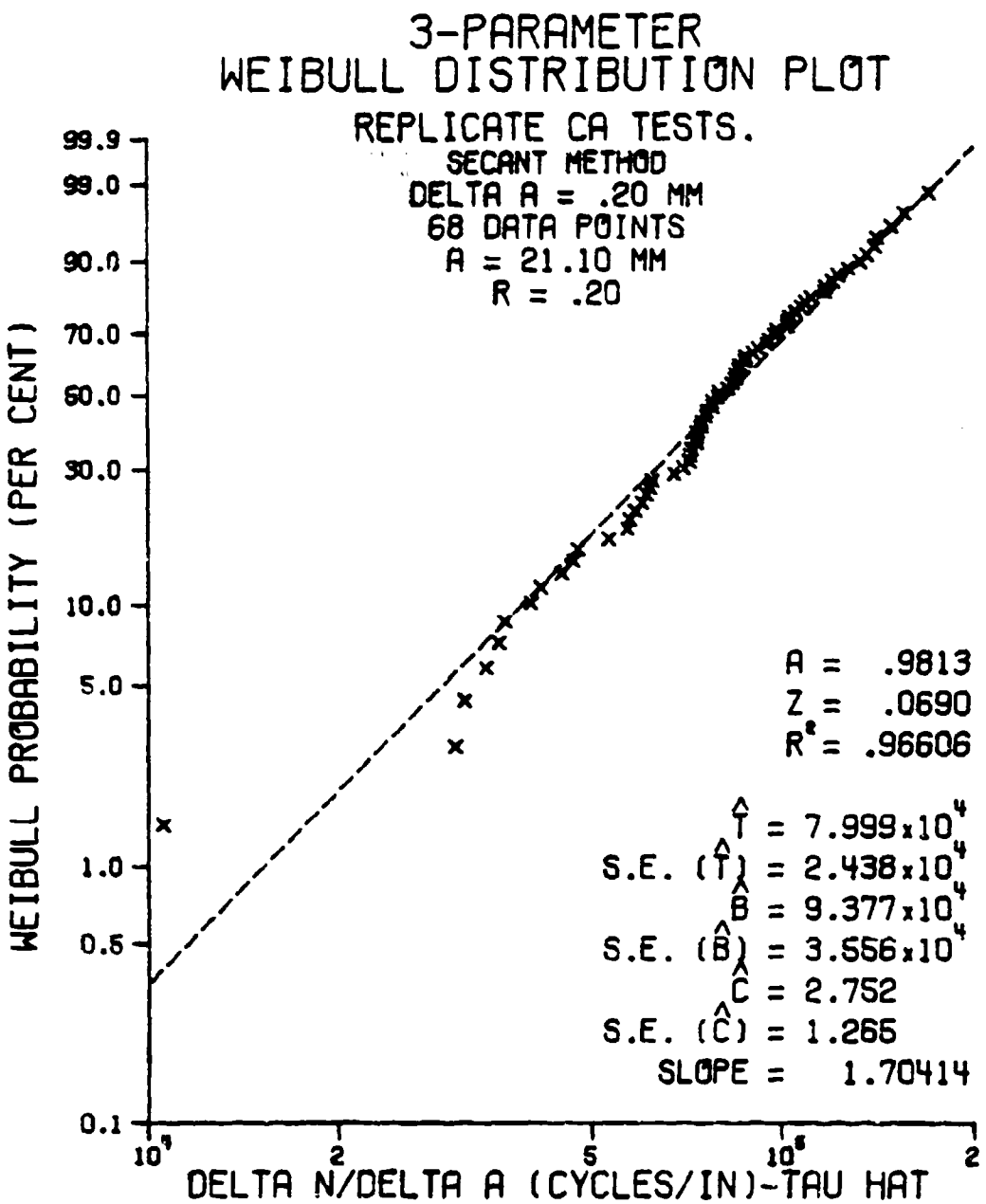

Figure 86. Typical Fit of Symmetric dN/da Data to the 3-Parameter Weibull Distribution

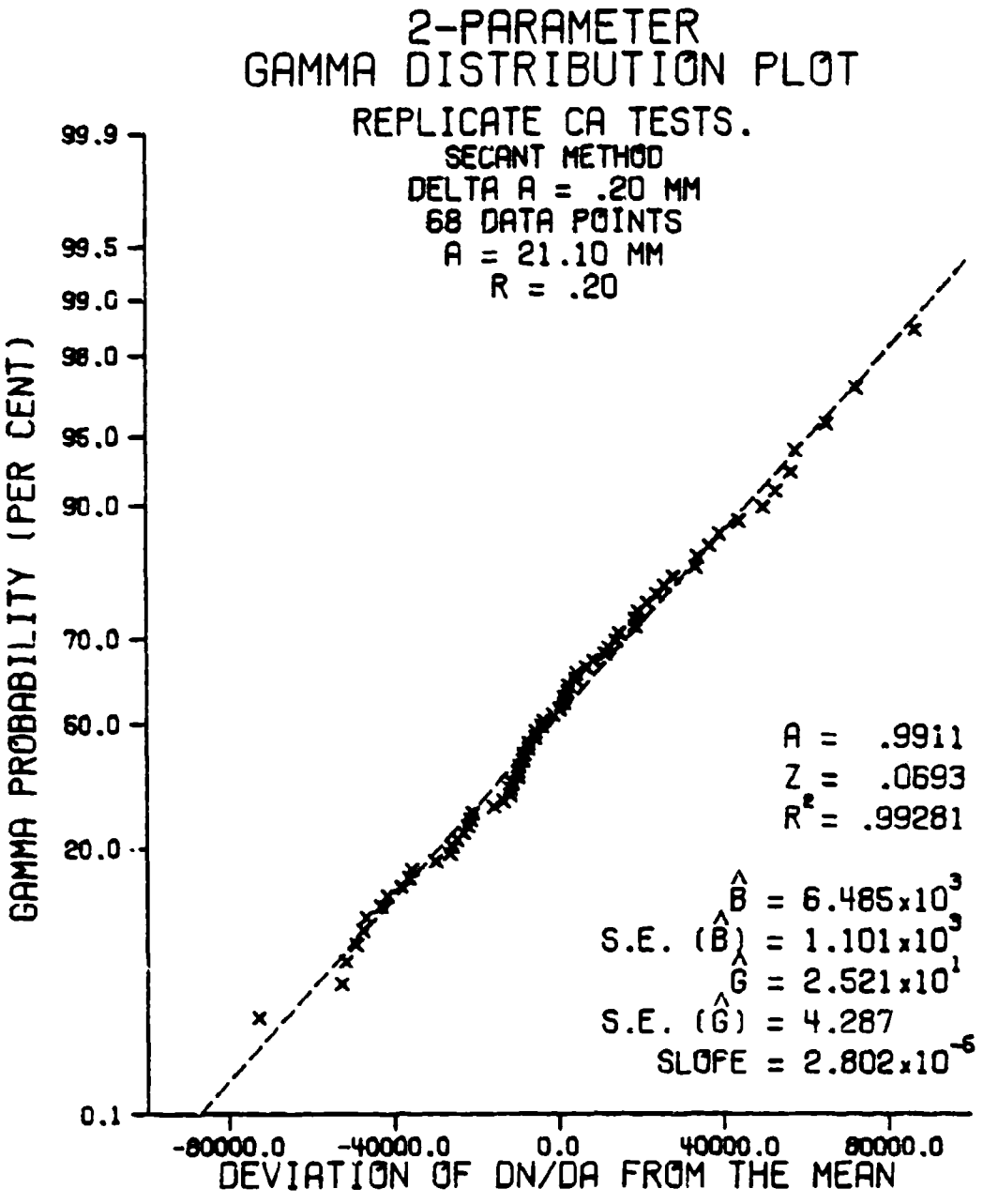

Figure 87. Typical Fit of Symmetric dN/da Data to the 2-Parameter Gamma Distribution

not in which variable is used to predict the data but rather in the assumption of independent adjacent growth rates.

When the cycle count data was predicted from the dN/da distribution parameters, the 3-parameter log normal distribution provided the best fit for the data as the estimates of the location parameter were all at anticipated values. This is an improvement over the prediction of cycle count data from the distribution parameters of da/dN, because the estimate of the location parameter was nearly always equal to zero. The use of this location parameter significantly improves the fit of the predicted cycle count data to the 3-parameter log normal distribution. Again, the values of $\hat{g}$ assumed maximum global values in both gamma distributions. This is most likely due to a lack of significant variance in the predicted cycle count data. When the distribution of predicted cycle count data was compared again to the distribution of actual cycle count data, the mean data was almost exactly predicted while the predicted standard deviation was again much less than the actual standard deviation, which can be seen by comparing Figure 59 with Figure 22.

The a vs. N data predicted from constant variance dN/da lines almost exactly reproduced a similar plot made from constant variance da/dN lines, as seen by comparing Figure 51 with Figure 65. Thus, the dN/da data seems to support the conclusion that the cycle count data fits the 3-parameter log normal distribution the best.

SECTION XII

CONCLUSIONS

The most significant conclusions of this investigation are summarized as follows:

1) The 2-parameter Weibull distribution was tried on previously generated fatigue crack propagation data and, due to its very poor performance, was dropped from the remainder of the statistical analysis (Section 8.1)

2) Actual replicate cycle count data followed a 3-parameter log normal distribution, with especially good fits at longer crack lengths (Section 11.2).

3) The modified secant method introduces the lowest amount of error into the da/dN data of the six growth rate calculation methods selected (Section 11.3).

4) The large amount of variance present in the da/dN vs. ΔK data prevented a consistent fit of the replicate da/dN data to any of the candidate distributions (Section 11.4).

5) Replicate dN/da data followed a 3-paramater log normal distribution (Section 11.6).

6) The method of predicting a vs. N data from the da/dN or dN/da distribution parameters was not completely successful due to the assumption of independent adjacent growth rates (Sections 11.5 and 11.6).

SECTION XIII

RECOMMENDATIONS FOR FURTHER WORK

The use of statistical methods in describing and predicting fatigue crack propagation behavior worked very well. However, accurate life prediction was not achieved because a total statistical description of the crack propagation process has not been determined. Only a minute percentage of the total possible experimental and analytical work needed to achieve this total statistical description was conducted under this investigation. Based on the observations, results, and conclusions of this investigation, the following topics need further investigation.

1) Experimental crack propagation data with N as the independent variable and a as the dependent variable is needed. From this the distribution of a as a function of N and the distribution of da/dN as a function of N can be obtained.
2) A study of the interdependence of growth rate data would be valuable for use in the prediction of a vs. N data from the distribution of growth rate data.
3) The effect of data density on the variance and distribution of growth rate data needs to be found to aid in more accurate data acquisition and analysis.
4) A study of the sudden growth rate changes in the original a vs. N data mentioned in Section 11.1 would aid considerably in the understanding of the crack propagation process.

5) A more reliable and accurate method of establishing the distribution rankings is needed. The goodness of fit criteria used in this investigation did not totally fulfill this need.

APPENDIX A

DERIVATION OF THE da/dN EQUATION FOR THE LINEAR LOG-LOG 7-POINT INCREMENTAL POLYNOMIAL METHOD

The fitted polynomial equation for the linear log-log 7-point incremental polynomial method is given by

$$\log_{10} a = b_o + b_1 N_{LS} \tag{A-1}$$

where N_{LS} is given by

$$N_{LS} = \frac{\log_{10} N - C_1}{C_2} \tag{A-2}$$

where C_1 and C_2 are given by the scaling equations (equations 7 and 8, Section 4.3). Substituting into equation A-1 for N_{LS},

$$\log_{10} a = b_o + b_1 \left[\frac{\log_{10} N - C_1}{C_2}\right] \tag{A-3}$$

Solving for a,

$$a = 10^{b_o + b_1 \left[\frac{\log_{10} N - C_1}{C_2}\right]}$$

$$= 10^{b_o - \frac{b_1 C_1}{C_2} + \frac{b_1 \log_{10} N}{C_2}}$$

$$= 10^{b_o - \frac{b_1 C_1}{C_2}} \cdot 10^{(\log_{10} N) \cdot \frac{b_1}{C_2}}$$

$$= 10^{b_o - \frac{b_1 C_1}{C_2}} \cdot N^{\frac{b_1}{C_2}} \tag{A-4}$$

Taking the derivative of a with respect to N and evaluating at the mid-point, N_i,

$$\frac{da}{dN_i} = 10^{b_o - \frac{b_1 C_1}{C_2}} \cdot \frac{b_1}{C_2} N_i^{\frac{b_1}{C_2} - 1} \qquad \text{(A-5)}$$

APPENDIX B

DERIVATION OF THE da/dN EQUATION FOR THE QUADRATIC LOG-LOG 7-POINT INCREMENTAL POLYNOMIAL METHOD

The fitted polynomial equation for the quadratic log-log 7-point incremental polynomial method is given by

$$\log_{10} a = b_o + b_1 N_{LS} + b_2 N_{LS}^2 \tag{B-1}$$

where N_{LS} is given by equation A-2. Substituting into Equation B-1 for N_{LS},

$$\log_{10} a = b_o + b_1 \left[\frac{\log_{10} N - C_1}{C_2}\right] + b_2 \left[\frac{\log_{10} N - C_1}{C_2}\right]^2 \tag{B-2}$$

Letting

$$U = \frac{\log_{10} N - C_1}{C_2} \tag{B-3}$$

$$\frac{dU}{dN} = \frac{1}{N \cdot \ln(10) \cdot C_2} \tag{B-4}$$

Then

$$\log_{10} a = b_o + b_1 U + b_2 U^2 \tag{B-5}$$

Solving for a,

$$a = 10^{b_o + b_1 U + b_2 U^2} \tag{B-6}$$

Taking the derivative of a with respect to U,

$$\frac{da}{dU} = 10^{b_o} \cdot \frac{d}{dU}\left[10^{b_1 U} \cdot 10^{b_2 U^2}\right] \tag{B-7}$$

where

$$\frac{d}{dU}\left[10^{b_1 U} \cdot 10^{b_2 U^2}\right] = \left[10^{b_1 U} \cdot 10^{b_2 U^2} \cdot 2\, b_2\, U \ln(10) + 10^{b_2 U^2} \cdot 10^{b_1 U} \cdot b_1 \ln(10)\right] \tag{B-8}$$

Then

$$\frac{da}{dU} = 10^{b_o} \cdot 10^{b_1 U} \cdot 10^{b_2 U^2} \cdot \ln(10) \cdot \left[2\, b_2\, U + b_1\right] \tag{B-9}$$

Using the chain rule,

$$\frac{da}{dN} = \frac{da}{dU} \cdot \frac{dU}{dN} \tag{B-10}$$

$$= 10^{b_o} \cdot 10^{b_1 U} \cdot 10^{b_2 U^2} \cdot \ln(10) \cdot \left[2\, b_2\, U + b_1\right] \cdot \left[\frac{1}{N \cdot \ln(10) \cdot C_2}\right]$$

$$= \frac{10^{b_o} \cdot 10^{b_1 U} \cdot 10^{b_2 U^2} \cdot (2 b_2 U + b_1)}{C_2 \cdot N} \tag{B-11}$$

Substituting for U and evaluating at the midpoint, N_i,

$$\frac{da}{dN_i} = \frac{10^{b_o} \cdot 10^{\left[\frac{b_1 \log N_i}{C_2} - \frac{b_1 C_1}{C_2}\right]} \cdot 10^{\left[b_2 (\log N_i)^2 - 2 b_2 C_1 \log N_i + b_2 C_1^2\right]}}{C_2 N_i} \cdot \left[\frac{2 b_2 \log N_i - 2 b_2 C_1}{C_2} + b_1\right] \tag{B-12}$$

APPENDIX C

DERIVATION OF C^2

From linear regression, the coefficient of multiple determination, R^2, is given by [34]

$$R^2 = 1 - \frac{SSRES}{TCSS} \qquad (C\text{-}1)$$

Where SSRES is the residual sum of squares and TCSS is the total corrected sum of squares. Since SSRES and TCSS are measured in the vertical direction, it was desirable to correct them so that their direction is normal to the slope, m. Let the slope be given by

$$m = J/K \qquad (C\text{-}2)$$

Where J is the side of a triangle along the least squares line and K is the side of the triangle perpendicular to the least squares line. From basic geometry,

$$I^2 = J^2 + K^2 \qquad (C\text{-}3)$$

Where I is the third side of the triangle. I is always in a vertical direction. Substituting from equation C-2 into C-3 for J,

$$I^2 = (m \cdot K)^2 + K^2$$

$$= K^2 (m^2 + 1) \qquad (C\text{-}4)$$

Solving for K^2,

$$K^2 = \frac{I^2}{m^2 + 1} \tag{C-5}$$

Solving for the correction of the slope, K^2/I^2,

$$\frac{K^2}{I^2} = \frac{1}{m^2 + 1} \tag{C-6}$$

Plugging this into equation C-1 to obtain R^2 corrected for the slope, called C^2,

$$C^2 = R^2 \cdot (K^2/I^2) \tag{C-7}$$

$$= \left[1 - \frac{SSRES}{TCSS}\right] \cdot \left[\frac{1}{m^2 + 1}\right] \tag{C-8}$$

APPENDIX D

DNDDPG DOCUMENTATION

This program consists of a main program and 25 subroutines. The main program (DNDDPG) reads in the desired Δa vs. ΔN data and calls subroutine DELTA to re-create the original a vs. N data. The program flow is then transferred to subroutine CLASS which divides the data into constant Δa data sets and then calculates the histogram frequencies for each constant Δa data set. The program flow is then transferred to subroutine STPLOT which determines the distribution.

Subroutine STPLOT uses, directly or indirectly, the following subroutines.

I. Parameter Estimation Subroutines
   1. GOLDEN
   2. CRVFIT

II. Scaling Subroutines
   1. PRBPLT
   2. WBLPRB
   3. LGSCAL
   4. LNSCAL
   5. INLNSC
   6. ODSCAL

III. Plotting Subroutines
   1. DOPLOT

2. NRMPLT

3. LOGPLT

4. WBLPLT

5. ODAXIS

IV. Output Subroutines

1. RITDAT

2. RITPAR

V. General Purpose Subroutines

1. LSTSQR

2. RANK

3. OUTLIR

4. NRMTAB

5. SIMPSN

6. MAXR

7. MAXI

A listing of this program can be obtained from:

Prof. B. M. Hillberry
School of Mechanical Engineering
Purdue University
West Lafayette, Indiana 47907
Phone (317) 494-1600

APPENDIX E

CCDDP DOCUMENTATION

This program consists of a main program, 53 subroutines, and 18 function subprograms. The main program (CCDDP) reads in the desired replicate cycle count data and writes it by calling subroutine RITDAT. The program flow is then transferred to subroutine CLASS which calculates the histogram frequencies for the data. The program flow is then passed to subroutine STPLOT which determines the distribution.

Subroutine STPLOT uses, directly or indirectly, the following subroutines and function subprograms.

I. Parameter Estimation Routines

A. Subroutines

1. MLELN
2. MLEW
3. MLEG
4. MLEGG
5. HJ

B. Supporting Function Subprograms

1. FLN
2. FW
3. FG
4. FGG

II. Statistical Parameters Subroutines

1. NRSTAT

2. WBSTAT

3. GMSTAT

III. Goodness of Fit Routines

A. Subroutines

1. CHISQR

2. KOLSMR

3. NRMCS

4. WBLCS

5. GAMCS

B. Supporting Function Subprograms

1. FNRM

2. FWBL

3. FGAM

IV. Output Subroutines

1. RITPAR

2. RITRES

3. PAROUT

V. Plotting Routines

A. Main Plotting Subroutines

1. AVNPLT

2. HISPLT

3. NRMPLT

4. LOGPLT

5. WBLPLT

6. GAMPLT

B. Supporting Plotting Subroutines

1. ODAXIS

2. LGAXIS

3. GMAXIS

4. SCINOT

VI. Scaling Subroutines

1. NRMSCL

2. WBLSCL

3. GAMSCL

4. LGSCAL

5. LNSCAL

6. INLNSC

7. ODSCAL

8. SCALEL

VII. Stress Intensity Calculation Routines

A. Subroutine

1. DELTAK

B. Function Subprogram

1. FAB

VIII. General Purpose Statistical Routines

A. Subroutines

1. NRMTAB

2. OUTLIR

B. Function Subprograms

1. FNORM

2. FGAMMA

3. FPSI

4. FTRIGM

5. FINGAM

6. FGM

7. FGMINT

8. FGMNEG

9. FSER

10. FFRAC

IX. General Purpose Subroutines

1. TABLEL

2. INTHAV

3. INTERP

4. INVINT

5. LSTSQR

6. INVMAT

7. RANK

8. MANCHA

9. INITR

10. ITOR

11. LOG

12. MAXR

13. MAXI

A listing of this program can be obtained from Professor B. M. Hillberry (Appendix D).

APPENDIX F

CGRDDP DOCUMENTATION

This program consists of a main program, 50 subroutines, and 17 function subprograms. This program is nearly identical to the CCDDP program (Appendix E) and only the main program (CGRDDP) and 3 subroutines are changed. These 3 subroutines are;

1. CLASS,
2. STPLOT, and
3. RITDAT.

This program requires an input of replicate growth rate data and has the same output as the CCDDP program. Subroutines DELTAK, ITOR, and MAXI and function subprogram FAB need not be loaded for this program. A listing of this program can be obtained from Professor B. M. Hillberry (Appendix D).

APPENDIX G

DNDDP DOCUMENTATION

This program consists of a main program, 49 subroutines, and 17 function subprograms. This program is nearly identical to the CGRDDP program (Appendix F) and only the main program (DNDDP), 9 subroutines, and 3 function subprograms are changed. The 9 subroutines that are changed are;

1. CLASS,
2. STPLOT,
3. MLEG,
4. MLEGG,
5. GMSTAT,
6. GAMCS,
7. RITDAT,
8. RITPAR, and
9. GAMPLT.

The 3 function subprograms that are changed are;

1. FG,
2. FGG, and
3. FGAM.

This program requires an input of replicate growth rate data and has the same output as the CGRDDP program. Subroutine INVMAT need not be loaded

for this program. A listing of this program can be obtained from Professor B. M. Hillberry (Appendix D).

APPENDIX H

DELTCP DOCUMENTATION

This program consists of a main program and 5 subroutines. The main program (DELTCP) reads in the desired a vs. N data and calls the proper subroutine(s) to calculate the Δa vs. ΔN data according to the desired calculation method chosen. The Δa vs. ΔN calculation subroutines are;

1. REMOVE,
2. STRIP, and
3. DELTA.

The main program then calls subroutine RITDAT to write the Δa vs. ΔN data. The only general purpose subroutine required is subroutine LSTSQR. A listing of this program can be obtained from Professor B. M. Hillberry (Appendix D).

APPENDIX I

DADNCP DOCUMENTATION

This program consists of a main program, 22 subroutines, and 1 function subprogram. The main program (DADNCP) reads in the desired a vs. N data set and calls, directly or indirectly, the following subroutines and function subprogram.

I. Growth Rate Calculation Subroutines
   1. DADN
   2. SECANT
   3. MODSEC
   4. STRIP
   5. EVAL

II. Error Determination Subroutines
   1. DELTA
   2. INTEGR
   3. ERROR

III. Output Subroutines
   1. RITDAT
   2. RITRES
   3. RESULT

IV. Plotting Subroutines
   1. AVEPLT
   2. LDPLT

V. Scaling Subroutine

1. LGSCAL

VI. Stress Intensity Calculation Routines

A. Subroutine

1. DELTAK

B. Function Subprogram

1. FAB

VII. General Purpose Subroutines

1. INITR

2. INITI

3. CHECK

4. ITOR

5. MAXR

6. LOC

7. LSTSQR

A listing of this program can be obtained from Professor B. M. Hillberry (Appendix D).

APPENDIX J

AVNPRD DOCUMENTATION

This program consists of a main program, 19 subroutines, and 8 function subprograms. The main program (AVNPRD) reads in the desired distribution parameters and calls, directly or indirectly, the following subroutines and function subprograms.

I. Random Number Generating Subroutine

1. RNGEN

II. Inverse Distribution Subroutines

1. INVDIS
2. INVNRM
3. INV2LN
4. INV3LN
5. INVWBL
6. INVGAM

III. Prediction Subroutines

1. PRD
2. SECANT
3. MODSEC
4. STRIP

IV. Output Subroutine

1. RITDAT

V. Plotting Subroutine

1. AVNPLT

VI. General Purpose Statistical Routines

A. Subroutine

1. NRMTAB

B. Function Subprograms

1. FNORM

2. FGAMMA

3. FINGAM

4. FGM

5. FGMINT

6. FGMNEG

7. FSER

8. FFRAC

VII. General Purpose Subroutines

1. TABLEL

2. INTHAV

3. INTERP

4. INVINT

5. MAXR

A listing of this program can be obtained from Professor B. M. Hillberry (Appendix D).

APPENDIX K

RANDOM ORDER OF EXPERIMENTAL TESTS

The randomised order of the 68 specimens used during testing is as follows.

1. 131	19. 141	37. 49	55. 127
2. 101	20. 60	38. 111	56. 6
3. 147	21. 85	39. 102	57. 71
4. 77	22. 50	40. 64	58. 58
5. 66	23. 134	41. 82	59. 78
6. 119	24. 55	42. 94	60. 106
7. 47	25. 14	43. 138	61. 129
8. 112	26. 21	44. 130	62. 31
9. 42	27. 7	45. 143	63. 125
10. 40	28. 2	46. 57	64. 32
11. 18	29. 70	47. 41	65. 116
12. 132	30. 19	48. 9	66. 62
13. 118	31. 52	49. 74	67. 12
14. 1	32. 83	50. 33	68. 121
15. 35	33. 149	51. 144	
16. 123	34. 80	52. 81	
17. 37	35. 97	53. 93	
18. 139	36. 96	54. 99	

REFERENCES

1. Van Vlack, L. H., Elements of Materials Science, 2nd edition, Addison-Wesley Publishing Co., 1964, pp. 160-165.

2. Frank, K. H. and Fisher, J. W., "Analysis of Error in Determining Fatigue Crack Growth Rates," Fritz Engineering Laboratory Report No. 358.10, Lehigh University, Bethlehem, Pa., March 1971.

3. Wilhem, D. P., "Fracture Mechanics Guidelines for Aircraft Structural Applications," AFFDL-TR-69-111, Air Force Flight Dynamics Laboratory, Wright-Patterson Air Force Base, Ohio, February 1970.

4. Gallagher, J. P. and Stalnaker, H. D., "Developing Methods for Tracking Crack Growth Damage in Aircraft," AIAA/ASME/SAE 17th Structures, Structural Dynamics and Materials Conference, Valley Forge, Pa., May 1976.

5. Hudak, S. J. Jr., "The Analysis of Fatigue Crack Growth Rate Data," E24.04 Committee Meeting, ASTM, Philadelphia, Pa., 1975.

6. Clark, W. G. Jr. and Hudak, S. J. Jr., "Variability in Fatigue Crack Growth Rate Testing," ASTM E24.04.01 Task Group Report, Westinghouse Research Laboratories, 1974.

7. Hudak, S. J. Jr., Saxena, A., Bucci, R. J., and Malcolm, R. C., "Development of Standard Methods of Testing and Analyzing Fatigue Crack Growth Rate Data (Third Semi-Annual Report)," Westinghouse Research Laboratories, 1977.

8. Pook, L. P., "Basic Statistics of Fatigue Crack Growth," NEL Report No. 595, National Engineering Laboratory, 1975.

9. Gallagher, J. P., "Fatigue Crack Growth Rate Laws Accounting for Stress Ratio Effects," ASTM Task Force E24.04.04 Report No. 1, Air Force Flight Dynamics Laboratory, Wright-Patterson Air Force Base, Ohio, 1974.

10. Juvinall, R. C., Engineering Considerations of Stress, Strain, and Strength, McGraw-Hill Book Co., 1967.

11. Ostle, B. and Mensing, R. W., Statistics in Research, 3rd edition, Iowa State University Press, 1975.

12. Walpole, R. E. and Myers, R. H., Probability and Statistics for Engineers and Scientists, Macmillan Publishing Co., Inc., 1972.

13. Goel, P. K., Statistics Department, Purdue University, W. Lafayette, Ind., 1977.

14. Aitchison, J. and Brown, J. A. C., The Lognormal Distribution, Cambridge University Press, 1957.

15. Wingo, D. R., "The Use of Interior Penalty Functions to Overcome Lognormal Distribution Parameter Estimation Anomalies," Journal of Statistical Computation and Simulation, Volume 4, 1975, pp. 49-61.

16. Lambert, J. A. "Estimation of Parameters in the Three-Parameter Lognormal Distribution," Austrailian Journal of Statistics, Volume 6, 1964, pp. 29-32.

17. Wirsching, P. H. and Yao, J. T. P., "Statistical Methods in Structural Fatigue," Journal of the Structural Division, American Society of Civil Engineers, Volume 96, No. ST6, 1970.

18. Lipson, C. and Sheth, N. J., Statistical Design and Analysis of Engineering Experiments, McGraw-Hill Book Co., 1973.

19. Zanakis, S. H., "Computational Experience with Some Nonlinear Optimization Algorithms in Deriving Maximum Likelihood Estimates for the Three-Parameter Weibull Distribution," Special Issue of Management Science on Computational Methods in Probability Models, 1976.

20. Lienhard, J. H. and Meyer, P. L., "A Physical Basis for the Generalized Gamma Distribution," Quarterly of Applied Mathematics, Volume 25, 1967, pp. 330-334.

21. Harter, H. L., "Asymptotic Variances and Covariances of Maximum Likelihood Estimators, from Censored Samples, of the Parameters of a Four-Parameter Generalized Gamma Population," Report 66-0158, Aerospace Research Laboratories, Office of Aerospace Research, U.S.A.F., Wright-Patterson Air Force Base, Ohio, 1966.

22. Parr, V. B. and Webster, J. T., "A Method for Discriminating Between Failure Density Functions used in Reliability Predictions," Technometrics, Volume 7, 1965, pp. 1-10.

23. Johnson, N. L. and Kotz, S., Continuous Univariate Distributions, Houghton Mifflin Co., 1970.

24. Hillberry, B. M., Mechanical Engineering Department, Purdue University, W. Lafayette, Ind. 1977.

25. Stacy, E. W. and Mihram, G. A., "Parameter Estimation for a Generalized Gamma Distribution," Technometrics, Volume 7, 1965, pp. 349-358.

26. Mischke, C. R., An Introduction to Computer-Aided Design, Prentice-Hall, Inc., 1968.

27. Wilk, M. B., Gnanadesikan, R., and Hayett, M. J., "Probability Plots for the Gamma Distribution," Technometrics, Volume 4, 1962, pp. 1-20.

28. Harter, H. L. and Moore, A. H., "Local Maximum Likelihood Estimation of the Parameters of Three-Parameter Lognormal Populations from Complete and Censored Samples," Journal of American Statistics Association, Volume 61, 1961, pp. 842-851.

29. Cohen, A. C. Jr., "Estimating Parameters of Logarithmic-Normal Distributions by Maximum Likelihood," American Statistical Association Journal, Volume 46, 1951, pp. 206-212.

30. Harter, H. L. and Moore, A. H., "Maximum Likelihood Estimation of the Parameters of Gamma and Weibull Populations from Complete and from Censored Samples," Technometrics, Volume 7, 1965, pp. 639-643.

31. Mann, N. R., Schafer, R. E., and Singpurwalla, N. D., Methods for Statistical Analysis of Reliability and Life Data, John Wiley and Sons, Inc., 1974.

32. Harter, H. L., "Maximum Likelihood Estimation of the Parameters of a Four-Parameter Generalized Gamma Population from Complete and Censored Samples," Technometrics, Volume 9, 1967, pp. 159-165.

33. Hooke, R. and Jeeves, T. A., "Direct Search Solution of Numerical and Statistical Problems," Journal of the Association of Computing Machinery, Volume 8, 1961, pp. 212-229.

34. Draper, N. R. and Smith, H., Applied Regression Analysis, John Wiley and Sons, Inc., 1966.

35. Dahiya, R. C. and Garland, J., "Pearson Chi-Squared Test of Fit with Random Intervals," Biometrika, Volume 59, 1972, pp. 147-153.

36. Massey, F. J. Jr., "The Kolmogorov-Smirnov Test for Goodness of Fit," Journal of American Statistical Association, Volume 46, 1951, pp. 68-78.

37. Alzos, W. X., "The Effects of Single Overload/Underload Cycles on Fatigue Crack Propagation," M.S. Thesis, Purdue University, 1975.

38. Hillberry, B. M., Alzos, W. X., and Skat, A. C. Jr., "The Fatigue Crack Propagation Delay Behavior in 2024-T3 Aluminum Alloy Due to Single Overload/Underload Sequences," AFFDL-TR-75-96, Air Force Flight Dynamics Laboratory, Wright-Patterson Air Force Base, Ohio, 1976.

39. Skat, A. C. Jr., "Evaluation of Extended Crack Closure in Fatigue Crack Delay Prediction for Single Overload/Underload Sequences," M.S. Thesis, Purdue University, 1975.

40. Virkler, D. A., Hillberry, B. M., and Goel, P. K., "An Investigation of the Statistical Distribution of Fatigue Crack Propagation Data," ASTM Meeting on Fracture Mechanics, Norfolk, Va., March 1977.

*U.S.Government Printing Office: 1978 — 757-080/708